SMART GRID STATE ESTIMATION AND ITS APPLICATIONS TO GRID STABILIZATION

by

MD MASUD RANA

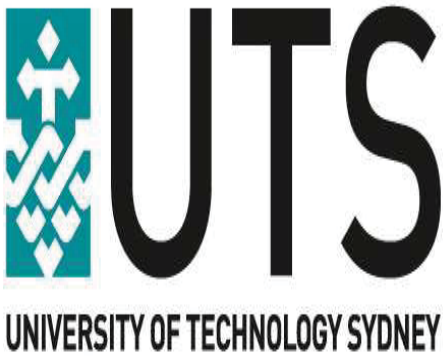

AN ABSTRACT OF A DISSERTATION

submitted partial fulfillment of the
requirements for the degree of

DOCTOR OF PHILOSOPHY

Faculty of Engineering and Information Technology
School of Electrical, Mechanical and Mechatronic Systems

UNIVERSITY OF TECHNOLOGY SYDNEY
Broadway, NSW 2007, Australia
February 2017

Dedicated to UTS students and staffs.

Abstract

The smart grid is expected to modernize the current electricity grid by commencing a new set of technologies and services that can make the electricity networks more secure, automated, cooperative and sustainable. The smart grid can integrate multiple distributed energy resources (DERs) into the main grid. The need for DERs is expected to become more important in the future smart grid due to the global warming and energy problems. Basically, the smart grid can spread the intelligence of the energy distribution and control system from the central unit to long-distance remote areas, thus enabling accurate state estimation and wide-area real-time monitoring of these intermittent energy sources. Reliable state estimation is a key technique to fulfil the control requirement and hence is an enabler for the automation of power grids. Driven by these motivations, this research explores the problem of state estimation and stabilization taking disturbances, cyber attacks and packet losses into consideration for the smart grid.

The first contribution of this dissertation is to develop a least square based Kalman filter (KF) algorithm for state estimation, and an optimal feedback control framework for stabilizing the microgrid states. To begin with, the environment-friendly renewable microgrid incorporating multiple DERs is modelled to obtain discrete-time state-space linear equations where sensors are deployed to obtain system state information. The proposed smart grid communication system provides an opportunity to address the state regulation challenge by offering two-way communication links for microgrid information collection, estimation and stabilization. Interestingly, the developed least square based centralised KF algorithm is able to estimate the system states properly even at the beginning of the dynamic process, and the proposed H_2 based optimal feedback controller is able to stabilize the microgrid states in a fairly short time.

Unfortunately, the smart grid is susceptible to malicious cyber attacks, which can create

serious technical, economic, social and control problems in power network operations. In contrast to the traditional cyber attack minimization techniques, this study proposes a recursive systematic convolutional (RSC) code and KF based method in the context of smart grids. The proposed RSC code is used to add redundancy in the microgrid states, and the log maximum a-posterior is used to recover the state information which is affected by random noises and cyber attacks. Once the estimated states are obtained, a semidefinite programming (SDP) based optimal feedback controller is proposed to regulate the system states. Test results show that the proposed approach can accurately mitigate the cyber attacks and properly estimate as well as regulate the system states.

The other significant contribution of this dissertation is to develop an adaptive-then-combine distributed dynamic approach for monitoring the grid under lossy communication links between wind turbines and the energy management system. Based on the mean squared error principle, an adaptive approach is proposed to estimate the local state information. The global estimation is designed by combining local estimation results with weighting factors, which are calculated by minimizing the estimation error covariances based on SDP. Afterwards, the convergence analysis indicates that the estimation error is gradually decreased, so the estimated state converges to the actual state. The efficacy of the developed approach is verified using the wind turbine and IEEE 6-bus distribution system.

Furthermore, the distribution power sub-systems are usually interconnected to each other, so this research investigates the interconnected optimal filtering problem for distributed dynamic state estimation considering packet losses. The optimal local and neighbouring gains are computed to reach a consensus estimation after exchanging their information with the neighbouring estimators. Then the convergence of the developed algorithm is theoretically proved. Afterwards, a distributed controller is designed based on the SDP approach. Simulation results demonstrate the accuracy of the developed approaches.

The penultimate contribution of this dissertation is to develop a distributed state estimation algorithm for interconnected power systems that only needs a consensus step. After modelling the interconnected synchronous generators, the optimal gain is determined to obtain a distributed state estimation. The consensus of the developed approach is proved based on the Lyapunov theory. From the circuit and system point of view, the proposed framework is useful for designing a practical energy management system as it has less computational complexity and provides accurate estimation results.

The distributed state estimation algorithm is further modified by considering different observation matrices with both local and consensus steps. The optimal local gain is computed after minimizing the mean squared error between the true and estimated states. The consensus gain is determined by a convex optimization process with a given local gain. Moreover, the convergence of the proposed scheme is analysed after stacking all the estimation error dynamics. The efficacy of the developed approach is demonstrated using the environment-friendly renewable microgrid and IEEE 30-bus power system.

Overall, the findings, theoretical development and analysis of this research represent a comprehensive source of information for smart grid state estimation and stabilization schemes, and will shed light on green smart energy management systems and monitoring centre design in future smart grid implementations. It is worth pointing out that the aforementioned contributions are very important in the smart grid community as communication impairments have a significant impact on grid stability and the distributed strategies can reduce communication burden and offer a sparse communication network.

Acknowledgements

At the University of Technology Sydney (UTS) I have had the opportunity to meet some wonderful people. First of all, I would like to thank my principal supervisor Dr. Li Li and my co-supervisor Dr. Steven W. Su. I cannot put into words what I have learnt from them. Their attitude to research and intellect have been my source of inspiration. It was a great honor to work with them and learn from them.

I am thankful to the Green Energy and Vehicle Innovations Centre, School of Electrical, Mechanical and Mechatronic systems at UTS for contributing to such a pleasant atmosphere. I thank the Faculty of Engineering and Information Technology and the Graduate School, UTS for the grant and financial support to finish this thesis. I also thank all the anonymous reviewers, for their appreciation and constructive feedback on my thesis and publications.

Finally, I would like to express my gratefulness to my adored wife and son for their unconditional support, devotion and love.

Statement of Originality

I certify that the work in this thesis has not previously been submitted for a degree nor has it been submitted as part of requirements for a degree except as fully acknowledged within the text.

I also certify that the thesis has been written by me. Any help that I have received in my research work and the preparation of the thesis itself has been acknowledged. In addition, I certify that all information sources and literature used are indicated in the thesis.

Md Masud Rana
Faculty of Engineering and Information Technology
University of Technology Sydney, Australia.

List of Publications

1. M. M. Rana, L. Li and S. W. Su, ”State estimation over unreliable communication networks with an application to smart grids,” *IEEE Transactions on Green Communications and Networking, vol. 1, no. 11, pp. 89-96, March 2017*.

2. M. M. Rana, L. Li and S. W. Su, ”Controlling the renewable microgrid using semidefinite programming technique,” *International Journal of Electrical Power and Energy Systems*, vol. 84, pp. 225-231, January 2017.

3. M. M. Rana, L. Li and S. W. Su, ”An adaptive-then-combine dynamic state estimation considering renewable generations in smart grids,” *IEEE Journal on Selected Areas in Communications*, vol. 34, no. 12, pp. 3954-3961, December 2016.

4. M. M. Rana, L. Li and S. W. Su, ”Microgrid state estimation and control using Kalman filter and semidefinite programming technique,” *International Energy Journal*, Thailand, vol. 2, pp. 47-56, June 2016.

5. M. M. Rana, L. Li and S. W. Su, ”Cyber attack protection and control of microgrids,” *IEEE/CAA Journal of Automatica Sinica (Acceptance notified on the 25th May, 2016, Appear in 2017)*.

6. M. M. Rana and L. Li, ”Renewable microgrid state estimation using the internet of things communication network,” *ICACT Transactions on Advanced Communications Technology*, South Korea, vol. 5, no. 2, pp. 823-829, May 2016.

7. M. M. Rana, L. Li and S. W. Su, ”Distributed state estimation using RSC coded smart grid communications,” *IEEE Access: Special Section on Smart Grids: A Hub of Interdisciplinary Research* , vol. 3, pp. 1340-1349, August 2015.

8. M. M. Rana and L. Li, ”An overview of distributed microgrid state estimation and control for smart grids,” *Sensors*, Switzerland, vol. 15, no. 2, pp. 4302-4325, February 2015.

9. M. M. Rana and L. Li, ”Microgrid state estimation and control for smart grid and Internet of Things communication network,” *Electronics Letters*, vol. 51, no. 2, pp. 149-151, January 2015.

10. M. M. Rana, L. Li and S. W. Su, ”Microgrid state estimation using the IoT with 5G technology,” *Internet of Things (IoT) in 5G Mobile Technologies. Springer International Publishing*, Germany, Chapter 9, pp. 175-195, June 2015.

11. M. M. Rana, L. Li and S. W. Su, ”Distributed dynamic state estimation over a lossy communication network with an application to smart grids,” *Proc. of the 55th IEEE Conference on Decision and Control*, pp. 6657-6662, USA, December 2016.

12. M. M. Rana, L. Li and S. W. Su, ”Distributed dynamic state estimation considering renewable generation and packet losses,” *Proc. of the 14th International Conference on Control, Automation, Robotics and Vision*, Thailand, November 2016.

13. M. M. Rana, L. Li and S. W. Su, ”Microgrid protection and control through reliable smart grid communication systems,” *Proc. of the 14th International Conference on Control, Automation, Robotics and Vision*, Thailand, November 2016.

14. M. M. Rana, L. Li and S. W. Su, ”Cyber attack protection and control in microgrids using channel code and semidefinite programming,” *Proc. of the IEEE Power and Energy Society General Meeting*, USA, July 2016.

15. M. M. Rana, L. Li and S. W. Su, ”Distributed condition monitoring of renewable microgrids using adaptive-then-combine algorithm,” *Proc. of the IEEE Power and Energy Society General Meeting*, USA, July 2016.

16. M. M. Rana, L. Li and S. W. Su, ”Kalman filter based microgrid state estimation and control using the IoT with 5G networks,” *Proc. of the IEEE PES Asia-Pacific Power and Energy Engineering Conference*, Australia, November 2015.

17. M. M. Rana, L. Li and S. W. Su, ”Kalman filter based distributed state estimation with communication systems,” *Proc. of the IEEE PES Asia-Pacific Power and Energy Engineering Conference*, Australia, November 2015.

18. M. M. Rana, L. Li and S. W. Su, "Distributed microgrid state estimation using smart grid communications," *Proc. of the IEEE PES Asia-Pacific Power and Energy Engineering Conference*, Australia, November 2015.

19. M. M. Rana and L. Li, "Distributed generation monitoring of smart grid using accuracy dependent Kalman filter with communication systems," *Proc. of the 12th International Conference on Information Technology-New Generations*, USA, April 2015.

20. M. M. Rana and L. Li, "Kalman filter based microgrid state estimation using the internet of things communication network," *Proc. of the 12th International Conference on Information Technology-New Generations*, USA, April 2015.

21. M. M. Rana and L. Li, "Controlling the distributed energy resources using smart grid communications," *Proc. of the 12th International Conference on Information Technology-New Generations*, USA, April 2015.

Awards and Scholarships

- Publications Award 2016 from the Faculty of Engineering and Information Technology, UTS, Australia.
- The Vice-Chancellor's Postgraduate Conference Travel Grant from the UTS Graduate Research School to attend the 14th International Conference on Control, Automation, Robotics and Vision, Thailand, November 2016.
- Student Scholarship Award from the IEEE PES Asia-Pacific Power and Energy Engineering Conference, Australia, November 2015.
- The Vice-Chancellor's Postgraduate Conference Travel Grant from the UTS Graduate Research School to attend the IEEE PES Asia-Pacific Power and Energy Engineering Conference, Australia, November 2015.
- Publications Award 2015 from the Faculty of Engineering and Information Technology, UTS, Australia.
- The UTS President's Scholarship (UTSP) during PhD study from the UTS, Australia.
- International Research Scholarship during PhD study from the UTS, Australia.

Contents

List of Figures

List of Tables

List of Acronyms

3G	Third Generation
4G	Fourth Generation
5G	Fifth Generation
AC	Alternating Current
AVR	Automatic Voltage Regulator
AWGN	Additive White Gaussian Noise
BP	Belief Propagation
BPSK	Binary Phase Shift Keying
CC	Convolutional Coding
DC	Direct Current
DER	Distributed Energy Resource
DSE	Dynamic State Estimation
DKF	Distributed Kalman Filter
EMS	Energy Management System
EKF	Extended Kalman Filter
GPS	Global Positioning System
ICT	Information and Communication Technology
IED	Intelligent Electronic Device
LAN	Local Area Network
LDPC	Low Density Parity Check
LMMSE	Linear Minimum Mean Square Error
LMS	Least Mean Squares
Log-MAP	Log-maximum a-posteriori
LQG	Linear Quadratic Gaussian
LQR	Linear Quadratic Regulator

LS	Least Square
EKF	Extended Kalman Filter
FAN	Field Area Network
IAN	Industrial Area Network
IID	Independent, Identically Distributed
KF	Kalman Filter
KCL	Kirchhoff's Current Law
KVL	Kirchhoff's Voltage Law
LLR	Log-Likelihood Ratio
LMI	Linear Matrix Inquality
LTE	Long Term Evolution
MAC	Multiple Access Channel
MASE	Multi-Area State Estimation
MAP	Maximum a-Posteriori Probability
MCSE	Modified Coordinated State Estimation
MPC	Model Predictive Control
NAN	Neighborhood Area Network
NBP	Nonparametric Belief Propagation
NLMS	Normalized Least Mean Square
PCC	Point of Common Coupling
PDF	Probability Distribution Function
PID	Proportional Integral Derivative
PF	Particle Filter
PLC	Power Line Communications
PMU	Phasor Measurement Units
RFID	Radio-Frequency Identification
RL	Resistor inductor
RLC	Resistor inductor Capacitor
RSC	Recursive Systematic Convolutional
SCADA	Supervisory Control and Data Acquisition
SDP	Semidefinite Programming
SE	State Estimation
SG	Smart Grid
SNR	Signal-to-Noise Ratio

RTU	Remote Terminal Unit
UKF	Unscented Kalman Filter
VSC	Voltage Source Converter
WAN	Wireless Area Network
WiFi	Wireless Fidelity
WLS	Weighted Least Square
WiMAX	Worldwide Interoperability for Microwave Access
WSN	Wireless Sensor Networks

List of Symbols

θ	Azimuth angle
$\otimes$	Kronecker product
Δ	Deviation
Δi_{dj}	Current deviation of DER_j
Δi_{tj}	Current deviation of transmission line
Δi_{lj}	Current deviation of load
Δv_j	PCC bus voltage deviation
Δt	Sampling period
δ	Rotor angle
ω	Rotor speed
λ	Packet arrival rate
a	Cyber attack
A	System state matrix
b	Sequence of bits
B	System input matrix
C	Observation matrix
C_j	Capacitance
$diag(\cdot)$	Diagonal matrix
D	Damping coefficient
e	Estimation error
E'	Transient voltage
$E(\cdot)$	Expectation operator
f_o	Frequency
F	State feedback gain
i	Current

$\mathbf{I}$	Identity matrix
J	Moment of inertia
k	Time step
$\mathbf{K}$	Kalman gain
$\mathbf{L}_r$	Received sequence length
$\mathbf{L}$	Neighbouring gain
L_{dj}	Inductance of VSC_j filter
L_{tj}	Inductance of transmission line
L_{lj}	Inductance of load
M_s	Number of states in the trellis
$\mathbf{n}$	Process noise
P_a	Turbine output power
$\mathbf{P}^-$	Predicted error covariance matrix
$\mathbf{P}$	Updated error covariance matrix
$\mathbf{Q}$	Process noise covariance matrix
$\mathbf{Q}_z$	Positive definite matrix
$\mathbf{r}$	Received sequence
$\mathbf{R}$	Measurement noise covariance matrix
R_{dj}	Resistance of VSC_j filter
R_{tj}	Resistance of transmission line
R_{lj}	Resistance of load
$\mathbf{s}$	Transmitted sequence
$tr(\cdot)$	Trace operator
T'_{doi}	Open-circuit transient time constant
T	Torque
v_{pi}	i-th DER input voltage
v_i	i-th PCC voltage
$\mathbf{w}$	Measurement noise
$\mathbf{x}$	Actual system states
$\hat{\mathbf{x}}$	Estimated system states
$\mathbf{y}$	Measurements
$\mathbf{y}_{rd}$	Dequantized and demodulated output bit sequence
$\mathbf{Y}$	Admittance matrix

Chapter 1

Introduction

This research explores the problem of state estimation and stabilization taking disturbances, cyber attacks and packet losses into consideration for the smart grid. The problem is becoming critical and challenging due to global warming, increase of green house gas emissions, and the dramatically increased computational burden of the centralized energy management system for the state estimation and stabilization of power networks [18], [19], [20]. Obviously, these kinds of impairments can seriously deteriorate the system performance and even lose network stability leading to a massive blackouts [21], [22]. Basically, the state estimation provides accurate information about the power system operating conditions and acts as a precursor to design the effective state feedback controller [23], [24]. To address the impending problem, the Kalman filter (KF) based smart grid state estimation and semidefinite programming (SDP) based stabilization approaches are proposed and verified. In light of the goals, this chapter presents the background, research challenges, objectives and contributions of the research.

1.1 Background

Today the most imperative problems all over the world are energy crisis and global warming, which is vulnerable to the natural disasters [25], [26], [27]. These impending issues are mainly due to the greenhouse gas (carbon dioxide, methane and nitrous oxide) emissions from the generation of electricity from the traditional coal and oil based power plants [28],

[29]. Unfortunately, the energy productivity is about 55% and clients suffer from power outages [30]. More than 95% of these outages are due to distribution systems (excluding the reason of generation deficiency). As the electricity customers are directly connected to the distribution system, its automation will need to guarantee the power supply quality and enhance the operating efficiency. The traditional electricity generation system can also cause power loss due to the long distance energy transmission and distribution, which increases the electricity cost. For example, the electricity production cost is approximately 3-5 EUROcent/kWh in European wholesale markets, but the retail price is about 10-15 EUROcent/kWh, which is due to the energy transmission from the point of production to the consumer [31]. Another reason for the high cost is due to the use of the power electronic interface between the microgrid and the main grid at the point of common coupling [32].

Fortunately, to mitigate the aforementioned inconveniences at an acceptable level, one of the effective solutions is to use a microgrid incorporating renewable distributed energy resources (DERs) for achieving a wiser and sustainable future [33]. For example, a typical photovoltaic (PV) generation system can minimise the power loss by roughly 40%, particularly in the rural distribution power networks [31]. Usually, a microgrid is designed and operated to meet the energy requirement of consumer household items such as pacemakers, home appliances, electric vehicles, cooling and heating, and to deliver excess power to the grid [31]. Certainly, one of the features of a smart grid is that it can integrate and manage the microgrid in a distributed way. For the purpose of illustration, Fig. 1.1 shows the main characteristic of a smart grid with the motivation of smart grid state estimations [1]. More precisely, the main feature of a smart grid is: self-healing, active participation by consumers, protection against cyber attacks, power quality enhancement, adapting all generation and storage options, enabling new product, services and real-time performance optimization [1], [34].

Generally speaking, the power generation pattern of the microgrid incorporating electricity generating circuits depends on the weather and surrounding ambient conditions [35]. Consequently, the microgrid state estimation is needed to estimate the system state in a distributed way so that it can operate in a normal and secure manner [1]. In other words, the state estimation can assist to identify the unmeasurable quantities of the microgrid such as voltage, current and power. After estimating the system states from the smart meter or sensor data, the operator knows the present status of the electricity network and can take necessary actions. The centralized state estimator is infeasible due to the communication burdens. Furthermore, the omnipotent decision maker is responsible for monitoring a large amount of

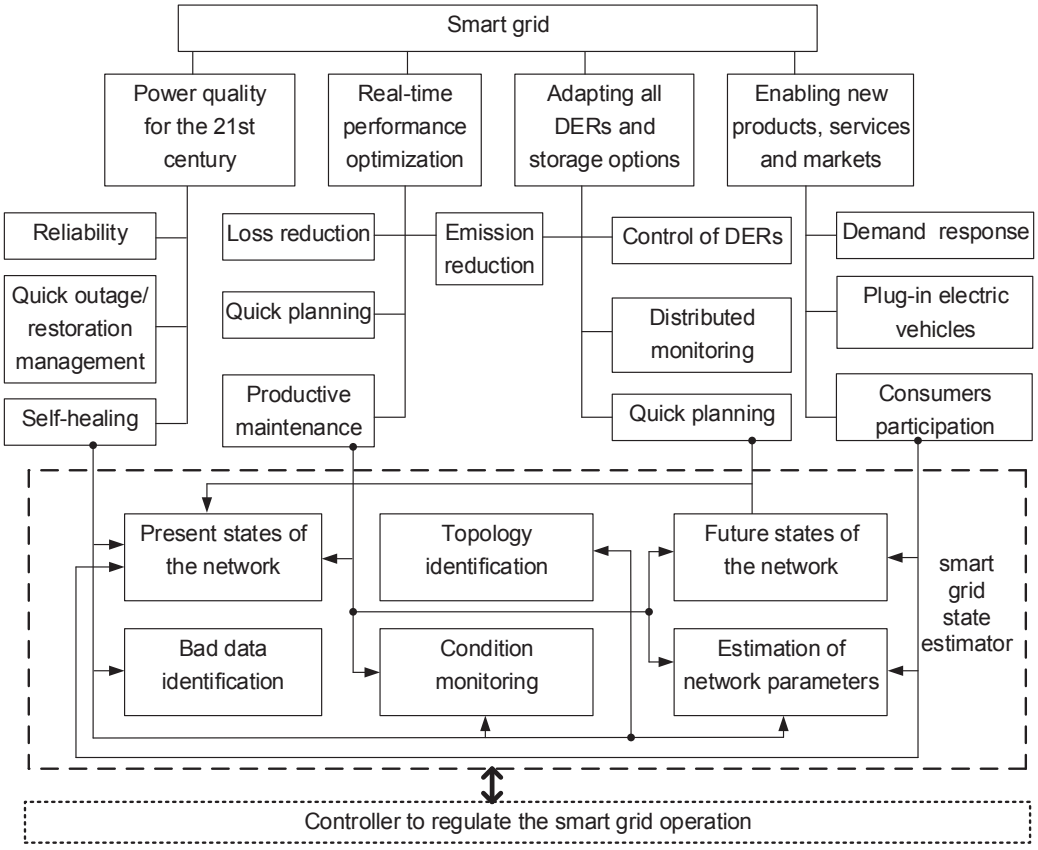

Figure 1.1: Features of a smart grid and its key state estimation functions [1].

generating equipment as well as end-user appliances and for purchasing energy [30]. Hence, the centralized state estimator may hardly monitor the future energy demand and supply [36].

Encouragingly, the community microgrid is modern, a supplement for the traditional bulk power grid and small-scale version of the centralized electricity network. To achieve the reliability, cost reduction and diversification of energy sources, the distributed microgrid state estimation is one of the promising research topics in academia, and for environmentalists and utility operators. To obtain the measurement, the utility operator deploys a set of smart sensors around the microgrid. Generally, the smart sensors, actuators and estimator are not physically collocated in the power network [37], [38]. Therefore, a communication network is clearly required for transferring information between the microgrid and the estimator at the energy management system (EMS). As a matter of fact, the performance of the estimation depends on the channel condition between the microgrid and the EMS. For instance, there may be packet losses due to the impairments of the communication medium such as wired,

wireless and hybrid networks.

There are several communication options available such as power line communications (PLC), copper-wire line, fiber optics, and a variety of wireless technologies for the grid integration of DERs [39]. Figure 1.2 shows different sensing and communication options in the smart grid. In comparison with wireline communications, wireless communications have the

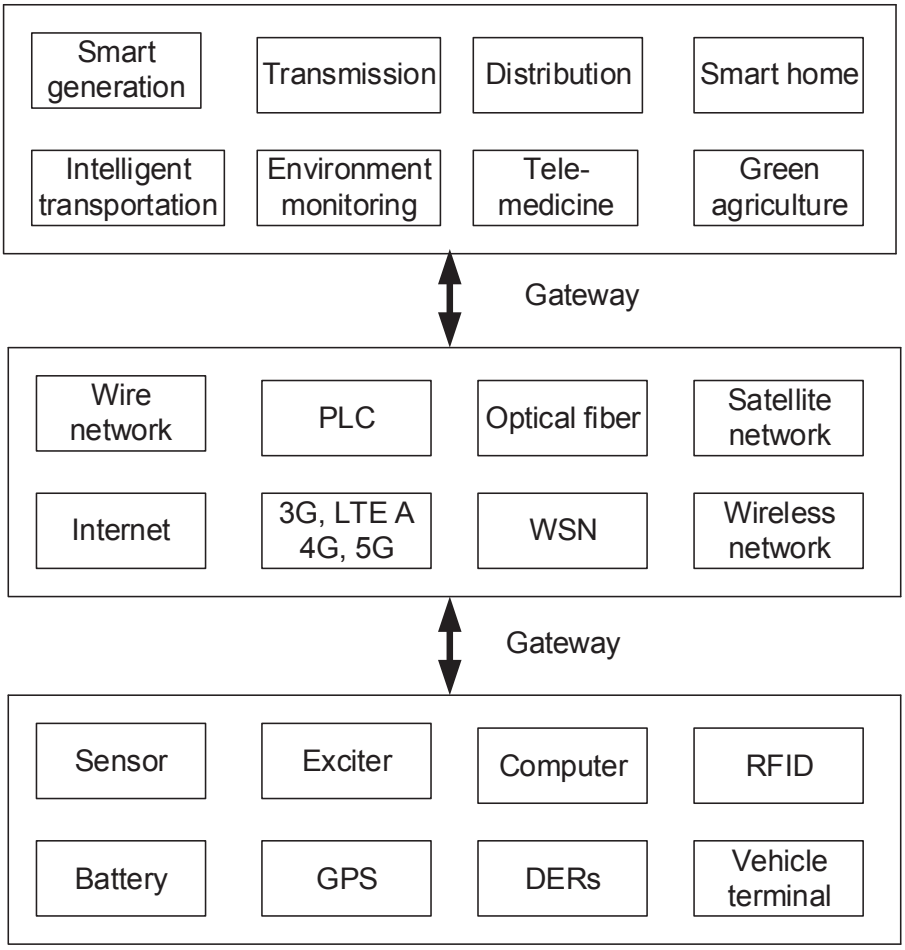

Figure 1.2: Different sensing and communication options in the smart grid [2].

advantages of easy mobility and installation, low deployment cost, remote area microgrid control and more user supported, and are gaining more and more interests from both industry and academia in future smart grids [2]. To achieve the vision of the smart grid through communication networks, the fifth generation (5G) communication infrastructure is used to collect data from the physical entities and take necessary actions based on observations [40]. The 5G technology comprises all type of advanced features such as ubiquitous computing,

smart aggregator and all IP platforms, which makes this technology more powerful to meet the massive demands in the future [41], [40]. The 5G networks will entail smart nodes with heterogeneous characteristics and capacities, which will result in a multi-tier architecture. This technology can effectively enable new facilities, security and high data rate services to everyone and every device [41], [40].

Research has been conducted on the power system state estimation in a centralized or distributed way. The centralized estimation means that the EMS uses all measurements from the local sensors to obtain a global estimation [42], [43], thus demanding huge communication and computation resources for processing all the measurements. The distributed system can process the subset of sensing information in a distributed way, leading to a very effective strategy for performing the wide-area distributed computation [44], [45]. In the distributed state estimation, every local estimator computes the state information based on its own measurements and sends it to the global estimator for obtaining a reliable estimation. From the smart grid and practical point of views, it improves scalability and computational efficiency [46], [42]. It is also relatively easier for monitoring the microgrid operating condition which changes after adding/removing the microgrid to/from the grid.

There are many estimation methods that deal with the centralized and distributed state estimation. First of all, weighted least squares is a classic method for estimating power system states [47]. The distributed KF (DKF) based dynamic state estimation is widely used in the literature [48]. Moreover, the extended KF and unscented KF algorithms are proposed in [49]. Nowadays, the consensus-based DKF methods have been proposed for sensor networks in [50], [51]. From the practical point of view, the diffusion strategy is widely used in the literature, where the global estimator linearly combines local results using a set of weighing factors [52], [53]. However, selecting an optimal weighting factor from the power system perspective is a quite difficult task. Furthermore, none of the above papers consider the packet losses in the distributed estimation process. Interestingly, the KF and linear quadratic Gaussian based optimal control for the networked controlled smart grid is suggested in [20]. Even though it considers packet losses, it is only suitable for the centralized power system state estimation and control. In fact, the microgrid state estimation with an unreliable communication channel is not considered in the literature specifically in a distributed way.

1.2 Research Challenges

Given the significant concerns regarding carbon emissions from fossil fuels, global warming and the energy crisis, renewable DERs are going to be integrated in smart grids, which will make the energy supply more reliable and decrease the costs and transmission losses [54], [55]. However, significant technical challenges arise in the planning, operation and control of DERs, due to the randomness and weather-dependence in the power generation [56]. This problem stimulates the deployment of smart sensors and actuators in smart grids so that the voltage can be stabilized. Motivated by this, voltage regulators should be installed at planned positions in the distribution feeders [57], [55]. Interestingly, the bidirectional smart grid communication between the microgrid and the control center can be leveraged to facilitate voltage regulation problems [58]. Another critical challenge is that the performance of the microgrid state estimation framework has to handle a hybrid system: a continuous dynamic system state and discrete information bits in communication systems and the estimation process [59]. Obviously, the introduction of time-varying parameters in the system model is needed for accurate representation of the DER behaviour, leading to more challenging problems in the estimation and control.

Generally speaking, the smart grid is susceptible to malicious cyber attacks, which can create serious technical, economic, social and control problems in power network operations such as blackouts in power systems, tampering with smart meter readings and changing the forecasted load profiles [3]. As shown in Fig. 1.3 system state estimation is an essential task for the monitoring and stabilization of the power network. Statistics in the energy sector in the USA show that more than 150 cyber attacks happened in 2013 and 79 in 2014 [11]. As a result, the power outage cost is about 80 billion US dollars per year in the USA. Usually, the utility operators amortize it by increasing the energy tariff, which is unfortunately transferred to consumer expenses [60]. Mostly, the wind farm and EMS are located far away from each other [61], so there is an unreliable communication link between them. The unreliable link can lead to packet losses which cause monitoring performance degradation and may give deceiving information to the utility operator [62], [63].

The power system state estimation commonly uses the KF algorithm. To utilize the KF estimator, one needs to specify the initial state value. Due to the lack of systematic methods for the estimation of initial states, the initial estimation is usually far away from the true initial

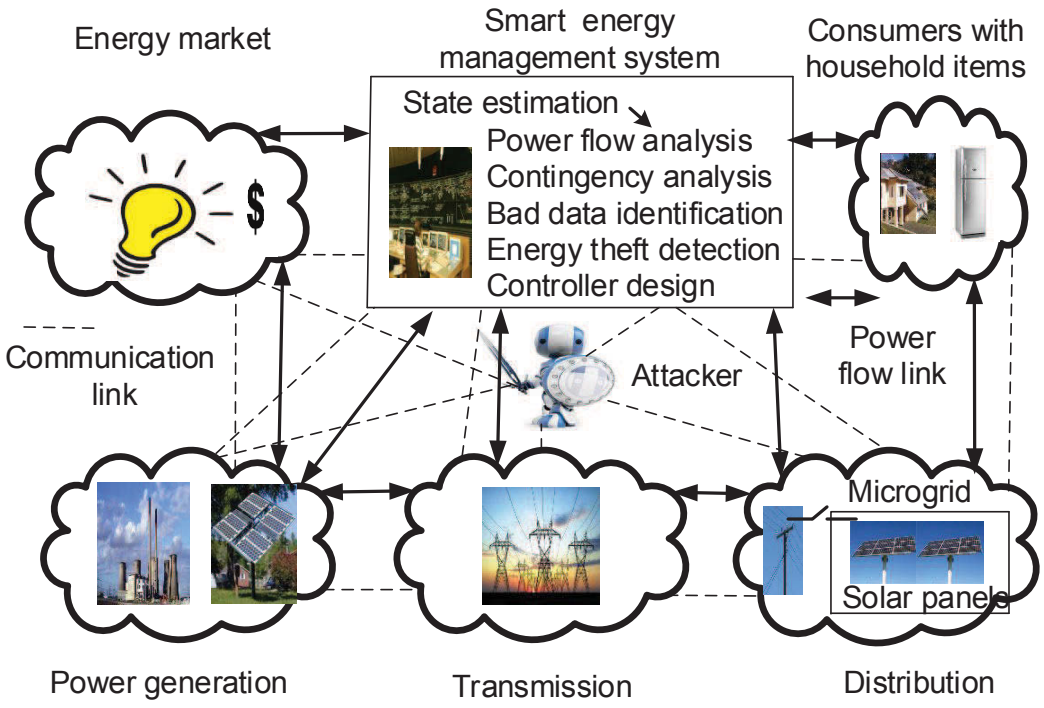

Figure 1.3: Flow of electricity and information between different sections of smart grids [3].

states. In the diffusion KF, the global estimator is linearly combined with the local estimation results with the set of weighting factors. However, in designing the optimal weighting sequence it is very difficult to get a consistent estimation. Finally, the distribution power sub-systems are usually interconnected to each other, so the design of the interconnected optimal filtering algorithm for distributed dynamic state estimation considering packet losses is a very challenging task. Driven by the aforementioned motivations and technical challenges, the following research gaps are identified and addressed in this thesis.

- *What is the suitable two-way communication infrastructure for sensing, estimating and controlling the microgrid incorporating multiple DERs? Based on the communication infrastructure, what is the optimal state estimation algorithm that can relax the initial assumption in the centralised KF? Based on the estimated states, what type of feedback control technique can be applied for stabilizing the grid?*

- *What is the reliable smart grid communication infrastructure that can tolerate cyber attacks? What type of centralised feedback control technique can be applied for controlling the microgrid states?*

- *How can the global estimator effectively combine local estimation results considering packet dropout in measurements? How can the convergence of the algorithm be proven from the continuous-time state space point of view?*
- *How should the estimators interact with each other so that the centralised processing can be avoided to reach a consensus on estimation? If such distributed estimation is feasible, how can the convergence of the algorithm be proven from the continuous-time state space point of view? What type of distributed feedback control technique should be applied for controlling the system states?*
- *How can the distributed estimator be designed such that it needs only a consensus step to reduce computational complexity? From the practical implementation point of view, how can the convergence of the algorithm be proven for a discrete-time system?*
- *How can the convergence of the distributed estimator be analysed considering different observation matrices with local and consensus steps?*

It is worth pointing out that the aforementioned problems are not trivial in the smart grid community as communication impairments have significant impact on grid stability and the distributed strategies can reduce communication burden and offer a sparse communication network.

1.3 Research Objectives

In recent years, the concept and framework of smart grid have gained acceptance in both industry and academia. Built upon ubiquitous sensors and integrated high speed interconnected communication networks, through the use of advanced information technology, control and decision support technologies, smart grid is seen as a modernisation of both transmission and distribution networks with the features of self-awareness, self-organising and self-recovery. In order to realise these features, one of the prerequisites is the observability of system state information such as power flows, voltages, currents, phases and frequency, across the grid. Reliable state estimation is a key technique to fulfil the observability requirement and hence is an enabler for the automation of power grids. We consider a state estimation problem in smart grids, where various sensors collect grid information and send it to the control centre

via wired or wireless channels, and then the control centre performs state estimation based on the received data. The specific aims of this research include the following aspects:

- A microgrid incorporating multiple DERs is represented as a discrete-time state-space linear system. A set of smart sensors are deployed to get microgrid information where measurements are disturbed by noises, cyber attacks and packet losses.
- Propose a reliable smart grid communication system to address the state regulation challenge by offering two-way communication links for microgrid information collection, estimation and stabilization.
- In order to properly monitor the intermittent energy sources, it will need centralized and distributed state estimation algorithms in the context of smart grids. For real-time applications, the convergence of the developed approaches will need to be proven.
- In order to regulate the microgrid states, this study will need to propose optimal feedback controllers such that they will act as precursors in terms of network stability and the operation of DERs.
- The efficacy of the developed approaches will need to be verified through numerical simulations. To sum up, Fig. 1.4 summarizes the flow diagram of the research objective.

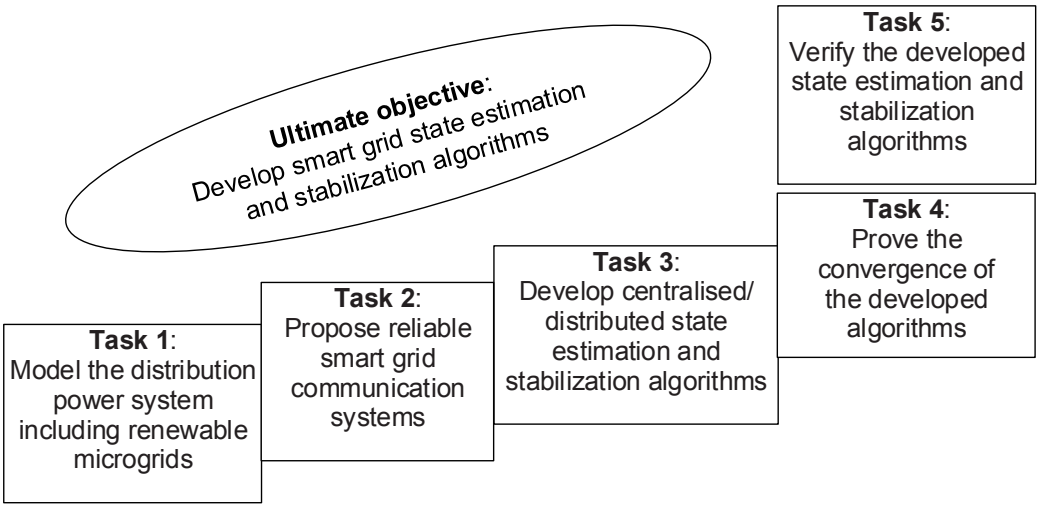

Figure 1.4: Flow diagram of the research objective.

1.4 Methodology

After modelling the microgrid, the observation information is obtained by a set of sensors. The sensing information is transmitted to the control center over a communication network where measurements may be disturbed by noises, cyber attacks and packet losses. In the control center, the data is fed to a state estimator program for estimating the system states. After estimating the system states, the feedback control strategy is developed to stabilize the grid. Figure 1.5 shows the detailed research methodology of this project. The following

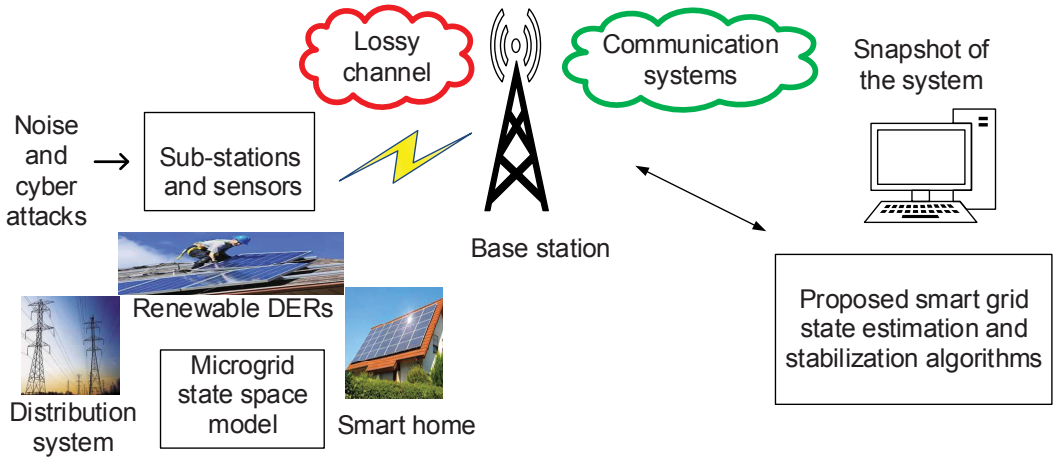

Figure 1.5: Research methodology.

tools will be used in this research: centralised KF, diffusion KF, distributed KF, least square, optimization theory, linear quadratic Gaussian (LQG), linear matrix inequality (LMI), SDP, H_2-optimal control, channel coding and communication theory. Using the appropriate tools and methodology, the key contributions are summarised in the next section.

1.5 Main Contributions

Driven by the aforementioned motivations and technical challenges, the main objective of this research is to develop KF based state estimation and stabilization algorithms in the context of smart grid communications. The research contributions and findings that will be discussed in this thesis have been presented in several conferences and published in journals

(see List of Publications). In meeting the goals of this project, the main contributions and expected outcomes of this research can be summarized as follows:

- A microgrid incorporating multiple DERs is modelled as a discrete-time linear state-space equation where sensors are deployed to obtain state information. In order to transmit the sensing information to the control center, a smart grid communication infrastructure is proposed. The proposed communication system provides an opportunity to address the state regulation challenge by offering two-way communication links for microgrid information collection, estimation and stabilization. Based on the communication infrastructure, the proposed least square based KF algorithm is able to estimate the system states properly even at the beginning of the dynamic process. After estimating the system states, an optimal H_2 feedback control strategy for stabilizing the microgrid states is explored based on the SDP approach. As a result, a new sensing, state estimation and control scheme for microgrids incorporating DERs is derived. The effectiveness of the developed approaches is verified by numerical simulations.

- The smart grid is generally susceptible to malicious cyber attacks, which can create serious technical, economic, social and control problems in power network operations. In contrast to the traditional cyber attack minimization techniques, this dissertation proposes a recursive systematic convolutional (RSC) code and KF based state estimation method in the context of smart grids. Specifically, the proposed RSC code is used to add redundancy in the microgrid states, and the log maximum a-posterior decoder is used to recover the state information which is affected by random noises and cyber attacks. Once the estimated states are obtained, an SDP based optimal feedback controller is proposed to regulate the system states. Test results show that the proposed approach can accurately mitigate the cyber attacks and properly estimate and regulate the system states.

- Environment-friendly wind turbine is described as a state-space framework, and the system measurements are obtained at EMS under unreliable communication links. In order to know the wind turbine operating conditions, an adaptive-then-combine distributed dynamic state estimation algorithm is proposed. After locally estimating the system states, the global estimator combines local estimation results through a set of weighting factors. The weighting coefficients are determined by minimizing estimation error covariances based on SDP. Convergence of the proposed approach is

analyzed based on the Lyapunov approach. The analysis is significantly important for validation of the algorithm and simulation results.

- The distribution power sub-systems are usually interconnected to each other, so this research investigates the interconnected optimal filtering problem for distributed dynamic state estimation considering packet losses. The proposed estimator is based on the mean squared error between the actual state and its estimate. To obtain the distributed estimation, the optimal local and neighbouring gains are computed to reach a consensus estimation after exchanging their information with the neighbouring estimators. Moreover, the convergence of the developed algorithm is theoretically proved. Afterwards, a distributed controller is designed based on the SDP approach. Simulation results demonstrate the accuracy of the developed approaches.

- The consensus of interconnected optimal filtering problem is further extended considering only the consensus step. The consensus of the developed algorithm is proved based on the information form of the discrete-time KF and matrix theory. Simulation results are demonstrated using the interconnected synchronous generators and loads.

- The distributed state estimation algorithm is further modified by considering different observation matrices with both local and consensus steps. The optimal local gain is computed after minimizing the mean squared error between the true and estimated states. The consensus gain is determined by a convex optimization process with a given local gain. Furthermore, the convergence of the proposed scheme is analysed after stacking all the estimation error dynamics. The efficacy of the developed approach is demonstrated using the environment-friendly renewable microgrid and IEEE 30-bus power system.

1.6 Thesis Organisation

The remainder of this thesis is organized as follows.

- Chapter 2 describes the necessity of state estimation for smart grid operations. The literature review for smart grid state estimation and control is presented.

- Chapter 3 presents the least square based centralized KF and H_2 stabilization approach. A microgrid incorporating multiple DERs is modelled, followed by the proposed algorithms. The efficacy of the developed approaches is verified through simulations.

- Chapter 4 describes the cyber attacks protection and optimal feedback control approach. After presenting the microgrid, the observation model and cyber attack process are described. Moreover, the KF based dynamic state estimation is presented. The proposed control technique is derived, followed by the simulation results and discussions.

- Chapter 5 captures the adaptive-then-combine distributed state estimation considering packet dropouts. After representing a community resilient wind turbine state-space model, an adaptive-then-combine diffusion algorithm and a weighting factor calculation method are proposed. Convergence of the proposed method is analyzed. The efficacy of the developed approaches is verified through simulations.

- Chapter 6 presents the distributed estimation and stabilization algorithms for interconnected systems over a lossy network. First of all, the proposed algorithm is derived and its stability analysed. Then the proposed distributed controller is designed. Finally, the distribution power system including microgrid and the numerical simulations are demonstrated.

- Chapter 7 describes the convergence of distributed estimation for the discrete-time systems. An interconnected network with multiple synchronous generators and its state-space model are illustrated. Afterwards, the proposed algorithm is derived and its convergence is analysed. The efficacy of the developed approaches is verified through simulations.

- Chapter 8 proposes the distributed state estimation algorithm by considering different observation matrices with both local and consensus steps. The convergence of the proposed algorithm is analysed after stacking all the estimation error dynamics. The efficacy of the developed approach is demonstrated using the environment-friendly renewable microgrid and IEEE 30-bus power system.

- Chapter 9 concludes the thesis with a summary of the original contributions and future work.

Chapter 2

Literature Review for Smart Grid State Estimation and Control

2.1 Introduction

The smart grid is a two-way flow of electricity and information between energy producers and consumers, which provides a widely-distributed and automatedly controlled energy delivery network [64]. By exploiting two-way communications, it becomes possible to replace the current power system with more intelligent infrastructures [65]. Therefore, the smart grid is seen as a modernization of both transmission and distribution power grids with the features of self-awareness, self-organisation and self-recovery [39, 65]. The main characteristics of a smart grid are illustrated in Fig. 2.1.

The smart grid is based on the development of communication infrastructures incorporated into the electrical grid to enhance the information exchange and achieve a fully-automated energy management system. From this point of view, the smart grid architecture is divided into four dominant layers: physical power layer, power control layer, communications layer and application layer [2]. The system architecture for the smart grid paradigm is demonstrated in Fig. 2.2. The physical power layer includes the power generation unit, transmission systems (delivering power from the plants to the substations) and distribution systems (delivering power from the substations to the consumers). The power control layer involves advanced sensing technologies, measurement devices, controls and monitoring equipment,

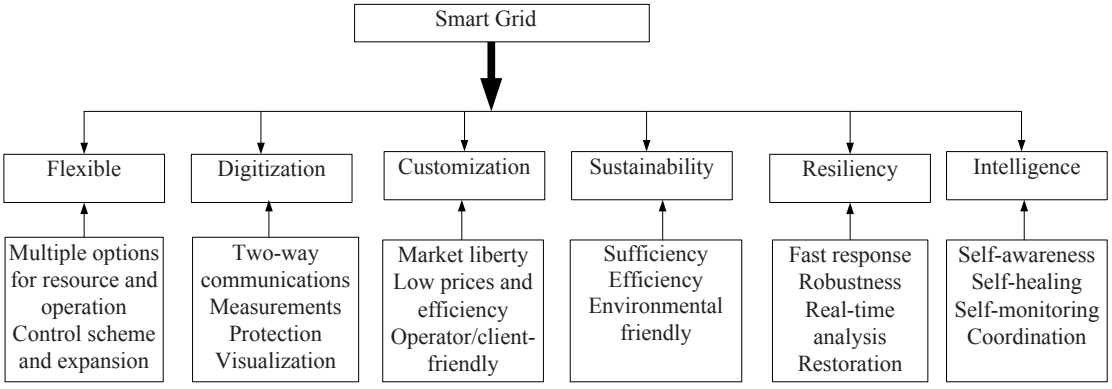

Figure 2.1: The main characteristics of a smart grid.

such as smart sensors, phasor measurement units, SCADA and actuators. The communications layer provides reliable, secure and effective information exchange between the layers. Lastly, the application layer supports all of the services provided to the end customers and utilities, such as automated metering and broadband access [65], [2].

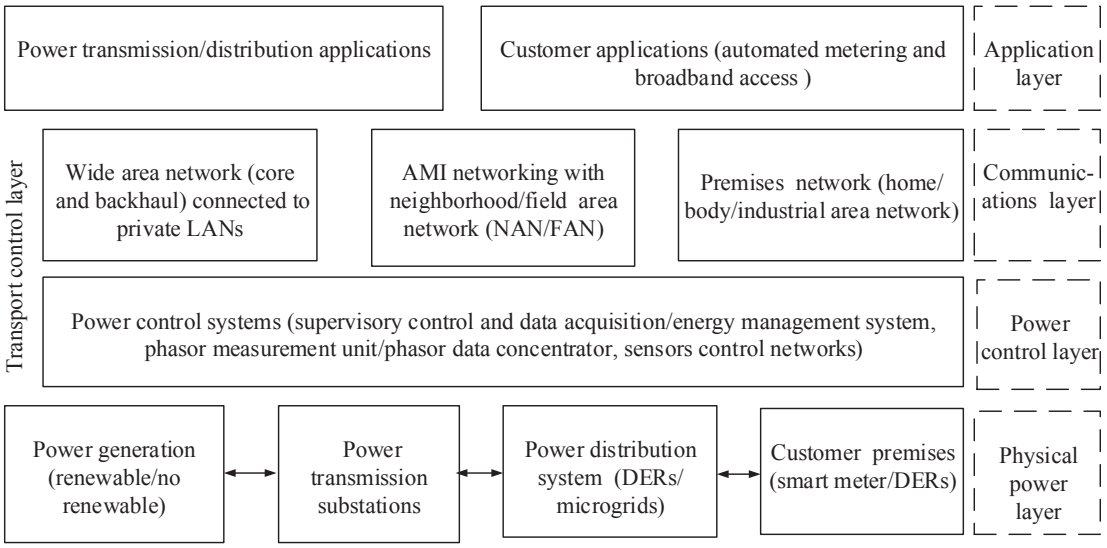

Figure 2.2: System architecture for the smart grid paradigm [2].

Furthermore, the communications layer has premises networks, neighborhood/field area network (NAN/FAN) and wide area network (WAN). The premises network, such as the home area network (HAN), building area network (BAN) and industrial area network (IAN), provides access to applications in the customer premises [66]. The NAN/FAN provides a rel-

atively long-distance communication link between smart meters, field devices, DERs, customer premises' networks and WAN. The WAN provides very long-distance communication links between the grid and the utility via a core network and FAN/NAN. However, the coverage area and data rate requirements for the customer premises' network, FAN/NAN and WAN vary for different communication standards (wired and wireless) and protocols. To illustrate, Fig. 2.3 shows different communication standards and protocols of a smart grid. The wireless communications are easier to deploy (especially in remote areas), more flexi-

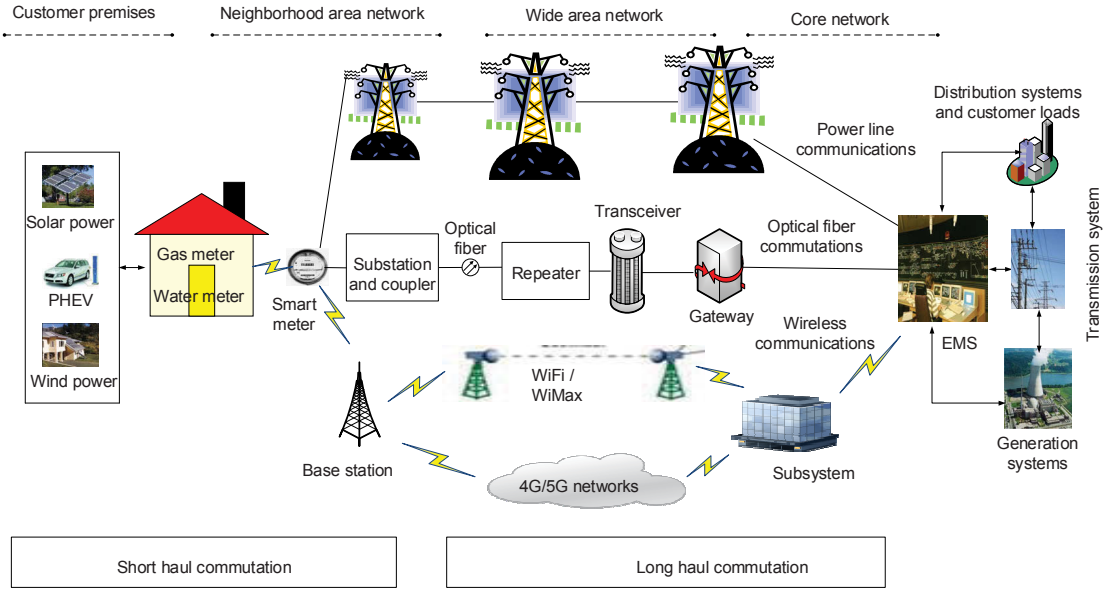

Figure 2.3: Different communication standards and protocols of a smart grid [4].

ble and portable than wired networks, such as power line communication (PLC) and optical fiber communication [2]. However, the security, reliability and power consumption are the main problems for this network [67]. In order to get the benefits of the future smart grid, the signal processing research community is trying to develop channel coding based communication technologies so that the smart grid becomes more intelligent, reliable, secure and user friendly [9], [68] [69].

2.2 Role of State Estimation and Controller in Smart Grids

The state variable defines the system's operating conditions of a power system such as bus voltage, branch current and power [70]. According to [22], the power system may move

into one of four possible states such as normal state, emergency state, in extremis state and restorative state, as the operating conditions change due to an unexpected event. In the nor-

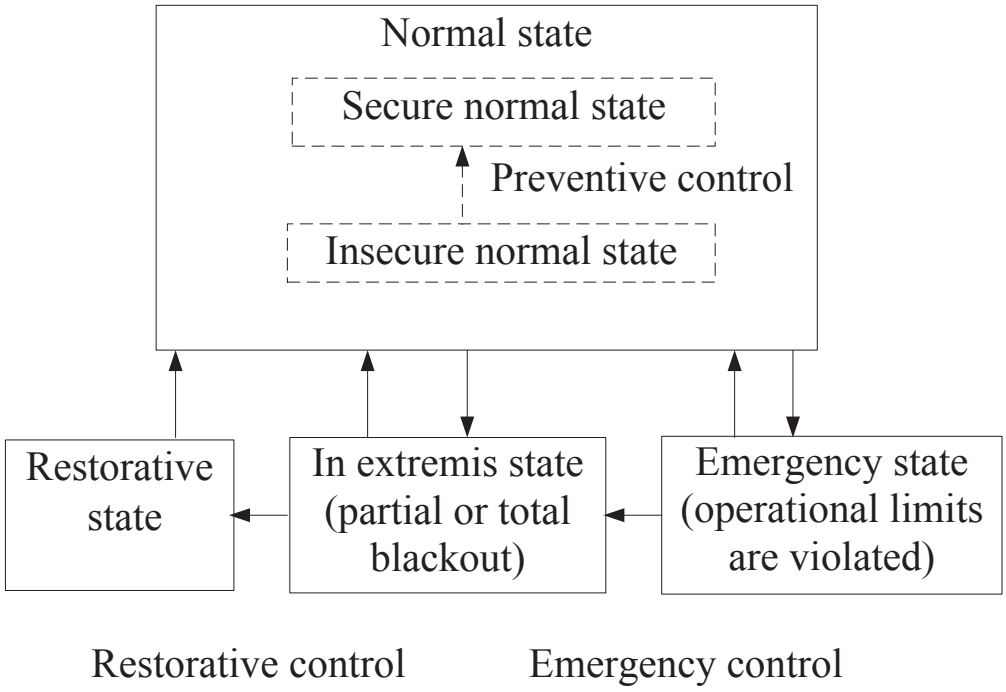

Figure 2.4: State diagram for smart grid operations [5].

mal secure state, a power system satisfies the energy demand of all clients without violating any operational constraints (all state variables are within the normal range). Otherwise, the normal state is classified as an insecure state when some important quantities (line currents or nodal voltages) exceed their operational constraints but the power system is still intact and supplies its clients. Overall, in the event of insecure, emergency and extremis cases, the utility company will take necessary action to restore the system to normal secure state [22], [71]. Otherwise, the system will blackout. In the USA 2003, about 50,000,000 people had their power interrupted and numerous plants shut down due to the nonreal-time information to monitor the power plant [72].

One of the important features of smart grid is that it can integrate the multiple DERs into the main grid. The distributed generation such as microturbines, photovoltaic cells, biomass, fuel cells, battery systems, solar panel and wind power generations can continue to generate power even when power from a utility is absent [73]. However, significant technical challenges arise in the planning, operation and control of DERs, due to the randomness and

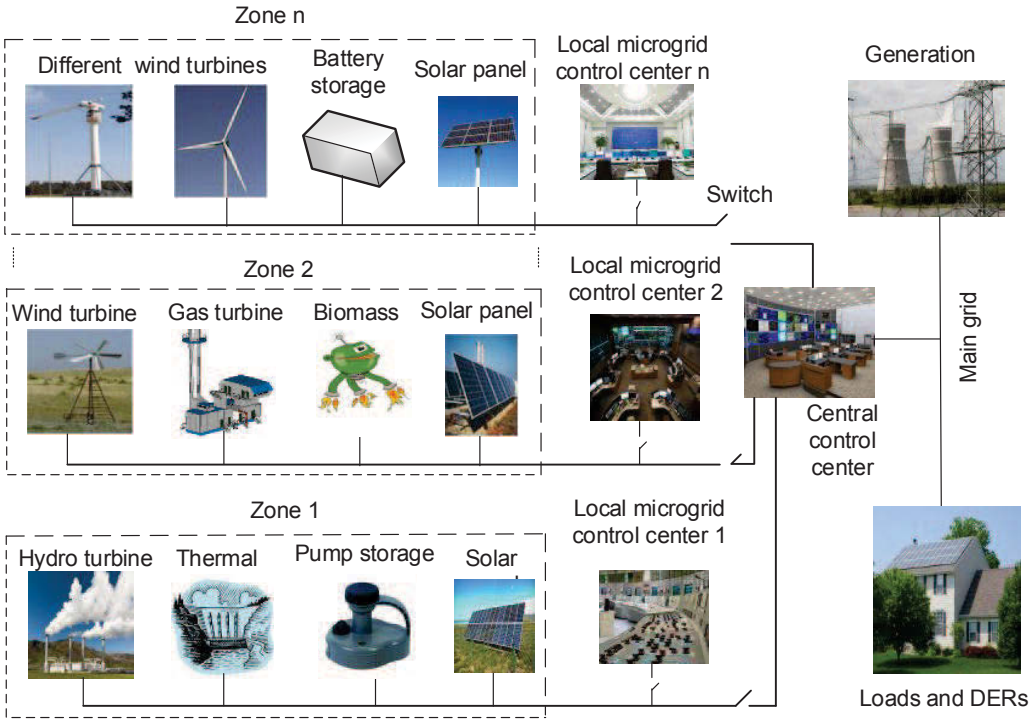

Figure 2.5: Integration of the multiple DERs and today's control center.

weather-dependence in the power generation [56]. Considering these factors, DERs need to monitor from the distribution level. Figure 2.5 shows the integration of the multiple DERs and todays centralized and distributed control centers. Interestingly, the bidirectional smart grid communication between the microgrid and the control center can be leveraged to facilitate smart grid state estimation problems [58].

In order to know the operating conditions of a power system, the utility company deploys many sensors in the substation levels. Substations are equipped with devices called remote terminal unit or intelligent electronic device which collect various types of measurements from the field. These devices are responsible for transmitting the sensing information from the DER to the control centre [22], [5]. In the control centre, the information is fed to a state estimator program for further analysis as shown in Fig. 2.6. The estimation is passed to the energy management system (EMS) applications such as the load forecasting, contingency analysis, power flow analysis and stability analysis [74], [75], [76]. The state estimation also allows the determination of power flows which are not directly metered. So, the state estimation provides a snapshot of the power system from the available measurements [77], [78]. Generally, the knowledge of the system states is necessary to apply the control strategy

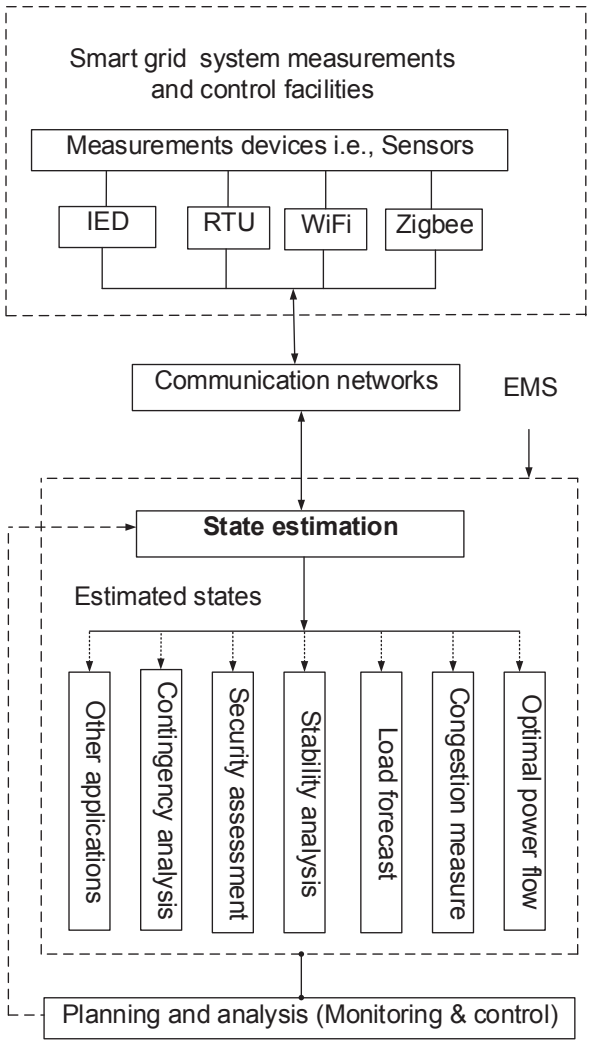

Figure 2.6: Role of state estimation in smart grid operations.

for grid stabilization. Before going to design EMS, the state-of-art smart grid state estimation and stabilization approaches will need to know in advance.

Research has been conducted on the smart grid state estimation in a centralized or distributed way. The centralized estimation means that the EMS uses all measurements from the local sensors to obtain a global estimation [46], [42], [43], thus demanding huge communication and computation resources for processing all measurements. On the other hand, the distributed system can process the subset of sensing information in a distributed way leading to a very effective strategy for performing the wide-area distributed computation [44], [45]. Sometimes the measurement information may be lost in the communication channel due to

fading, link failure, packet dropouts and delays [38]. After estimation, the state feedback controller is necessary for proper operation and maintaining the grid stability. Driven by this motivation, the literature review for the centralised and distributed state estimation with ideal and lossy channel is presented first, followed by the state feedback controllers.

2.3 Centralised State Estimation Over an Ideal Channel

The centralised state estimation over an ideal channel means the EMS processes all available measurements to estimate the system states, which are disturbed by noises only. In other words, there are no measurement losses due to communication impairments such as packet losses, cyber attacks, link failures and delays.

There are many algorithms and tools that have been adopted for smart grid centralised state estimation over an ideal communication channel. To begin with, the static state estimators are widely used in power systems, which rely on a single set of measurements [79]. In order to regularly estimate the system states, this process is repeated at suitable intervals of time [80], [81], [82]. Interestingly, the first step toward the dynamic estimator is taken by Debs and Larson in [83], where a simple state transition model is considered. It is assumed that the power system is a quasi-static scheme, and the states change slowly with time. It provides a better performance; however, it requires an accurate dynamic model and incurs relatively more computational complexity. In multi-area power systems, several different estimation stages are used [79]. In local state estimation stages, the estimators gather measurements from the system and estimate the states, which are shared with the neighbouring local estimators. Next, the global estimator combines the local estimation information and re-calculates the system states [84], [85]. In order to know the system states, the specific algorithm needs to be known, which is discussed in the following paragraphs.

Power system state estimation frequently uses the weighted least squares (WLS) method that minimizes the sum of the squares of the weighted residuals [86]. The main problem of the WLS method is that the gain matrix may be ill-conditioned. Thereby, the solution may fail to converge, and system states cannot be obtained accurately [87], [77]. The numerically ill-conditioned problem is successfully solved by the trust region method with quadratic regulation factorization, but the convergence problem still exists [88]. Besides, the estimation

process of telemetering measurements is treated individually as an additional constraint to the WLS method [89]. Then, the constrained minimization problem is solved by the Lagrange multiplier method [90]. In [89], a similar constrained WLS problem is formulated, where the explicit optimization variables are the measurement residuals. In order to overcome the WLS problem, the least mean squares (LMS) and Kalman filter (KF) based iterative algorithms are widely used for power system state estimations.

The LMS based power system state estimation is implemented in [91], [92]. However, it is very difficult to tune the step size parameter of this LMS algorithm. The normalized LMS (NLMS) algorithm is explored for state estimations [91], [93]. This NLMS algorithm normalises the input signal so that the step size parameter guarantees stability of the algorithm. Then, the variable step size based LMS algorithm for system state estimations is proposed in [94], [95]. This method provides an optimum convergence rate, but there is a trade-off between rate and performance. Moreover, an artificial intelligence based dynamic state estimation is presented in [96]. This technique does not require a mathematical dynamic model. However, in stability analysis of large-scale power systems, it is often preferable to have an exact model. From this perspective, the model based KF algorithm is widely used for dynamic system state estimations [97], [20], [98].

A joint state and parameter estimation method in power systems is proposed in [99], [100], but it fails to properly identify any dynamic pattern. The next breakthrough in dynamic state estimation comes from [101], which provides an appropriate state transition model. This model uses a KF and an exponential smoothing algorithm for state forecast [101, 102]. Generally, the KF based state estimation is widely used in the literature and provides a recursive update of the state during system operations. Furthermore, a robust forecast-aided state estimation algorithm is presented in [103], which is considered an alternative form of the KF approach. Moreover, the KF together with the linear quadratic Gaussian (LQG) control method is explored in [55], [104], [105]. To utilize the KF estimator, one needs to specify the initial state values. Due to the lacking of systematic methods for the estimation of initial states, the associated estimation is usually far away from the true states. Fundamentally, the KF is only applied for a linear system, but most of the power system dynamics in the real world are non-linear.

Generally speaking, the extended KF (EKF) and unscented KF (UKF) algorithms are commonly used in the literature for non-linear power systems. In [106], the EKF based state

estimation process is applied to a fourth-order synchronous generator. In [107], the fault tolerant EKF based state estimation framework is proposed with the application to smart grids. It shows that when the system is highly non-linear, the linear prediction is not appropriate [108]. In other words, the main drawback of EKF is that it will need linearized system parameters such as partial derivative of the state transition matrix. Apart from the difficulty of obtaining derivatives for a large-scale power system, if the initial state estimation is wrong, the filter error may diverge. To deal with these shortcomings, the fractional order EKF is used for estimating the system states, whereby fractional order partial derivatives can be employed [109], [110]. In order to avoid the calculation of Jacobians, the UKF based power system state estimation is explored in [106], [111], [112], and it shows that the UKF preserves high-order estimation accuracy compared with the EKF. This improvement is due to the fact that the UKF calculates the mean and covariance of state variables accurately that undergo a non-linear transformation [113], [112]. The aforementioned techniques are suitable for the non-linear power systems with the Gaussian distribution noises.

The particle filter (PF) is adopted for power system state estimations, which can be applied in non-linear and non-Gaussian systems [114], [23]. Generally, the PF computes the prior and posterior probability density functions based on measurements with particle weights [114], [115]. When a new measurement is available, the probabilities can be updated by changing the values and weights of the particles through Monte Carlo simulation [23]. Specifically, the PF based scheme to estimate the phase angle of the utility grid in the presence of voltage unbalance and frequency variation is proposed in [116]. It shows that the PF provides better performance compared with the EKF as the power system states are highly non-linear, while their reverse performance results are reported in [117]. Moreover, the modified PF is employed in [114] for permanent magnet synchronous machine flux linkage estimations. In this scheme, the prior and posterior probability density functions are approximated by the set of particle weights, and the weight of the particles are then adjusted based on the modified probabilities. Furthermore, the hybrid particle swarm optimization algorithm is developed in [118]. The method is tested on standard IEEE 13 and 123-bus unbalanced test systems, and it indicates that the hybrid particle swarm optimization algorithm outperforms the WLS approach. In addition, the PF approach to dynamically estimate the states of a synchronous generator in a multi-machine setting is presented in [119], [120]. Interestingly, a comparison between the PF, EKF and UKF is provided in [23], and it demonstrates that the PF captures the transient responses of the dynamic states more accurately than the UKF

and EKF. Unfortunately, the PF requires a higher computational complexity. Fortunately, the signal processing research community is trying to add a new flavour in the smart grid state estimation by introducing different message passing algorithms.

From the signal processing point of view, the belief propagation (BP) based static state estimator for the IEEE 4-bus distributed system is proposed in [121]. However, the system states continuously change over time. In fact, the BP algorithm for unregulated dynamic state estimation for a virtual microgrid is proposed in [9]. Unfortunately, the computational complexity of the BP approach is very high, even though the performance is almost the same as KF at a high signal-to-noise ratio. A comparison between the EKF and nonparametric BP (NBP) has been investigated for dynamic state estimation [122]. Basically, the sum-product message passing algorithm to estimate the system state is developed, showing that the performance of the NBP is better than that of the EKF algorithm. In [123], [124], a factor graph based message passing algorithm for power system state estimation is presented. Actually, the factor graph consists of variable and factor nodes. Typically, the factor nodes are the logical representation of the sensor observation information, whereas the variable nodes do not exist physically [123]. Usually, the message can be processed and passed between the variable and factor nodes with certain sum-product rules [123], [124]. A BP algorithm has interesting structural properties corresponding to non-linear feedback dynamical systems in the context of decoding the received signal [125]. Overall, the BP based statistical estimation techniques can provide a better performance if there is no loop in the graph [126]. In other words, this algorithm can converge to the true system states in the Bayesian tree like structure. When loops are present in the graph, the algorithm may cause oscillation and the estimated state may diverge from the true state [126], [127].

Overall, most of the existing smart grid state estimation techniques are centralised in the literature [128], [129]. This means, a huge amount of state information is collected and processed at the central state estimation unit. This not only causes communication and computational burdens but also creates a possibility for central point failure leading to massive blackout [128], [130]. For this reason, the distributed estimation approaches are a striking alternate as they may need less communication bandwidth and allow parallel processing [131].

2.4 Distributed State Estimation Over an Ideal Channel

In order to estimate the system states, various distributed state estimation algorithms and tools have been proposed in the literature. To begin with, the hierarchical two-level static state estimation is proposed in [132]. Afterwards, the two-level state estimation for multiarea power systems is studied in [133], [134], [135]. These approaches use a conventional WLS in a distributed way. Moreover, a brief literature survey for system decomposition techniques can be found in [136]. Next, a survey of multiarea state estimation is given in [137]. Different types of multilevel computation and communication architectures are described for large-scale interconnected power systems. Particularly, the distributed state estimation method for multiarea power systems is presented in [138]. Each area performs its own state estimation based on the local information and exchanges the border information with a global state estimator. Next, a fully distributed modified coordinated state estimation (MCSE) algorithm is proposed for interconnected power systems [130]. This static MCSE method estimates the entire system state information and communicates their estimation results with pre-specified neighbouring areas. The idea is then extended in [139], where a fully distributed Gauss-Newton algorithm for power system state estimations is presented. In this framework, the matrix-splitting techniques are utilized to carry out the matrix inversion required for the Gauss-Newton iteration.

Interestingly, the distributed KF (DKF) has received considerable attention in the smart grid research community. In [48], the distributed hierarchical structure is provided in which the local state estimation is computed independently by the local KF at each sensor node. In [128], the distributed extended information filter and unscented information filter are considered for condition monitoring of power transmission and distribution systems. Here, the local estimated states and covariance matrices are fed to an aggregator filter. The performance of the method totally depends upon the covariance matrices with the assumption that each measurement is similar. However, in practice, the measurement for each local KF is different and these big covariance matrices lead to a large communication burden. Next, the DKF with a weighted averaging method is adopted in [140], which requires the global information of the state error covariance matrix.

Recently, the consensus based DKF methods have been proposed for sensor networks, where the local observations are exchanged with neighbours in order to get the global state estima-

tion [141], [51], [142]. The DKF algorithm in [141] consists of micro-Kalman filters and each is embedded with a low-pass and a band-pass consensus filter, while in [50] a micro-filter architecture with identical high-pass consensus filters is proposed for the sensors with different observation matrices. It is assumed that each sensor node can communicate its measurement, covariance information and output matrix with its neighbours [50]. Then, a trust based DKF approach to state estimation in power systems is proposed in [143]. This method uses an accuracy dependent consensus step in the standard KF steps. Generally, this method imposes the requirement of intermediate averaging among subsystems that leads to additional communication burden [144]. Moreover, the distributed information consensus filter for simultaneous input and state estimation is explored in [145]. However, the calculations of gain and error covariance in all preceding methods are based on the suboptimal filter.

Different from the consensus approaches, the diffusion strategy is widely used in the literature, where the estimates are linearly combined using a set of weights [52], [53]. This method is more practical when dealing with dynamic systems where new measurements must be processed in a timely manner instead of running consensus [146], [147]. However, finding the optimal combination of weights is one of the important problems for enhancing the estimation performance. To do so, the Metropolis optimal weights are generally chosen to yield fast consensus, and it is a strong candidate for distributed consensus. Therefore, it requires knowledge of the local topology to get a faster mixing with the guaranteed convergence of average consensus [148]. Generally speaking, the local state estimators are interconnected with each other, so there are cross-covariances between them. Considering this factor in an aggregator filter, it can play an important role in improving the estimation performance. To achieve a better performance, the diffusion KF based covariance intersection is investigated in [149], [150], [151]. Moreover, the diffusion EKF based covariance intersection for power system state estimations is explored in [128]. Finally, the diffusion LMS based distributed static state estimation is proposed in [152], [153]. However, the system states continuously change over time, so the static estimation may not be suitable. Moreover, in the aforementioned methods, it is assumed that communication is perfect and convergence is not analysed.

While diffusion KF gives the best estimation for white Gaussian noises, it may not produce good estimation if the noise is not Gaussian distributed. If the statistical information of the noise is not known, the H_∞ filtering approach is useful [154], [155]. Essentially, it minimizes

the H_∞ norm between the estimation errors and disturbances. First of all, the distributed H_∞ robust filtering approach is proposed in [156]. In this scheme, the gradient descent type algorithm is presented, which allows the nodes to be estimated system states in a decentralized manner. The sufficient condition to guarantee the suboptimal level of disagreement of estimates is also derived. The idea is then extended in [157], where state estimator is designed based on a set of coupled LMIs, which are computed in a decentralized fashion. In [158], presents the H_∞ based Round-Robin interconnection protocol for distributed observers. The designed scheme allows one to use sampled-data communications between the observers in the network, and does not require a combinational gain scheduling. Consequently, the observers are shown to be capable of achieving the H_∞ consensus with their neighbors. In [159], describes a distributed filtering algorithm by utilizing an H_∞ minimum-energy filtering framework to design the constituent filters. The algorithm employs a decoupled computation of the individual filter coefficients. Finally, the distributed implementation of the PF is presented for state estimation in large-scale interconnected power systems [160].

The smart grid can provide an efficient way of supplying and consuming energy by providing two-way energy flow and communication [11]. The associated connectivity and advanced information/communication infrastructure make the smart grid susceptible to cyber attacks and packet dropouts [11], [161]. These types of catastrophic phenomena are much easier to be committed in microgrids, so they create much more serious problems in the smart grid compared with the traditional grid [60]. Therefore, the system state estimation under cyber attacks and packet losses for smart grids have drawn significant interest in the energy industry and signal processing based information and communication societies.

2.5 State Estimation Considering Cyber Attacks and Packet Dropouts

Many studies have been carried out to investigate the cyber attacks in smart grid state estimations. To begin with, most of the state estimation methods use the WLS technique under cyber attacks [162], [163], [164]. Chi-Square detector is also used to detect those attacks. Even though this approach is easy to be implemented for non-linear systems, it is computationally intensive and does not eliminate the attacks properly [162], [3]. To this end,

the WLS based l_1 optimization method is explored in [165]. Furthermore, a new detection scheme to detect the false data injection attack is proposed in [166]. It employs a Kullback-Leibler method to calculate the distance between the probability distributions derived from the observation variations. A sequential detection of false data injection into smart grids is investigated in [161]. It adopts a centralized detector based on the generalized likelihood ratio and cumulative sum algorithm. Note that this detector usually depends on the parametric inferences, so it is inapplicable for nonparametric inferences [166]. A SDP based AC power system state estimation is proposed in [167]. Thereafter, the KF based microgrid energy theft detection algorithm is presented in [60].

A lot of efforts have been devoted towards the power system state estimation under the condition of unreliable communication channels. Generally, the attackers have limited attacking energy to jam the channel in order to achieve the desired goals [168]. So, the sensor data scheduling for state estimation with energy constraints is studied in [169]. In this research, the sensor has to decide whether to send its data to a remote estimator or not based on its energy and estimation error covariance matrix. This idea is further extended in [170], where both the sensor and attacker have energy constraints for sending information and attacking the system. The considered attack is on the communication channel between a sensor and a remote estimator. Basically, the sensor aims to minimize the average estimation error covariance matrix, while attackers try to maximize it. So, an iterative game theory is used to solve the optimization problem. Due to the motivation of unknown attacking patterns, authors in [168], [171] investigated how the attacker can design the attacking policy so the estimation performance can be deteriorated. Then the average estimation error covariance based optimal scheduling strategy is proposed to avoid such kind of attacks.

Generally speaking, the sensing measurements are affected by communication impairments when they are transmitted through an unreliable communication network [37]. The unreliable link such as packet losses causes monitoring performance degradation and may give deceiving information to the utility operator [62], [63]. The KF based state estimation via wireless sensor networks over fading channels and missing measurements are presented in [172], [20]. Hence, the packet losses are considered as another form of power system contingency which may lead to a massive blackout if suitable actions from the operator are not taken on time. Moreover, the EKF algorithm for power system state estimation considering the missing measurements is proposed in [173]. In this scheme, the measurements are treated as inequality constraints on the states with the aid of the statistical criterion, and the

estimation problem is solved by the particle swarm optimization scheme. The LQG control strategy under the condition of packet losses is presented in [20]. This networked control system is suitable for the centralized state estimation and its stability analysis for Markovian jump systems. Usually, the system state information is unavailable, so the estimation with controller design remains an open question in the signal processing, control and smart grid communities.

2.6 Feedback Controllers

Many state feedback centralised controllers have been proposed to regulate the system. First of all, a classic LQG controller for the power system is proposed in [20], [105], [174]. This controller is comprised of an LQ regulator and a KF that minimizes the error between the output signals and their estimations. Then the cooperative control problem of AC microgrids is proposed in [175]. This method uses a feedforward approach which only requires local state measurements and reference signals from neighbors. Furthermore, an output voltage differential feedback and output current differential feedforward control strategy is presented in [176]. This technique eliminates the output voltage steady-state errors so that it can improve dynamic system response under different load disturbances. Following that an adaptive sliding mode based robust control scheme for a multi-bus islanded microgrid is recommended in [177]. This method is performed based on local measurements and is designed independently from topology, parameters, and dynamics of the microgrid loads. Interestingly, three types of H_∞ based centralised feedback controllers, namely static output feedback controllers, dynamic output feedback controllers, and observer based output feedback controllers are investigated for linear discrete-time systems in [178]. The controller synthesis in discrete-time linear systems with uncertainty is explored in [179]. Moreover, the model predictive control (MPC) for grid connected converters is illustrated in [180], [181]. However, MPC requires a large computational complexity leading to a considerable time delay in the actuation. In [182], [183], [184], the controllers are designed using partial feedback linearization which can partially linearize the system and enable the controllers design scheme for reduced-order systems. The full-order nonlinear observer based excitation controller is designed for interconnected power systems in [185].

There are several state feedback algorithms that consider the communication impairments.

The LQG networked control strategy under the condition of packet losses is presented in [20]. Furthermore, the LQG based detecting techniques for cyber integrity attacks on the sensors of a control system is proposed in [168], [186]. It shows that the residual error based chi-squared detection technique is not suitable when the attacker does not know the system dynamics. Based on this analysis, they consider the cyber attack model as an i.i.d (independent, identically distributed) Gaussian distribution, then the LQG objective function is modified. At the end, they developed a sufficient condition to detect the false alarm probability and proposed an optimization algorithm to minimize it. In [187], a new strategy is recommended for designing a communication and control infrastructure in a distribution system based on the virtual microgrid concept. It is shown in [188], [189] that designing a state feedback control framework for a general case of polynomial discrete-time system is quite challenging because the solution is non-convex. Recently, the time-delay switch attack based on the simple proportional integral derivative (PID) centralized controller is adapted in the context of smart grids [190]. It is considered that delays can be introduced in the sensing loop or control lines so the packet may be lost. In order to reduce the computation cost, the distributed feedback controller is gaining significant interest in the smart grid community.

Each controller only communicates information with its neighbours in the distributed control strategy [44], [45]. Recently, a unified distributed control strategy for the DC microgrid is proposed in [21]. It shows that the standard distributed PI controllers are no longer able to regulate the average DC microgrid bus voltage, so the distributed voltage controllers are replaced by double integrator controllers. In addition, the distributed MPC for a class of discrete-time Markovian jump linear systems is presented in [191]. Moreover, the H_∞ and H_2 based distributed controllers for identical dynamically coupled systems are proposed in [192]. In this framework, it assumes that the state-space model satisfies a certain structural property. In order to avoid the higher state feedback gain, a sub-optimal H_∞ controller is proposed in [193]. Due to the simplicity and easy implementation point of view, the static state feedback controller is preferred in discrete-time systems.

2.7 Summary

This chapter has presented a comprehensive literature review for smart grid state estimations and its applications to grid stabilization. After presenting the smart grid features, the avail-

able communication infrastructure is illustrated. The state-of-art literature review for smart grid state estimations and stabilization approaches are presented. Specifically, different kind of state estimation algorithms such as WLS, LMS, KF, EKF, UKF, PF, DKF as well as H_∞, and their advantages as well as disadvantages are discussed. Then the LQG, PID, MPC, H_2 and H_∞ controllers, and their benefits as well as drawbacks are presented. In the following chapter, the smart grid state estimation and H_2 based centralised feedback controller is proposed and verified.

Chapter 3

Least Square Based Centralized KF Algorithm and H_2 Controller

3.1 Introduction

Given the significant concerns regarding carbon emissions from fossil fuels, global warming and the energy crisis, renewable distributed energy resources (DERs) are going to be integrated in smart grids, which will make the energy supply more reliable and decrease the costs and transmission losses. However, significant technical challenges arise in the planning, operation and control of DERs, due to the randomness and weather-dependence in the power generation patterns [56], [58], [57]. Interestingly, the bidirectional communication between the microgrid and control center can be leveraged to facilitate state estimation and stabilization problems [58]. Based on information and communication technologies, the smart grid can spread the intelligence of the distribution system from the central unit to long-distance remote areas, thus enabling accurate state estimation and wide-area real-time monitoring of intermittent renewable energy sources [39] [194]. The power system state estimation commonly uses the weighted least squares technique that minimizes the sum squares of weighted residuals, but the gain matrix may be ill-conditioned [47]. Furthermore, a minimum mean squared error based optimal state estimation in the context of smart grids is studied in [195]. Moreover, the KF together with the simple linear-quadratic-Gaussian controller is presented in [55], [104], [105]. To utilize the KF estimator, one needs to specify the initial state val-

uess. Due to the lacking of systematic methods for the initial state estimation, the initial estimation is usually far away from the true initial states. In [187], a new strategy is recommended for designing a communication and control infrastructure in a distribution system based on the virtual microgrid concept. It is shown in [188], [189] that designing a state feedback control framework for a general case of polynomial discrete-time system is quite challenging because the optimization problem is non-convex. On the other hand, the convex optimization based controller design has gained growing interest in the research community.

This chapter proposes a least square based centralised KF algorithm and a H_2 feedback controller for microgrid state estimation and stabilization. A microgrid incorporating multiple DERs is modelled as a discrete-time linear state-space equation where sensors are deployed to obtain state information. In order to transmit the sensing information to the control center, a smart grid communication infrastructure is proposed. The proposed communication system provides an opportunity to address the state regulation challenge by offering two-way communication links for microgrid information collection, estimation and stabilization. Based on the communication infrastructure, this study proposes a least square based KF algorithm for state estimation and a H_2 feedback control framework for stabilizing the microgrid states. The efficacy of the developed approaches is demonstrated using a microgrid incorporating multiple DERs.

3.2 Microgrid and Distributed Energy Resources

A microgrid incorporating DERs is a small-scale power generation unit that is used to deliver an alternative to or an enhancement of the traditional electricity network. So, the typical microgrid can be described as a cluster of DERs and local loads. The micro-sources such as photovoltaic panels and wind turbines improve the efficiency of energy supply and reduce the electricity delivery costs and carbon footprint [57], [196]. Generally, the microgrid is capable of operating at either the islanded mode or grid-connected mode. A microgrid has a switch installed at the point of common coupling (PCC) of the utility side [55]. Under abnormal conditions, this switch can be opened in a very short time. In this case, DERs can still supply power for load points in the islanded portion of the distribution network. In the case of grid connected mode, the microgrid is connected to the main grid at the PCC to deliver/receive power to/from the main grid [197]. Therefore, seamless transition is one of

the technical challenges in the microgrid control.

The microgrid is categorized into AC and DC microgrid based on the bus to which the component systems are connected. The main benefit of the AC microgrid is that the existing AC power grid technologies are readily applicable [198]. However, expensive power electronic devices are needed to convert DC to AC. In DC microgrids, there is no need to control the frequency, phase and reactive power [199]. Furthermore, they can minimize the energy losses in the transmission and distribution networks as the green energy is generated near the consumption. Therefore, the DC microgrid is envisaged as a promising building block for future smart power distribution systems specifically in industrial and residential zones such as rural or mountain areas, electric aircraft and ships, data centers and smart buildings [200], [201], [202].

3.2.1 Microgrid Incorporating Multiple DERs

The schematic diagram of an electronically coupled microgrid incorporating multiple DERs is depicted in Fig. 3.1 [6]. There are N interconnected renewable DERs in the microgrid. Similar to [55], [203], [204], [16], this study considers a DC microgrid operating in the islanded mode. It contains multiple DER units connected with each other through a DC distribution line. From Fig. 3.1, it can be seen that the DER is interfaced to the local load through a converter. Each DER is represented by a DC voltage source in series with a voltage source converter (VSC) and a series resistive inductive (RL) filter. The VSC is fed with DC voltage sources representing renewable energy resource such as solar cells, microturbine and photovoltaic systems. For instance, in each DER unit a Buck converter is presented to supply local loads connected to the PCC through an RL filter [203]. This means that the DER unit utilizes a VSC as the coupling medium [6]. The local load is represented by a resistive inductive capacitive (RLC) load at the PCC.

Now based on Kirchhoff's voltage law and Kirchhoff's current law, the dynamics of N DERs

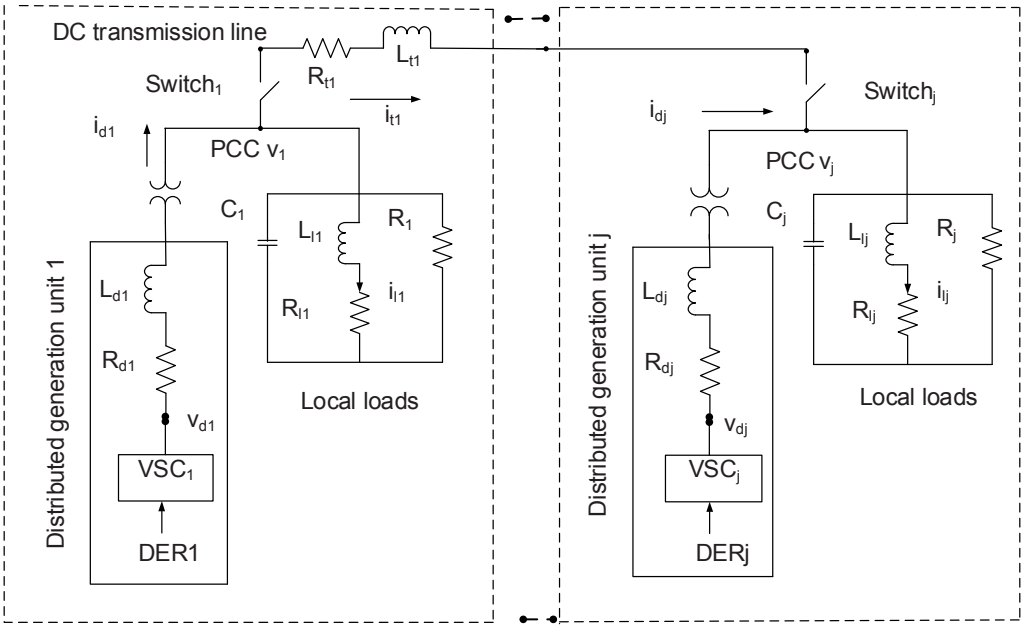

Figure 3.1: Schematic diagram of DC microgrid integrating multiple DERs [6].

can be expressed as follows:

$$\Delta\dot{i}_{lj} = (-R_{lj}\Delta i_{lj} + \Delta v_j)/L_{lj}, j = 1, ..., N. \tag{3.1}$$

$$\Delta\dot{i}_{dj} = (-R_{dj}\Delta i_{dj} - \Delta v_j + \Delta v_{dj})/L_{dj}, j = 1, ..., N. \tag{3.2}$$

$$\Delta\dot{i}_{tj} = (-R_{tj}\Delta i_{tj} - \Delta v_j + \Delta v_{j+1})/L_{tj}, j = 1, ..., N-1. \tag{3.3}$$

$$\Delta\dot{v}_j = -\Delta i_{lj} + \Delta i_{dj} - \Delta i_{tj} - \Delta v_j/R_j)/C_j, \quad \text{if } j = 1. \tag{3.4}$$

$$= [-\Delta i_{lj} + \Delta i_{dj} - \Delta i_{tj} - \Delta v_j/R_j + \Delta i_{t(j-1)}]/C_j, \quad \text{if } j = 2, \cdots, N-1. \tag{3.5}$$

$$= [-\Delta i_{lj} + \Delta i_{dj} - \Delta v_j/R_j + \Delta i_{t(j-1)}]/C_j, \quad \text{if } j = N. \tag{3.6}$$

Here, Δi_{dj},Δi_{tj} and Δi_{lj} are the current deviation of DER_j, transmission line and load, respectively. R_{dj}, R_{tj} and R_{lj} are the resistances of VSC_j filter, transmission line and load, respectively. L_{dj}, L_{tj} and L_{lj} are the inductances of VSC_j filter, transmission line and load, respectively. C_j is the capacitance and Δv_j is the PCC bus voltage deviation. Here, the variables are locally linearized around the operating points $x^\star$, leading to the deviation $\Delta x = x - x^\star$ [55].

For the sake of simplicity and similar to [203], we consider the case that three DERs are connected to one bus acting in the islanded mode of operations. Note that the system in Fig. 3.1 is not restrictive, and can have the general topology, i.e., the method proposed in this

paper is independent of the type and size of microgrids.

3.2.2 Discretisation of the Microgrid State-Space Framework

The above continuous-time system described by (3.1)-(3.6) can be written in the following discrete form:

$$\mathbf{x}(k+1) = \mathbf{A}_d\mathbf{x}(k) + \mathbf{B}_d\mathbf{u}(k) + \mathbf{n}_d(k), \tag{3.7}$$

where $\mathbf{x} = [\Delta i_{l1}\ \Delta i_{d1}\ \Delta i_{t1}\ \Delta v_1\ \Delta i_{l2}\ \Delta i_{d2}\ \Delta i_{t2}\ \Delta v_2\ \Delta i_{l3}\ \Delta i_{d3}\ \Delta v_3]'$, $\mathbf{u} = [\Delta v_{d1}\ \Delta v_{d2}\ \Delta v_{d3}]'$, $\mathbf{A}_d = \mathbf{I} + \mathbf{A}\Delta t$, Δt is the sampling period and $\mathbf{B}_d = \mathbf{B}\Delta t$, $\mathbf{A}$, and $\mathbf{B}$ are given by:

$$\mathbf{A} = \begin{bmatrix}
\frac{-R_{l1}}{L_{l1}} & 0 & 0 & \frac{1}{L_{l1}} & 0 & 0 & 0 & 0 & 0 & 0 & 0 \\
0 & \frac{-R_{d1}}{L_{d1}} & 0 & \frac{-1}{L_{d1}} & 0 & 0 & 0 & 0 & 0 & 0 & 0 \\
0 & 0 & \frac{-R_{t1}}{L_{t1}} & \frac{-1}{L_{t1}} & 0 & 0 & 0 & \frac{1}{L_{t1}} & 0 & 0 & 0 \\
\frac{-1}{C_1} & \frac{1}{C_1} & \frac{-1}{C_1} & \frac{-1}{R_1C_1} & 0 & 0 & 0 & 0 & 0 & 0 & 0 \\
0 & 0 & 0 & 0 & \frac{-R_{l2}}{L_{l2}} & 0 & 0 & \frac{1}{L_{l2}} & 0 & 0 & 0 \\
0 & 0 & 0 & 0 & 0 & \frac{-R_{d2}}{L_{d2}} & 0 & \frac{-1}{L_{d2}} & 0 & 0 & 0 \\
0 & 0 & 0 & 0 & 0 & 0 & \frac{-R_{t2}}{L_{t2}} & \frac{-1}{L_{t2}} & 0 & 0 & \frac{1}{L_{t2}} \\
0 & 0 & \frac{1}{C_2} & 0 & \frac{-1}{C_2} & \frac{1}{C_2} & \frac{-1}{C_2} & \frac{-1}{R_2C_2} & 0 & 0 & 0 \\
0 & 0 & 0 & 0 & 0 & 0 & 0 & 0 & \frac{-R_{l3}}{L_{l3}} & 0 & \frac{1}{L_{l3}} \\
0 & 0 & 0 & 0 & 0 & 0 & 0 & 0 & 0 & \frac{-R_{d3}}{L_{d3}} & \frac{-1}{L_{d3}} \\
0 & 0 & 0 & 0 & 0 & 0 & \frac{1}{C_3} & 0 & \frac{-1}{C_3} & \frac{1}{C_3} & \frac{-1}{R_3C_3}
\end{bmatrix},$$

$$\mathbf{B} = \begin{bmatrix}
0 & \frac{1}{L_{d1}} & 0 & 0 & 0 & 0 & 0 & 0 & 0 & 0 & 0 \\
0 & 0 & 0 & 0 & 0 & \frac{1}{L_{d2}} & 0 & 0 & 0 & 0 & 0 \\
0 & 0 & 0 & 0 & 0 & 0 & 0 & 0 & 0 & \frac{1}{L_{d3}} & 0
\end{bmatrix}'.$$

The symbol $\mathbf{n}_d(k)$ is the process uncertainties due to discretisation and variations in DERs parameters by the surrounding ambient conditions. The process noise $\mathbf{n}_d(k)$ is the zero mean Gaussian distribution [106], [107], [113] whose covariance matrix is $\mathbf{Q}_n(k)$. For discretizing a continuous-time system into a discrete-time system, there are several techniques available in the literature such as traditional approximation method, delta operator and shift operator [106], [205], [206], [207]. Similar to [106], [207], this study adopts the traditional approximation method ignoring discretization errors.

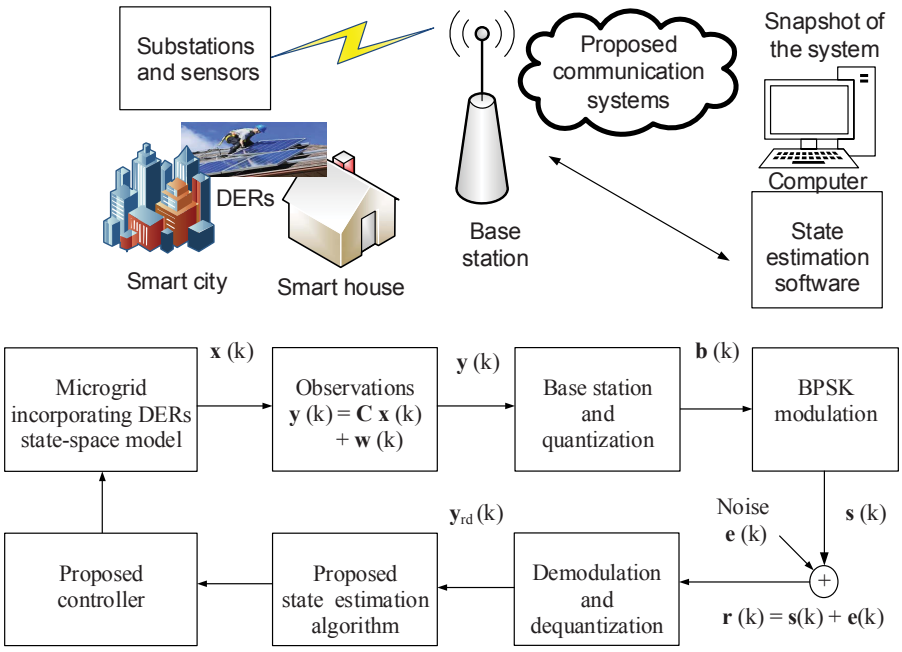

Figure 3.2: The proposed smart grid communication system.

3.3 Proposed Smart Grid Communication Systems

Generally, the communication network brings about new perspectives to energy management systems and covers a diverse range of communication technologies including sensing, networking, information processing and intelligent control technologies [39]. To achieve the goal, the utility company deploys a lot of sensors in the electricity network for monitoring system states [55], [57]. The measurements of the microgrid states are obtained by a set of sensors as follows:

$$\mathbf{y}(k) = \mathbf{C}\mathbf{x}(k) + \mathbf{w}(k), \tag{3.8}$$

where $\mathbf{y}(k)$ is the measurements, $\mathbf{C}$ is the sensing matrix and $\mathbf{w}(k)$ is the zero mean Gaussian distribution [106], [107], [113] whose covariance matrix is $\mathbf{R}_w(k)$. The observation information is transmitted to the nearby base station. After that, the uniform quantizer of this base station maps each observation signal to a sequence of bits $\mathbf{b}(k)$. Then $\mathbf{b}(k)$ is passed through the BPSK, and the modulated signal $\mathbf{s}(k)$ is obtained. To illustrate, Fig. 3.2 shows the proposed communication systems in the context of microgrid state estimation. At the

end, the received signal is given by:

$$\mathbf{r}(k) = \mathbf{s}(k) + \mathbf{e}(k), \tag{3.9}$$

where $\mathbf{e}(k)$ is the additive white Gaussian noise (AWGN). Followed by demodulation and dequantization, the resulting signal is then used for state estimation of the dynamic system.

3.4 Proposed Least Square Based KF Algorithm and H_2 Feedback Controller

This section tries to answer the following questions: (i) What is the optimal smart grid state estimation method for the microgrid incorporating multiple DERs? (ii) Based on the estimated states, what type of feedback control technique is applied for controlling the microgrid states? This section attempts to answer these questions by presenting the least square based KF algorithm and H_2 feedback controller.

3.4.1 Proposed Least Square Based Centralized KF Algorithm

The KF algorithm is a set of mathematical equations that provide an efficient recursive means to estimate the state of a process in a way that minimizes the mean square error (MSE) over time. Moreover, the KF algorithm can use the complete system information including the statistical information of process noise, observation noise, process value and measurement value to obtain the optimal estimation of the DER states. This estimation technique works in two steps: time prediction step and measurement update step. In the prediction stage, the KF estimates the current state variables along with their uncertainties [155]. In the correction phase, the predicted estimation is further updated based on the measurement to get the desired state estimation. In other words, a KF is required to save the DER state values and covariances at the previous step in each estimation process. The energy management system computes the following KF steps as follows [155]:

$$\hat{\mathbf{x}}^{-}(k) = \mathbf{A}_d\hat{\mathbf{x}}(k-1) + \mathbf{B}_d\mathbf{u}(k-1), \tag{3.10}$$

where $\hat{\mathbf{x}}(k-1)$ is the estimate states of the previous step. The predicted estimate covariance matrix is given by:

$$\mathbf{P}^{-}(k) = \mathbf{A}_d\mathbf{P}(k-1)\mathbf{A}_d^T + \mathbf{Q}_n(k-1), \tag{3.11}$$

where $\mathbf{P}(k-1)$ is the estimate covariance matrix of the previous step. The measurement residual $\mathbf{d}(k)$ is given by:

$$\mathbf{d}(k) = \mathbf{y}_{rd}(k) - \mathbf{C}\hat{\mathbf{x}}^{-}(k), \tag{3.12}$$

where $\mathbf{y}_{rd}(k)$ is the dequantized and demodulated output bit sequences. The Kalman gain is given by:

$$\mathbf{K}(k) = \mathbf{P}^{-}(k)\mathbf{C}^T[\mathbf{C}\mathbf{P}^{-}(k)\mathbf{C}^T + \mathbf{R}_w(k)]^{-1}. \tag{3.13}$$

The updated state estimation is given by:

$$\hat{\mathbf{x}}(k) = \hat{\mathbf{x}}^{-}(k) + \mathbf{K}(k)\mathbf{d}(k). \tag{3.14}$$

The updated estimate covariance matrix $\mathbf{P}(k)$ is given by:

$$\mathbf{P}(k) = \mathbf{P}^{-}(k) - \mathbf{K}(k)\mathbf{C}\mathbf{P}^{-}(k). \tag{3.15}$$

The equations infer that the amount of output correction is determined by $\mathbf{K}(k)$ which is dependent on the predicted covariance matrix $\mathbf{P}^{-}(k)$ over time. From (3.10), it can be seen that one needs to specify the initial state value $\hat{\mathbf{x}}(k=0)$ to run the KF algorithm. There are no general procedures to estimate the initial state value [208]. In practice, researchers often set $\hat{\mathbf{x}}(0) = \mathbf{0}$ as an estimate of the initial state value [208], [209]. As a result, the initial estimation is usually far away from the true initial state value. To obtain a good initial estimation to reduce the error propagations, this paper adopts a least square estimation method for the KF step [209]. For instance, given that $\mathbf{C}$ is of full row rank, one can obtain the initial state estimation $\hat{\mathbf{x}}(0)$ as follows:

$$\hat{\mathbf{x}}(0) = \mathbf{C}^T(\mathbf{C}\mathbf{C}^T)^{-1}\mathbf{y}_{rd}(0). \tag{3.16}$$

Here, $\mathbf{y}_{rd}(0)$ is the initial observation value. In summary, the flow chart of the proposed estimation algorithm is depicted in Fig. 3.3. After initializing the system parameters, one can obtain the initial state estimation using (3.16). This least square estimation is applied together with the KF algorithm to accelerate the convergence. Then one can compute the predicted state estimation and error covariance matrix. Once the Kalman gain has been determined, the state estimation and covariance matrix are calculated. After estimating the system states, the proposed control method is applied for stabilizing the DER states as shown in the following section.

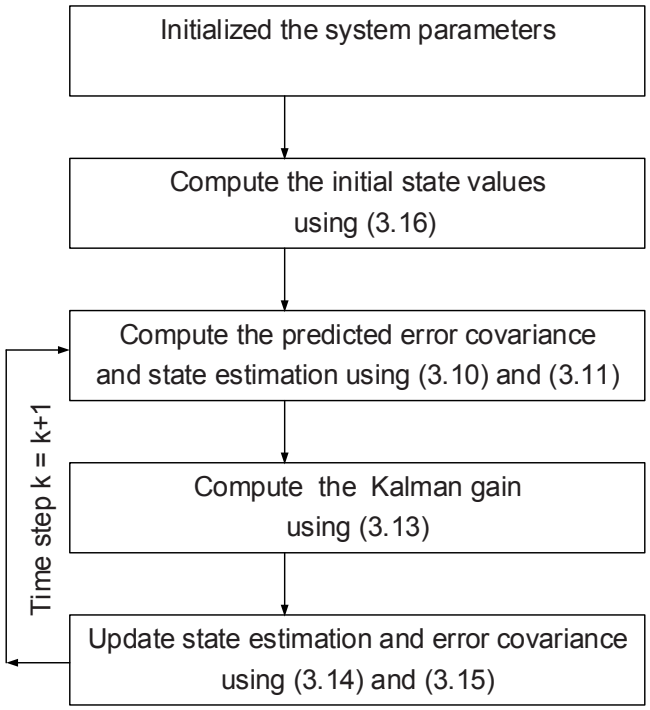

Figure 3.3: Flow chart of the proposed estimation algorithm.

3.4.2 Proposed Centralized H_2 Feedback Controller

According to the separation principle, the feedback control strategy and the state estimator can be designed separately [210, p. 427]. Therefore, it is assumed that $\mathbf{x}(k) \approx \hat{\mathbf{x}}(k)$ for applying the control method as the states are already estimated. In order to regulate the microgrid states, consider the following performance output signal:

$$\mathbf{z}(k) = \begin{bmatrix} \mathbf{Q}_z^{1/2} \\ \mathbf{0} \end{bmatrix} \mathbf{x}(k) + \begin{bmatrix} \mathbf{0} \\ \mathbf{R}_z^{1/2} \end{bmatrix} \mathbf{u}(k), \tag{3.17}$$

where $\mathbf{Q}_z$ and $\mathbf{R}_z$ are strict positive definite matrices. Define the following state feedback control law:

$$\mathbf{u}(k) = -\mathbf{F}\mathbf{x}(k), \tag{3.18}$$

by minimizing the H_2 norm of the closed-loop system [211], [212]. Here, $\mathbf{F}$ is the state feedback gain matrix. For the state feedback (3.18), the closed-loop system is described

by [212]:

$$\mathbf{x}(k+1) = (\mathbf{A}_d - \mathbf{B}_d\mathbf{F})\mathbf{x}(k) + \mathbf{n}_d(k), \tag{3.19}$$

$$\mathbf{z}(k) = \begin{bmatrix} \mathbf{Q}_z^{1/2} \\ -\mathbf{R}_z^{1/2}\mathbf{F} \end{bmatrix} \mathbf{x}(k). \tag{3.20}$$

In order to find the optimal feedback gain, one can search for the feedback gain matrix $\mathbf{F}$ that solves the H_2 norm minimization problem as follows:

$$\text{minimise} \qquad trace[\mathbf{P}], \quad \mathbf{P} > \mathbf{0} \tag{3.21}$$

$$\text{subject to} \qquad \mathbf{P} - (\mathbf{A}_d - \mathbf{B}_d\mathbf{F})^T\mathbf{P}(\mathbf{A}_d - \mathbf{B}_d\mathbf{F}) < \mathbf{Q}_z + \mathbf{F}^T\mathbf{R}_z\mathbf{F}. \tag{3.22}$$

In order to solve the above problem by using semidefinite programming, define $\tilde{\mathbf{P}} = \mathbf{P}^{-1}$. Then (3.21)-(3.22) can be transformed into the following form:

$$\text{minimise} \qquad trace[\tilde{\mathbf{P}}^{-1}], \quad \tilde{\mathbf{P}} > \mathbf{0} \tag{3.23}$$

$$\text{subject to} \qquad (\mathbf{A}_d - \mathbf{B}_d\mathbf{F})^T\tilde{\mathbf{P}}^{-1}(\mathbf{A}_d - \mathbf{B}_d\mathbf{F}) - \tilde{\mathbf{P}}^{-1} + \mathbf{Q}_z + \mathbf{F}^T\mathbf{R}_z\mathbf{F} < \mathbf{0}. \tag{3.24}$$

After the congruence transformation by $\tilde{\mathbf{P}}$, (3.23)-(3.24) can be transformed into the following form:

$$\text{minimise} \qquad trace[\tilde{\mathbf{P}}^{-1}], \quad \tilde{\mathbf{P}} > \mathbf{0} \tag{3.25}$$

$$\text{subject to} \qquad \tilde{\mathbf{P}}(\mathbf{A}_d - \mathbf{B}_d\mathbf{F})^T\tilde{\mathbf{P}}^{-1}(\mathbf{A}_d - \mathbf{B}_d\mathbf{F})\tilde{\mathbf{P}} - \tilde{\mathbf{P}} + \tilde{\mathbf{P}}\mathbf{Q}_z\tilde{\mathbf{P}} + \tilde{\mathbf{P}}\mathbf{F}^T\mathbf{R}_z\mathbf{F}\tilde{\mathbf{P}} < \mathbf{0}. \tag{3.26}$$

By introducing a new variable $\mathbf{X} = \mathbf{F}\tilde{\mathbf{P}}$, (3.26) can be rewritten as follows:

$$(\mathbf{A}_d\tilde{\mathbf{P}} - \mathbf{B}_d\mathbf{X})^T\tilde{\mathbf{P}}^{-1}(\mathbf{A}_d\tilde{\mathbf{P}} - \mathbf{B}_d\mathbf{X}) - \tilde{\mathbf{P}} + \tilde{\mathbf{P}}\mathbf{Q}_z\tilde{\mathbf{P}} + \mathbf{X}^T\mathbf{R}_z\mathbf{X} < \mathbf{0}. \tag{3.27}$$

According to the Schur's complement, (3.27) can be transformed into the following form:

$$\begin{bmatrix} -\tilde{\mathbf{P}} & \tilde{\mathbf{P}} & \mathbf{X}^T & \tilde{\mathbf{P}}\mathbf{A}_d^T - \mathbf{X}^T\mathbf{B}_d^T \\ \tilde{\mathbf{P}} & -\mathbf{Q}_z^{-1} & \mathbf{0} & \mathbf{0} \\ \mathbf{X} & \mathbf{0} & -\mathbf{R}_z^{-1} & \mathbf{0} \\ \mathbf{A}_d\tilde{\mathbf{P}} - \mathbf{B}_d\mathbf{X} & \mathbf{0} & \mathbf{0} & -\tilde{\mathbf{P}} \end{bmatrix} < \mathbf{0}. \tag{3.28}$$

If the term $\tilde{\mathbf{P}}^{-1}$ in (3.25) is replaced by $\mathbf{S}$, the above optimization problem can be formulated as follows:

$$\text{minimise} \qquad trace[\mathbf{S}] \tag{3.29}$$

$$\text{subject to} \qquad \tilde{\mathbf{P}}^{-1} - \mathbf{S} < \mathbf{0}, \tag{3.30}$$

$$Hold\ (3.28).$$

According to the Schur's complement, one can rewrite (3.30) as follows:

$$\begin{bmatrix} -\mathbf{S} & \mathbf{I} \\ \mathbf{I} & -\tilde{\mathbf{P}} \end{bmatrix} < \mathbf{0}. \tag{3.31}$$

In order to stablize the DER states, one can finally formulate the proposed optimization problem as follows:

$$\begin{aligned} &\text{minimise} && trace[\mathbf{S}] \\ &\text{subject to} && Hold\ (3.28)\ and\ (3.31). \end{aligned} \tag{3.32}$$

Finally, the feedback gain matrix is computed as follows:

$$\mathbf{F} = \mathbf{X}\tilde{\mathbf{P}}^{-1}. \tag{3.33}$$

One can use the standard YALMIP toolbox to solve the proposed optimization problem [213]. The performance of the proposed method is analysed in the next section.

3.5 Simulation Results Using the Least Square Based KF and H_2 Controller

The performance of the aforementioned algorithms are explored by performing extensive numerical simulations.

3.5.1 Performance of the Proposed Estimation Algorithm

The simulation parameters under the balanced load conditions are summarized in Table 3.1 [6], [106]. Generally, the process noise covariance matrix is determined by the modeling error. That is, when a model is established, its error will account for the process noise covariance. The considered process and measurement noise covariances are diagonal matrices [106], [107], [113] and their values are given in Table 3.1. This is due to the fact that the observation noises are uncorrelated with and independent of each other. Secondly, the individual sensor can be used to estimate the system states and its accuracy is affected by its noise covariance. From the microgrid model, it can be seen that the measurement

information is the current and voltage magnitudes. Typically, the measurement accuracy is affected by the observation noises [106], [111]. The uniform quantization is used to obtain bit sequence for transmission of the signal.

Table 3.1: System parameters under the balanced load conditions.

Parameters	Values	Parameters	Values
R_{lj}	76 Ohm	R_{j}	76 Ohm
i_{lj}	76 Amp	R_{t1}	1 Ohm
R_{t2}	5 Ohm	R_{t3}	10 Ohm
i_{t1}	0.1 Amp	i_{t2}	10 Amp
Quantization	Uniform	R_{d1}	1.5 Ohm
R_{d2}	6 Ohm	R_{d3}	10 Ohm
i_{d1}	300 Amp	i_{d2}	900 Amp
i_{d3}	1500 Amp	C_{j}	0.9 F
L_{j}	76 H	Δt	0.001
$\mathbf{Q}_{n}$	0.0005*$\mathbf{I}$	$\mathbf{R}_{w}$	0.05*$\mathbf{I}$

Under the balanced load conditions, the numerical simulation results are presented in Figs. 3.4-3.6. From the results, it is clearly observed that the proposed approach is able to estimate the system state properly compared with the existing method [104]. This accurate estimation is obtained using the proposed least square based KF estimation method. Note that the small fluctuations come from the statistical information such as process, observation and channel noises.

3.5.2 Performance of the Proposed Controller

As this is an open-loop system without control the system dynamics can not be guaranteed to be stable. That is, as can be seen in the simulation results, the state will fluctuate which is determined by the open-loop system state matrix $\mathbf{A}$. Therefore, it is necessary to apply a proper control method, so that the PCC voltages are stabilized. After applying the proposed control method, it can be seen in Fig.3.7 that the proposed method is able to stabilise the system states at a fairly short time steps. This is because the proposed control framework can properly determine the feedback gain such that the system states can be stabilizable.

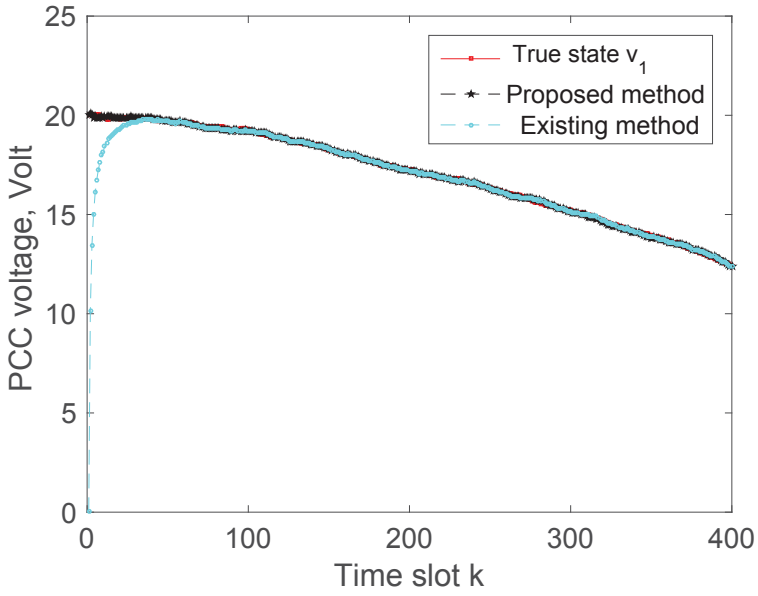

Figure 3.4: v_1 comparison between the true and estimated state.

In order to see the capacitor effect in the regulation process, consider the unbalanced load conditions with its corresponding parameters as shown in Table 3.2. The unbalanced condi-

Table 3.2: System parameters under the unbalanced load conditions.

Parameters	Values	Parameters	Values
R_{l1}	76 Ohm	R_{l2}	10 Ohm
R_{l3}	30 Ohm	i_{l1}	76 Amp
i_{l2}	10 Amp	i_{l3}	30 Amp
R_1	100 Ohm	R_2	200 Ohm
R_3	300 Ohm	C_1	10 F
C_2	20 F	C_3	30 F
L_{l1}	76 H	L_{l2}	10 H (L_{l3} = 30 H)

tions are considered as a sudden change of loads and variation of distributed network parameters due to weather conditions. The simulation result under the unbalanced load conditions is demonstrated in Fig. 3.8. It can be seen that if the capacitances are increased, it will need more time to stabilize the system states as expected in [214].

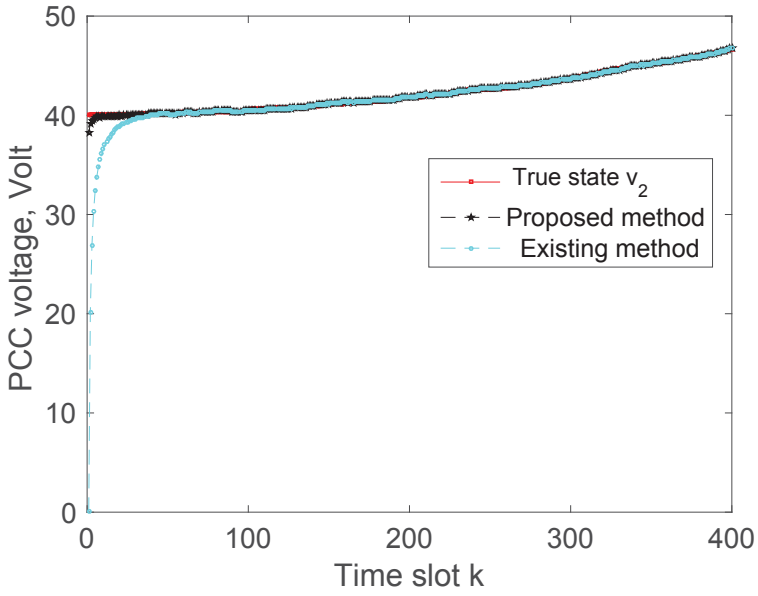

Figure 3.5: v_2 comparison between the true and estimated state.

3.6 Summary

This study addresses the microgrid state estimation and its stabilization problem from the communication perspective. To do so, the sensor networks have been applied in the microgrid to coordinate DER states regulation. In order to transmit the sensing information to the observer, the proposed smart grid communication systems have been utilized. Based on the infrastructure, this paper proposes a least square based KF algorithm for microgrid state estimations. In order to regulate the microgrid states, this study proposes a novel optimal control strategy based on a semidefinite programming approach. As a result, a new sensing, state estimation and control scheme for microgrids incorporating DERs is derived. At the end, the effectiveness of the developed approaches is verified by numerical simulations. It is worth pointing out that the aforementioned problems are not considered trivial and simple in the smart grid and control communities.

Recently, the smart grid has been considered as a next-generation power system to modernize the traditional grid to improve its security, connectivity, efficiency and sustainability. Unfortunately, the smart grid is susceptible to malicious cyber attacks, which can create serious technical, economical, social and control problems in power network operations [3], [11]. The following chapter proposes a recursive systematic convolutional (RSC) code and KF

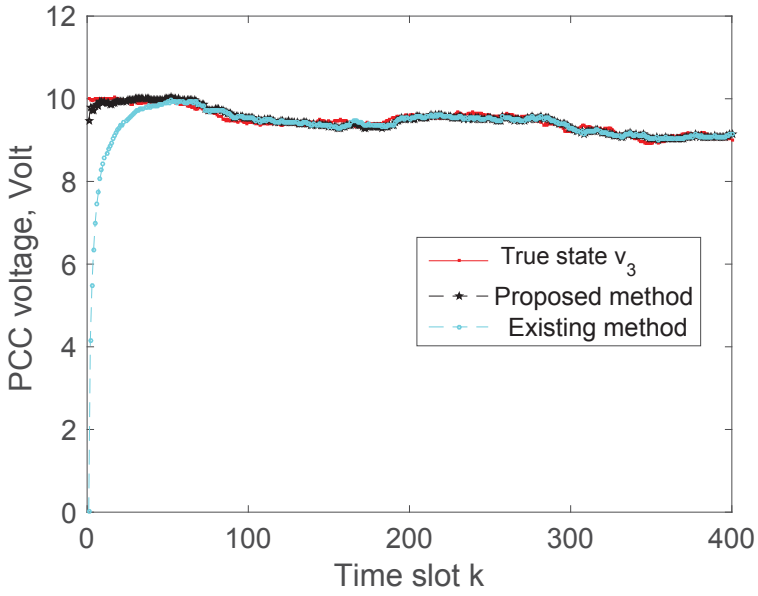

Figure 3.6: v_3 comparison between the true and estimated state.

based cyber attack minimization technique in the context of smart grids.

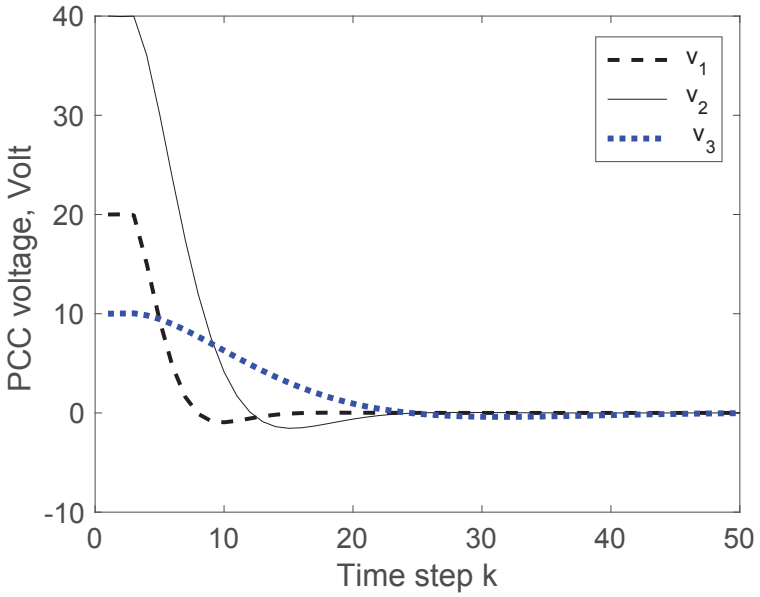

Figure 3.7: Voltage control trajectory under balanced load conditions.

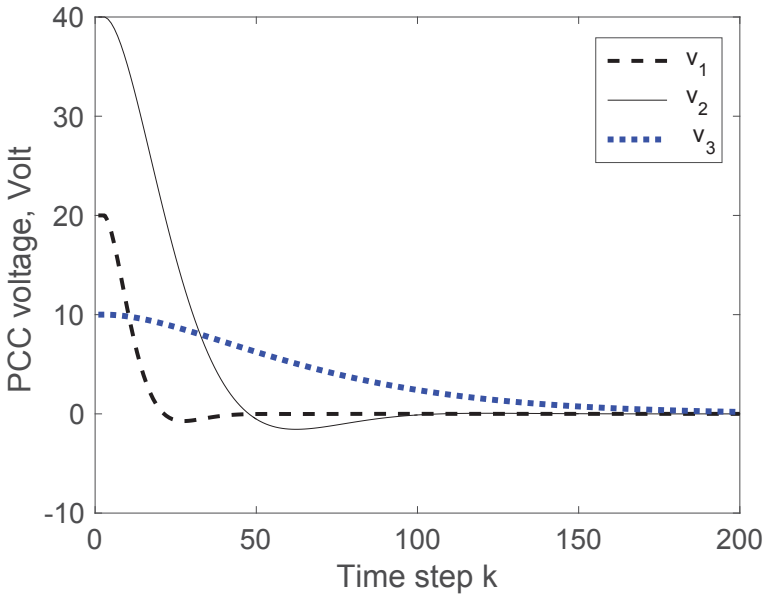

Figure 3.8: Capacitors effect for voltage regulation considering unbalanced load conditions.

Chapter 4

Cyber Attack Protection and Optimal Feedback Controller

4.1 Introduction

Recently, smart grid has been considered as a next-generation power system to modernize the traditional grid to improve its security, connectivity, efficiency and sustainability. Unfortunately, smart grid is susceptible to malicious cyber attacks, which can create serious technical, economical, social and control problems in power network operations [162], [163], [164]. Many studies have been carried out to investigate the cyber attacks in smart grid state estimations. Most of the state estimation methods use the weighted least squared (WLS) technique under cyber attacks [162], [163], [164]. Chi-Square detector is also used to detect those attacks. Even though this approach is easy to be implemented for nonlinear systems, it is computationally intensive and it cannot eliminate the attacks properly [162], [3]. To this end, the WLS based l_1 optimization method is explored in [165]. Furthermore, a new detection scheme to detect the false data injection attack is proposed in [166]. It employs a Kullback-Leibler method to calculate the distance between the probability distributions derived from the observation variations. A sequential detection of false data injection in smart grids is investigated in [161]. It adopts a centralized detector based on the generalized likelihood ratio and cumulative sum algorithm. A SDP based AC power system state estimation is proposed in [167]. Thereafter, the KF based microgrid energy theft detection algorithm is

presented in [60].

It is not feasible for utility operators at controller points, to find out cyber attacks by trial and error, so a joint cyber attack protection and state estimation scheme is necessary for the stabilization of the power network. Driven by the aforementioned motivations, this study proposes a recursive systematic convolutional (RSC) code and KF based cyber attack minimization technique in the context of smart grids. Specifically, the proposed RSC code is used to add redundancy in the system states, and the log-maximum a-posterior decoding is used to recover the state information, which is affected by random noises and cyber attacks. Once the estimated states are obtained by KF algorithm, a SDP based optimal feedback controller is proposed to regulate the system states. Test results show that the proposed approach can accurately mitigate the cyber attacks and properly estimate and stabilize the system states. These results can be used to provide an insight to distribution grid planners for contingency analysis, energy theft detections and power network control. Consequently, this work is valuable for the energy industry and households towards a smart and secure energy system in the future.

4.2 DERs Connected to the IEEE 4-Bus System

A microgrid is a small-scale power network that can operate independently or be connected to the main grid. To mitigate global warming at an acceptable level by reducing green house gas emissions and diversification of energy sources, the renewable microgrid is one of the most promising research topics in academia [1]. As renewable power generation patterns are generally intermittent in nature, they need to be properly monitored. Generally, the microgrid incorporating multiple DERs is connected to the distribution power system.

Fig. 4.1 shows the IEEE 4-bus distribution test feeder that is interfaced to the local load through the converter [8]. In addition, the model of multiple DERs connecting to the power network is shown in Fig. 4.2 [8]. The considered N DERs in this study are connected to the main grid. For simplicity, we assume that N=4 solar panels are connected through the IEEE 4-bus test feeder as shown in Fig. 4.2 [215], [8]. Here, the input voltages are denoted by $\mathbf{v}_p = (v_{p1}\ v_{p2}\ v_{p3}\ v_{p4})^T$, where v_{pi} is the i-th DER input voltage. The four DERs are connected to the power network at the corresponding points of common coupling (PCCs)

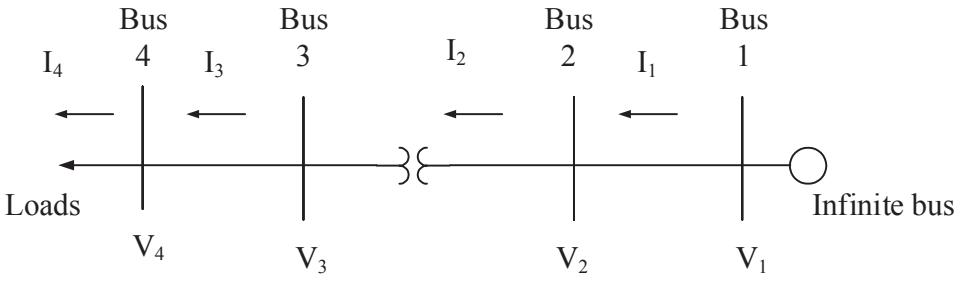

Figure 4.1: An illustration of the IEEE 4-bus distribution system [7].

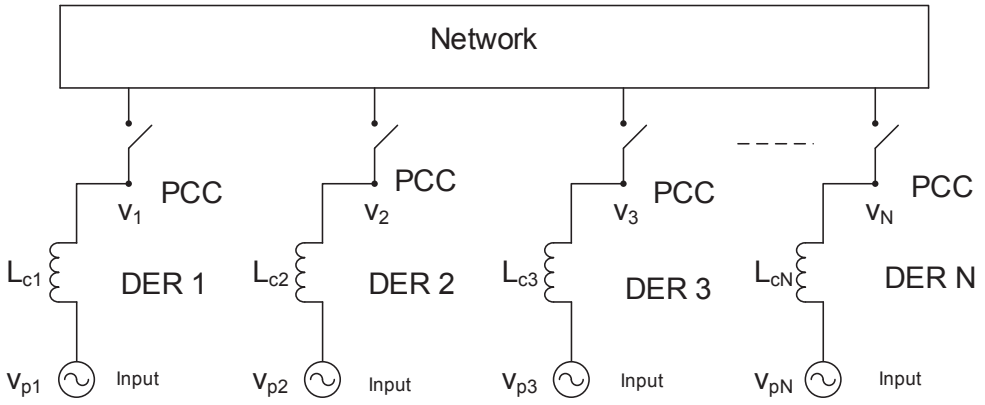

Figure 4.2: DERs are connected to the power network [8].

whose voltages are denoted by $\mathbf{v}_s = (v_1\ v_2\ v_3\ v_4)^T$, where v_i is the i-th PCC voltage. In order to maintain the proper operation of DERs, these PCC voltages need to be kept at their reference values. A coupling inductor exists between each DER and the rest of the electricity network.

Now by applying Laplace transformation, the nodal voltage equation can be obtained as follows [8]:

$$\mathbf{Y}(s)\mathbf{v}_s(s) = \frac{1}{s}\mathbf{L}_c^{-1}\mathbf{v}_p(s), \tag{4.1}$$

where $\mathbf{L}_c = diag(L_{c_1},\ L_{c_2},\ L_{c_3},\ L_{c_4})$ is the coupling inductance and $\mathbf{Y}(s)$ is the admittance matrix of the entire power network incorporating four DERs. Based on the typical specifications of the IEEE 4-bus distribution feeder [215], [8], [7], the admittance matrix is as

follows:

$$\mathbf{Y}(s) = (\mathbf{L}_c s)^{-1} + \begin{bmatrix} \frac{1}{0.1750+0.0005s} & \frac{-1}{0.1750+0.0005s} \\ \frac{-1}{0.1750+0.0005s} & \frac{1}{0.1750+0.0005s} + \frac{1}{0.1667+0.0004s} \\ 0 & \frac{-1}{0.1667+0.0004s} \\ 0 & 0 \end{bmatrix}$$

$$\begin{bmatrix} 0 & 0 \\ \frac{-1}{0.1667+0.0004s} & 0 \\ \frac{1}{0.1667+0.0004s} + \frac{1}{0.2187+0.0006s} & \frac{-1}{0.2187+0.0006s} \\ \frac{-1}{0.2187+0.0006s} & \frac{1}{0.2187+0.0006s} + \frac{1}{12.3413+0.0148s} \end{bmatrix}.$$

Now we can convert the transfer function into the state-space framework [8]. The discrete-time linear dynamic system can be described as follows:

$$\mathbf{x}(k+1) = \mathbf{A}_d \mathbf{x}(k) + \mathbf{B}_d \mathbf{u}(k) + \mathbf{n}_d(k), \tag{4.2}$$

where $\mathbf{x} = \mathbf{v}_s - \mathbf{v}_{ref}$ is the PCC state voltage deviation, $\mathbf{v}_{ref}$ is the PCC reference voltage, $\mathbf{u} = \mathbf{v}_p - \mathbf{v}_{pref}$ is the DER control input deviation, $\mathbf{v}_{pref}$ is the reference control effort, $\mathbf{n}_d$ is the zero mean process noise whose covariance matrix is $\mathbf{Q}_n$, $\mathbf{A}_d = \mathbf{I} + \mathbf{A}\Delta t$ is the system state matrix, Δt is the sampling period and $\mathbf{B}_d = \mathbf{B}\Delta t$ is the input matrix. After applying Kirchhoff's laws with the given IEEE 4-bus specifications in [7], [8], [215], the matrices $\mathbf{A}$, and $\mathbf{B}$ are given by [8], [215]:

$$\mathbf{A} = \begin{bmatrix} 175.9 & 176.8 & 511 & 103.6 \\ -350 & 0 & 0 & 0 \\ -544.2 & -474.8 & -408.8 & -828.8 \\ -119.7 & -554.6 & -968.8 & -1077.5 \end{bmatrix}, \tag{4.3}$$

$$\mathbf{B} = \begin{bmatrix} 0.8 & 334.2 & 525.1 & -103.6 \\ -350 & 0 & 0 & 0 \\ -69.3 & -66.1 & -420.1 & -828.8 \\ -434.9 & -414.2 & -108.7 & -1077.5 \end{bmatrix}. \tag{4.4}$$

In the following section, the observation model and attack process is explored.

4.3 Measurements and Cyber Attacks

In order to monitor the microgrid, the utility company deploys a set of sensors around it. The measurements of the microgrid states are obtained by a set of sensors and can be modelled as follows:

$$\mathbf{z}(k) = \mathbf{C}\mathbf{x}(k) + \mathbf{w}(k), \tag{4.5}$$

where $\mathbf{z}(k)$ is the measurements, $\mathbf{C}$ is the measurement matrix and $\mathbf{w}(k)$ is the zero mean sensor measurement noise whose covariance matrix is $\mathbf{R}_w(k)$.

Due to dramatically rising energy demand worldwide, the power system is often run near the operational and technical limits, where unexpected trivial disturbances can cause possible massive blackouts. Cyber attacks on smart grid communication are one of the impending threats to cause large-scale cascading outage. Generally speaking, in smart grids the communication infrastructure is used to send information from sensors to the EMS. However, vulnerabilities of the infrastructure make modern smart grids prone to cyber attacks. Generally, the objective of attackers is to insert false data into the observations as follows:

$$\mathbf{y}(k) = \mathbf{C}\mathbf{x}(k) + \mathbf{w}(k) + \mathbf{a}(k), \tag{4.6}$$

where $\mathbf{a}(k)$ is the false data inserted by the attacker [11], [161], [60]. The attackers have complete access to the system infrastructure so that they can hijack, record and manipulate data according to their best interest. In this study, the cyber attack pattern is similar to those illustrated in [11], [161], [216]. Figure 4.3 shows the observation model and cyber attack process in the context of smart grid state estimations. It can be seen that the measurement information is disturbed by noises and cyber attacks.

4.4 Proposed Cyber Attack Protection and Optimal Controller

Normally, a smart grid is likely to combine communication infrastructure, control and computation to improve efficiency, security and reliability [217]. Even though the communication infrastructure in supporting the monitoring and control of smart grid is secured, it

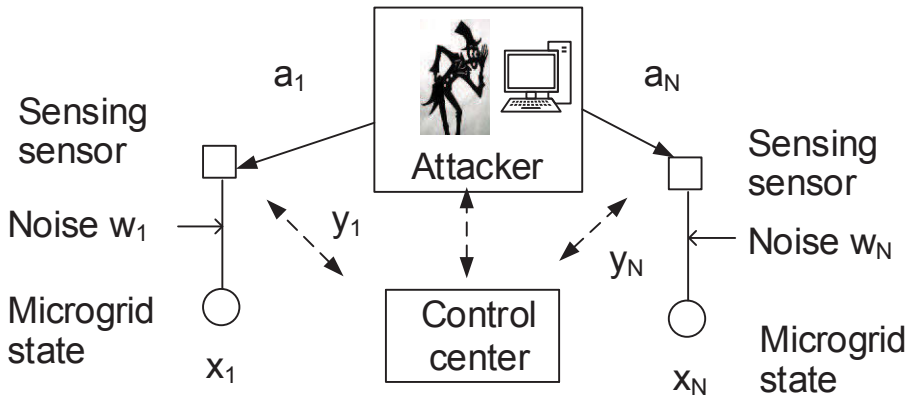

Figure 4.3: Observation information with cyber attack in the microgrid.

still can be vulnerable to intended attacks. To secure the system states, the channel code is commonly used in the signal processing research community. To design a reliable communication infrastructure, the cyber attack protection and optimal feedback controller are described in this section.

4.4.1 Cyber Attack Protection Using the RSC Channel Code

The channel code is used to protect data sent over it for storage or retrieval even in the presence of noise (errors). Inspired by the convolutional coding concept (current output state depends on the previous state and input), the outer coding is considered similar to the microgrid state-space and the observation models. Motivated by the convolutional coding concept, the microgrid state-space and measurements are regarded as the outer code [10], [9]. Then the standard uniform quantizer performs quantization to get the sequence of bits $\mathbf{b}(k)$. $\mathbf{b}(k)$ is encoded by RSC channel code which is regarded as the inner code. Figure 4.4 shows this encoding process in detail. The main reason for using RSC code is to mitigate impairments and introduce redundancy in the system to protect the grid information. As a result, it improves the system performance significantly.

Generally speaking, the RSC code is characterized by three parameters: the codeword length n, the message length l, and the constraint length m i.e., (n, l, m). The quantity l/n refers to the code rate which indicates the amount of parity bits added to the data stream. The constraint length specifies $m-1$ memory elements which represents the number of bits in the encoder memory that affects the RSC generation output bits. If the constraint length

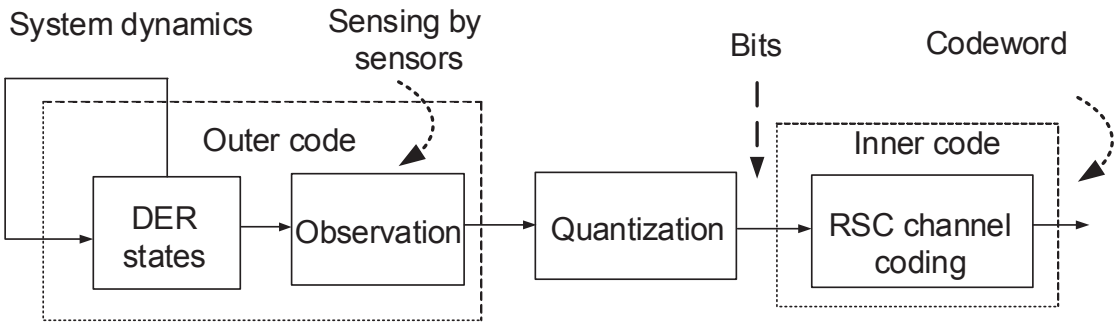

Figure 4.4: A concatenated coding structure of a dynamic power system [9].

m increases, the encoding process intrinsically needs a longer time to execute the logical operations. Other advantages of the RSC code compared with the convolutional and turbo encoder include its reduced computation complexity, systematic output features and no error floor [218]. From this point of view, this study considers a (2, 1, 3) RSC code and (1 0 1, 1 1 1) code generator polynomial in the feedback process. According to the RSC features, the code rate is $1/2$ and there are two memories in the RSC process. As shown in Fig. 4.5, this RSC code produces two outputs and can convert an entire data stream into one single codeword. The state transition and trellis diagrams of the RSC code are illustrated in Figs.

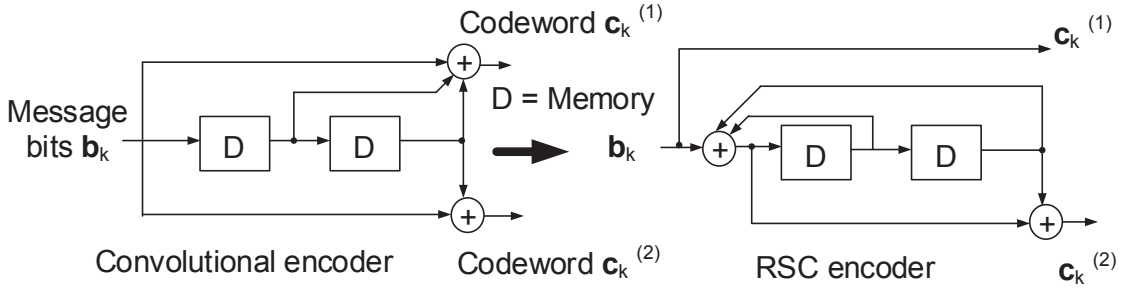

Figure 4.5: A convolutional encoder is equivalent to the RSC encoder [10].

4.6 and 4.7.

The codeword is then passed through the binary phase shift keying (BPSK) to obtain modulated signal $\mathbf{s}(k)$. $\mathbf{s}(k)$ is passed through the additive white Gaussian noisy (AWGN) channel. To illustrate, Fig. 4.8 shows the proposed cyber attack protection procedure in the context of smart grids. At the end, the received signal is given by:

$$\mathbf{r}(k) = \mathbf{s}(k) + \mathbf{e}(k), \tag{4.7}$$

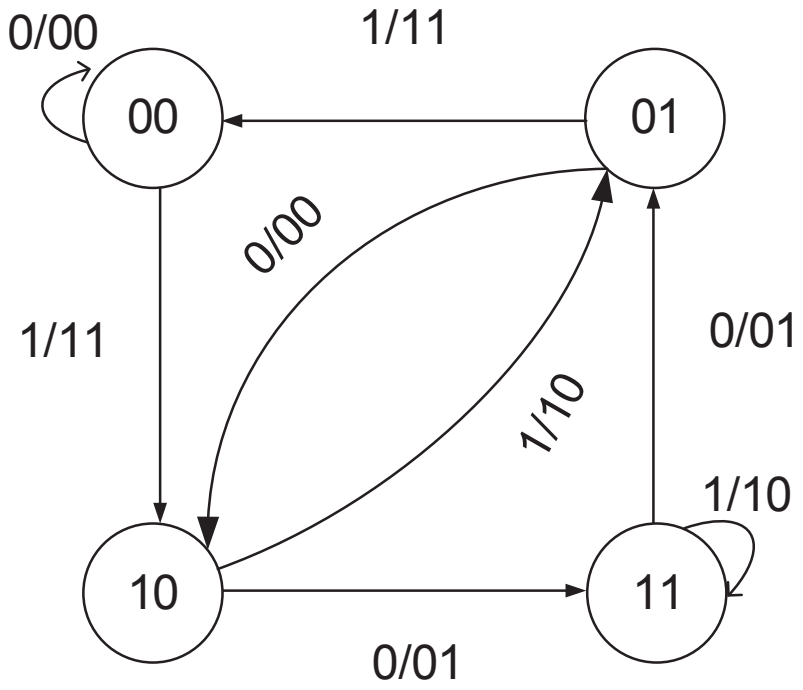

Figure 4.6: State transition diagram for the RSC code [10].

where $\mathbf{e}(k)$ is the AWGN noise. The received signal is followed by the log-maximum a-posteriori (Log-MAP) decoding for this dynamic system. The Log-MAP works recursively from the forward path to the backward path to recover the state information [10]. For each transmitted symbol it generates its hard estimate and soft output in the form of a posteriori probability on the basis of received sequences [10], [219]. The Log-MAP output information is sent to demodulation and dequantization processes, followed by the state estimation scheme.

Our cyber-attacks protection algorithm is different from the external faults in two ways. Firstly, our scheme can identify the external faults and give alarm to the utility operator for taking necessary actions. In this way, the external faults can be minimized so the power system can operate properly. Secondly, the external faults are due to the system failures, and the fault patterns can be easily identified. On the other hand, the proposed RSC code is used to add redundancy in the system states so that it can tolerate the malicious cyber-attacks without identify them.

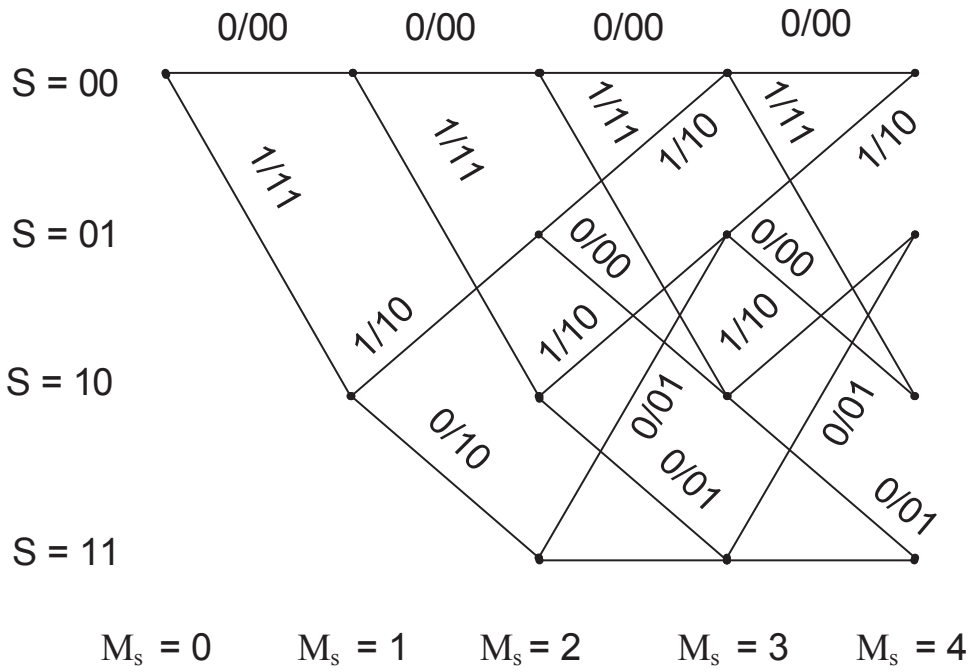

Figure 4.7: Trellis diagram for the RSC code [10].

4.4.2 Proposed Centralised Estimation Framework

The proposed framework uses the KF to estimate the system states. The KF operates recursively on observation information to produce the optimal state estimation. Generally, the forecasted system state estimate is expressed as follows [155]:

$$\hat{\mathbf{x}}^{-}(k) = \mathbf{A}_d\hat{\mathbf{x}}(k-1) + \mathbf{B}_d\mathbf{u}(k-1), \tag{4.8}$$

where $\hat{\mathbf{x}}(k-1)$ is the estimated state of the last step. Then the forecasted error covariance matrix is given by:

$$\mathbf{P}^{-}(k) = \mathbf{A}_d\mathbf{P}(k-1)\mathbf{A}_d' + \mathbf{Q}_n(k-1), \tag{4.9}$$

where $\mathbf{P}(k-1)$ is the estimated error covariance matrix of the last step. The observation innovation residual $\mathbf{d}(k)$ is given by:

$$\mathbf{d}(k) = \mathbf{y}_{rd}(k) - \mathbf{C}\hat{\mathbf{x}}^{-}(k), \tag{4.10}$$

where $\mathbf{y}_{rd}(k)$ is the dequantized and demodulated output bit sequence. The Kalman gain matrix can be written as:

$$\mathbf{K}(k) = \mathbf{P}^{-}(k)\mathbf{C}'[\mathbf{C}\mathbf{P}^{-}(k)\mathbf{C}' + \mathbf{R}_w(k)]^{-1}. \tag{4.11}$$

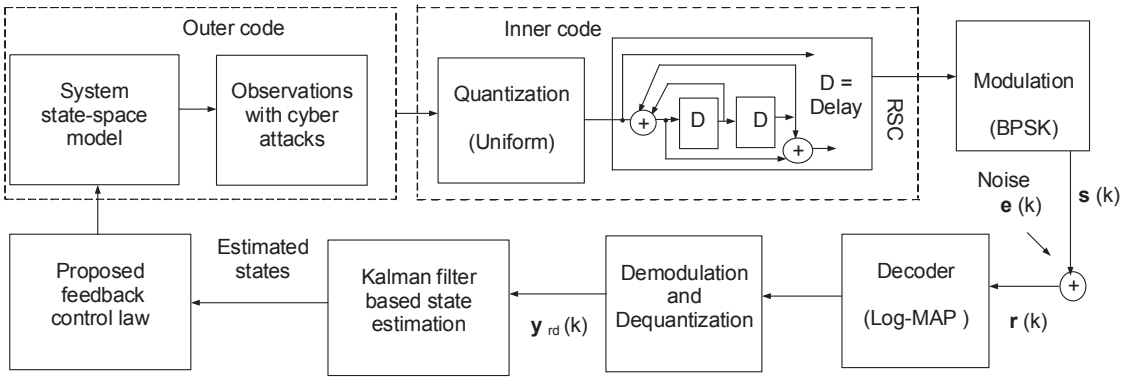

Figure 4.8: An illustration of the cyber attack protection in smart grids.

The updated state estimation is given by:

$$\hat{\mathbf{x}}(k) = \hat{\mathbf{x}}^{-}(k) + \mathbf{K}(k)\mathbf{d}(k). \tag{4.12}$$

Finally, the updated estimated error covariance matrix $\mathbf{P}(k)$ is expressed as follows:

$$\mathbf{P}(k) = \mathbf{P}^{-}(k) - \mathbf{K}(k)\mathbf{C}\mathbf{P}^{-}(k). \tag{4.13}$$

After estimating the system state, the proposed control strategy is applied for regulating the microgrid states as shown in the next section.

4.4.3 Proposed Centralized Optimal Feedback Controller

In the simulation section, it has been shown that the proposed method is able to well estimate the system states. So, here we assume the microgrid state information is available. In order to regulate the microgrid states, define the following feedback control law [20], [212]:

$$\mathbf{u}(k) = \mathbf{F}\mathbf{x}(k), \tag{4.14}$$

by minimizing the following cost function:

$$J = E[\lim_{N\to\infty} 1/N \sum_{k=0}^{N-1} \{\mathbf{x}'(k)\mathbf{Q}_z\mathbf{x}(k) + \mathbf{u}'(k)\mathbf{R}_z\mathbf{u}(k)\}]. \tag{4.15}$$

Here, $E(\cdot)$ denotes the expectation operator, and $\mathbf{F}$ is the state feedback gain matrix, $\mathbf{Q}_z$ and $\mathbf{R}_z$ are the positive-definite state and control weighting matrices, respectively. Then the closed loop system is described as follows:

$$\mathbf{x}(k+1) = (\mathbf{A}_d + \mathbf{B}_d\mathbf{F})\mathbf{x}(k) + \mathbf{n}_d(k). \tag{4.16}$$

By using (4.14) and standard trace operator $(m'Dn = tr[Dnm'])$, (4.15) can be expressed as follows:

$$\begin{aligned} J =& E[\lim_{N\to\infty} 1/N \sum_{k=0}^{N-1} tr\{\mathbf{Q}_z\mathbf{x}(k)\mathbf{x}'(k) + \mathbf{F}'\mathbf{R}_z\mathbf{F}\mathbf{x}(k)\mathbf{x}'(k)\}] \\ =& tr[\mathbf{Q}_z + \mathbf{F}'\mathbf{R}_z\mathbf{F}]\mathbf{P}, \end{aligned} \tag{4.17}$$

where $\mathbf{P} = E[\lim_{N\to\infty} 1/N \sum_{k=0}^{N-1} \mathbf{x}(k)\mathbf{x}'(k)]$, and it can be written as follows:

$$\begin{aligned} \mathbf{P} =& E[\lim_{N\to\infty} 1/N \sum_{k=0}^{N-2} \mathbf{x}(k+1)\mathbf{x}'(k+1)] + \lim_{N\to\infty} 1/N E[\mathbf{x}(0)\mathbf{x}'(0)] \\ =& E[\lim_{N\to\infty} 1/N \sum_{k=0}^{N-2} (\mathbf{A}_d + \mathbf{B}_d\mathbf{F})\mathbf{x}(k)\mathbf{x}'(k)(\mathbf{A}_d + \mathbf{B}_d\mathbf{F})'] + \mathbf{Q}_n. \end{aligned} \tag{4.18}$$

Then (4.18) can be written as follows:

$$\mathbf{P} = (\mathbf{A}_d + \mathbf{B}_d\mathbf{F})\mathbf{P}(\mathbf{A}_d + \mathbf{B}_d\mathbf{F})' + \mathbf{Q}_n. \tag{4.19}$$

Now, one can consider the following inequality,

$$\begin{aligned} &(\mathbf{A}_d + \mathbf{B}_d\mathbf{F})\mathbf{P}(\mathbf{A}_d + \mathbf{B}_d\mathbf{F})' - \mathbf{P} + \mathbf{Q}_n < \mathbf{0} \\ &(\mathbf{A}_d + \mathbf{B}_d\mathbf{F})\mathbf{P}\mathbf{P}^{-1}\mathbf{P}(\mathbf{A}_d + \mathbf{B}_d\mathbf{F})' - \mathbf{P} + \mathbf{Q}_n < \mathbf{0}. \end{aligned} \tag{4.20}$$

One can introduce a new variable $\mathbf{H} = \mathbf{F}\mathbf{P}$ and rewrite (4.20) as follows:

$$(\mathbf{A}_d\mathbf{P} + \mathbf{B}_d\mathbf{H})\mathbf{P}^{-1}(\mathbf{A}_d\mathbf{P} + \mathbf{B}_d\mathbf{H})' - \mathbf{P} + \mathbf{Q}_n < \mathbf{0}. \tag{4.21}$$

According to the Schur's complement, (4.21) can be transformed into the following form:

$$\begin{bmatrix} \mathbf{Q}_n - \mathbf{P} & \mathbf{A}_d\mathbf{P} + \mathbf{B}_d\mathbf{H} \\ (\mathbf{A}_d\mathbf{P} + \mathbf{B}_d\mathbf{H})' & -\mathbf{P} \end{bmatrix} < \mathbf{0}. \tag{4.22}$$

From (4.17), $\mathbf{F}$ and $\mathbf{P}$ can be found by minimising the following expression:

$$\begin{aligned} &\underset{\mathbf{P},\mathbf{F}}{\text{minimise}} && tr[\mathbf{Q}_z + \mathbf{F}'\mathbf{R}_z\mathbf{F}]\mathbf{P} && (4.23) \\ &\text{subject to} && (4.22). \end{aligned}$$

Based on $\mathbf{H} = \mathbf{F}\mathbf{P}$, (4.23) can be transformed as follows:

$$\begin{aligned} &\underset{\mathbf{P},\mathbf{S},\mathbf{H}}{\text{minimise}} && tr[\mathbf{Q}_z\mathbf{P}] + tr[\mathbf{S}] && (4.24) \\ &\text{subject to} && \mathbf{S} > \mathbf{R}_z^{1/2}\mathbf{H}\mathbf{P}^{-1}\mathbf{H}'\mathbf{R}_z^{1/2} && (4.25) \\ & && Hold\ Eq.\ (4.22). \end{aligned}$$

According to the Schur's complement, one can rewrite (4.25) as follows:

$$\begin{bmatrix} \mathbf{S} & \mathbf{R}_z^{1/2}\mathbf{H} \\ \mathbf{H}'\mathbf{R}_z^{1/2} & \mathbf{P} \end{bmatrix} > \mathbf{0}. \tag{4.26}$$

Then one can formulate the proposed optimization problem as follows:

$$\underset{\mathbf{P},\mathbf{S},\mathbf{H}}{\text{minimise}} \quad tr[\mathbf{Q}_z\mathbf{P}] + tr[\mathbf{S}] \tag{4.27}$$

$$\text{subject to} \quad Hold\ Eq.\ (4.22), Hold\ Eq.\ (4.26). \tag{4.28}$$

Finally, the feedback gain matrix is computed as follows:

$$\mathbf{F} = \mathbf{H}\mathbf{P}^{-1}. \tag{4.29}$$

The proposed convex problem can be solved effectively and efficiently using a number of available softwares such as YALMIP [213].

4.5 Simulation Results Using the RSC Code and Optimal Controller

In this section, we evaluate the performance of the proposed approaches under cyber attacks in smart grids. An overall system level diagram for system state estimation and control is illustrated in Fig. 4.9. After sensing and quantizing the system states, the RSC channel code is proposed to add redundancy into the data stream in a controlled manner to give the Log-MAP decoder to correct errors at EMS. Once the estimated system states are obtained, a SDP based optimal feedback controller is proposed to regulate the system states. The simulation is performed using the microgrid connected to the IEEE 4-bus distribution feeder and the individual IEEE 9-bus distribution system.

4.5.1 Estimation Results Using the Microgrid

The simulation parameters are summarized in Table 4.1. The mean squared error (MSE) versus signal-to-noise ratio (SNR) is presented in Fig. 4.10. It can be observed that the proposed method provides significant performance improvement compared with the existing

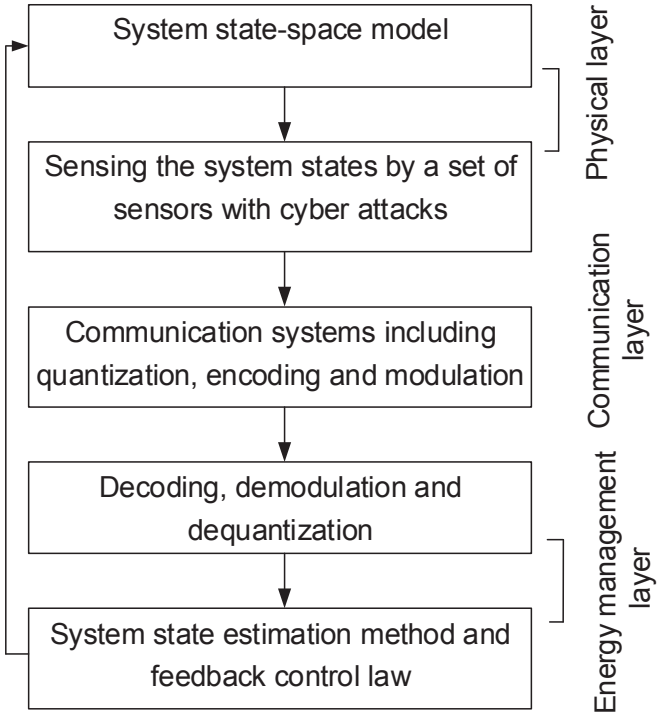

Figure 4.9: System level diagram for the state estimation and control.

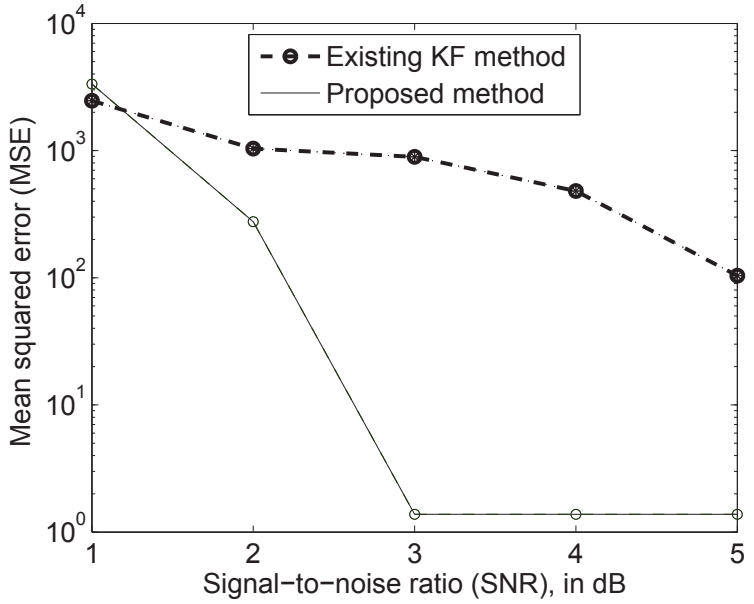

Figure 4.10: MSE versus SNR performance comparison.

Table 4.1: System parameters for the simulation.

Parameters	Values	Parameters	Values
$\mathbf{Q}_z$	$diag(10^{-2}, 10^{-2}, 10^{1}, 10^{-3})$	$\mathbf{R}_z$	$0.01 * \mathbf{I}_4$
Codes generator	$5/7$	Δt	0.0001
Quantization	Uniform 16 bits	Decoding	Log-MAP
Code rate	$1/2$	Channel	AWGN
$\mathbf{Q}_n$	$0.005 * \mathbf{I}_4$	$\mathbf{R}_w$	$0.05 * \mathbf{I}_4$

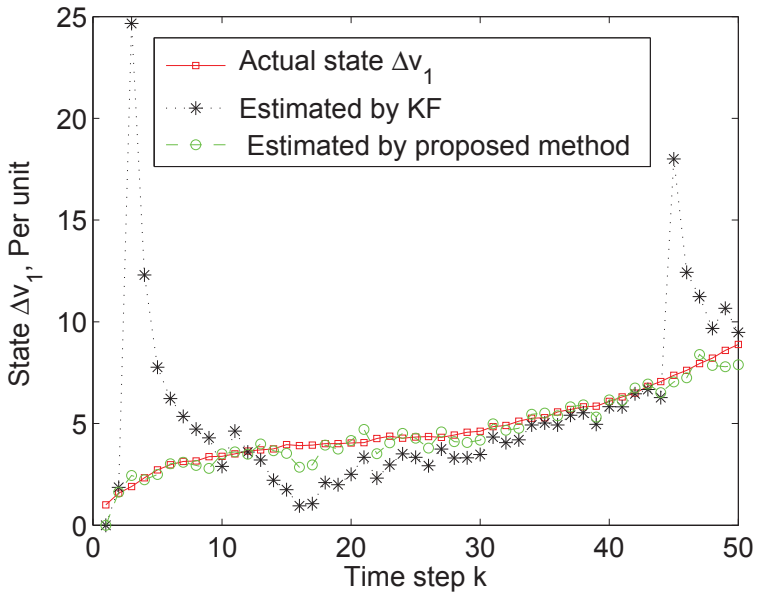

Figure 4.11: State trajectory of Δv_1 and its estimate.

method [11]. The reason is that the RSC code is used to protect the system from cyber attacks and noises by adding redundancy in the system states. It can also protect the state information from the unreliable lossy communication networks. Furthermore, the Log-MAP decoding can also facilitate the accurate extraction of the system state. For better visualization of the cyber attack, the system states versus time step are illustrated in Figs. 4.11–4.14. It can be observed and expected that the cyber attack still affects the system states seriously when the existing method is used to estimate system states [11]. In other words, there is a significant fluctuation due to the noises and cyber attacks. Interestingly, the proposed RSC based cyber attack protection technique can tolerate the system impairments by introducing redundancy and protection in the system states. As a result, the proposed method can estimate microgrid

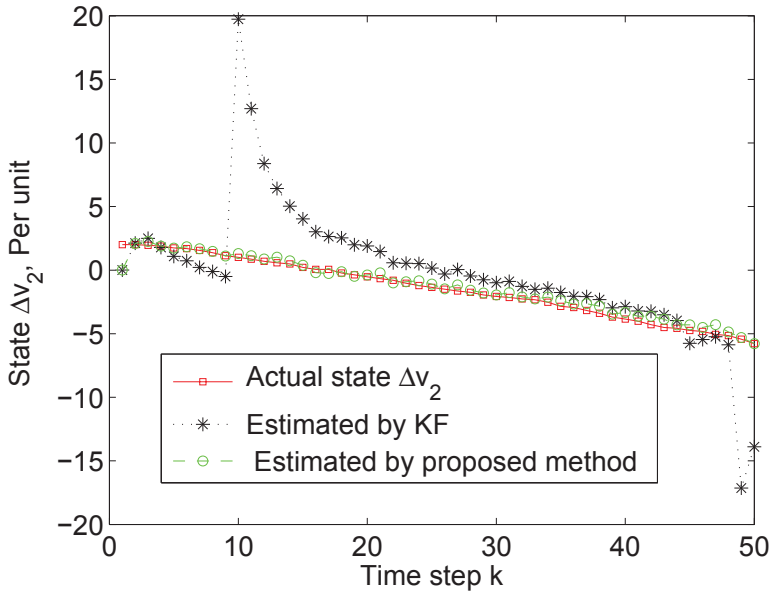

Figure 4.12: State trajectory of Δv_2 and its estimate.

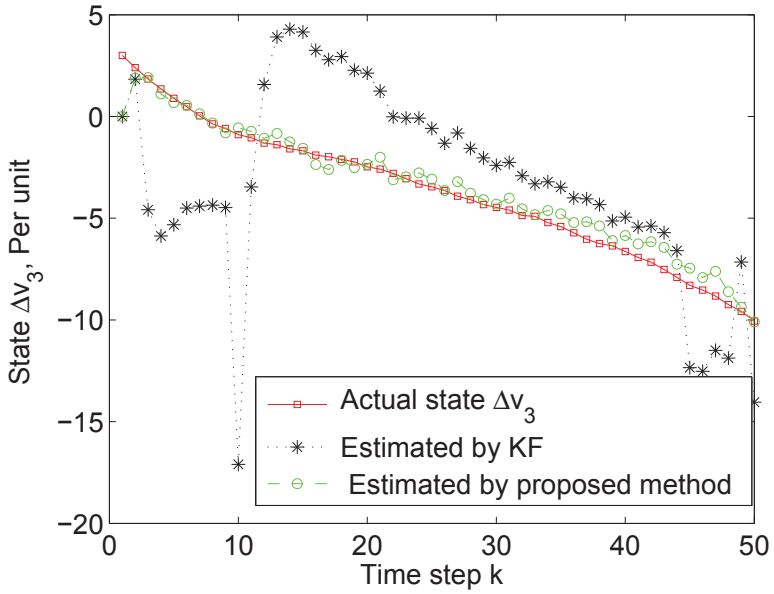

Figure 4.13: State trajectory of Δv_3 and its estimate.

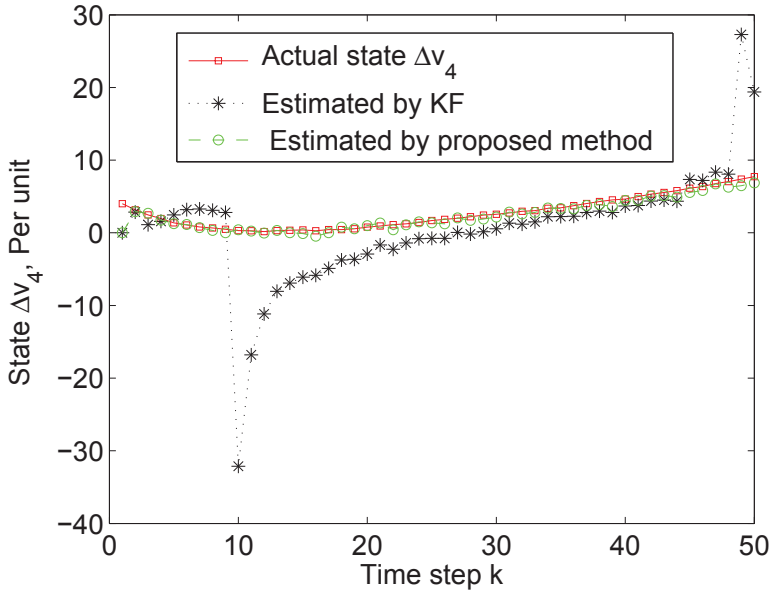

Figure 4.14: State trajectory of Δv_4 and its estimate.

states accurately even if there are cyber attacks and noises.

4.5.2 Estimation Results Using the IEEE 9-Bus System

In order to prove the robustness of the proposed method, it is applied to the IEEE 9-bus test feeder. To illustrate, Fig. 4.15 shows a single-line diagram of the IEEE 9-bus distribution system [11]. The parameters of the standard IEEE 9-bus system can be found in [220]. The system state vector is comprised of the bus voltage and phase angles. Normally, for a power system with N buses, the system state $\mathbf{x}$ can be defined as $\mathbf{x} = [\Theta_1\ \Theta_2 \cdots\ \Theta_N\ V_1\ V_2\ \cdots\ V_N]'$, where Θ_i is the i-th phase angle and V_i is the i-th bus voltage magnitude. Here, Θ_1 is considered as a reference phase angle. The IEEE 9-bus test system can be modelled as (4.2) with the parameters $\mathbf{A}_d = 0.98\mathbf{I}_{18}$ and $\mathbf{B}_d = 0.02\mathbf{I}_{18}$ [221]. The simulation is carried out in Matlab with the Matpower package [220]. The nominal phase angles and bus voltage magnitudes in $\mathbf{u}$ are shown in Table 4.2.

From the simulation results in Figs 4.16-4.19, it is observed that the proposed cyber attack minimization technique can have a better estimation performance compared with the traditional KF method [11]. This is due to the fact that the RSC channel coding and Log-MAP

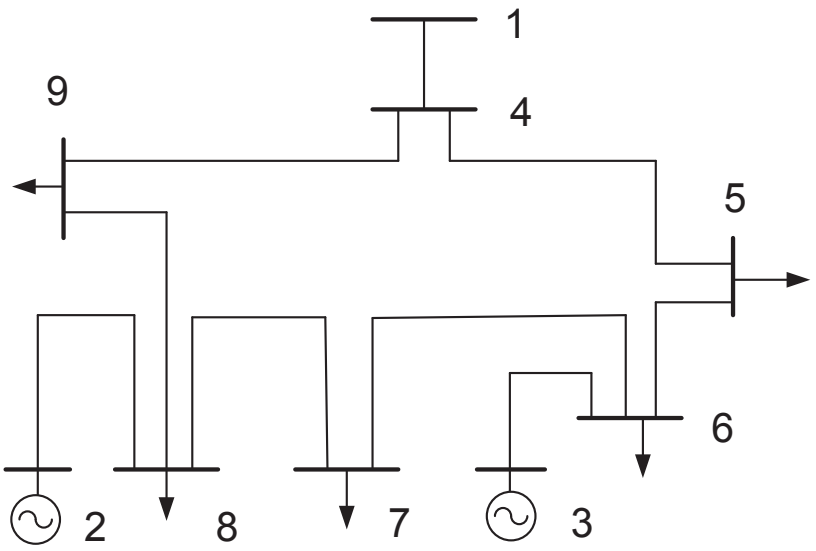

Figure 4.15: Single-line diagram of the IEEE 9-bus distribution feeder [11].

Table 4.2: The nominal state values of the IEEE 9-bus power system.

Bus No.	Phase angle Θ_N (degree)	Voltage magnitude V_N (per unit)
1	0.000	1
2	9.669	1
3	4.771	1
4	-2.407	0.987
5	-4.017	0.975
6	1.926	1.003
7	0.622	0.986
8	3.799	0.996
9	-4.350	0.958

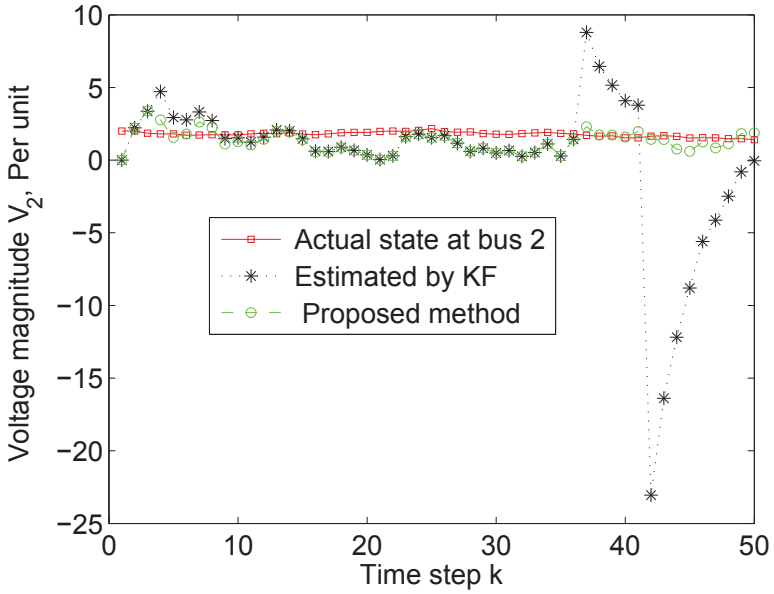

Figure 4.16: State trajectory of V_2 and its estimate at bus 2.

decoding can mitigate the impairments from the system states. It can be concluded that for smart grid communication it is better to use the RSC code with Log-MAP to mitigate impairments.

4.5.3 Stabilizing the Microgrid States

Unfortunately, it is noticed that the actual PCC state deviations increase dramatically (Figs. 4.11–4.14), which is very dangerous in terms of network stability and microgrid operation. Thus, it is necessary to apply a suitable control technique, so that the PCC voltage deviations are driven to zero. After applying the proposed control method to the microgrid connected to the IEEE 4-bus distribution system, it can be seen from Figs. 4.20-4.21 that the proposed controller is able to keep the voltage deviations to zero by the time k=200, which acts as a precursor in terms of network stability and proper operation of microgrids. Besides, the corresponding control input of each DER is shown in Fig. 4.21, which implies that it requires a small amount of control input.

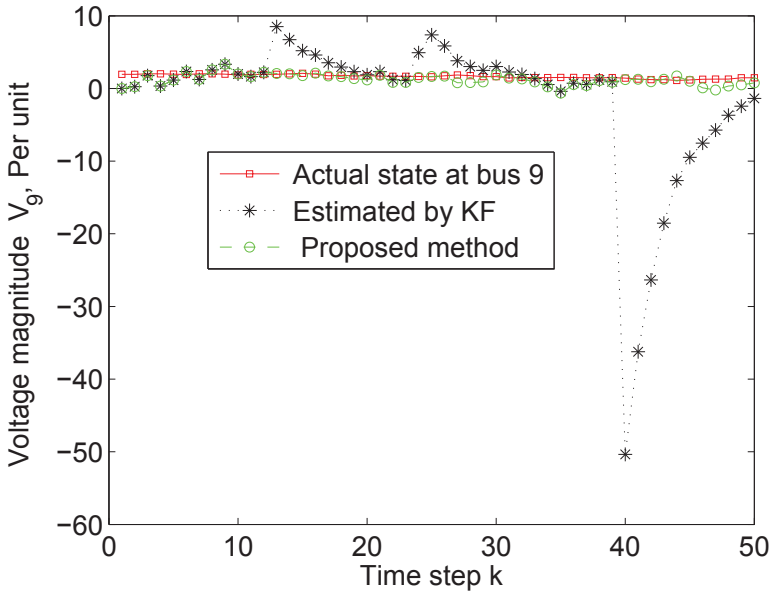

Figure 4.17: State trajectory of V_9 and its estimate at bus 9.

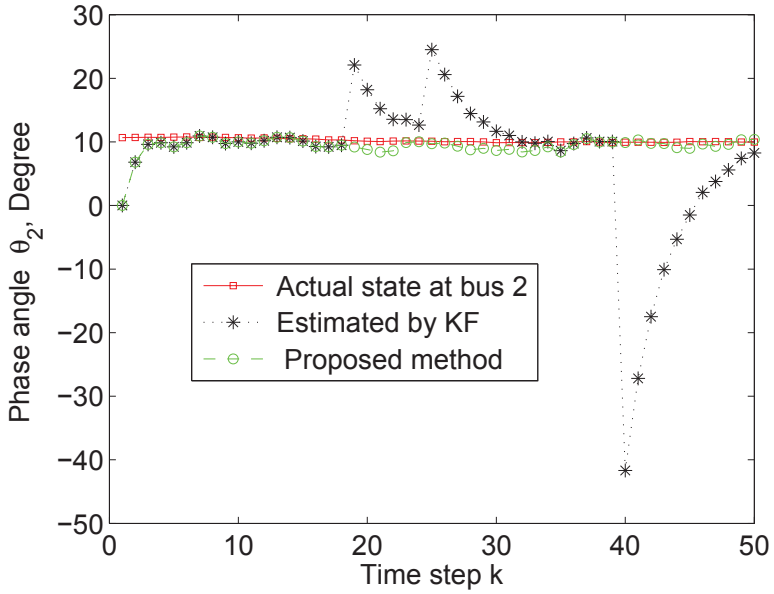

Figure 4.18: State trajectory of θ_2 and its estimate at bus 2.

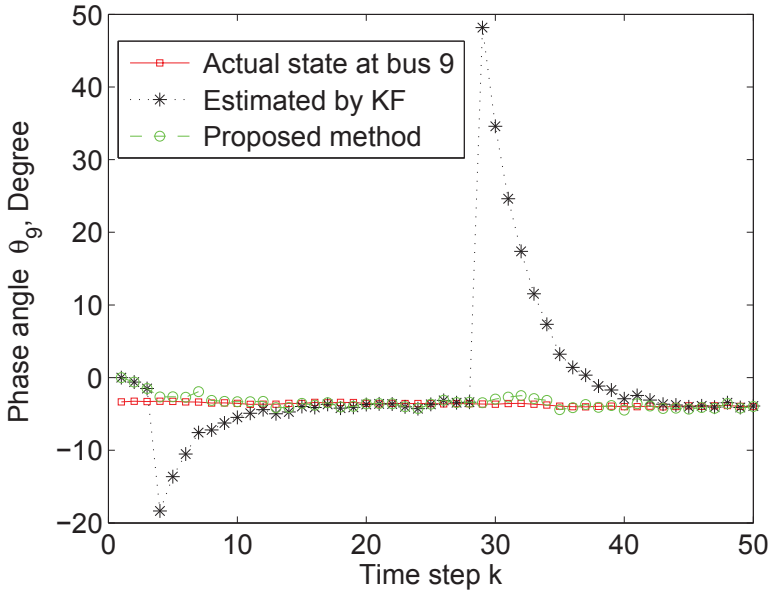

Figure 4.19: State trajectory of θ_9 and its estimate at bus 9.

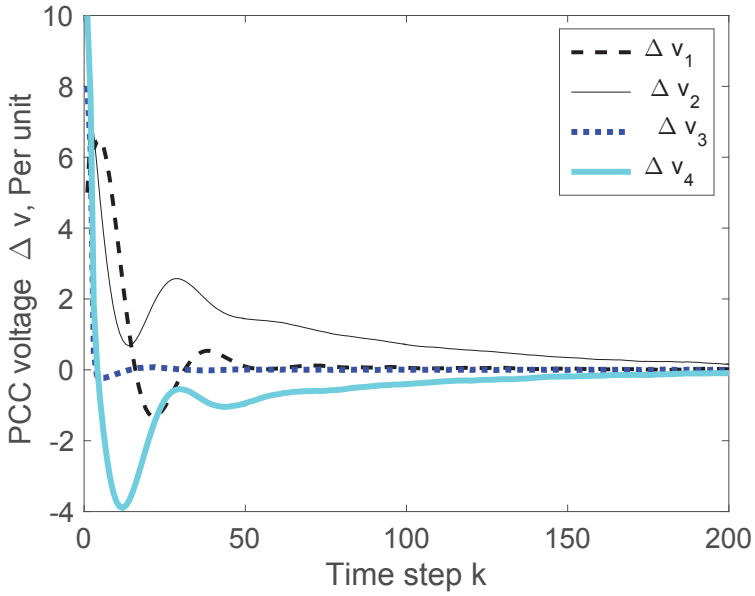

Figure 4.20: Controlling the states trajectory.

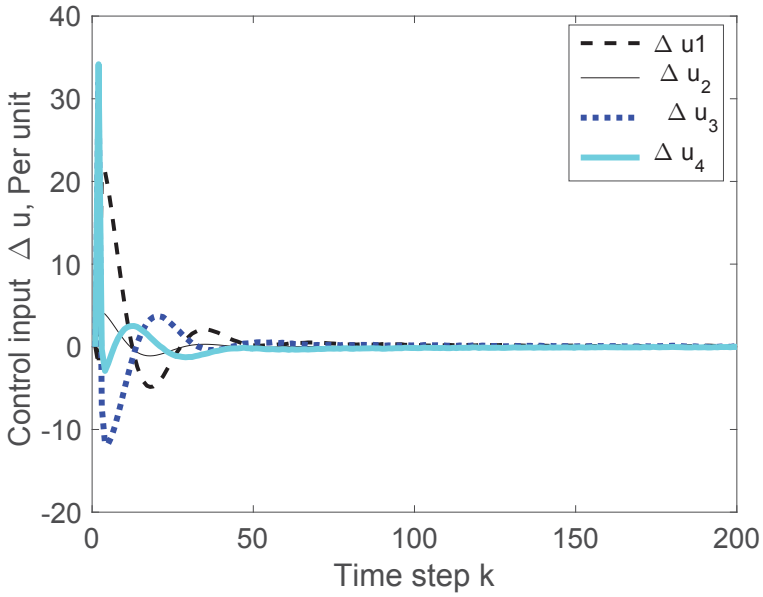

Figure 4.21: Control input trajectory.

4.6 Summary

This chapter proposes a cyber attack minimization based dynamic state estimation technique and feedback control algorithm in smart grids. An RSC coded cyber attack protection technique is proposed to add redundancy in the system states. Then a Log-MAP decoding can assist to extract the system states from the received signal which is polluted by noises and cyber attacks. In order to regulate the system states, this study proposes a SDP based optimal feedback controller. The effectiveness of the developed approaches is verified by numerical simulations. These findings can help to design the future smart control center under cyber attacks. Consequently, it is encouraged to use an environmentally friendly renewable microgrid, and the utility operator can monitor and control the power network properly.

It can be seen that the EMS is highly dependent on measurements, and it has different measurement-dependent signal processing modules including state estimation program, control functionalities, contingency analysis, forecasting, and optimal power flow [165]. Therefore, the cyber attacks that change the system measurements can intrinsically force in wrong estimations within these modules, which can lead to potential systematic problems and cascading failures [222]. Apart from the cyber attacks, the measurement information is obviously lost during the transmission of the sensing information to the EMS. In the following

chapter, the packet dropouts is considered in the measurements for distributed state estimations.

Chapter 5

Adaptive-then-Combine Distributed State Estimation Considering Packet Dropouts

5.1 Introduction

The penetration of renewable distributed energy resources such as wind turbines has dramatically increased in distribution power networks. Due to the intermittent nature of winds, the wind power generation patterns vary, which may be a cause of risk to the distribution network operations. Consequently, it is intrinsically necessary to monitor the wind turbines in a distributed way. In the distributed state estimation, every local estimator computes the state information based on its own measurements and sends it to the global estimator for obtaining a reliable estimation [46], [42]. The distributed KF (DKF) based dynamic state estimation is widely used in the literature [48]. Nowadays, the consensus-based DKF methods have been proposed for sensor networks in [50], [141]. From the practical point of view, the diffusion strategy is widely used in the literature, where the global estimator linearly combines local results using a set of weighing factors [52], [53]. However, selecting an optimal weighting factor from the power system perspective is a quite difficult task. Furthermore, none of the above papers consider the packet losses in the distributed estimation process. Interestingly, the KF and linear quadratic Gaussian based optimal control for the networked controlled

smart grid is suggested in [20]. Even though it considers packet losses, it is only suitable for the centralized power system state estimation and control. In fact, the microgrid state estimation with an unreliable communication channel is not considered in the literature specifically in a distributed way.

This chapter presents an adaptive-then-combine distributed dynamic algorithm for monitoring the grid over lossy communication links between the wind turbines and energy management system. Firstly, the wind turbine is represented by a state-space linear model where sensors are deployed to the obtain the system state information. Based on the mean squared error principle, an adaptive approach is proposed to estimate the local state information. At the end, the global estimator is designed by combining local estimation results with weighting factors, which are calculated by minimizing the estimation error covariances based on semidefinite programming. Convergence of the proposed approach is analyzed based on the Lyapunov approach. The efficacy of the developed approach is verified using the wind turbine and IEEE 6-bus distribution system.

5.2 State-Space Representation of Wind Turbine

Usually, wind turbines are the most important and promising distributed energy resources which are contributing considerably to the world's power generation [223]. The wind turbine converts the wind kinetic energy into electrical energy. In other words, the power generated by the wind turbine is transferred to the grid through the inverter and step up transformer. To illustrate, the structure of a wind turbine is shown in Fig. 5.1 [12]. It consists of an aerodynamic rotor, drive train (mechanical part) and generator (electrical part) [224]. The drive train is the connection between the rotor and generator. The rotor of the turbine is driven by blades. The blade converts the wind kinetic energy into torque. Then the drive train converts it into high rotational speed to drive the generator [12], [225]. Generally, wind turbines are designed to generate high torque at predominately low wind speeds. The turbine output power P_a is determined as follows: [223]:

$$P_a = \frac{1}{2} s \rho v^3 = \frac{1}{2} \pi r^2 \rho v^3, \tag{5.1}$$

where $s = \pi r^2$ is the area covered by rotor, r is the rotor radius, ρ is the air density and v is the wind speed. As the wind speed v increases, the captured power rises as roughly the cube

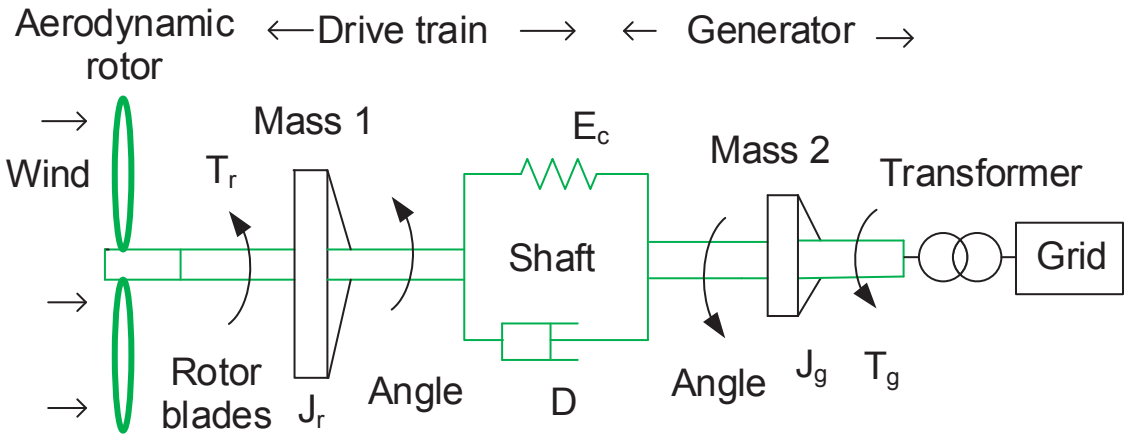

Figure 5.1: Two-mass wind turbine model [12].

of the speed. Normally, the power that can be converted by rotor is limited by the power coefficient [226], so the mechanical power P_{ext} extraction from the wind can be written as follows:

$$P_{ext} = \frac{1}{2} s\rho c_p(\chi, \beta) v^3, \tag{5.2}$$

where β is the rotor blade pitch angle and $c_p(\chi, \beta)$ is the power coefficient. The power coefficient is a nonlinear function of β and tip speed ratio $\chi = \omega_r r/v$, where ω_r is the rotor rotational speed.

Mostly, the mechanical power generated by the wind turbine is transferred from the rotor to the generator terminal. This connection is called the drive train, and the dynamic model of the drive train is represented by the following second order differential equations:

$$J_r \ddot{\theta}_r = T_r - T_s. \tag{5.3}$$

$$J_g \ddot{\theta}_g = T_s - T_g. \tag{5.4}$$

Here, J_r, T_r, and θ_r are the moment of inertia, torque and azimuth angle of the wind turbine, respectively. J_g, T_g, and θ_g are the moment of inertia, torque and azimuth angle of the generator, respectively. As shown in Fig. 5.1 the shaft of the wind turbine is represented by a two-mass model, where the first mass represents a low speed turbine, and the second mass represents a high speed generator. The two-mass connection is modelled as a spring and a damper [227], [228]. The equivalent shaft torque T_s is given by:

$$T_s = D(\dot{\theta}_r - \dot{\theta}_g) + E_c(\theta_r - \theta_g), \tag{5.5}$$

where D is the damping coefficient and E_c is the spring elastic coefficient of the shaft. Perturbation in the shaft torque δT_s can be expressed as follows:

$$\delta T_s = D(\delta\dot{\theta}_r - \delta\dot{\theta}_g) + E_c(\delta\theta_r - \delta\theta_g). \tag{5.6}$$

Using the Tailor series, T_r is expressed at the operating points ω_{r0}, v_0, and β_0 as follows:

$$T_r(\omega_r, v, \beta) = T_r(\omega_{r0}, v_0, \beta_0) + \delta T_r, \tag{5.7}$$

where $\delta T_r = \alpha\delta v + \zeta\delta w_r + \xi\delta\beta$ with $\alpha = \frac{\partial T_r}{\partial v}\mid_{(\omega_{r0},v_0,\beta_0)}$, $\zeta = \frac{\partial T_r}{\partial \omega_r}\mid_{(\omega_{r0},v_0,\beta_0)}$, and $\xi = \frac{\partial T_r}{\partial \beta}\mid_{(\omega_{r0},v_0,\beta_0)}$. The perturbation in rotor is expressed by the following second order differential equation:

$$J_r\delta\ddot{\theta}_r = T_r + \delta T_r - T_s - \delta T_s. \tag{5.8}$$

At the operating point, the perturbation in rotor and generator deviation are zero. Let T_{ro}, T_{s0}, and T_{g0} be the rotor, shaft, and generator torque at the operating points, respectively. Overall, the system dynamic can be represented by the following differential equations [12]:

$$J_r\delta\ddot{\theta}_r = \alpha\delta v + \zeta\delta\omega_r + \xi\delta\beta - D(\delta\dot{\theta}_r - \delta\dot{\theta}_g) - E_c(\delta\theta_r - \delta\theta_g). \tag{5.9}$$

$$J_g\delta\ddot{\theta}_g = D(\delta\dot{\theta}_r - \delta\dot{\theta}_g) + E_c(\delta\theta_r - \delta\theta_g) - \delta T_g. \tag{5.10}$$

For the sake of simplicity, define $x_1 = \delta\dot{\theta}_r = \delta\omega_r$, $x_2 = T_d = E_c(\delta\theta_r - \delta\theta_g)$, and $x_3 = \delta\dot{\theta}_g = \delta\omega_g$; then the system dynamic equations can be rewritten as follows:

$$J_r\dot{x}_1 = \alpha\delta v + \zeta x_1 + \xi\delta\beta - D(x_1 - x_3) - x_2. \tag{5.11}$$

$$\dot{x}_2 = E_c(x_1 - x_3). \tag{5.12}$$

$$J_g\dot{x}_3 = D(x_1 - x_3) + x_2 - \delta T_g. \tag{5.13}$$

If the generator runs at the rated speed, $\delta T_g = 0$, so the wind turbine model is expressed as a state-space linear equation as follows:

$$\dot{\mathbf{x}} = \mathbf{A}\mathbf{x} + \mathbf{B}u + \mathbf{G}n. \tag{5.14}$$

Here, the turbine system state $\mathbf{x} = [x_1\ x_2\ x_3]' = [\delta\omega_r, T_d, \delta\omega_g]'$, system input $u = \delta\beta$, $n = \delta v$, $\mathbf{A} = \begin{bmatrix} (\zeta - D)/J_r & -1/J_r & D/J_r \\ E_c & 0 & -E_c \\ D/J_g & 1/J_g & -D/J_g \end{bmatrix}$, $\mathbf{B} = [\xi/J_r\ 0\ 0]'$, and $\mathbf{G} = [\alpha/J_r\ 0\ 0]'$. Now, the wind turbine model is expressed as a discrete-time state-space linear equation as follows:

$$\mathbf{x}_{k+1} = \mathbf{A}_d\mathbf{x}_k + \mathbf{B}_d u_k + \mathbf{G}_d n_k, \tag{5.15}$$

where $\mathbf{A}_d = \mathbf{I} + \mathbf{A}\Delta t$, Δt is the discretization step size parameter, $\mathbf{B}_d = \mathbf{B}\Delta t$, $\mathbf{G}_d = \mathbf{G}\Delta t$, and n_k is the zero mean process noise whose covariance matrix is $\mathbf{Q}_k$.

5.3 Distributed Measurements and Packet Loss Model

This section describes the distributed observations and packet loss model.

5.3.1 Distributed Observation Stations

The proposed distributed estimation scheme considering packet losses is described in Fig. 5.2. In order to simplify the discussion, it is assumed there are $N = 4$ observation stations in the distribution power network[1]. The measurements of the system are described by a set of sensors as follows:

$$\mathbf{z}_k^i = \mathbf{C}^i \mathbf{x}_k + \mathbf{w}_k^i, \tag{5.16}$$

where $\mathbf{z}_k^i$ is the observation information for the i-th estimator at the time instant k, $\mathbf{C}^i$ is the observation matrix and $\mathbf{w}_k^i$ is the zero mean measurement noise whose covariance matrix is $\mathbf{R}_k^i$.

Mostly, the wind farm and EMS are located far away from each other [61], so there is an unreliable communication link among them. [37] illustrates that the sensing measurements are affected by communication impairments when they are transmitted through an unreliable communication network. Impairments, such as packet losses, lead to an unreliable link which can cause monitoring performance degradation and may give deceiving information to the utility operator [62], [63].

5.3.2 Packet Loss Model

Taking into account the packet loss, (5.16) can be written as follows:

$$\mathbf{y}_k^i = \alpha_k^i \mathbf{C}^i \mathbf{x}_k + \alpha_k^i \mathbf{w}_k^i, \tag{5.17}$$

where $\mathbf{y}_k^i$ is the received measurements under the condition of packet losses, and $\alpha_k^i \in \{0, 1\}$ is the Bernoulli distribution considered as a packet loss model in this work [20]. Mathemat-

[1]The proposed work can be easily extended to the generic case.

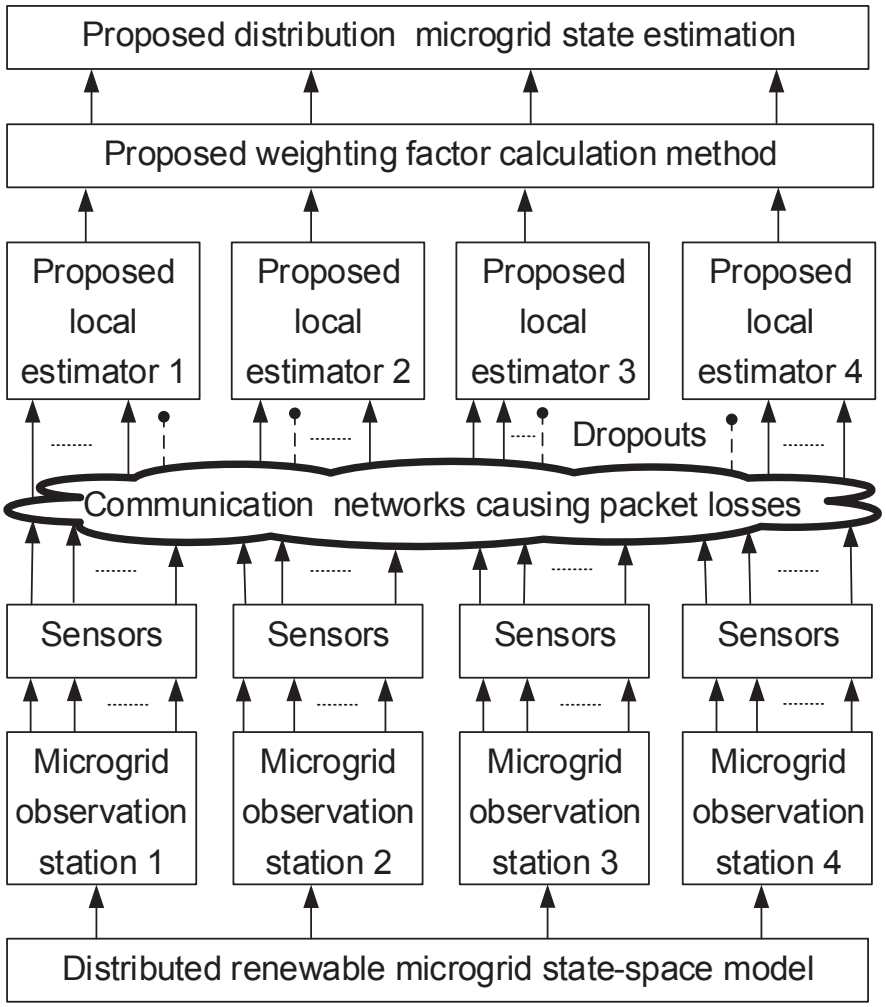

Figure 5.2: Proposed distributed microgrid state estimation considering packet losses.

ically, the packet loss can be modelled as follows:

$$\alpha_k^i = \begin{cases} 1, & \text{with probability of } \lambda_k^i \text{ ,} \\ 0, & \text{with probability of } 1 - \lambda_k^i \text{ ,} \end{cases}$$

where λ_k^i is the packet arrival rate reaching the estimator.

Remark: The assumption of a Bernoulli packet loss model is inappropriate when the communication channel is congested [20], [229], [230]. In a congested channel the packet loss occurs in bursts, and follows a two-state Markov chain model, also known as the Gilbert model [20], [229], [230].

5.4 Problem Formulation for Distributed Estimations

The local state estimation considering the packet losses is written as follows:

$$\hat{\mathbf{x}}^i_{k|k} = \hat{\mathbf{x}}^i_{k|k-1} + \mathbf{K}^i_k[\mathbf{y}^i_k - \alpha^i_k \mathbf{C}^i \hat{\mathbf{x}}^i_{k|k-1}]. \tag{5.18}$$

Here, $\hat{\mathbf{x}}^i_{k|k}$ is the local updated state estimation, $\hat{\mathbf{x}}^i_{k|k-1}$ is the predicted state estimation and $\mathbf{K}^i_k$ is the gain. The predicted state and error covariance are computed as follows:

$$\hat{\mathbf{x}}^i_{k|k-1} = \mathbf{A}_d \hat{\mathbf{x}}^i_{k-1|k-1} + \mathbf{B}_d u_k. \tag{5.19}$$

$$\mathbf{P}^i_{k|k-1} = \mathbf{A}_d \mathbf{P}^i_{k-1|k-1} \mathbf{A}'_d + \mathbf{G}_d \mathbf{Q}^i_k \mathbf{G}'_d. \tag{5.20}$$

Here, $\hat{\mathbf{x}}^i_{k-1|k-1}$ is the estimated state of the previous step and $\mathbf{P}^i_{k-1|k-1}$ is the error covariance matrix of the previous step. Based on the above filtering process, the first objective in this part of the study is to design the optimal gain $\mathbf{K}^i_k$. The second objective is to find a set of optimal weighting factors so that an accurate state estimation can be obtained by optimally combining the weighted local estimations. The final objective is to analyze the convergence of the proposed algorithm, so that the developed scheme can apply to the real-time applications. Driven by these motivations, the proposed scheme is demonstrated in Fig. 5.3. This research

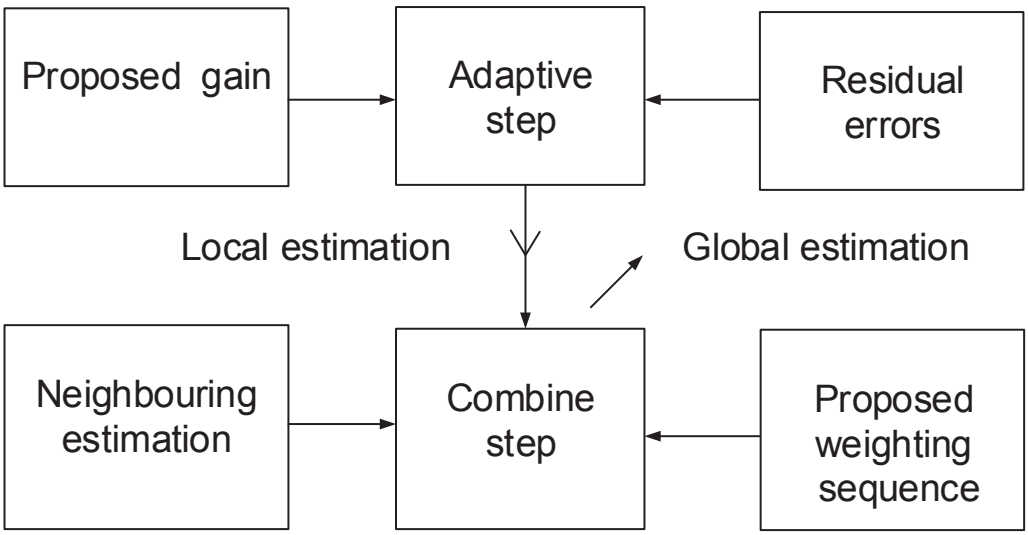

Figure 5.3: Problem formulation and proposed strategy.

tries to answer these questions by presenting an adaptive-then-combine distributed dynamic algorithm in the following section.

5.5 Proposed Adaptive-then-Combine Distributed Estimation Algorithm

Let, $\mathbf{e}^i$ denote the estimation error between the actual system state and estimated state of the i-th estimator, which can be expressed as follows:

$$\mathbf{e}^i_{k|k-1} = \mathbf{x}_k - \hat{\mathbf{x}}^i_{k|k-1}. \tag{5.21}$$

$$\mathbf{e}^i_{k|k} = \mathbf{x}_k - \hat{\mathbf{x}}^i_{k|k}. \tag{5.22}$$

Now substituting (5.18) into (5.22), one can obtain the following expression:

$$\begin{aligned}
\mathbf{e}^i_{k|k} &= \mathbf{x}_k - \hat{\mathbf{x}}^i_{k|k-1} - \mathbf{K}^i_k[\mathbf{y}^i_k - \alpha^i_k\mathbf{C}^i\hat{\mathbf{x}}^i_{k|k-1}] \\
&= \mathbf{x}_k - \hat{\mathbf{x}}^i_{k|k-1} - \mathbf{K}^i_k[\alpha^i_k\mathbf{C}^i\mathbf{x}_k + \alpha^i_k\mathbf{w}^i_k - \alpha^i_k\mathbf{C}^i\hat{\mathbf{x}}^i_{k|k-1}] \\
&= [\mathbf{I} - \alpha^i_k\mathbf{K}^i_k\mathbf{C}^i][\mathbf{x}_k - \hat{\mathbf{x}}^i_{k|k-1}] - \alpha^i_k\mathbf{K}^i_k\mathbf{w}^i_k \\
&= [\mathbf{I} - \alpha^i_k\mathbf{K}^i_k\mathbf{C}^i]\mathbf{e}^i_{k|k-1} - \alpha^i_k\mathbf{K}^i_k\mathbf{w}^i_k.
\end{aligned} \tag{5.23}$$

Now, the estimation error covariance matrix is defined by:

$$\mathbf{P}^i_{k|k} = E[\mathbf{e}^i_{k|k}\mathbf{e}'^i_{k|k}]. \tag{5.24}$$

By substituting (5.23) into (5.24), one can obtain the following estimation error covariance matrix as follows:

$$\mathbf{P}^i_{k|k} = \lambda^i_k[\mathbf{I} - \mathbf{K}^i_k\mathbf{C}^i]\mathbf{P}^i_{k|k-1}[\mathbf{I} - \mathbf{K}^i_k\mathbf{C}^i]' + \lambda^i_k\mathbf{K}^i_k\mathbf{R}^i_k\mathbf{K}'^i_k + (1-\lambda^i_k)\mathbf{P}^i_{k|k-1}. \tag{5.25}$$

For any two compatible matrices $\mathbf{X}$ and $\mathbf{Y}$, the following partial derivatives hold [51]:

$$\frac{\partial tr(\mathbf{YX})}{\partial \mathbf{X}} = \mathbf{Y}'. \tag{5.26}$$

$$\frac{\partial tr(\mathbf{XYX}')}{\partial \mathbf{X}} = \mathbf{X}(\mathbf{Y} + \mathbf{Y}'). \tag{5.27}$$

Taking the partial derivative of (5.25) with respect to $\mathbf{K}^i_k$ and applying (5.26) and (5.27) yields:

$$\frac{\partial[tr\mathbf{P}^i_{k|k}]}{\partial \mathbf{K}^i_k} = -2\lambda^i_k\mathbf{P}^i_{k|k-1}\mathbf{C}'^i + 2\lambda^i_k\mathbf{K}^i_k\mathbf{C}^i\mathbf{P}^i_{k|k-1}\mathbf{C}'^i + 2\lambda^i_k\mathbf{K}^i_k\mathbf{R}^i_k. \tag{5.28}$$

Setting $\frac{\partial[tr\mathbf{P}^i_{k|k}]}{\partial \mathbf{K}^i_k} = 0$, the optimal Kalman gain is given by:

$$\mathbf{K}^i_k = \mathbf{P}^i_{k|k-1}\mathbf{C}'^i[\mathbf{C}^i\mathbf{P}^i_{k|k-1}\mathbf{C}'^i + \mathbf{R}^i_k]^{-1}. \tag{5.29}$$

Next, an optimal linear estimator to fuse the local state estimations is designed as follows:

$$\hat{\mathbf{x}}^{g}_{k|k} = \sum_{i=1}^{N} w_k^{(i)} \hat{\mathbf{x}}^{i}_{k|k}. \tag{5.30}$$

Here, $\hat{\mathbf{x}}^{i}_{k|k}$ is the local estimation and $w_k^{(i)}$ is the weighting factor to be designed. It can be observed that designing an optimal set of weighing factors plays a vital role for the distributed state estimation in the context of smart grids. In order to find the optimal weighting factors, this study proposes the following optimization process (assuming $N = 4$):

$$\begin{aligned}
&\text{minimise } s \\
&\text{subject to } (w_k^{(1)})^2 d^{(1)}_{k|k} + (w_k^{(2)})^2 d^{(2)}_{k|k} + (w_k^{(3)})^2 d^{(3)}_{k|k} + (w_k^{(4)})^2 d^{(4)}_{k|k} \leq s, && (5.31)\\
&\qquad w_k^{(1)} + w_k^{(2)} + w_k^{(3)} + w_k^{(4)} = 1, && (5.32)
\end{aligned}$$

where $d^{(i)}_{k|k} = tr(\mathbf{P}^{i}_{k|k})$, and s is an auxiliary variable for minimizing the trace of the global estimator error covariance. Consequently, the error covariance is minimized, so that the estimated states match the true states. By using the SDP variable s, the distributed estimation problem is converted to a convex problem which can be solved effectively and efficiently. Based on Schur's complement, (5.31) can be formulated as a linear matrix inequality:

$$\begin{bmatrix}
-s & w_k^{(1)} & w_k^{(2)} & w_k^{(3)} & w_k^{(4)} \\
w_k^{(1)} & -(d^{(1)}_{k|k})^{-1} & 0 & 0 & 0 \\
w_k^{(2)} & 0 & -(d^{(2)}_{k|k})^{-1} & 0 & 0 \\
w_k^{(3)} & 0 & 0 & -(d^{(3)}_{k|k})^{-1} & 0 \\
w_k^{(4)} & 0 & 0 & 0 & -(d^{(4)}_{k|k})^{-1}
\end{bmatrix} \leq 0. \tag{5.33}$$

Finally, one can formulate the proposed optimization problem as follows:

$$\begin{aligned}
&\text{minimise } s \\
&\text{subject to } Hold\ (5.32),\ and\ (5.33).
\end{aligned} \tag{5.34}$$

In summary, the proposed distributed state estimation algorithm in the context of smart grids is summarized in Table 5.1. Note that the error covariances between different estimations are assumed to be zero; consideration of the theses error covariances and their scalar values of weighting factors are well-studied in [143], [231], [232]. Now the question is how can we guarantee the convergence of the proposed state estimation method.

Table 5.1: Proposed distributed state estimation algorithm.

Initialization for observation station i:

Input: $\hat{\mathbf{x}}^i_{0|0}$ and $\mathbf{P}^i_{0|0}$.

Take the local measurements $\mathbf{y}_i$ from the observation stations.

1: Predict the system state and covariance matrix:

$\hat{\mathbf{x}}^i_{k|k-1} = \mathbf{A}_d\hat{\mathbf{x}}^i_{k-1|k-1} + \mathbf{B}_d u_k,$

$\mathbf{P}^i_{k|k-1} = \mathbf{A}_d\mathbf{P}^i_{k-1|k-1}\mathbf{A}'_d + \mathbf{G}_d\mathbf{Q}^i_k\mathbf{G}'_d.$

2: Estimate the local system state and covariance matrix:

$\mathbf{K}^i_k = \mathbf{P}^i_{k|k-1}\mathbf{C}'^i[\mathbf{C}^i\mathbf{P}^i_{k|k-1}\mathbf{C}'^i + \mathbf{R}^i_k]^{-1}.$

$\hat{\mathbf{x}}^i_{k|k} = \hat{\mathbf{x}}^i_{k|k-1} + \mathbf{K}^i_k[\mathbf{y}^i_k - \boldsymbol{\alpha}^i_k\mathbf{C}^i\hat{\mathbf{x}}^i_{k|k-1}].$

$\hat{\mathbf{P}}^i_{k|k} = \lambda^i_k[\mathbf{I} - \mathbf{K}^i_k\mathbf{C}^i]\mathbf{P}^i_{k|k-1}[\mathbf{I} - \mathbf{K}^i_k\mathbf{C}^i]' + \lambda^i_k\mathbf{K}^i_k\mathbf{R}^i_k\mathbf{K}'^i_k + (1-\lambda^i_k)\mathbf{P}^i_{k|k-1}.$

3: Diffusion step:

$\hat{\mathbf{x}}^g_{k|k} = \sum_{i=1}^N w^{(i)}_k\hat{\mathbf{x}}^i_{k|k},$

where $w^{(i)}_k$ is determined by solving (5.34).

5.6 Convergence Analysis

From the engineering perspective, the discrete-time system is easy to implement in the digital platforms, while the continuous system is easy to analyze from the mathematical point of view [233]. Motivated by this realistic dilemma and similar to [50], the convergence analysis of the adaptive-then-combine algorithm is completed based on the convergence analysis of the continuous system. Similar to the discrete-time system, the estimator applies the following step:

$$\dot{\hat{\mathbf{x}}}^i = \mathbf{A}\hat{\mathbf{x}}^i + \mathbf{B}u + \mathbf{K}^i[\mathbf{y}^i - \boldsymbol{\alpha}^i\mathbf{C}^i\hat{\mathbf{x}}^i]. \tag{5.35}$$

The estimation error $\mathbf{e}^i$ can be expressed as follows:

$$\mathbf{e}^i = \mathbf{x} - \hat{\mathbf{x}}^i. \tag{5.36}$$

By direct differentiating (5.36), with (5.14) and (5.17), the estimation error dynamics is in the following form:

$$\begin{aligned}\dot{\mathbf{e}}^i &= \dot{\mathbf{x}} - \dot{\hat{\mathbf{x}}}^i \\ &= \mathbf{A}\mathbf{x} + \mathbf{B}u + \mathbf{G}n - \mathbf{A}\hat{\mathbf{x}}^i - \mathbf{B}u - \alpha^i\mathbf{K}^i[\mathbf{C}^i\mathbf{x} + \mathbf{w}^i - \mathbf{C}^i\hat{\mathbf{x}}^i] \\ &= (\mathbf{A} - \alpha^i\mathbf{K}^i\mathbf{C}^i)\mathbf{e}^i + \mathbf{G}n - \alpha^i\mathbf{K}^i\mathbf{w}^i.\end{aligned} \tag{5.37}$$

The error covariance matrix under the condition of losses is written as follows:

$$\begin{aligned}\dot{\mathbf{P}}^i &= (\mathbf{A}-\lambda^i\mathbf{K}^i\mathbf{C}^i)\mathbf{P}^i+\mathbf{P}^i(\mathbf{A}-\lambda^i\mathbf{K}^i\mathbf{C}^i)'+\mathbf{GQG}'+\lambda^i\mathbf{K}^i\mathbf{R}^i\mathbf{K}'^i \\ &= \mathbf{AP}^i+\mathbf{P}^i\mathbf{A}'+\mathbf{GQG}'-\lambda^i\mathbf{K}^i\mathbf{C}^i\mathbf{P}^i-\lambda^i\mathbf{P}^i\mathbf{C}'^i\mathbf{K}'^i+\lambda^i\mathbf{K}^i\mathbf{R}^i\mathbf{K}'^i. \end{aligned} \tag{5.38}$$

Taking the partial derivative of (5.38) with respect to $\mathbf{K}^i$ and applying (5.26) and (5.27) yields:

$$\frac{\partial[tr\dot{\mathbf{P}}^i]}{\partial\mathbf{K}^i} = -2\lambda^i\mathbf{P}^i\mathbf{C}'^i + 2\lambda^i\mathbf{K}^i\mathbf{R}^i. \tag{5.39}$$

Setting $\frac{\partial[tr\dot{\mathbf{P}}^i]}{\partial\mathbf{K}^i} = 0$, the optimal Kalman gain is given by:

$$\mathbf{K}^i = \mathbf{P}^i\mathbf{C}'^i(\mathbf{R}^i)^{-1}. \tag{5.40}$$

Substituting (5.40) into (5.38), one can obtain the following error covariance matrix:

$$\begin{aligned}\dot{\mathbf{P}}^i &= \mathbf{AP}^i + \mathbf{P}^i\mathbf{A}' + \mathbf{GQG}' - \lambda^i\mathbf{P}^i\mathbf{C}'^i(\mathbf{R}^i)^{-1}\mathbf{C}^i\mathbf{P}^i - \\ &\quad \lambda^i\mathbf{P}^i\mathbf{C}'^i(\mathbf{R}^i)^{-1}\mathbf{C}^i\mathbf{P}^i + \lambda^i\mathbf{P}^i\mathbf{C}'^i(\mathbf{R}^i)^{-1}\mathbf{C}^i\mathbf{P}^i \\ &= \mathbf{AP}^i + \mathbf{P}^i\mathbf{A}' + \mathbf{GQG}' - \lambda^i\mathbf{P}^i\mathbf{C}'^i(\mathbf{R}^i)^{-1}\mathbf{C}^i\mathbf{P}^i. \end{aligned} \tag{5.41}$$

In order to analyze the stability of the proposed approach, considering only the nominal system of (5.37) gives:

$$\dot{\mathbf{e}}^i = (\mathbf{A} - \alpha^i\mathbf{K}^i\mathbf{C}^i)\mathbf{e}^i. \tag{5.42}$$

Consider the following Lyapunov function:

$$V = \sum_{i=1}^{N}\mathbf{e}'^i(\mathbf{P}^i)^{-1}\mathbf{e}^i. \tag{5.43}$$

Now taking the partial derivative and expectation of (5.43) and using (5.40), (5.41) and (5.42), the Lyapunov function can be written as follows:

$$\begin{aligned}\dot{V} &= \sum_{i=1}^{N}\{\dot{\mathbf{e}}'^i(\mathbf{P}^i)^{-1}\mathbf{e}^i + \mathbf{e}'^i(\mathbf{P}^i)^{-1}\dot{\mathbf{e}}^i - \mathbf{e}'^i(\mathbf{P}^i)^{-1}\dot{\mathbf{P}}^i(\mathbf{P}^i)^{-1}\mathbf{e}^i\} \\ &= \sum_{i=1}^{N}\mathbf{e}'^i[-\lambda^i\mathbf{C}'^i(\mathbf{R}^i)^{-1}\mathbf{C}^i - \lambda^i\mathbf{C}'^i(\mathbf{R}^i)^{-1}\mathbf{C}^i - \\ &\quad (\mathbf{P}^i)^{-1}\mathbf{GQG}'(\mathbf{P}^i)^{-1} + \lambda^i\mathbf{C}'^i(\mathbf{R}^i)^{-1}\mathbf{C}^i]\mathbf{e}^i \\ &= -\sum_{i=1}^{N}\mathbf{e}'^i[\lambda^i\mathbf{C}'^i(\mathbf{R}^i)^{-1}\mathbf{C}^i + (\mathbf{P}^i)^{-1}\mathbf{GQG}'(\mathbf{P}^i)^{-1}]\mathbf{e}^i < 0. \end{aligned} \tag{5.44}$$

The inequality (5.44) shows that the Lyapunov function is gradually decreasing, so the error function (5.42) is asymptotically stable. Consequently, the estimated state $\hat{\mathbf{x}}^i$ converges to the actual system state $\mathbf{x}$. This shows the proposed filtering algorithm is convergent, which is significantly important for real-time applications. For testing the performance of the proposed distributed state estimation approach, the simulation results are presented in the following section.

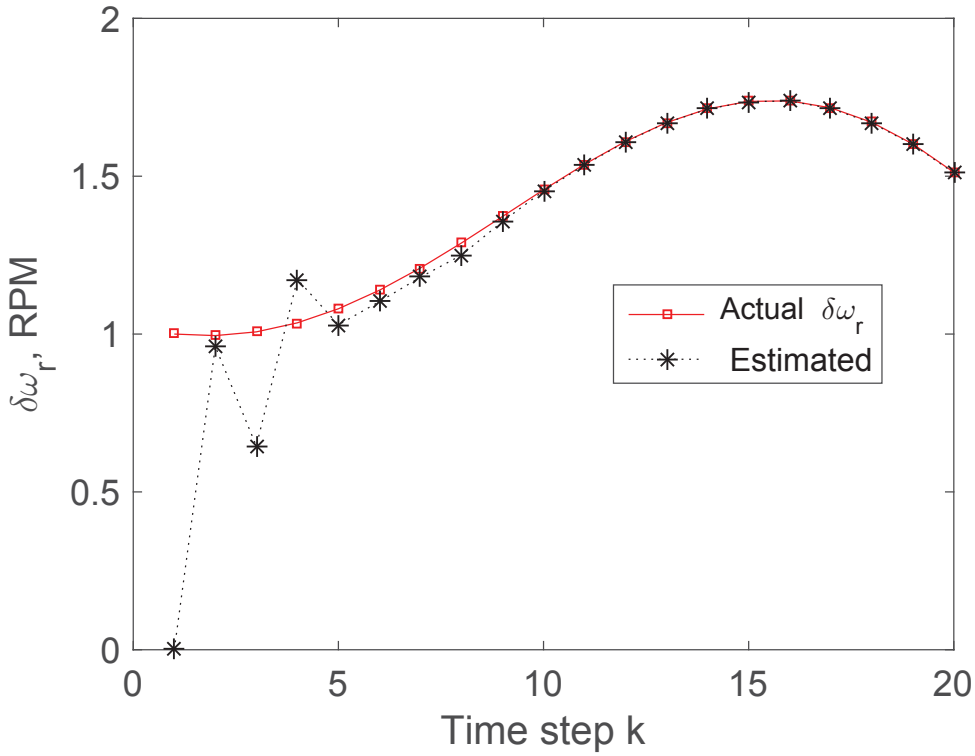

Figure 5.4: Rotor speed deviation $\delta\omega_r$ and its estimation.

5.7 Case Studies and Discussion Using the Adaptive-then-Combine Algorithm

In this section, the proposed algorithm is tested, and the results are demonstrated using the wind turbine and IEEE 6-bus distribution system, respectively. The system parameters are shown in Table 5.2 [12], [225]. The simulation has been carried out using the Matlab, Matpower [220] and YALMIP softwares [213].

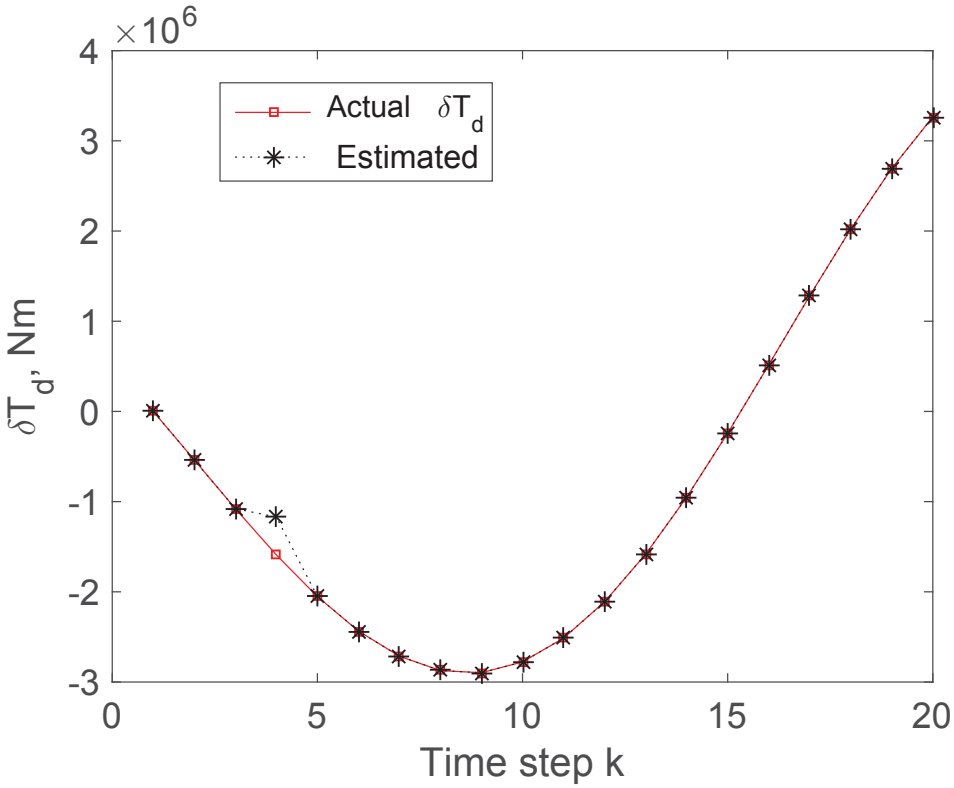

Figure 5.5: Drive-train torsional spring force deviation δT_d and its estimation.

5.7.1 Estimation Results Based on the Wind Turbine

Figures 5.4-5.6 show the system states versus time step for the wind turbine. It can be seen that the proposed method can estimate the turbine states with a reasonable accuracy. This is because the local estimators are able to track the system states after rejecting the statistical impairments as much as possible. In other words, the mean squared error based designed gain provides accurate influence to remove the system impairments. Then the global estimator properly calculates the optimal weighting factors by minimizing the estimated error covariances. Consequently, the fusion estimator can greatly reduce the global estimation error, so the estimated state converges to the true system state. Basically, the proposed SDP based estimator can efficiently solve the distributed state estimation problem to find the optimal solution. It can be seen from Fig.5.4 that the proposed method requires a maximum of 0.1 second $(k \times \Delta t = 10 \times 0.01)$ to estimate the system state. Technically, it means that the developed approach requires much less time compared with the standard estimation time of 1 second [47]. Note that small fluctuations come from system impairments, but this does not

Table 5.2: Simulation parameters.

Symbols	Values	Symbols	Values
ω_{ro}	42 RPM	v_0	$18\ m/s$
β_0	$12\ deg$	E_c	$2.691 \times 10^7 Nm/deg.$
r	21.65 m	D	0 Nm/deg-s
J_r	3.2175×10^5	J_g	6.4103×10^4
Δt	0.01	λ^1	0.93
λ^2	0.95	λ^3	0.98
λ^4	0.97	$\mathbf{R}^1$	0.0001*$\mathbf{I}$
$\mathbf{R}^2$	0.00012*$\mathbf{I}$	$\mathbf{R}^3$	0.00014*$\mathbf{I}$
$\mathbf{R}^4$	0.00015*$\mathbf{I}$	$\mathbf{Q}^i$	0.00001*$\mathbf{I}$

affect the estimation accuracy. In other words, the estimation result would not mislead the utility operator even though there are missing measurements. As this is an open-loop system without control, the system dynamics cannot be guaranteed to be stable. As can be seen in the simulation results, the state is unstable which is determined by the open-loop system state matrix **A**.

5.7.2 Estimation Results Based on the IEEE 6-Bus System

The IEEE 6-bus testing system is employed to demonstrate the performance of the proposed approach. A single-line diagram of the IEEE 6-bus distribution test system is depicted in Fig. 5.7. The system has three generators on buses 1, 2 and 6 and three loads on buses 3, 4 and 5. It has the total generation capacity 217.88 MW and load capacity 210 MW. The nominal phase angles and bus voltage magnitudes are shown in Table 5.3.

Table 5.3: The nominal values of the IEEE 6-bus system.

Bus	Θ_N	V_N	Bus	Θ_N	V_N
1	0	1.050	4	-4.196	0.989
2	-3.671	1.050	5	-5.276	0.985
3	-4.273	1.070	6	-5.947	1.004

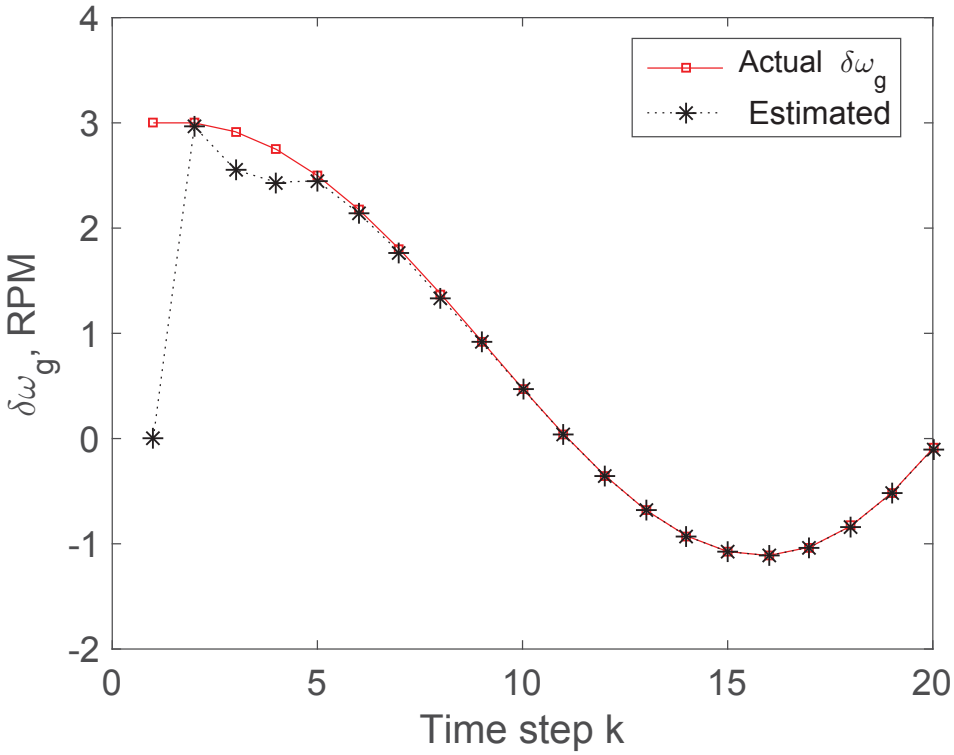

Figure 5.6: Generator speed deviation $\delta\omega_g$ and its estimation.

It is evident from the dynamic responses in Figs. 5.8-5.9 that the estimation results match the actual system states within a few time steps. This clearly implies that the explored method can reliably reject the system impairments and accurately monitor the system states.

5.8 Summary

The increasing penetration of renewable energy presents a series of technical challenges in power system operations. To monitor such a system under lossy network conditions, this study proposes an adaptive-then-combine distributed dynamic state estimation algorithm based on the mean squared error and SDP approaches. After estimating the local information, the global estimator combines the locally estimated results with a set of weighting factors, which are calculated by the proposed convex optimization algorithm. The convergence of the developed algorithm is proved. Simulation results demonstrate that the developed scheme can well estimate the system states. Overall, these findings are valuable for

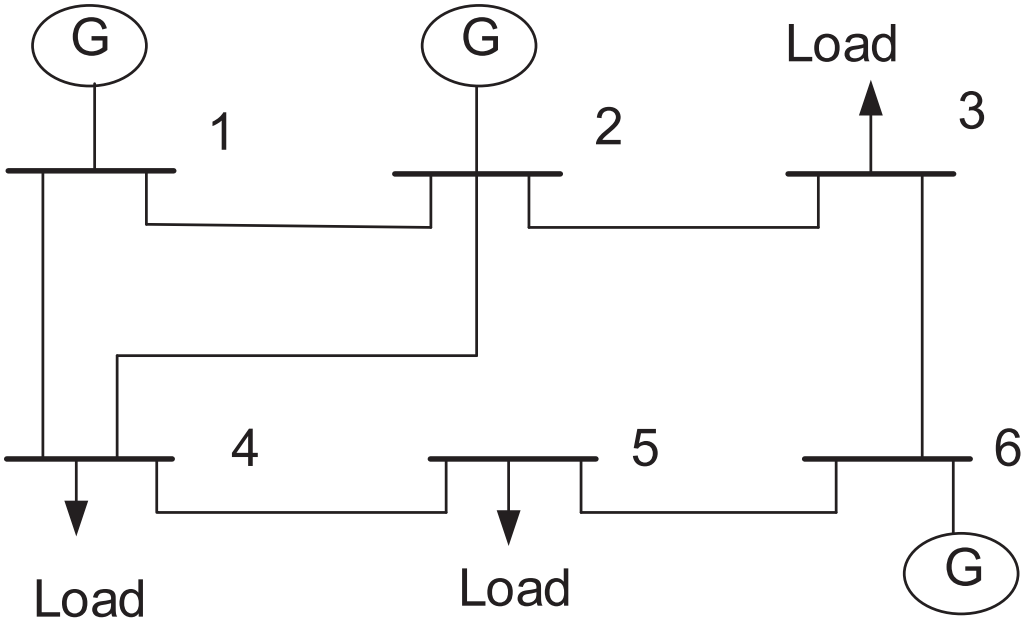

Figure 5.7: Single-line diagram of the 6-bus power distribution system [13].

green communication, households, and provides the knowledge towards smart EMS design.

It can be seen that the generated wind turbine states are not stable due to open-loop characteristic of the system without controller. This will create a problem for microgrid operations and maintaining grid stability. Furthermore, the distribution power sub-systems are interconnected to each other. To address this problem, the distributed state estimation and stabilization algorithms for interconnected systems are developed in the following chapter.

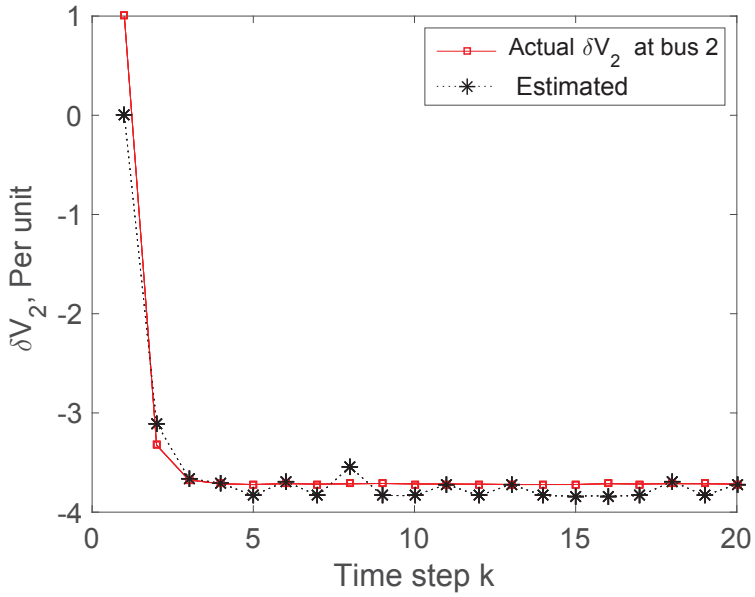

Figure 5.8: Voltage deviation δV_2 and its estimation using the IEEE 6-bus.

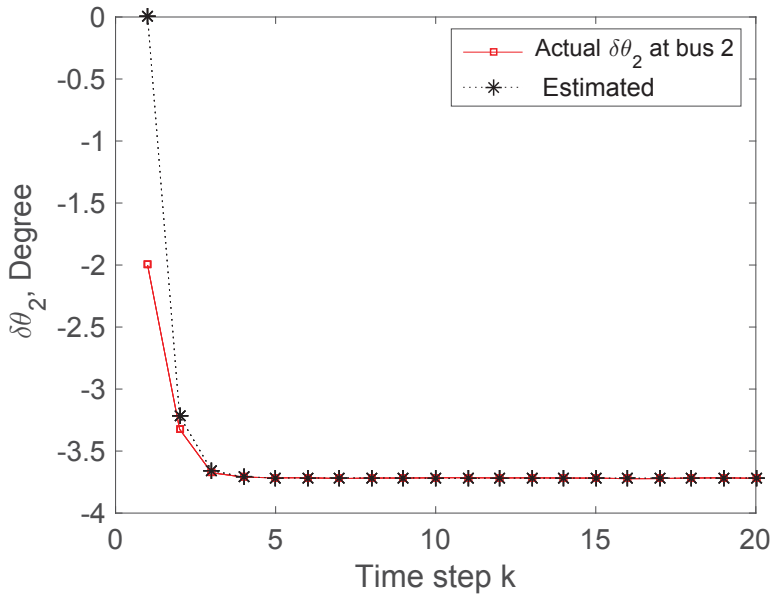

Figure 5.9: Phase angle deviation $\delta\theta_2$ and its estimation using the IEEE 6-bus.

Chapter 6

Distributed Estimation and Control for Interconnected Systems over a Lossy Network

6.1 Introduction

Generally speaking, the industrial domain application becomes more and more distributed due to advanced information and communication technologies [234], [235]. In other words, the automation system is mostly designed based on the distributed architecture and its signal processing algorithms. As the measurements are locally processed, it can accurately handle more data, offer flexible communication infrastructure, deliver required functionality and services in sustainable and efficient ways, for example, monitoring and controlling the power system incorporating microgrids in a distributed way. As the power substations and energy management system are generally far away, so the measurements are normally lost in the communication channel [62], [63]. It is therefore imperative to estimate the power system states and apply a suitable control strategy, so the system can operate properly [20]. In other words, the power network intrinsically requires to expect stability over a lossy communication channel between the microgrid and EMS.

There is a wealth of research related to the power system state estimation in a distributed way. To begin with, a distributed weighted least square state estimation method using ad-

ditive Schwarz domain decomposition technique is proposed in [236]. This decomposition divides the data set into several subsets to reduce the execution time. Unfortunately, it is assumed that the communication is perfect with no measurement losses. A KF based state estimation via wireless sensor networks over fading channels is presented in [172]. This kind of centralized estimation technique is generally not only in need of huge amount of communication and computation resources but also vulnerable to the central point failures which may lead to massive blackouts. To deal with the communication impairments, a distributed fusion based KF algorithm for sensor networks is developed in [237], [238]. The fusion centre linearly combines the local estimators through a set of designed weighting factors. In order to obtain a suitable set of weighting factors, a weighted density function based recursive algorithm is proposed under the condition of reliable communication channels [239]. In order to accommodate the effects of random delay in measurements, an extended KF based power system state estimation method is proposed in [240]. All of the aforementioned papers consider the centralised estimation or reliable communication channel.

In contrast to the traditional centralised power system state estimation methods, this study investigates the interconnected filtering problem for distributed dynamic state estimations considering packet losses. Basically, the sensing information is transmitted to the energy management system through a lossy communication network where measurements are lost. The proposed estimator is based on the mean squared error between the actual state and its estimate. To obtain the distributed estimation, the optimal local and neighbouring gains are computed to reach a consensus estimation after exchanging their information with the neighbouring estimators. Afterwards, the convergence of the developed algorithm is theoretically proved. Finally, a distributed controller is designed based on the SDP approach. The efficacy of the proposed approaches is demonstrated by applying it to the microgrid.

6.2 Observation and Packet Losses

Consider the following discrete-time system:

$$\mathbf{x}_{k+1} = \mathbf{A}_d\mathbf{x}_k + \mathbf{B}_d\mathbf{u}_k + \mathbf{n}_k, \tag{6.1}$$

where $\mathbf{x}_k$ is the system state at time instant k, $\mathbf{u}_k$ is the control effort and $\mathbf{n}_k$ is process noise whose covariance matrix is $\mathbf{Q}_k$. Generally speaking, the state variable defines the

system's operating conditions of a power system such as bus voltages, branch currents and power [70]. Basically, $\mathbf{A}_d$ is the system state matrix and $\mathbf{B}_d$ represents the system input matrix. These matrices can be obtained by a set of algebraic equations, which are obtained using Kirchhoff's laws. For instance, the system state matrix $\mathbf{A}_d$ and input matrix $\mathbf{B}_d$ are obtained from the microgrid using Kirchhoff's voltage law and Kirchhoff's current law with the given circuit parameters such as resistors, capacitors and inductors [6], [17].

The system measurements are obtained by a set of sensors as follows:

$$\mathbf{z}_k^i = \mathbf{C}^i \mathbf{x}_k + \mathbf{w}_k^i, \tag{6.2}$$

where $\mathbf{z}_k^i$ is the observation information by the i-th estimator at time instant k, $\mathbf{C}^i$ is the observation matrix and $\mathbf{w}_k^i$ is the measurement noise with zero mean and the covariance matrix $\mathbf{R}_k^i$. Realistically, the sensing measurements transmit through a lossy communication network which causes packet dropouts. Taking into account the packet loss, (6.2) can be written as follows:

$$\mathbf{y}_k^i = \alpha_k^i \mathbf{C}^i \mathbf{x}_k + \alpha_k^i \mathbf{w}_k^i, \tag{6.3}$$

where $\mathbf{y}_k^i$ is the received measurements under the condition of packet losses, and $\alpha_k^i \in \{0, 1\}$ is the Bernoulli distribution modelled as follows [63]:

$$\alpha_k^i = \begin{cases} 1, & \text{with probability of } \lambda_k^i, \\ 0, & \text{with probability of } 1 - \lambda_k^i, \end{cases}$$

where λ_k^i is the packet arrival rate reaching the estimator. Inspired by [241], [141], [242], and for the sake of mathematical simplicity, it assumes that the observation matrices and packet loss distribution are identical to each other. The assumptions are probably due to the fact that the distributed estimators are not far away from the power sub-stations but as usual information transmits through an unreliable network. Secondly, the sensors have limited power and processing capability. Thirdly, the service provider deploys similar kinds of sensors in the distribution power network. Finally, from Eq. (6.3) it can be seen that the measurement noises are different from each observation point, so only for the sake of mathematical simplicity in Eq. (6.7), it assumes that the observation matrices are identical to each other.

6.3 Problem Formulation for Interconnected Systems

Generally speaking, the filtering infrastructure is interconnected with each other to know the operating conditions of the distribution power network. For instance, the proposed interconnected filtering scheme is depicted in Fig. 6.1. It can be seen that the sensing information at the sub-systems can be shared with the connected estimators. Considering the packet losses,

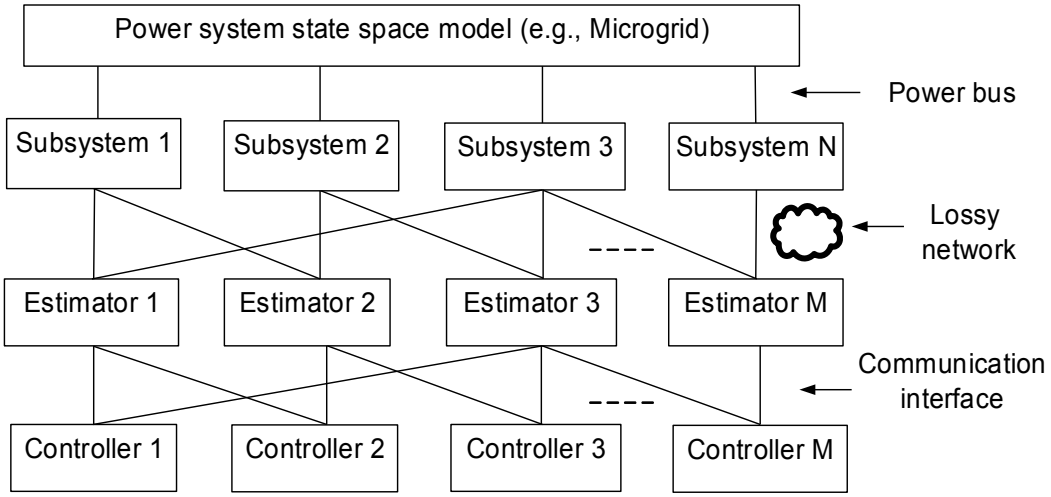

Figure 6.1: Proposed interconnected filtering scheme.

the proposed distributed dynamic state estimator is written as follows:

$$\hat{\mathbf{x}}^i_{k|k} = \hat{\mathbf{x}}^i_{k|k-1} + \mathbf{K}^i_k[\mathbf{y}^i_k - \alpha_k \mathbf{C}\hat{\mathbf{x}}^i_{k|k-1}] + \mathbf{L}^i_k \sum_{j \in N^i_k} [\mathbf{y}^j_k - \alpha_k \mathbf{C}\hat{\mathbf{x}}^i_{k|k-1}]. \tag{6.4}$$

Here, $\hat{\mathbf{x}}^i_{k|k}$ is the updated state estimation at the i-th estimator, $\hat{\mathbf{x}}^i_{k|k-1}$ is the predicted states estimate, $\mathbf{K}^i_k$ is the local gain, $\mathbf{L}^i_k$ is the neighbouring gain and N^i_k denotes the set of neighbouring estimators. Based on the above modelling structure, the first objective in this part of the study is to design the optimal gains $\mathbf{K}^i_k$ and $\mathbf{L}^i_k$, so that the estimated state converges to the actual system state.

6.4 Proposed Distributed Estimator and Controller

This section derives a distributed state estimation and control under the condition of packet losses. Based on the mean squared error principle, the optimal local and neighbouring gains

are determined to obtain a distributed dynamic state estimation in the context of smart grids. Each estimator exchanges information with the neighbouring estimators for reaching a consensus estimation even though there are packet losses. The convergence of the developed approach is theoretically proved based on the continuous-time domain analysis due to its mathematical simplicity. For proper operation and maintaining the stability of the microgrid, a distributed controller is proposed based on the SDP approach. The designed sparse feedback gain is calculated by an iterative optimization process which is less conservative as it effectively and efficiently computes the Lyapunov matrix $\mathbf{P}$ with no structure constraints on it.

6.4.1 Proposed Distributed Estimation Algorithm

Let $\mathbf{e}^i$ denote the estimation error between the actual state and estimated state of the i-th estimator:

$$\mathbf{e}^i_{k|k-1} = \mathbf{x}_k - \hat{\mathbf{x}}^i_{k|k-1}. \tag{6.5}$$

$$\mathbf{e}^i_{k|k} = \mathbf{x}_k - \hat{\mathbf{x}}^i_{k|k}. \tag{6.6}$$

Let $n^i_k = n^i_k(N^i_k)$ represents the cardinality of N^i_k. Substituting (6.4) into (6.6), and using (6.3) one can obtain:

$$\begin{aligned}\mathbf{e}^i_{k|k} &= \mathbf{x}_k - \hat{\mathbf{x}}^i_{k|k-1} - \mathbf{K}^i_k[\mathbf{y}^i_k - \alpha_k\mathbf{C}\hat{\mathbf{x}}^i_{k|k-1}] - \mathbf{L}^i_k\sum_{l\in N^i_k}[\mathbf{y}^l_k - \alpha_k\mathbf{C}\hat{\mathbf{x}}^i_{k|k-1}] \\ &= [\mathbf{I} - \alpha_k\mathbf{K}^i_k\mathbf{C} - \alpha_k n^i_k\mathbf{L}^i_k\mathbf{C}]\mathbf{e}^i_{k|k-1} - \alpha_k\mathbf{K}^i_k\mathbf{w}^i_k - \alpha_k\mathbf{L}^i_k\sum_{l\in N^i_k}\mathbf{w}^l_k.\end{aligned} \tag{6.7}$$

Now the estimation error covariance matrix $\mathbf{P}^i_{k|k}$ is defined by:

$$\mathbf{P}^i_{k|k} = E[\mathbf{e}^i_{k|k}\mathbf{e}'^i_{k|k}]. \tag{6.8}$$

Substituting (6.7) into (6.8), one can obtain:

$$\begin{aligned}\mathbf{P}^i_{k|k} &= \lambda_k[\mathbf{I} - \mathbf{K}^i_k\mathbf{C} - n^i_k\mathbf{L}^i_k\mathbf{C}]\mathbf{P}^i_{k|k-1}[\mathbf{I} - \mathbf{K}^i_k\mathbf{C} - n^i_k\mathbf{L}^i_k\mathbf{C}]' \\ &\quad + (\mathbf{I} - \lambda_k)\mathbf{P}^i_{k|k-1} + \lambda_k\mathbf{K}^i_k\mathbf{R}^i_k\mathbf{K}'^i_k + \lambda_k\mathbf{L}^i_k\sum_{l\in N^i_k}\mathbf{R}^l_k\mathbf{L}'^i_k.\end{aligned} \tag{6.9}$$

Here, $\mathbf{P}^i_{k|k-1} = E[\mathbf{e}^i_{k|k-1}\mathbf{e}'^i_{k|k-1}]$. For any two compatible matrices $\mathbf{X}$ and $\mathbf{Y}$, the following partial derivatives hold:

$$\frac{\partial tr(\mathbf{YX})}{\partial \mathbf{X}} = \mathbf{Y}'. \tag{6.10}$$

$$\frac{\partial tr(\mathbf{XYX}')}{\partial \mathbf{X}} = \mathbf{X}(\mathbf{Y} + \mathbf{Y}'). \tag{6.11}$$

In order to find the optimal gain $\mathbf{K}^i_k$, taking the partial derivative of $\mathbf{P}^i_{k|k}$ in (6.9) with respect to $\mathbf{K}^i_k$ and applying (6.10), (6.11) yields:

$$\frac{\partial[tr\mathbf{P}^i_{k|k}]}{\partial \mathbf{K}^i_k} = -2\lambda_k(\mathbf{I} - n^i_k\mathbf{L}^i_k\mathbf{C})\mathbf{P}^i_{k|k-1}\mathbf{C}' + 2\lambda_k\mathbf{K}^i_k(\mathbf{C}\mathbf{P}^i_{k|k-1}\mathbf{C}' + \mathbf{R}^i_k). \tag{6.12}$$

Now putting $\frac{\partial[tr\mathbf{P}^i_{k|k}]}{\partial \mathbf{K}^i_k} = 0$ in (6.12), the optimal local gain $\mathbf{K}^i_k$ is given by:

$$\mathbf{K}^i_k = [\mathbf{P}^i_{k|k-1}\mathbf{C}' - n^i_k\mathbf{L}^i_k\mathbf{C}\mathbf{P}^i_{k|k-1}\mathbf{C}'][\mathbf{C}\mathbf{P}^i_{k|k-1}\mathbf{C}' + \mathbf{R}^i_k]^{-1}. \tag{6.13}$$

Similarly, taking the partial derivative of (6.9) with respect to $\mathbf{L}^i_k$ and applying (6.10), (6.11) obtains:

$$\frac{\partial[tr\mathbf{P}^i_{k|k}]}{\partial \mathbf{L}^i_k} = -2n^i_k\lambda_k(\mathbf{I} - \mathbf{K}^i_k\mathbf{C})'\mathbf{P}^i_{k|k-1}\mathbf{C} + 2(n^i_k)^2\lambda_k\mathbf{L}^i_k\mathbf{C}\mathbf{P}^i_{k|k-1}\mathbf{C}' + 2\lambda_k\mathbf{L}^i_k\sum_{l\in N^i_k}\mathbf{R}^l_k. \tag{6.14}$$

Setting $\frac{\partial[tr\mathbf{P}^i_{k|k}]}{\partial \mathbf{L}^i_k} = 0$ in (6.14), $\mathbf{L}^i_k$ is derived as follows:

$$\mathbf{L}^i_k = [n^i_k\mathbf{P}^i_{k|k-1}\mathbf{C}' - n^i_k\mathbf{K}^i_k\mathbf{C}\mathbf{P}^i_{k|k-1}\mathbf{C}'][(n^i_k)^2\mathbf{C}\mathbf{P}^i_{k|k-1}\mathbf{C}' + \sum_{l\in N^i_k}\mathbf{R}^l_k]^{-1}. \tag{6.15}$$

For simplicity, define $\mathbf{H}^i_k = \mathbf{C}\mathbf{P}^i_{k|k-1}\mathbf{C}'$, $\mathbf{F}^i_k = (\mathbf{H}^i_k + \mathbf{R}^i_k)^{-1}$, and $\mathbf{G}^i_k = [(n^i_k)^2\mathbf{H}^i_k + \sum_{l\in N^i_k}\mathbf{R}^l_k]^{-1}$. Then (6.13) and (6.15) can be rewritten as follows:

$$\begin{aligned}\mathbf{K}^i_k &= [\mathbf{P}^i_{k|k-1}\mathbf{C}' - n^i_k\mathbf{L}^i_k\mathbf{C}\mathbf{P}^i_{k|k-1}\mathbf{C}']\mathbf{F}^i_k \\ &= \mathbf{P}^i_{k|k-1}\mathbf{C}'\mathbf{F}^i_k - n^i_k\mathbf{L}^i_k\mathbf{H}^i_k\mathbf{F}^i_k. \end{aligned}\tag{6.16}$$

$$\begin{aligned}\mathbf{L}^i_k &= [n^i_k\mathbf{P}^i_{k|k-1}\mathbf{C}' - n^i_k\mathbf{K}^i_k\mathbf{C}\mathbf{P}^i_{k|k-1}\mathbf{C}']\mathbf{G}^i_k \\ &= n^i_k\mathbf{P}^i_{k|k-1}\mathbf{C}'\mathbf{G}^i_k - n^i_k\mathbf{K}^i_k\mathbf{H}^i_k\mathbf{G}^i_k. \end{aligned}\tag{6.17}$$

In order to obtain the optimal gain $\mathbf{K}^i_k$, substituting (6.17) into (6.16) leads to:

$$\mathbf{K}^i_k = [\mathbf{P}^i_{k|k-1}\mathbf{C}'\mathbf{F}^i_k - (n^i_k)^2\mathbf{P}^i_{k|k-1}\mathbf{C}'\mathbf{G}^i_k\mathbf{H}^i_k\mathbf{F}^i_k][\mathbf{I} - (n^i_k)^2\mathbf{H}^i_k\mathbf{G}^i_k\mathbf{H}^i_k\mathbf{F}^i_k]^{-1}. \tag{6.18}$$

Similarly,

$$\mathbf{L}_k^i = [n_k^i \mathbf{P}_{k|k-1}^i \mathbf{C}' \mathbf{G}_k^i - n_k^i \mathbf{P}_{k|k-1}^i \mathbf{C}' \mathbf{F}_k^i \mathbf{H}_k^i \mathbf{G}_k^i][\mathbf{I} - (n_k^i)^2 \mathbf{H}_k^i \mathbf{F}_k^i \mathbf{H}_k^i \mathbf{G}_k^i]^{-1}. \tag{6.19}$$

In summary, after initialization of the system parameters such as $\mathbf{P}_{k|k-1}^i$ and $\hat{\mathbf{x}}_{k|k-1}^i$ through the KF based prediction step, each estimator computes the optimal local and neighbouring gains by (6.18) and (6.19). $\hat{\mathbf{x}}_{k+1|k}^i$ and $\mathbf{P}_{k+1|k}^i$ are given by:

$$\hat{\mathbf{x}}_{k+1|k}^i = \mathbf{A}_d \hat{\mathbf{x}}_{k|k}^i + \mathbf{B}_d u_k, \tag{6.20}$$

$$\mathbf{P}_{k+1|k}^i = \mathbf{A}_d \mathbf{P}_{k|k}^i \mathbf{A}_d' + \mathbf{Q}_k. \tag{6.21}$$

Afterwards, each estimator computes the state estimation and its update covariance matrix by (6.4) and (6.9). Now the next problem is how we can guarantee the consensus of the proposed distributed state estimation method, so that the developed approach can apply to real-time applications.

6.4.2 Consensus Analysis of the Distributed Estimation Algorithm

From the engineering perspective, the discrete-time system is easy to implement in the digital platforms, while the continuous system is easy to analyze from the mathematical point of view [233]. Motivated by this realistic dilemma and similar to [50], the consensus analysis of the proposed algorithm is completed based on the consensus analysis of the continuous system. Similar to the discrete-time case, the estimator applies the following step:

$$\dot{\hat{\mathbf{x}}}^i = \mathbf{A}\hat{\mathbf{x}}^i + \mathbf{B}\mathbf{u} + \mathbf{K}^i[\mathbf{y}^i - \alpha \mathbf{C}\hat{\mathbf{x}}^i] + \mathbf{L}^i \sum_{j \in N^i} [\mathbf{y}^j - \alpha \mathbf{C}\hat{\mathbf{x}}^i]. \tag{6.22}$$

The estimation error $\mathbf{e}^i$ can be expressed as follows:

$$\mathbf{e}^i = \mathbf{x} - \hat{\mathbf{x}}^i. \tag{6.23}$$

By direct differentiation of (6.23), one can obtain:

$$\begin{aligned}
\dot{\mathbf{e}}^i &= \dot{\mathbf{x}} - \mathbf{A}\hat{\mathbf{x}}^i - \mathbf{B}\mathbf{u} - \mathbf{K}^i[\mathbf{y}^i - \alpha \mathbf{C}\hat{\mathbf{x}}^i] - \mathbf{L}^i \sum_{j \in N^i} [\mathbf{y}^j - \alpha \mathbf{C}\hat{\mathbf{x}}^i] \\
&= (\mathbf{A} - \alpha \mathbf{K}^i \mathbf{C} - n^i \alpha \mathbf{L}^i \mathbf{C})\mathbf{x} - (\mathbf{A} - \alpha \mathbf{K}^i \mathbf{C} - n^i \alpha \mathbf{L}^i \mathbf{C})\hat{\mathbf{x}}^i + \mathbf{n} - \alpha \mathbf{K}^i \mathbf{w}^i - \alpha \mathbf{L}^i \sum_{l \in N^i} \mathbf{w}^l \\
&= (\mathbf{A} - \alpha \mathbf{K}^i \mathbf{C} - n^i \alpha \mathbf{L}^i \mathbf{C})\mathbf{e}^i + \mathbf{n} - \alpha^i \mathbf{K}^i \mathbf{w}^i - \alpha^i \mathbf{L}^i \sum_{l \in N^i} \mathbf{w}^l.
\end{aligned} \tag{6.24}$$

The error covariance matrix is written as follows:

$$\begin{aligned}\dot{\mathbf{P}}^i &= (\mathbf{A}-\lambda\mathbf{K}^i\mathbf{C}-n^i\lambda\mathbf{L}^i\mathbf{C})\mathbf{P}^i+\mathbf{P}^i(\mathbf{A}-\lambda\mathbf{K}^i\mathbf{C}-n^i\lambda\mathbf{L}^i\mathbf{C})'+\mathbf{Q}+\lambda\mathbf{K}^i\mathbf{R}^i\mathbf{K}'^i+\lambda\mathbf{L}^i\sum_{l\in N^i}\mathbf{R}^l\mathbf{L}'^i \\ &= \mathbf{A}\mathbf{P}^i+\mathbf{P}^i\mathbf{A}'+\mathbf{Q}-\lambda\mathbf{K}^i\mathbf{C}\mathbf{P}^i-\lambda\mathbf{P}^i\mathbf{C}'\mathbf{K}'^i+\lambda\mathbf{K}^i\mathbf{R}^i\mathbf{K}'^i-n^i\lambda\mathbf{L}^i\mathbf{C}\mathbf{P}^i-n^i\lambda\mathbf{P}^i\mathbf{C}'\mathbf{L}'^i+\lambda\mathbf{L}^i\sum_{l\in N^i}\mathbf{R}^l\mathbf{L}'^i.\end{aligned} \tag{6.25}$$

Taking the partial derivative of (6.25) with respect to $\mathbf{K}^i$ and applying (6.10), (6.11) yields:

$$\frac{\partial[tr\dot{\mathbf{P}}^i]}{\partial\mathbf{K}^i} = -2\lambda\mathbf{P}^i\mathbf{C}'+2\lambda\mathbf{K}^i\mathbf{R}^i. \tag{6.26}$$

Setting $\frac{\partial[tr\dot{\mathbf{P}}^i]}{\partial\mathbf{K}^i}=0$ in (6.26), then the gain matrix is given by:

$$\mathbf{K}^i = \mathbf{P}^i\mathbf{C}'(\mathbf{R}^i)^{-1}. \tag{6.27}$$

Taking the partial derivative of (6.25) with respect to $\mathbf{L}^i$ and applying (6.10), (6.11) leads to:

$$\frac{\partial[tr\dot{\mathbf{P}}^i]}{\partial\mathbf{L}^i} = -2n^i\lambda\mathbf{P}^i\mathbf{C}'+2\lambda\mathbf{L}^i\sum_{l\in N^i}\mathbf{R}^l. \tag{6.28}$$

Putting $\frac{\partial[tr\dot{\mathbf{P}}^i]}{\partial\mathbf{L}^i}=0$ in (6.28), then the gain matrix is obtained as follows:

$$\mathbf{L}^i = n^i\mathbf{P}^i\mathbf{C}'(\sum_{l\in N^i}\mathbf{R}^l)^{-1}. \tag{6.29}$$

Substituting (6.27) and (6.29) into (6.25), one can obtain:

$$\begin{aligned}\dot{\mathbf{P}}^i &= \mathbf{A}\mathbf{P}^i+\mathbf{P}^i\mathbf{A}'+\mathbf{Q}-\lambda\mathbf{P}^i\mathbf{C}'(\mathbf{R}^i)^{-1}\mathbf{C}\mathbf{P}^i-\lambda\mathbf{P}^i\mathbf{C}'(\mathbf{R}^i)^{-1}\mathbf{C}\mathbf{P}^i+\lambda\mathbf{P}^i\mathbf{C}'(\mathbf{R}^i)^{-1}\mathbf{C}\mathbf{P}^i- \\ &\quad n^i\lambda\mathbf{P}^i\mathbf{C}'(\sum_{l\in N^i}\mathbf{R}^l)^{-1}\mathbf{C}\mathbf{P}^i-n^i\lambda\mathbf{P}^i\mathbf{C}'(\sum_{l\in N^i}\mathbf{R}^l)^{-1}\mathbf{C}\mathbf{P}^i+(n^i)^2\lambda\mathbf{P}^i\mathbf{C}'(\sum_{l\in N^i}\mathbf{R}^l)^{-1}\mathbf{C}\mathbf{P}^i \\ &= \mathbf{A}\mathbf{P}^i+\mathbf{P}^i\mathbf{A}'+\mathbf{Q}-\lambda\mathbf{P}^i\mathbf{C}'(\mathbf{R}^i)^{-1}\mathbf{C}\mathbf{P}^i+[(n^i)^2-2n^i]\lambda\mathbf{P}^i\mathbf{C}'(\sum_{l\in N^i}\mathbf{R}^l)^{-1}\mathbf{C}\mathbf{P}^i.\end{aligned} \tag{6.30}$$

In order to analyze the consensus of the developed algorithm, consider only the nominal system of (6.24) to obtain:

$$\dot{\mathbf{e}}^i = (\mathbf{A}-\alpha\mathbf{K}^i\mathbf{C}-n^i\alpha\mathbf{L}^i\mathbf{C})\mathbf{e}^i. \tag{6.31}$$

Consider the following Lyapunov function:

$$V = \sum_{i=1}^{M}\mathbf{e}'^i(\mathbf{P}^i)^{-1}\mathbf{e}^i. \tag{6.32}$$

Now taking the partial derivative and expectation of (6.32), and using (6.27), (6.29), (6.30) and (6.31), one can obtain:

$$
\begin{aligned}
\dot{V} &= \sum_{i=1}^{M} \{\dot{\mathbf{e}}'^{i}(\mathbf{P}^i)^{-1}\mathbf{e}^i + \mathbf{e}'^{i}(\mathbf{P}^i)^{-1}\dot{\mathbf{e}}^i - \mathbf{e}'^{i}(\mathbf{P}^i)^{-1}\dot{\mathbf{P}}^i(\mathbf{P}^i)^{-1}\mathbf{e}^i\} \\
&= \sum_{i=1}^{M} \mathbf{e}'^{i}[(\mathbf{A}-\lambda\mathbf{K}^i\mathbf{C}-n^i\lambda\mathbf{L}^i\mathbf{C})'(\mathbf{P}^i)^{-1}+(\mathbf{P}^i)^{-1}(\mathbf{A}-\lambda\mathbf{K}^i\mathbf{C}-n^i\lambda\mathbf{L}^i\mathbf{C})-(\mathbf{P}^i)^{-1}\mathbf{A}-\mathbf{A}'(\mathbf{P}^i)^{-1} \\
&\quad -(\mathbf{P}^i)^{-1}\mathbf{Q}(\mathbf{P}^i)^{-1} +\lambda\mathbf{C}'(\mathbf{R}^i)^{-1}\mathbf{C}-[(n^i)^2-2n^i]\lambda\mathbf{C}'(\sum_{l\in N^i}\mathbf{R}^l)^{-1}\mathbf{C}]\mathbf{e}^i \\
&= \sum_{i=1}^{M} \mathbf{e}'^{i}[-\lambda(\mathbf{P}^i)^{-1}\mathbf{K}^i\mathbf{C} - \lambda\mathbf{C}'\mathbf{K}'^{i}(\mathbf{P}^i)^{-1} - n^i\lambda(\mathbf{P}^i)^{-1}\mathbf{L}^i\mathbf{C} - n^i\lambda\mathbf{C}'\mathbf{L}'^{i}(\mathbf{P}^i)^{-1} - \\
&\quad (\mathbf{P}^i)^{-1}\mathbf{Q}(\mathbf{P}^i)^{-1} + \lambda\mathbf{C}'(\mathbf{R}^i)^{-1}\mathbf{C} - [(n^i)^2-2n^i]\lambda\mathbf{C}'(\sum_{l\in N^i}\mathbf{R}^l)^{-1}\mathbf{C}]\mathbf{e}^i \\
&= \sum_{i=1}^{M} \mathbf{e}'^{i}[-\lambda\mathbf{C}'(\mathbf{R}^i)^{-1}\mathbf{C} - \lambda\mathbf{C}'(\mathbf{R}^i)^{-1}\mathbf{C} - n^i\lambda\mathbf{C}'(\sum_{l\in N^i}\mathbf{R}^l)^{-1}\mathbf{C} - n^i\lambda\mathbf{C}'(\sum_{l\in N^i}\mathbf{R}^l)^{-1}\mathbf{C} - \\
&\quad (\mathbf{P}^i)^{-1}\mathbf{Q}(\mathbf{P}^i)^{-1} + \lambda\mathbf{C}'(\mathbf{R}^i)^{-1}\mathbf{C} - [(n^i)^2-2n^i]\lambda\mathbf{C}'(\sum_{l\in N^i}\mathbf{R}^l)^{-1}\mathbf{C}]\mathbf{e}^i \\
&= -\sum_{i=1}^{M} \mathbf{e}'^{i}[\lambda\mathbf{C}'(\mathbf{R}^i)^{-1}\mathbf{C} + (\mathbf{P}^i)^{-1}\mathbf{Q}(\mathbf{P}^i)^{-1} + (n^i)^2\lambda\mathbf{C}'(\sum_{l\in N^i}\mathbf{R}^l)^{-1}\mathbf{C}]\mathbf{e}^i \leq 0. \qquad (6.33)
\end{aligned}
$$

The inequality shows that the Lyapunov function is gradually decreasing so the error function is asymptotically stable. Consequently, the estimated state $\hat{\mathbf{x}}^i$ converges to the actual system state $\mathbf{x}$. After estimating the system states, the designer needs to apply a control strategy for maintaining the stability of the network.

6.4.3 Proposed Distributed Controller

Generally, computing machines have finite memory and temporal resolution [190], so the distributed controller is obviously preferred from the engineering aspects. In this study, the distributed feedback controller is employed to regulate the microgrid states. The feedback controller is given by:

$$\mathbf{u}_k = \mathbf{F}\hat{\mathbf{x}}_{k|k}. \qquad (6.34)$$

Here, $\mathbf{F}$ is the distributed feedback gain matrix to be designed. If there is no connection between sub-system/estimator and controller then the corresponding element of $\mathbf{F}$ is zero.

For instance, from the Fig. 6.1 the designed gain matrix $\mathbf{F}$ belongs to the following structure set (assuming[1] M = 4):

$$\mathbf{F}^{\circ} = \{\mathbf{F} \mid \mathbf{F} = \begin{bmatrix} F_{11} & F_{12} & 0 & 0 \\ 0 & F_{22} & F_{23} & 0 \\ F_{31} & 0 & F_{33} & F_{34} \\ 0 & 0 & 0 & F_{44} \end{bmatrix}\}. \tag{6.35}$$

Here, the feedback element F_{NM} is the connection between subsystem sensor N and controller M. This type of distributed feedback gain structure offers sparse communication between the grid and EMS [21].

According to the separation principle [210, p. 427], the feedback control strategy and the state estimation can be designed separately. So, one can implement the control law $\mathbf{u}_k = \mathbf{F}\mathbf{x}_k$ [20]. Using $\mathbf{u}_k$, (6.1) can be written as follows:

$$\mathbf{x}_{k+1} = \tilde{\mathbf{A}}_d \mathbf{x}_k + \mathbf{n}_k, \tag{6.36}$$

where $\tilde{\mathbf{A}}_d = \mathbf{A}_d + \mathbf{B}_d\mathbf{F}$ is the closed loop state matrix. If there exists a stabilizing gain matrix $\mathbf{F} \in \mathbf{F}^{\circ}$, then the following LMI holds:

$$\begin{aligned} &\tilde{\mathbf{A}}'_d \mathbf{P} \tilde{\mathbf{A}}_d - \mathbf{P} < \mathbf{0} \\ &(\mathbf{A}_d + \mathbf{B}_d\mathbf{F})' \mathbf{P} (\mathbf{A}_d + \mathbf{B}_d\mathbf{F}) - \mathbf{P} < \mathbf{0}. \end{aligned} \tag{6.37}$$

In order to obtain a feasible solution so that the distributed feedback can be applied, $\mathbf{P}$ is computed as follows:

$$(\beta\mathbf{A}_d)' \mathbf{P} (\beta\mathbf{A}_d) - \mathbf{P} < \mathbf{0}, \tag{6.38}$$

where $\beta = 1/[\gamma\ max\ \{eig(\mathbf{A}_d)\}]$, $\gamma > 1$ is a free parameter and $max\ \{eig(\mathbf{A}_d)\}$ is the maximum eigen values of $\mathbf{A}_d$. The quantity γ ensures eigenvalues of the scaled close loop system strictly less than one. According to the standard Schur's complement, (6.38) can be transformed into the following LMI form:

$$\begin{bmatrix} -\mathbf{P} & \beta\mathbf{A}'_d\mathbf{P} \\ \beta\mathbf{P}\mathbf{A}_d & -\mathbf{P} \end{bmatrix} < \mathbf{0}. \tag{6.39}$$

[1]The proposed work can be easily extended to the generic case.

After computing $\mathbf{P}$ in (6.39) and with the help of (6.37), one can obtain $\mathbf{F} \in \mathbf{F}^{\circ}$ by considering the following optimization problem:

$$\begin{aligned} &\text{minimise} && \zeta && (6.40)\\ &\text{subject to} && (\mathbf{A}_d + \mathbf{B}_d\mathbf{F})'\mathbf{P}(\mathbf{A}_d + \mathbf{B}_d\mathbf{F}) - \mathbf{P} + \zeta\mathbf{I} < \mathbf{0}. && (6.41) \end{aligned}$$

where ζ is the semidefinite programming variable. Given $\mathbf{P}$, applying the Schur's complement to (6.41) yields:

$$\begin{bmatrix} -\mathbf{P} + \zeta\mathbf{I} & (\mathbf{A}_d + \mathbf{B}_d\mathbf{F})'\mathbf{P} \\ \mathbf{P}(\mathbf{A}_d + \mathbf{B}_d\mathbf{F}) & -\mathbf{P} \end{bmatrix} < \mathbf{0}. \tag{6.42}$$

Finally, one can formulate the proposed optimization problem as follows:

$$\begin{aligned} &\text{minimise} && \zeta \\ &\text{subject to} && Hold\ (6.42), \mathbf{F} \in \mathbf{F}^{\circ}. && (6.43) \end{aligned}$$

One can use the standard YALMIP toolbox to solve the proposed optimization problem [213]. As the feedback structure offers sparse communication, the developed approach reduces computation costs.

6.5 Simulation Results Using the Proposed Distributed Approaches

This chapter proposes a distributed state estimator and optimal controller under the condition of packet losses. In this section, the proposed distributed algorithms are applied to the microgrid connected to the IEEE-4 bus system which is described in Chapter 4.2. The proposed algorithm is tested on the microgrids with both large and small disturbances.

6.5.1 State Estimation Performance Considering Small Disturbances

The simulation is conducted through Matlab and YALMIP, and the parameters are shown in Table 6.1. It can be seen that the process and measurement disturbance variances are considered small.

Table 6.1: Simulation parameters.

Parameters	Values	Parameters	Values
$\mathbf{Q}$	$0.0000001 * \mathbf{I}_4$	$\mathbf{R}^1$	$0.000001 * \mathbf{I}_4$
$\mathbf{R}^2$	$0.000002 * \mathbf{I}_4$	$\mathbf{R}^3$	$0.000003 * \mathbf{I}_4$
$\mathbf{R}^4$	$0.000004 * \mathbf{I}_4$	λ_K	0.90-0.95
γ	2	Δt	0.0001

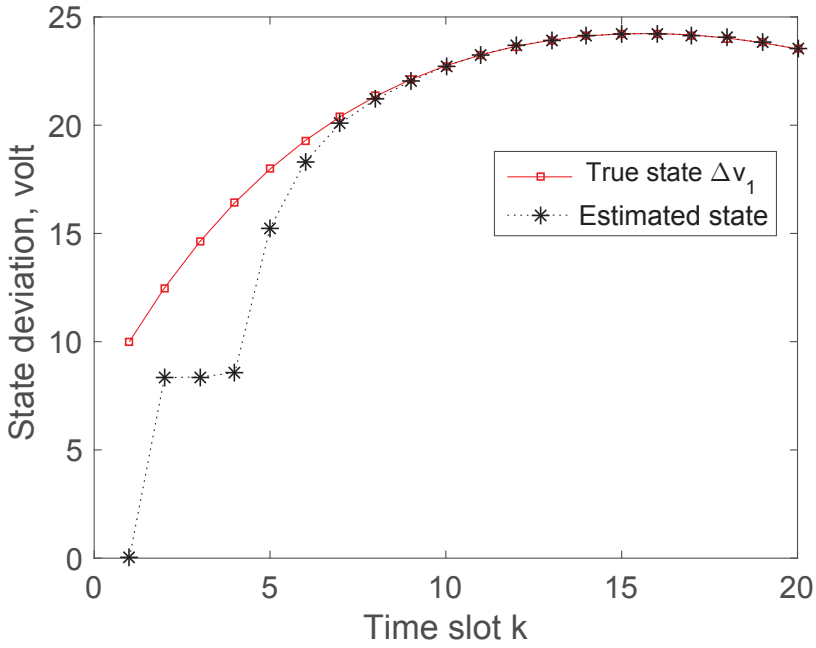

Figure 6.2: State trajectory of Δv_1 and its estimate with small disturbances.

From the simulation, the system state versus time step results are demonstrated in Figs. 6.2–6.5. It can be observed that the packet loss significantly affects the system states but the proposed algorithm can well estimate the system states. This is due to the fact that the proposed algorithm can find the optimal gains to extract the system state information from adversaries. It can also be seen that it requires only 0.015 seconds $(k \times \Delta t)$ to estimate the system states which is much less than the standard estimation time frame of 1 second [47]. Note that the small fluctuation comes from the packet losses and random noises.

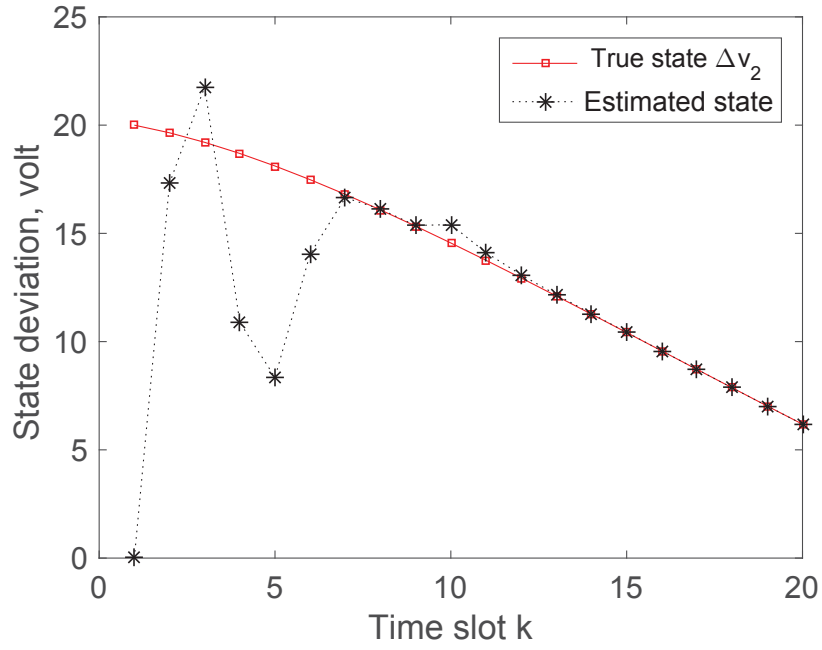

Figure 6.3: State trajectory of Δv_2 and its estimate with small disturbances.

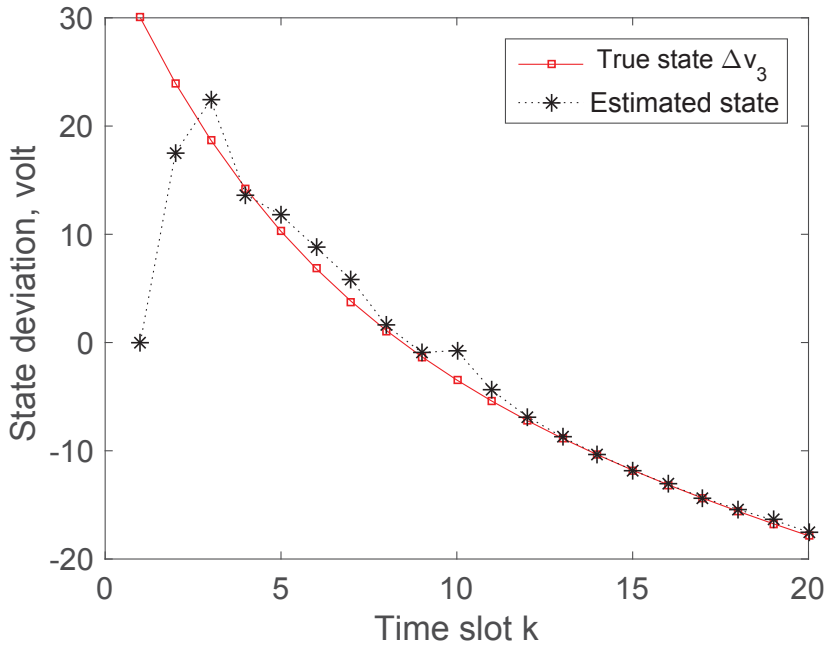

Figure 6.4: State trajectory of Δv_3 and its estimate with small disturbances.

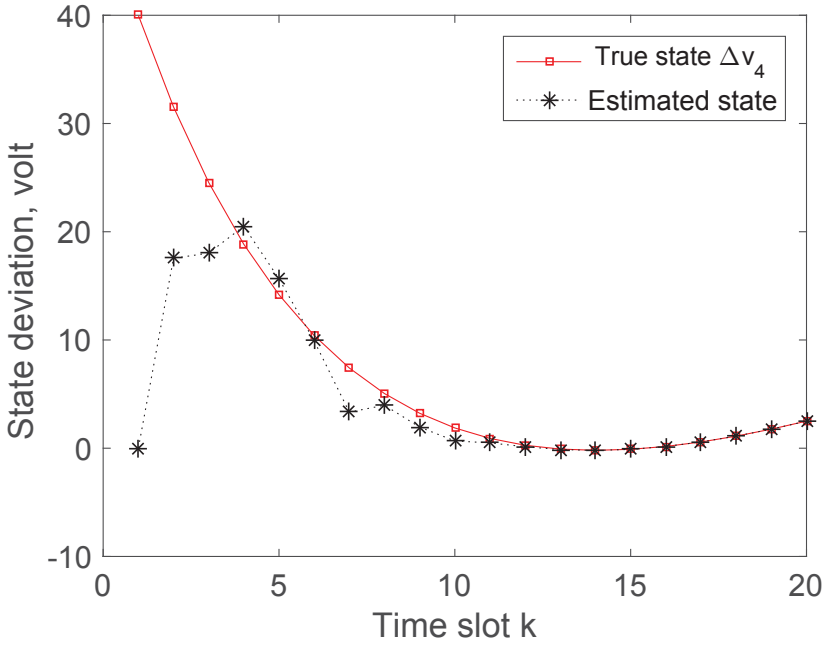

Figure 6.5: State trajectory of Δv_4 and its estimate with small disturbances.

6.5.2 State Estimation Performance Considering Large Disturbances

In order to investigate the impacts of process and measurement noises on the estimation performance, the variance of the process noise is increased from $0.0000001 * \mathbf{I}_4$ to $0.5 * \mathbf{I}_4$, and the measurement noise variance for estimator 1, 2, 3 and 4 are set as $0.6 * \mathbf{I}_4$, $0.7 * \mathbf{I}_4$, $0.8 * \mathbf{I}_4$ and $0.9 * \mathbf{I}_4$, respectively [243]. The step size is decreased from 0.0001 to 0.00001, while other system parameters are kept the same as that in case 1. The simulation results are presented in Figs. 6.6-6.9. It can be seen that the results are greatly affected by heavy disturbances, but the estimation accuracy is still high. Even if there are large disturbances in the system, the proposed algorithm can estimate well the system states.

6.5.3 Controller Performance Analysis

Basically, it can be seen that the actual PCC state deviations increase dramatically over time, which is very dangerous in terms of power network stability and microgrid operation. Thus, it is intrinsically essential to apply a suitable control technique, so that the PCC voltage deviations are driven to zero in a short time. After applying the proposed distributed control

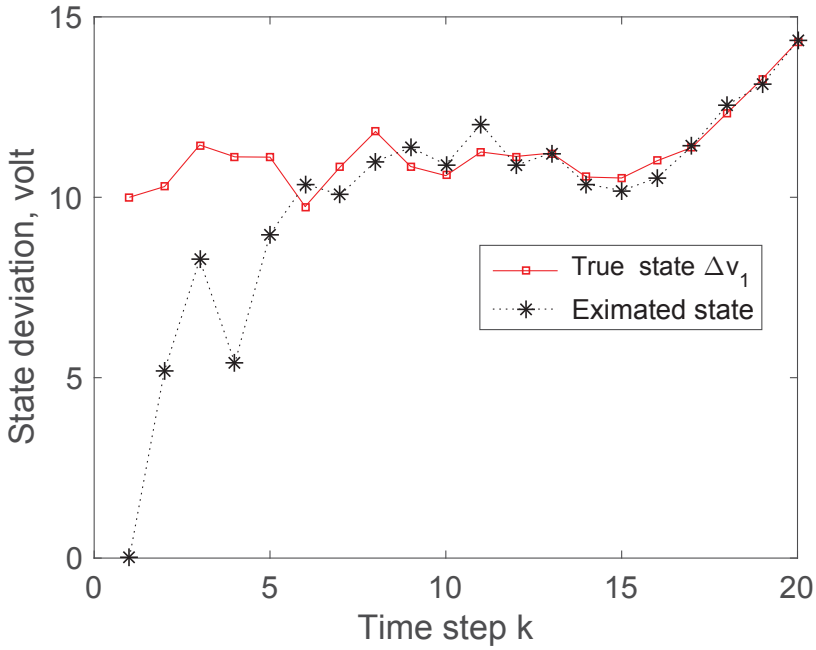

Figure 6.6: State trajectory of Δv_1 and its estimate with large disturbances.

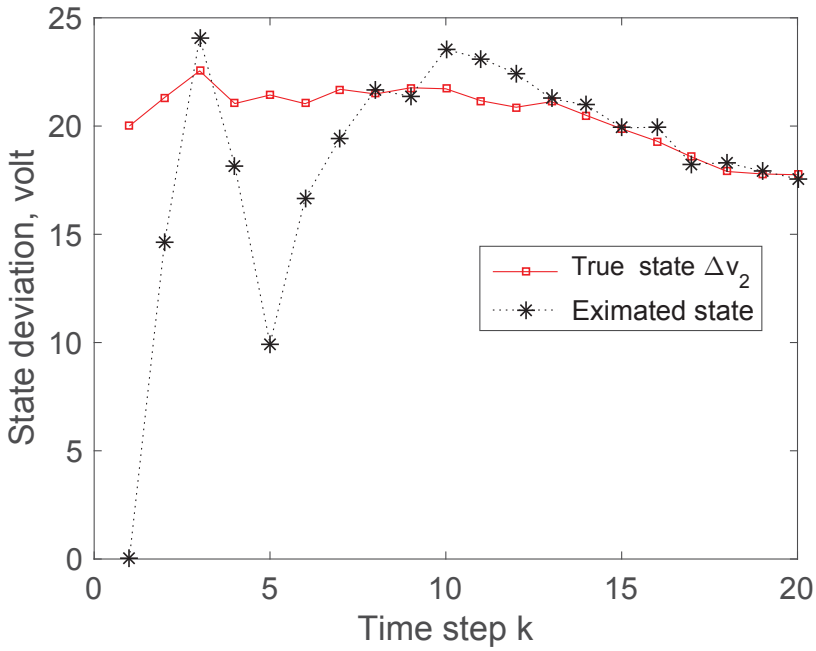

Figure 6.7: State trajectory of Δv_2 and its estimate with large disturbances.

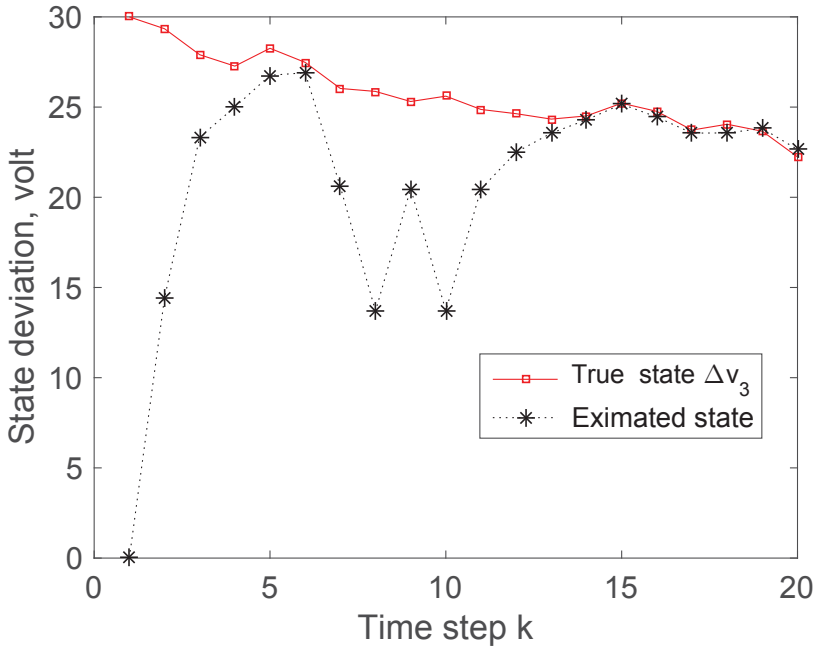

Figure 6.8: State trajectory of Δv_3 and its estimate with large disturbances.

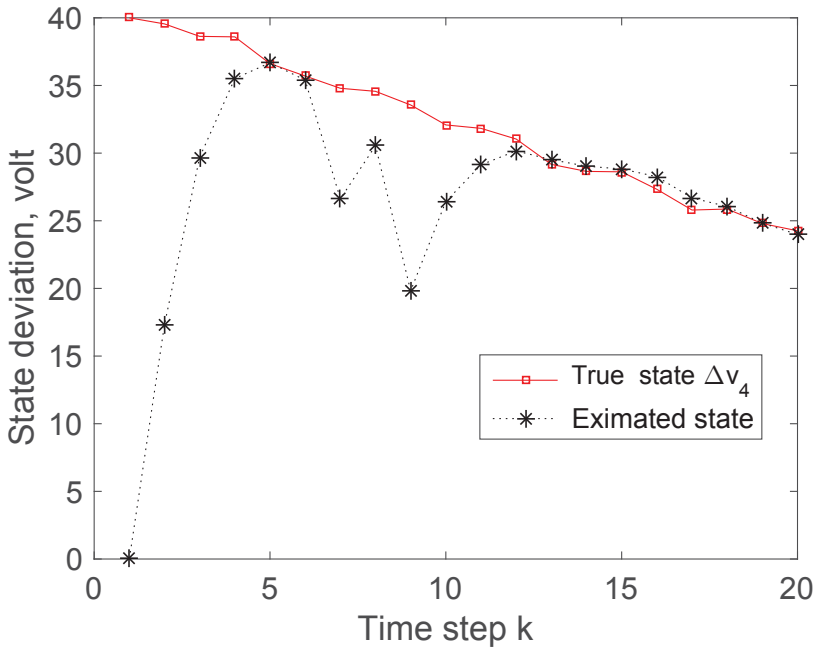

Figure 6.9: State trajectory of Δv_4 and its estimate with large disturbances.

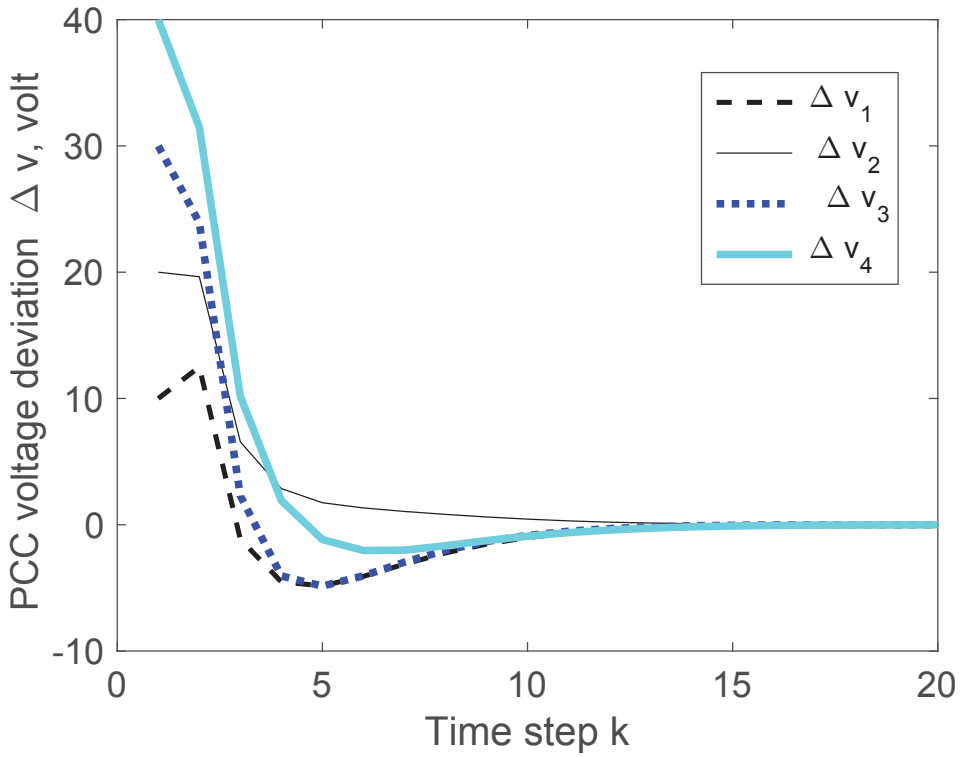

Figure 6.10: Controlling the states trajectory.

method, it can be seen from Fig. 6.10 that the proposed controller is able to keep the voltage deviations to zero in approximately 0.01 seconds $(k \times \Delta t)$, which acts as a precursor for stability and microgrid operations. Technically, it means that the developed approach requires much less time to keep the voltage as a reference value compared with the standard stability time frame $1 - 5$ seconds [47].

6.6 Summary

This chapter presents a distributed state estimation and control strategy considering packet losses. The developed distributed estimator is based on the mean squared error, so it can accurately compute the optimal gains to extract the actual system states. In order to regulate the system states, this study proposes a SDP based distributed controller in the context of smart grid communication. The proposed distributed control framework could properly determine the sparse gain such that the system states can be stabilized in a fairly short time. These ap-

proaches can help to design the future smart EMS under the condition of uncertainties. It is worth pointing out that the aforementioned problems are not trivial in the smart grid community as the communication impairments have significant impact on the grid stability and the distributed strategies can reduce communication burden and offer a sparse communication network.

Similar to [50], [51], the proposed distributed state estimation algorithm requires both local and consensus steps with their corresponding gain. That is, the derived covariance expression is not scalable in the number of estimators; therefore, sometimes its needs a *suboptimal filter* [51]. Generally, including the consensus step in the filter structure, the computational complexity of the gain and error covariance is significantly increased. To address this issue, the following chapter proposes a distributed state estimation algorithm that will only need to compute the neighboring gain for interconnected systems. The convergence of the developed approach is proved considering the discrete time system.

Chapter 7

Convergence Analysis of the Distributed Estimation Algorithm for a Discrete-Time System

7.1 Introduction

Generally speaking, power systems are continuously monitored in order to maintain the normal and secure operating conditions. The state estimation provides accurate information about the power system operating conditions. Due to the increasing size and complexity of power systems, the traditional centralised estimation method is no longer suitable [244]. Moreover, the implementation of the centralised state estimation over a whole interconnected power system is becoming a challenging problem. So, the distributed state estimation is gaining significant interest both in academic and industrial domains. In the distributed estimation approach, the estimator exchanges information with the neighbouring connected nodes to reach a consensus on estimation. The consensus-based distributed state estimation algorithms for sensor networks have been proposed in [141], [51], [142]. Moreover, the distributed information consensus filter for simultaneous input and state estimation is explored in [145]. However, the calculations of gain and error covariance in all preceding methods are based on the *suboptimal filter*. Therefore, it can be considered that the optimal consensus analysis has not been fully investigated as it does not trace back to the original system in the

optimal sense. In other words, the approximation of the error function does not reflect the optimal consensus analysis, so the algorithms might not be the best to be applied in real-time applications.

Motivated by the aforementioned research gaps in the smart grid research community, this research proposes a distributed dynamic state estimation method with the optimal observation gain, and its convergence is analysed without approximations. Specifically, the interconnected synchronous generators are modelled as a state-space linear equation where sensors are deployed to obtain measurements. As the synchronous generator states are unknown, the estimation needs to know the overall operating conditions of power networks. Availability of the system states gives the designer an accurate picture of power networks to avoid blackouts. Basically, the proposed algorithm is based on the minimization of the mean squared estimation error, and the optimal gain is computed by exchanging information with neighboring estimators. Afterwards, the convergence of the developed algorithm is proved so that it can be applied to real-time applications in modern smart grids. Simulation results demonstrate the efficacy of the developed approach.

7.2 Problem Statement

There is a strong drive in the power industry to design, create and analyse the system in a distributed way considering flexible communication infrastructure [245]. In order to develop a distributed estimation approach, consider the following discrete-time system:

$$\mathbf{x}_{k+1} = \mathbf{A}_d\mathbf{x}_k + \mathbf{B}_d\mathbf{u}_k + \mathbf{n}_k, \tag{7.1}$$

where $\mathbf{x}_k$ is the system state at time instant k, $\mathbf{u}_k$ is the control effort, $\mathbf{n}_k$ is the zero-mean process noise whose covariance matrix is $\mathbf{Q}_k$, and all other variables are previously well described. The system measurements are obtained by a set of sensors as follows:

$$\mathbf{y}_k^i = \mathbf{C}\mathbf{x}_k + \mathbf{w}_k^i,\ i = 1, 2, \cdots, n \tag{7.2}$$

where $\mathbf{y}_k^i$ is the observation information by the i-th estimator at time instant k, $\mathbf{C}$ is the observation matrix and $\mathbf{w}_k^i$ is the measurement noise with zero mean and the covariance matrix $\mathbf{R}_k^i$. Similar to [141], [246], we assume that the measurements are same, but the observation noises are different from each other. The assumption is probably due to the

fact that the system operators deploy a similar number of sensors that are interconnected in the distribution power system. Secondly, the deployed sensors have similar power and processing capability.

Generally speaking, the distribution power sub-systems are interconnected to each other as shown in Fig. 7.1. When the estimator exchanges information with the connected neigh-

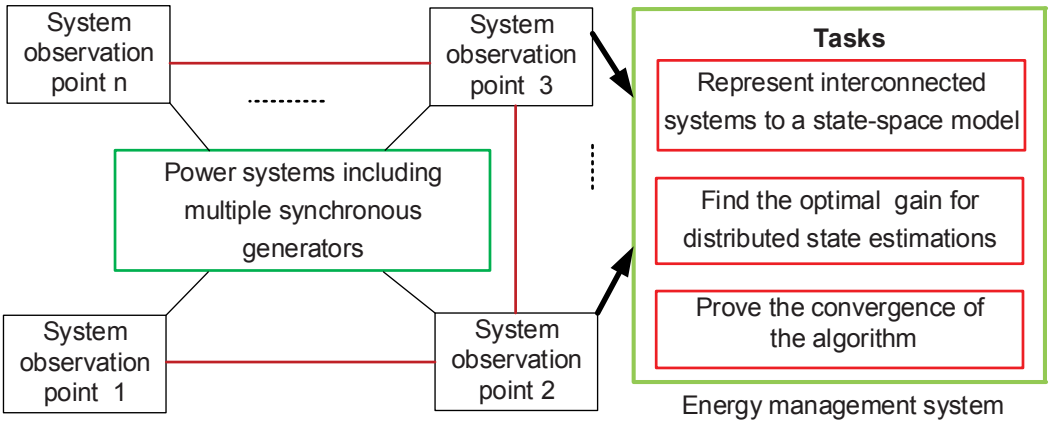

Figure 7.1: A framework for distributed estimations and its research questionnaires.

bouring nodes, it is called the distributed estimation [51], [237]. In this way, each estimator reaches its consensus estimation, so the estimated state converges to the true state. Basically, this research assumes the sub-stations have communication capabilities to exchange information with each other. Mathematically, the proposed distributed dynamic state estimator is written as follows:

$$\hat{\mathbf{x}}^i_{k+1|k} = \mathbf{A}_d \hat{\mathbf{x}}^i_{k|k} + \mathbf{B}_d \mathbf{u}_k. \tag{7.3}$$

$$\hat{\mathbf{x}}^i_{k|k} = \hat{\mathbf{x}}^i_{k|k-1} + \mathbf{K}^i_k \sum_{l \in N^i} (\mathbf{y}^l_k - \mathbf{C}\hat{\mathbf{x}}^i_{k|k-1}). \tag{7.4}$$

Here, $\hat{\mathbf{x}}^i_{k|k}$ is the updated state estimation at the i-th estimator, $\hat{\mathbf{x}}^i_{k|k-1}$ is the predicted state estimation, $\mathbf{K}^i_k$ is the local gain and N^i denotes the set of neighbouring estimators including node i. The second term in (7.4) is used to exchange information with the neighbouring estimators for reaching a consensus on estimations. In the traditional distributed state estimation methods [50], [51], it requires both local and consensus steps with their corresponding gain. That is, the derived covariance expression is not scalable in the number of estimators, so it needs to approximate which leads to a *suboptimal filter* [51]. Therefore, it can be considered that the optimal consensus analysis has not been fully investigated as it does not trace back

to the original system in the optimal sense. In other words, the approximation of the error function does not reflect the optimal consensus analysis, so the algorithms might not be the best to be applied in real-time applications. Generally, including the consensus step in the filter structure, the computational complexity of the gain and error covariance is significantly increased.

The first problem is how to express the interconnected power systems in a state-space framework, which is easy to analyse. The second problem is to design the optimal gain without approximations. The next problem is to prove the convergence of the proposed algorithm, so that the developed approach can be applied in smart grid industry. Generally, the consensus analysis confirms the consistency of the estimation over the interconnected networks. The problem statement is summarised as follows:
Develop a distributed state estimation algorithm for complex power systems such that all estimators reach a consensus on estimation.

This chapter tries to answer these questions by presenting a distributed state estimation scheme with the optimal gain for interconnected synchronous generators, and algorithmic convergence is analysed without approximations.

7.3 Discrete-Time State-Space Representation of Synchronous Generators

The power grid can be represented by diverse stages of complexity which depend on the planned applications of the system model. Generally speaking, there are many synchronous generators and loads are connected to the complex power networks. To illustrate, Fig. 7.2 shows the typical synchronous generators and loads which are connected to the 8-bus distribution lines [106], [14]. Basically, the ith-synchronous generator can be represented by the following third order differential equations as follows [14], [247], [5]:

$$\Delta\dot{\delta}_i = \Delta\omega_i. \tag{7.5}$$

$$\Delta\dot{\omega}_i = -\frac{D_i}{H_i}\Delta\omega_i - \frac{\Delta P_{ei}}{H_i}. \tag{7.6}$$

$$\Delta\dot{E}'_{qi} = -\frac{\Delta E'_{qi}}{T'_{doi}} + \frac{\Delta E_{fi}}{T'_{doi}} + \frac{X_{di}}{T'_{doi}}\Delta i_{di} - \frac{X'_{di}}{T'_{doi}}\Delta i_{di}. \tag{7.7}$$

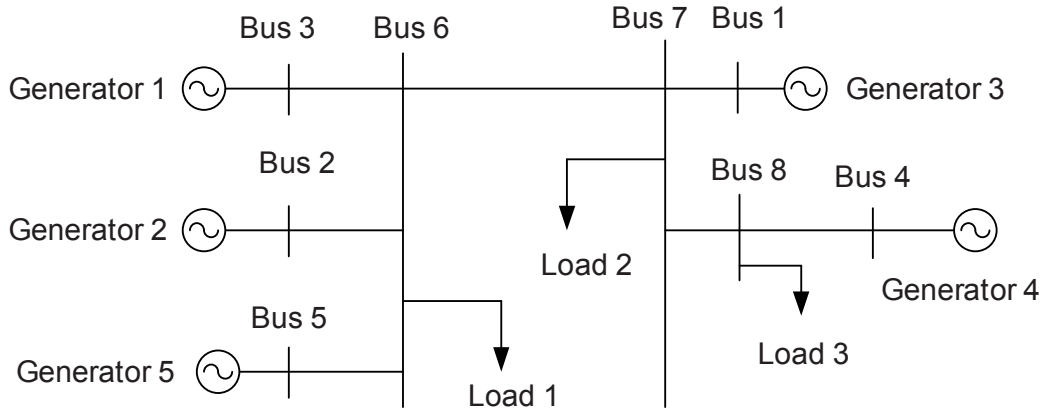

Figure 7.2: Synchronous generators are connected to the distribution system [14], [15].

Here, δ_i is the rotor angle, ω_i is the rotor speed, H_i is the inertia constant, D_i is the damping constant, P_e is the active power delivered at the terminal, E'_{qi} is the quadrature-axis transient voltage, E_{fi} is the exciter output voltage, T'_{doi} is the direct-axis open-circuit transient time constant, X_{di} is the direct-axis synchronous reactance, X'_{di} is the direct-axis transient reactance and i_{di} is the direct-axis current [106].

Usually, the typical automatic voltage regulator (AVR) is used to control the excitation current which leads to control the terminal voltage [14], [15]. A second-order transfer function is used to represent the AVR whose dynamic equations are given by [14]:

$$\Delta E_{fi} = b_{0i} z_{1i} + b_{1i} z_{2i}. \tag{7.8}$$

$$\dot{z_{1i}} = z_{2i}. \tag{7.9}$$

$$\dot{z_{2i}} = -c_{1i} z_{2i} - c_{0i} z_{1i} + \Delta v_i. \tag{7.10}$$

Here, z_{1i} and z_{2i} are the AVR internal states, b_{0i} and b_{1i} are transfer function coefficients of the voltage control, c_{0i} and c_{1i} are the transfer function coefficients of the excitation system and Δv_i is the control input signal.

If there are N generators in the system, the d-axis current I_{di} and electrical power P_{ei} are expressed as follows [15]:

$$I_{di} = \sum_{j=1}^{N} \Delta E'_{qi} [B_{ij}\, cos(\delta_i - \delta_j) - G_{ij}\, sin(\delta_i - \delta_j)]. \tag{7.11}$$

$$P_{ei} = \Delta E'_{qi} \sum_{j=1}^{N} [B_{ij}\, sin(\delta_i - \delta_j) + G_{ij}\, cos(\delta_i - \delta_j)] \Delta E'_{qj}. \tag{7.12}$$

Here, $i, j \in \{1, \cdots, N\}$, G_{ij} and B_{ij} are the real and imaginary part of the network admittance matrix $\mathbf{Y}$, which is given in the Appendix A.

After linearizing (7.11) and (7.12) at the operating points $\boldsymbol{\delta} = \boldsymbol{\delta}^{\star}$ and $\mathbf{E}'_q = \mathbf{E}'^{\star}_q$, the power increment ΔP_{ei} and current increment ΔI_{di} are given by [14]:

$$\Delta P_{ei} = \left[\frac{\partial P_{ei}}{\partial \boldsymbol{\delta}} \quad \frac{\partial P_{ei}}{\partial \boldsymbol{E'_q}}\right]_{\substack{\boldsymbol{\delta}=\boldsymbol{\delta}^{\star} \\ \mathbf{E}'_q=\mathbf{E}'^{\star}_q}} \begin{bmatrix} \Delta\boldsymbol{\delta} \\ \Delta\boldsymbol{E'_q} \end{bmatrix}. \tag{7.13}$$

$$\Delta I_{di} = \left[\frac{\partial I_{di}}{\partial \boldsymbol{\delta}} \quad \frac{\partial I_{di}}{\partial \boldsymbol{E'_q}}\right]_{\substack{\boldsymbol{\delta}=\boldsymbol{\delta}^{\star} \\ \mathbf{E}'_q=\mathbf{E}'^{\star}_q}} \begin{bmatrix} \Delta\boldsymbol{\delta} \\ \Delta\boldsymbol{E'_q} \end{bmatrix}. \tag{7.14}$$

Here, $\Delta\boldsymbol{\delta}$ and $\Delta\mathbf{E}'_q$ are the rotor angle deviations and transient voltage deviations. By combining (7.5)-(7.10) and (7.13)-(7.14), the system dynamics can be written as follows:

$$\dot{\mathbf{x}}_i = \mathbf{A}_i\mathbf{x}_i + \mathbf{B}_i u_i + \sum_{j \in N_i} \mathbf{A}_{ij}\mathbf{x}_j. \tag{7.15}$$

Here, the ith-generator state $\mathbf{x}_i = [\Delta\delta_i \ \Delta\omega_i \ \Delta E'_{qi} \ z_{2i} \ z_{1i}]'$, the input signal $u_i = \Delta v_i$, N_i denotes the set of generators that are physically connected with the ith-generator, the system matrices $\mathbf{A}_i \in \mathbb{R}^{5\times5}$, $\mathbf{B}_i \in \mathbb{R}^{5\times1}$ and $\mathbf{A}_{ij} \in \mathbb{R}^{5\times5}$ are given in Appendix B.

Furthermore, the interconnected power system is expressed as a linearised continuous-time state-space framework as follows [14], [15]:

$$\dot{\mathbf{x}} = \mathbf{A}\mathbf{x} + \mathbf{B}\mathbf{u} + \mathbf{n}. \tag{7.16}$$

Here, $\mathbf{x} \in \mathbb{R}^{5N\times1}$ and $\mathbf{u} \in \mathbb{R}^{N\times1}$ are the states and input signals of all N generators, $\mathbf{n} \in \mathbb{R}^{5N\times1}$ is the process noise with covariance matrix $\mathbf{Q} \in \mathbb{R}^{5N\times5N}$, the system state matrix $\mathbf{A} \in \mathbb{R}^{5N\times5N}$ and input matrix $\mathbf{B} \in \mathbb{R}^{5N\times N}$ are given by: $\mathbf{A} = \begin{bmatrix} \mathbf{A}_1 & \mathbf{A}_{12} & \cdots \mathbf{A}_{1N} \\ \mathbf{A}_{21} & \mathbf{A}_2 & \cdots \mathbf{A}_{2N} \\ \vdots & \vdots & \vdots \\ \mathbf{A}_{N1} & \mathbf{A}_{N2} & \cdots \mathbf{A}_N \end{bmatrix}$ and $\mathbf{B} = diag(\mathbf{B}_1 \cdots \mathbf{B}_N)$.

Now, the above system is expressed as a discrete-time state-space linear model as follows:

$$\mathbf{x}_{k+1} = \mathbf{A}_d\mathbf{x}_k + \mathbf{B}_d\mathbf{u}_k + \mathbf{n}_k, \tag{7.17}$$

where $\mathbf{A}_d = \mathbf{I} + \mathbf{A}\Delta t$, $\mathbf{I}$ is the identity matrix, Δt is the sampling period and $\mathbf{B}_d = \mathbf{B}\Delta t$.

In order to sense and monitor the distribution power systems, the system operators deploy a set of sensors around the grid. The system measurements are described by (7.2). Afterwards, the sensing information is transmitted to the energy management system where the estimators run in a distributed way.

7.4 Solution to the Optimal Distributed Estimator

The following result gives the optimal gain $\mathbf{K}_k^i$ in (7.4).

Theorem 7.1: For the given system (7.1), and observation (7.2), the minimization of mean squared error $E[(\mathbf{x}_k - \hat{\mathbf{x}}_{k|k}^i)(\mathbf{x}_k - \hat{\mathbf{x}}_{k|k}^i)']$ can be achieved, if one can obtain the optimal gain as follows:

$$\mathbf{K}_k^i = n^i \mathbf{P}_{k|k-1}^i \mathbf{C}' [(n^i)^2 \mathbf{C} \mathbf{P}_{k|k-1}^i \mathbf{C}' + \sum_{l \in N^i} \mathbf{R}_k^l]^{-1}. \tag{7.18}$$

The error covariance $\mathbf{P}_{k|k}^i = E[(\mathbf{x}_k - \hat{\mathbf{x}}_{k|k}^i)(\mathbf{x}_k - \hat{\mathbf{x}}_{k|k}^i)']$ is the solution to the following expression:

$$\mathbf{P}_{k|k}^i = (\mathbf{I} - n^i \mathbf{K}_k^i \mathbf{C}) \mathbf{P}_{k|k-1}^i (\mathbf{I} - n^i \mathbf{K}_k^i \mathbf{C})' + \mathbf{K}_k^i \sum_{l \in N^i} \mathbf{R}_k^l \mathbf{K}_k'^i. \tag{7.19}$$

Here, $n^i = n^i(N^i)$ represents the cardinality of N^i, $\mathbf{P}_{k|k-1}^i = \mathbf{A}_d \mathbf{P}_{k-1|k-1}^i \mathbf{A}_d' + \mathbf{Q}_{k-1}$ is the predicted error covariance matrix and $\mathbf{P}_{k-1|k-1}^i$ is the error covariance matrix of the previous step. The proof is derived in Appendix C.

Analytically, finding an optimal estimator does not guarantee reaching a consensus on estimation. Driven by this motivation, the next problem is to confirm the convergence of the proposed algorithm so that it can be applied for monitoring the power network.

7.5 Convergence Analysis of the Estimation Algorithm

Let $\mathbf{e}^i$ denote the estimation error between the actual state and estimated state of the i-th estimator, which can be expressed as follows:

$$\mathbf{e}^i_{k|k} = \mathbf{x}_k - \hat{\mathbf{x}}^i_{k|k}. \tag{7.20}$$

$$\mathbf{e}^i_{k|k-1} = \mathbf{x}_k - \hat{\mathbf{x}}^i_{k|k-1}. \tag{7.21}$$

Let's take the Lyapunov function as follows:

$$V(e_{k|k}) = \sum_{i=1}^{N} \mathbf{e}'^i_{k|k} (\mathbf{P}^i_{k|k})^{-1} \mathbf{e}^i_{k|k}. \tag{7.22}$$

The first difference of the Lyapunov function can be expressed as follows:

$$\begin{aligned} E[\Delta V(e_{k|k})] &= E[V(e_{k+1|k+1}) - V(e_{k|k})] \\ &= E[\sum_{i=1}^{N} \{\mathbf{e}'^i_{k+1|k+1} (\mathbf{P}^i_{k+1|k+1})^{-1} \mathbf{e}^i_{k+1|k+1} - \mathbf{e}'^i_{k|k} (\mathbf{P}^i_{k|k})^{-1} \mathbf{e}^i_{k|k}\}]. \end{aligned} \tag{7.23}$$

The following lemmas are used to simplify the above expression.

Lemma 7.1: Defining the information matrix $\mathbf{S}^i_k = (n^i)^2 \mathbf{C}' (\sum_{l \in N^i} \mathbf{R}^l_k)^{-1} \mathbf{C}$, then $\mathbf{P}^i_{k|k} = [(\mathbf{P}^i_{k|k-1})^{-1} + \mathbf{S}^i_k]^{-1}$.

Proof: See Appendix D.

Lemma 7.2: The following statement holds: $\mathbf{P}^i_{k+1|k+1} = \mathbf{F}^i_{k+1} \mathbf{G}^i_{k+1} \mathbf{F}'^i_{k+1}$ with the simplified terms $\mathbf{G}^i_{k+1} = \mathbf{A}_d \mathbf{P}^i_{k|k} \mathbf{A}'_d + \mathbf{W}^i_{k+1}$, $\mathbf{W}^i_{k+1} = \mathbf{Q}_k + \mathbf{P}^i_{k+1|k} \mathbf{S}^i_{k+1} \mathbf{P}^i_{k+1|k}$ and $\mathbf{F}^i_{k+1} = [\mathbf{I} - n^i \mathbf{K}^i_{k+1} \mathbf{C}]$.

Proof: See Appendix E.

Now $\mathbf{e}^i_{k+1|k+1}$ can be expressed as follows:

$$\begin{aligned} \mathbf{e}^i_{k+1|k+1} &= \mathbf{x}_{k+1} - \hat{\mathbf{x}}^i_{k+1|k+1} \\ &= \mathbf{x}_{k+1} - \hat{\mathbf{x}}^i_{k+1|k} - \mathbf{K}^i_{k+1} \sum_{l \in N^i} (\mathbf{y}^l_{k+1} - \mathbf{C} \hat{\mathbf{x}}^i_{k+1|k}) \\ &= [\mathbf{I} - n^i \mathbf{K}^i_{k+1} \mathbf{C}][\mathbf{A}_d (\mathbf{x}_k - \hat{\mathbf{x}}^i_{k|k}) + \mathbf{n}_k] - \mathbf{K}^i_{k+1} \sum_{l \in N^i} \mathbf{w}^l_{k+1} \\ &= (\mathbf{I} - n^i \mathbf{K}^i_{k+1} \mathbf{C})(\mathbf{A}_d \mathbf{e}^i_{k|k} + \mathbf{n}_k) - \mathbf{K}_{k+1} \sum_{l \in N^i} \mathbf{w}^l_{k+1}. \end{aligned} \tag{7.24}$$

For simplicity of the convergence analysis, it is assumed that there are no noisy terms in (7.24), and it can be rewritten as follows:

$$\begin{aligned}\mathbf{e}^i_{k+1|k+1} &= (\mathbf{I} - n^i\mathbf{K}^i_{k+1}\mathbf{C})\mathbf{A}_d\mathbf{e}^i_{k|k} \\ &= \mathbf{F}^i_{k+1}\mathbf{A}_d\mathbf{e}^i_{k|k}. \end{aligned} \tag{7.25}$$

Here, $\mathbf{F}^i_{k+1} = [\mathbf{I} - n^i\mathbf{K}^i_{k+1}\mathbf{C}]$.

For the expression of $E[\Delta V(e_{k|k})]$, (7.23) is used together with (7.25) to yield:

$$E[\Delta V(e_{k|k})] = \sum_{i=1}^{N} \mathbf{e}'^i_{k|k}[\mathbf{A}'_d\mathbf{F}'^i_{k+1}(\mathbf{P}^i_{k+1|k+1})^{-1}\mathbf{F}^i_{k+1}\mathbf{A}_d - (\mathbf{P}^i_{k|k})^{-1}]\mathbf{e}^i_{k|k}. \tag{7.26}$$

Using Lemma 2, (7.26) can be written as follows:

$$\begin{aligned} E[\Delta V(e_{k|k})] &= \sum_{i=1}^{N} \mathbf{e}'^i_{k|k}[\mathbf{A}'_d(\mathbf{G}^i_{k+1})^{-1}\mathbf{A}_d - (\mathbf{P}^i_{k|k})^{-1}]\mathbf{e}^i_{k|k} \\ &= -\sum_{i=1}^{N} \mathbf{e}'^i_{k|k}[(\mathbf{P}^i_{k|k})^{-1} - \mathbf{A}'_d(\mathbf{G}^i_{k+1})^{-1}\mathbf{A}_d]\mathbf{e}^i_{k|k} \\ \Rightarrow E[\Delta V(e_{k|k})] &= -\sum_{i=1}^{N} \mathbf{e}'^i_{k|k}\mathbf{\Lambda}^i_{k+1}\mathbf{e}^i_{k|k}, \end{aligned} \tag{7.27}$$

where $\mathbf{\Lambda}^i_{k+1}$ is defined as follows:

$$\mathbf{\Lambda}^i_{k+1} = (\mathbf{P}^i_{k|k})^{-1} - \mathbf{A}'_d(\mathbf{G}^i_{k+1})^{-1}\mathbf{A}_d. \tag{7.28}$$

In order to apply the well-known matrix inversion Lemma, $(\mathbf{A}+\mathbf{BCD})^{-1} = \mathbf{A}^{-1} - \mathbf{A}^{-1}\mathbf{B}(\mathbf{C}^{-1} + \mathbf{DA}^{-1}\mathbf{B})^{-1}\mathbf{DA}^{-1}$ [51], pre and post-multiplying (7.28) by $\mathbf{P}^i_{k|k}$ yields:

$$\begin{aligned}\mathbf{P}^i_{k|k}\mathbf{\Lambda}^i_{k+1}\mathbf{P}^i_{k|k} &= \mathbf{P}^i_{k|k} - \mathbf{P}^i_{k|k}\mathbf{A}'_d(\mathbf{W}^i_{k+1} + \mathbf{A}_d\mathbf{P}^i_{k|k}\mathbf{A}'_d)^{-1}\mathbf{A}_d\mathbf{P}^i_{k|k} \\ &= [(\mathbf{P}^i_{k|k})^{-1} + \mathbf{A}'_d(\mathbf{W}^i_{k+1})^{-1}\mathbf{A}_d]^{-1}. \end{aligned} \tag{7.29}$$

Now pre and post-multiplying (7.29) by $(\mathbf{P}^i_{k|k})^{-1}$ leads to:

$$\mathbf{\Lambda}^i_{k+1} = (\mathbf{P}^i_{k|k})^{-1}[(\mathbf{P}^i_{k|k})^{-1} + \mathbf{A}'_d(\mathbf{W}^i_{k+1})^{-1}\mathbf{A}_d]^{-1}(\mathbf{P}^i_{k|k})^{-1}. \tag{7.30}$$

This shows that $\mathbf{\Lambda}^i_{k|k}$ is a symmetric and positive definite matrix. This ensures that (7.27) becomes:

$$E[\Delta V(e_{k|k})] = -\sum_{i=1}^{N} \mathbf{e}'^i_{k|k}\mathbf{\Lambda}^i_{k+1}\mathbf{e}^i_{k|k} < 0. \tag{7.31}$$

This confirms that the incremental Lyapunov function is less than zero, so the estimation error dynamic is asymptotically stable. This proves that the proposed algorithm is convergent. The performance of the aforementioned algorithm is explored by performing numerical simulations in the following section.

7.6 Simulation Results and Discussions

In order to simplify our discussion, here, it is assumed there are n=4 observation stations and N=5 synchronous generators in the distribution power networks as shown in Figs. 7.1-7.2. The proposed work can be easily extended to the generic case. The simulation is implemented in Matlab where the parameters are summarized in Tables 7.1 and 7.2 [14], [15]. Moreover, the considered process and measurement noise covariances are diagonal matrices [106], [107], [113] and their values are $\mathbf{Q} = 0.00001\mathbf{I}$, $\mathbf{R}^1 = 0.003\mathbf{I}$, $\mathbf{R}^2 = 0.004\mathbf{I}$ $\mathbf{R}^3 = 0.005\mathbf{I}$ and $\mathbf{R}^4 = 0.006\mathbf{I}$. The sampling period for discretization is 0.0015 seconds.

Table 7.1: Parameters of five generators G1-G5 [14], [15].

Parameters	G1	G2	G3	G4	G5
H_i	4.6	4.75	4.53	4.04	5
D_i	3.14	3.77	3.45	4.08	3.5
X_{di}	0.1026	0.1026	1.0260	0.1026	1.0260
X'_{di}	0.0339	0.0339	0.3390	0.0339	0.3390
T'_{doi}	5.67	5.67	5.67	5.67	5.67
b_{1i}	1332	1332	1332	1332	1332
b_{oi}	666	666	666	666	666
c_{1i}	33.3	33.3	33.3	33.3	33.3
c_{oi}	3.33	3.33	3.33	3.33	3.33
V	1.05	1.03	1.025	1.05	1.025
θ	0	0.1051	0.0943	0.0361	0.0907
P	3.1621	4.1026	0.4708	4.0678	0.1647
Q	2.9241	1.3921	0.4197	2.1902	0.3479

Table 7.2: Transmission line parameters [14], [15].

Node i	Node j	R_{ij}	X_{ij}	B_{ij}
1	7	0.00435	0.01067	0.01536
2	6	0.00213	0.00468	0.00404
3	6	0.02004	0.06244	0.06406
4	8	0.00524	0.01184	0.01756
5	6	0.00711	0.02331	0.02732
6	7	0.04032	0.12785	0.15858
7	8	0.01724	0.04153	0.06014

Figures 7.3-7.17 show the system's true and estimated states versus time step. It can be seen that the proposed method can estimate the system states with reasonable accuracy. This is because the developed approach can effectively solve the distributed estimation problem to find the optimal solution. So, the estimated states reflect the true state within a few steps. For instance, it can be seen from Fig. 7.3 that the explored method requires 0.0150 seconds $(k \times \Delta t = 10 \times 0.0015)$ to estimate the rotor angle of generator 1. Similar kind of estimation performance is obtained for other states. From the technical point of view, it means that the proposed algorithm requires much less time compared with the standard estimation time of 1 second [47]. As the five generators have different specifications so their true states are different which are also well estimated by the proposed approach. Note that the small fluctuations come from the system noise.

7.7 Summary

This chapter presents a distributed approach for estimating the synchronous generator states. The simulation results show the validity of the analytical approach. The results point out the applicability of the proposed scheme for estimating the multiple synchronous generator states. Finally, the consensus of the explored algorithm is also proved so that it can be applied to practical applications in modern smart grids. Consequently, these contributions are valuable for designing the distributed smart energy management system as it provides precise estimation performance and requires less computational resources in the estimation

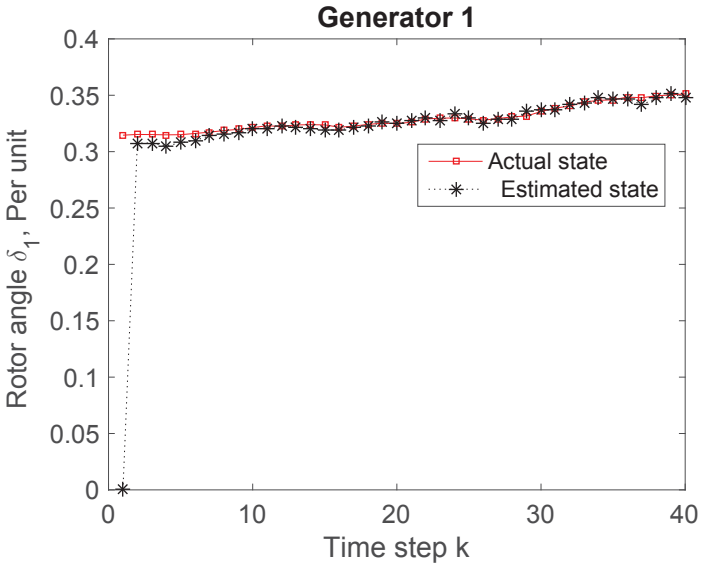

Figure 7.3: Rotor angle δ_1 and its estimation.

process.

The following chapter considers a more realistic filtering process for interconnected systems. That is, the upcoming distributed state estimation algorithm is derived by considering different observation matrices and the discrete-time system for convergence analysis.

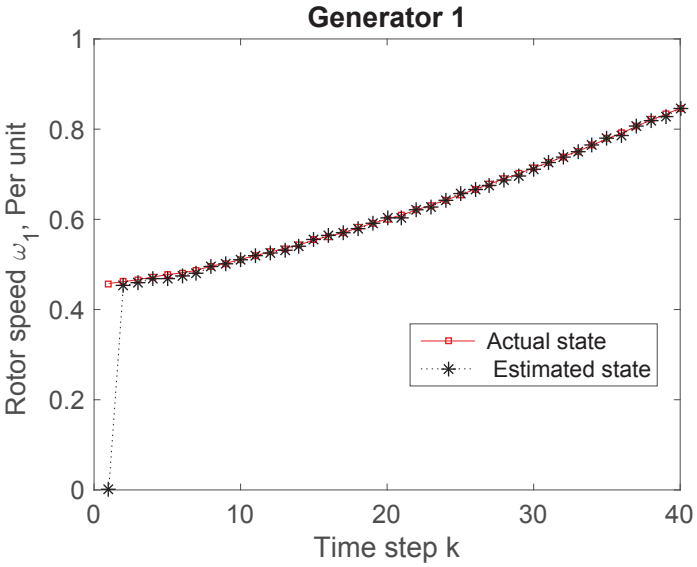

Figure 7.4: Rotor speed ω_1 and its estimation.

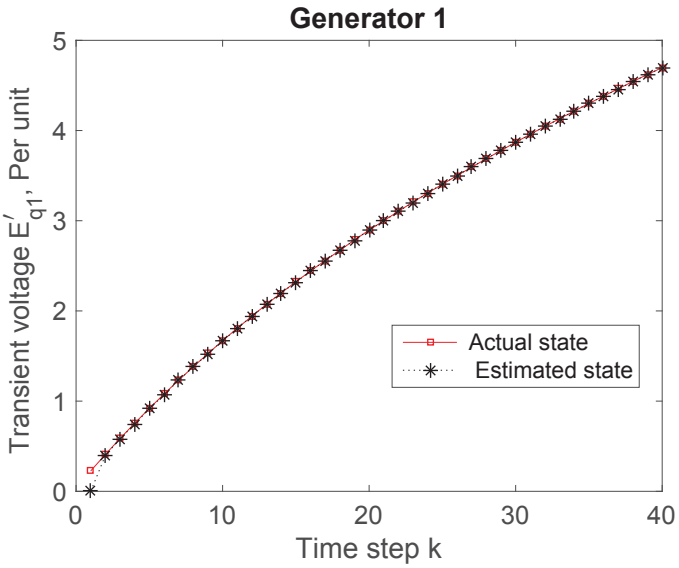

Figure 7.5: Transient voltage E'_{q1} and its estimation.

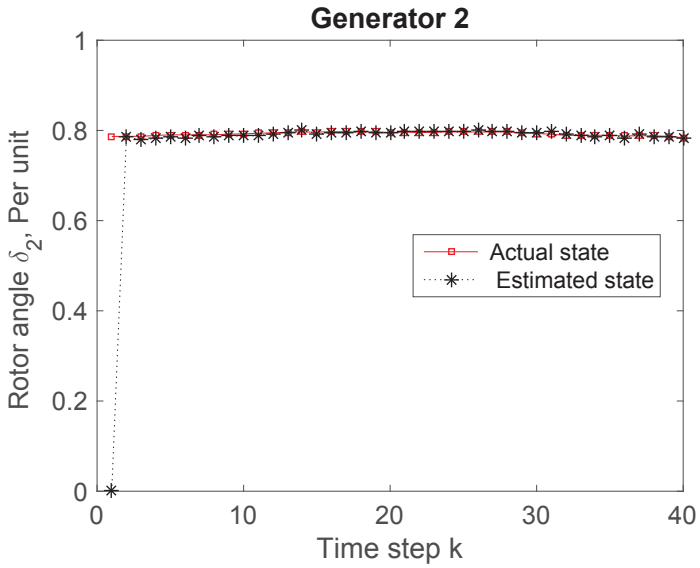

Figure 7.6: Rotor angle δ_2 and its estimation.

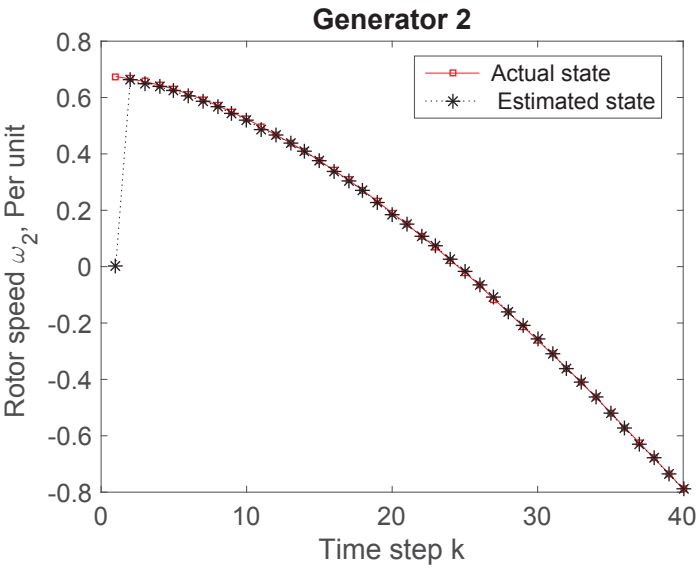

Figure 7.7: Rotor speed ω_2 and its estimation.

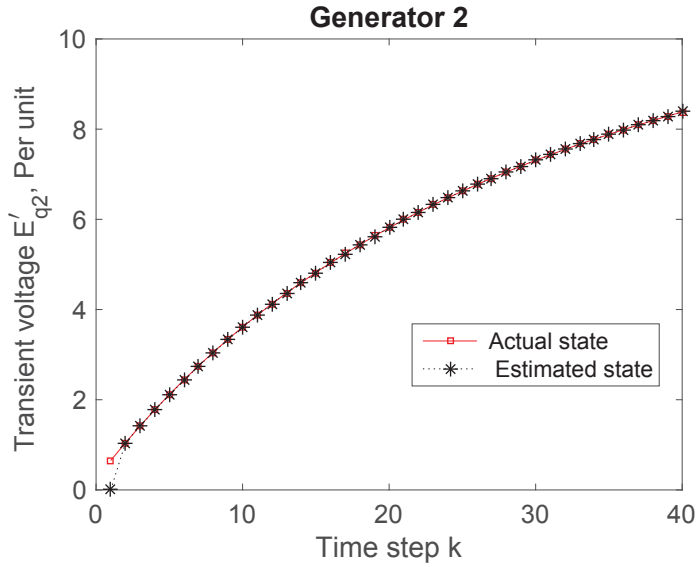

Figure 7.8: Transient voltage E'_{q2} and its estimation.

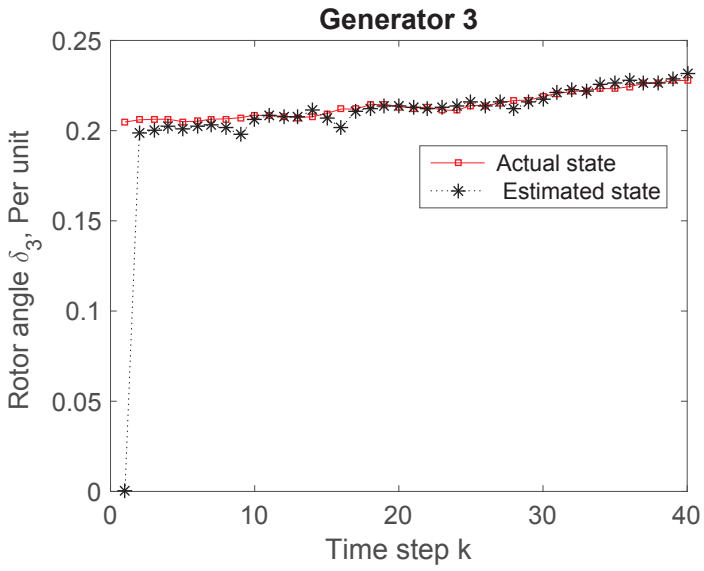

Figure 7.9: Rotor angle δ_3 and its estimation.

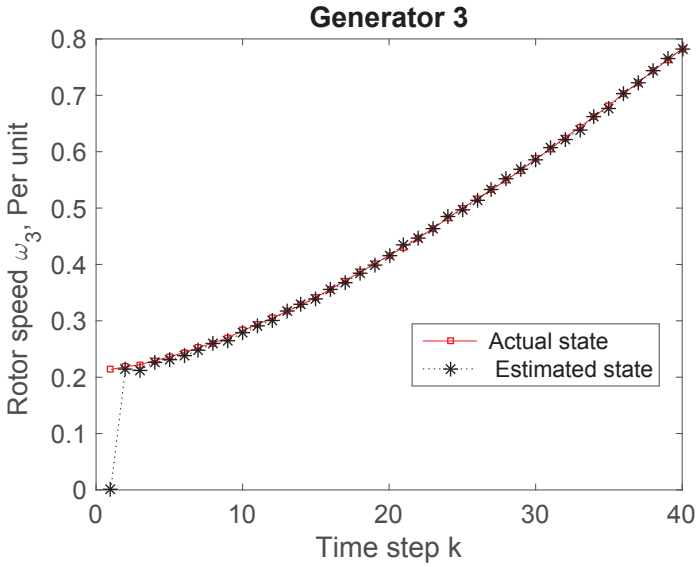

Figure 7.10: Rotor speed ω_3 and its estimation.

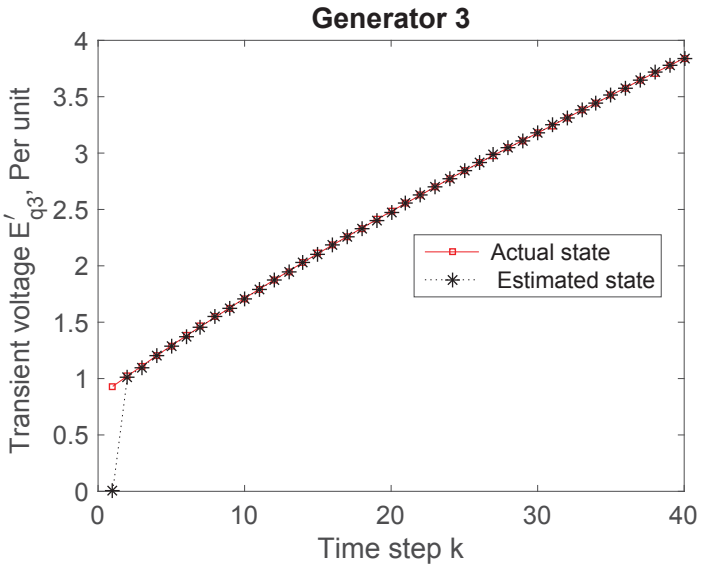

Figure 7.11: Transient voltage E'_{q3} and its estimation.

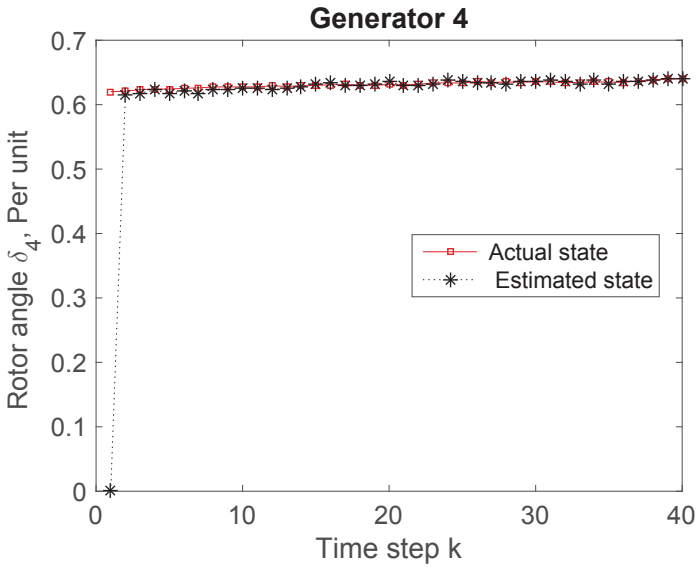

Figure 7.12: Rotor angle δ_4 and its estimation.

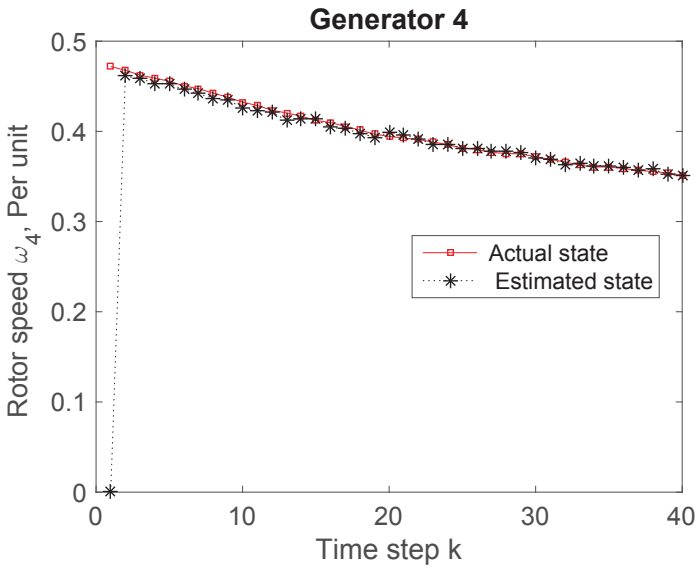

Figure 7.13: Rotor speed ω_4 and its estimation.

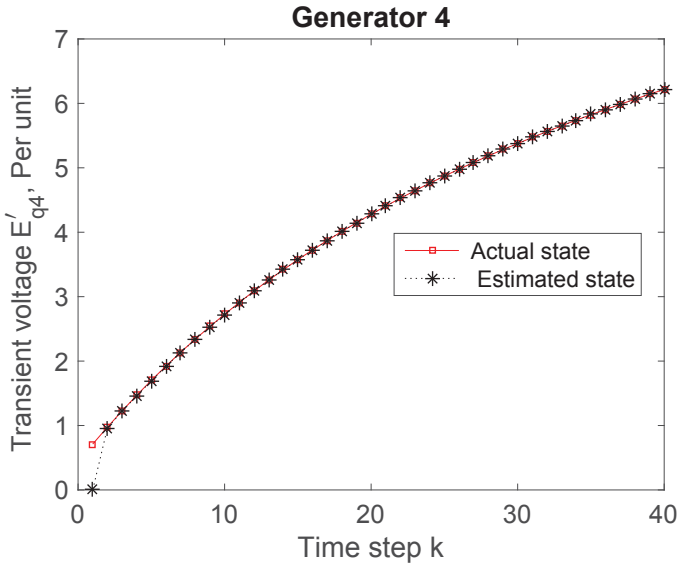

Figure 7.14: Transient voltage E'_{q4} and its estimation.

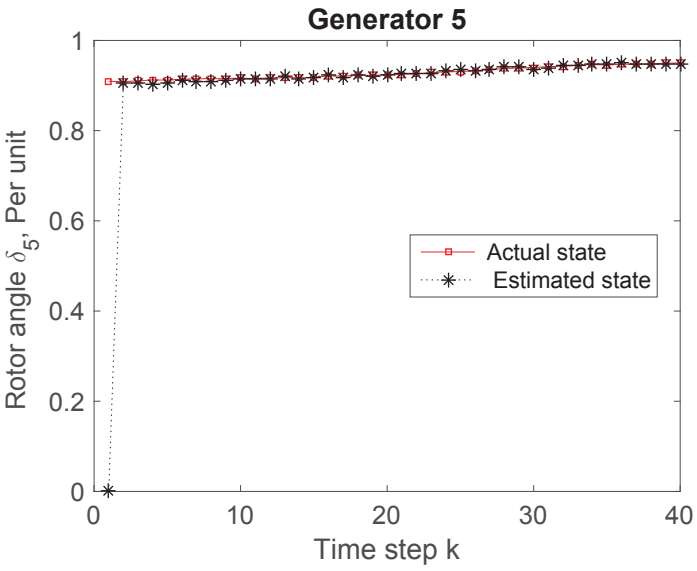

Figure 7.15: Rotor angle δ_5 and its estimation.

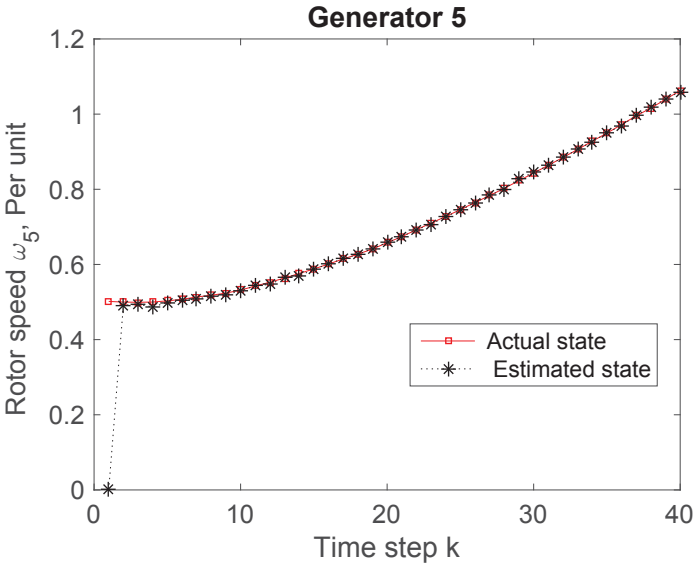

Figure 7.16: Rotor speed ω_5 and its estimation.

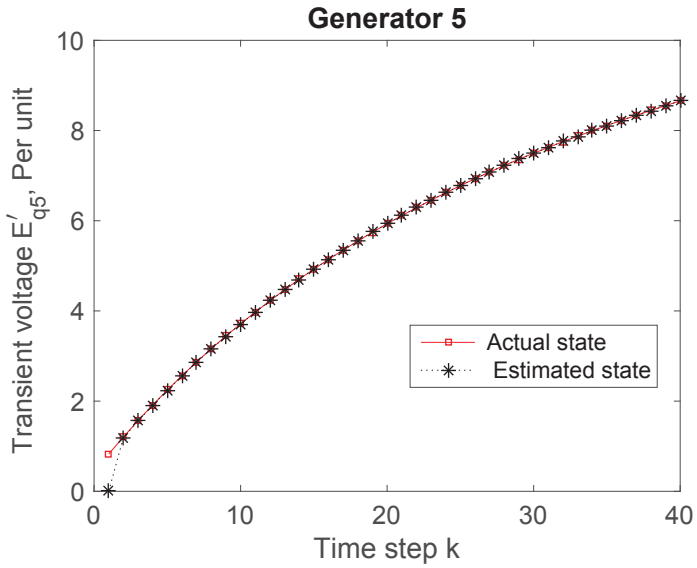

Figure 7.17: Transient voltage E'_{q5} and its estimation.

Chapter 8

Distributed Kalman Consensus Algorithm with its Convergence Analysis

8.1 Introduction

State estimation is essential to know the operating condition of power systems as the microgrid incorporating the renewable distributed energy resources (DERs) is integrated into the grid [22], [248]. Generally, the microgrid internal dynamic states such as rotor angle are inaccessible, so the estimation is not only required to know the system states but also imperative to design the controller [106]. However, transmitting the massive amount of grid data to the traditional centralised estimator is not only infeasible but also expensive [245]. Interestingly, the distributed estimation scheme is efficient, accurate and implementable for complex power systems [249]. However, there is little attention for the distributed smart grid state estimation that also incorporates the renewable microgrids. For instance, the least-square type modified coordinated state estimation is proposed for multi-area power systems in [130], [250], [153]. It is worth mentioning that it does not require either local observability or a central coordinator as it is completely distributed. Regrettably, the performance of this scheme is totally dependent on tuning parameters. Moreover, the linear minimum mean square error (LMMSE) based distributed estimation in sensor networks is introduced in [251]. The correlation between measurements is also considered in [62], and the LMMSE technique can mitigate the estimation errors for improving estimation performance. In [252],

author establishes a distributed estimation and collaborative control scheme for wireless sensor networks. These techniques mainly focus on an optimization approach for accurate and timely control of the event after minimizing the energy consumption of each actuator. The consensus-based distributed state estimation algorithms for sensor networks are proposed in [141], [51], [142].

This chapter proposes a novel distributed consensus filter based dynamic state estimation algorithm with its convergence analysis for modern power systems. The novelty of the scheme is that the algorithm is designed based on the mean squared error and semidefinite programming approaches. Specifically, the optimal local gain is computed after minimizing the mean squared error between the true and estimated states. The consensus gain is determined by a convex optimization process with a given local gain. Furthermore, the convergence of the proposed scheme is analysed after stacking all the estimation error dynamics. The Laplacian operator is used to represent the interconnected filter structure as a compact error dynamic for deriving the convergence condition of the algorithm. The developed approach is verified by using the mathematical dynamic model of the renewable microgrid and IEEE 30-bus power system. It shows that the proposed distributed scheme is effective to properly estimate the system states and does not need to transmit the remote sensing signals to the central estimator. Consequently, this work is valuable for the design of a distributed smart energy management system and will ready for implementing control strategies when the estimated system state is available.

8.2 Problem Description

In order to develop a distributed estimator, consider the following discrete-time system:

$$\mathbf{x}(k+1) = \mathbf{A}_d\mathbf{x}(k) + \mathbf{B}_d\mathbf{u}(k) + \mathbf{n}_d(k), \tag{8.1}$$

where $\mathbf{x}(k) \in \mathbb{R}^q$ is the system state variable at time instant k, $\mathbf{u}(k) \in \mathbb{R}^r$ is the control effort, $\mathbf{n}_d(k) \in \mathbb{R}^q$ is the process noise (Gaussian distribution) with zero mean and covariance matrix $\mathbf{Q}$, and $\mathbf{A}_d \in \mathbb{R}^{q\times q}$ as well as $\mathbf{B}_d \in \mathbb{R}^{q\times r}$ are the system state and input matrices.

In order to sense and monitor the above system, the system operators deploy a set of sensors

around the grid whose measurements are described by:

$$\mathbf{y}^i(k) = \mathbf{C}^i\mathbf{x}(k) + \mathbf{w}^i(k),\ i = 1, 2, \cdots, n \tag{8.2}$$

where $\mathbf{y}^i(k)$ is the observation information by the i-th estimator, $\mathbf{C}^i$ is the sensing matrix and $\mathbf{w}^i(k)$ is the measurement noise (Gaussian distribution) with zero mean and covariance matrix $\mathbf{R}^i$.

Assumption 1: $(\mathbf{A}_d, \mathbf{C}^i)$ is observable for all i.

Generally speaking, the distribution power sub-systems are interconnected to each other as shown in Fig. 8.1. Basically, this research assumes that the sub-stations have communication capabilities to exchange information with each other. The proposed distributed estimation is written as follows:

$$\hat{\mathbf{x}}^i(k+1) = \mathbf{A}_d\hat{\mathbf{x}}^i(k) + \mathbf{B}_d\mathbf{u}(k) + \mathbf{K}^i(k)[\mathbf{y}^i(k) - \mathbf{C}^i\hat{\mathbf{x}}^i(k)] + \mathbf{L}^i(k)\sum_{j\in N_i}[\hat{\mathbf{x}}^j(k) - \hat{\mathbf{x}}^i(k)]. \tag{8.3}$$

Here, $\hat{\mathbf{x}}^i(k+1)$ is the updated state estimation at the i-th estimator, $\hat{\mathbf{x}}^i(k)$ is the estimated state of the previous step, $\mathbf{K}^i(k)$ is the local gain, $\mathbf{L}^i(k)$ is the neighbouring gain and N_i denotes the set of neighbouring estimators. Basically, the first two terms are considered as a prediction step, while others are the correction part. Particularly, the third term in (8.3) is used for local estimation, while the fourth term is employed to share information with the connected estimators to reach a consensus on state estimation. Based on the aforementioned filter structure, the first problem is to design the optimal gains, so that the estimated state converges to the actual system state. The next problem is to analyse the convergence of the developed algorithm so that it can be applied in real-time applications. Overall, the pictorial view of the proposed distributed estimation and its research questions are summarized in Fig. 8.1.

To address the aforementioned issues, this study proposes a distributed dynamic state estimation algorithm, and its convergence is analysed. To estimate the system states, the local and neighbouring gains are derived based on the mean squared error and linear matrix inequality approaches, respectively. From a practical implementation point of view, the convergence condition of the developed approach is derived and verified. For doing this, the interconnected error dynamic is expressed in a compact framework using the Laplacian operator. A

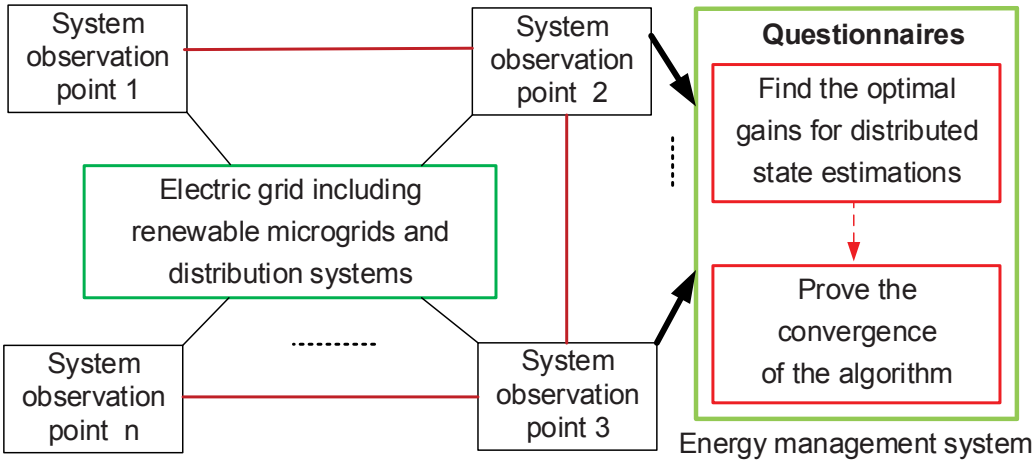

Figure 8.1: A framework for distributed estimation and its research questions.

sufficient condition for the convergence of the algorithm is that the spectral radius of error dynamic is less than one. The efficacy of the developed approach is demonstrated using the environment-friendly renewable microgrid and IEEE 30-bus power system.

8.3 State-Space Representation of Microgrid

The electricity produced by the renewable microgrid is generally cleaner, greener, more affordable and locally harvested in many parts of the world [248], [253]. Driven by this motivation, this study considers a renewable microgrid which incorporates multiple DERs such as solar cells and wind turbines. The single-line diagram of the studied microgrid incorporating electricity generating electronic circuits is described in Fig. 8.2 [16], [17], where two parallel DERs are connected to it [16]. It consists of DC voltage sources (representing renewable resources), voltage source converters (VSC), filters, step-up transformers and loads [6], [254]. In each DER, the generic renewable resource is modelled as a DC voltage source, and the converter is used to supply power to loads. The step-up transformer is utilised to connect DERs at the common coupling point (PCC). From this diagram, it can be seen that the two DERs are denoted by DER i and DER j which are connected through a three-phase transmission line with line impedance (consisting of resistance and inductance). The shunt capacitance C_t is used for regulating the high-frequency harmonics of load voltages [255].

After applying Kirchhoff's voltage and current laws, the system dynamic in the dq-rotating

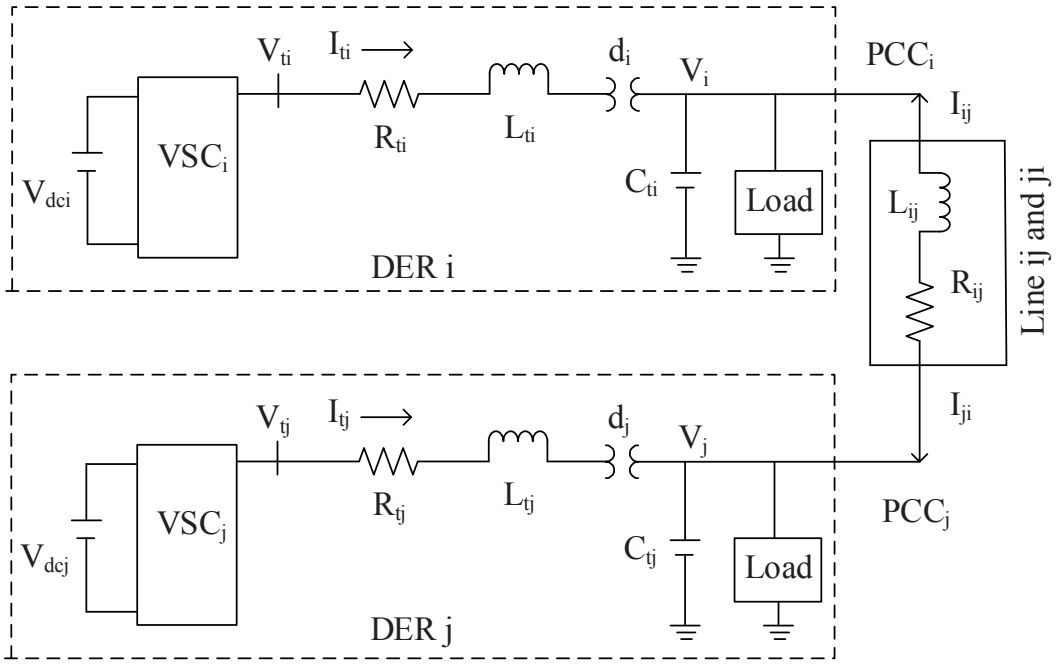

Figure 8.2: Electricity generating electronic circuits and loads [16], [17].

frame with speed ω_0 can be written as follows [16]:

$$DERi \begin{cases} \dot{V}_{i,dq} = -j\omega_o V_{i,dq} + (d_i I_{ti,dq} + I_{ij,dq})/C_{ti}. \\ \dot{I}_{ti,dq} = -j\omega_o I_{ti,dq} - (d_i V_{i,dq} + R_{ti,dq} I_{ti,dq} - V_{ti,dq})/L_{ti}. \end{cases} \tag{8.4}$$

$$DERj \begin{cases} \dot{V}_{j,dq} = -j\omega_o V_{j,dq} + (d_j I_{tj,dq} + I_{ji,dq})/C_{tj}. \\ \dot{I}_{tj,dq} = -j\omega_o I_{tj,dq} - (d_j V_{j,dq} + R_{tj,dq} I_{tj,dq} - V_{tj,dq})/L_{tj}. \end{cases} \tag{8.5}$$

$$Line\ ij : \dot{I}_{ij,dq} = -j\omega_o I_{ij,dq} + (V_{j,dq} - R_{ij,dq} I_{ij,dq} - V_{i,dq})/L_{ij}. \tag{8.6}$$

$$Line\ ji : \dot{I}_{ji,dq} = -j\omega_o I_{ji,dq} + (V_{i,dq} - R_{ji,dq} I_{ji,dq} - V_{j,dq})/L_{ji}. \tag{8.7}$$

Here, $(V_{i,dq}, V_{j,dq})$, $(V_{ti,dq}, V_{tj,dq})$, $(I_{ti,dq}, I_{tj,dq})$ and $(I_{ij,dq}, I_{ji,dq})$ are the dq components of PCC voltages, VSC terminal voltages, filter currents and line currents, respectively, d_i is the transformer ratio, and $w_0 = 2\pi f_o$, where f_o is the frequency of the microgrid. Basically, each expression has two components: real part d-frame and imaginary part q-frame. The above system can be written in the following continuous-time state-space framework as follows:

$$\dot{\mathbf{x}} = \mathbf{A}\mathbf{x} + \mathbf{B}\mathbf{u}. \tag{8.8}$$

Here, the microgrid state $\mathbf{x} = [V_{i,d},\ V_{i,q},\ I_{ti,d},\ I_{ti,q},\ I_{ij,d},\ I_{ij,q},\ I_{ji,d},\ I_{ji,q},\ V_{j,d},\ V_{j,q},\ I_{tj,d},\ I_{tj,q}]'$

$$\mathbf{A} = \begin{bmatrix}
0 & \omega_o & \frac{d_i}{C_{ti}} & 0 & \frac{1}{C_{ti}} & 0 & 0 & 0 & 0 & 0 & 0 & 0 \\
-\omega_o & 0 & 0 & \frac{d_i}{C_{ti}} & 0 & \frac{1}{C_{ti}} & 0 & 0 & 0 & 0 & 0 & 0 \\
-\frac{d_i}{C_{ti}} & 0 & -\frac{R_{ti}}{L_{ti}} & \omega_o & 0 & 0 & 0 & 0 & 0 & 0 & 0 & 0 \\
0 & -\frac{d_i}{C_{ti}} & -\omega_o & -\frac{R_{ti}}{L_{ti}} & 0 & 0 & 0 & 0 & 0 & 0 & 0 & 0 \\
-\frac{1}{L_{ij}} & 0 & 0 & 0 & -\frac{R_{ij}}{L_{ij}} & \omega_o & 0 & 0 & \frac{1}{L_{ij}} & 0 & 0 & 0 \\
0 & -\frac{1}{L_{ij}} & 0 & 0 & -\omega_o & -\frac{R_{ij}}{L_{ii}} & 0 & 0 & 0 & \frac{1}{L_{ij}} & 0 & 0 \\
\frac{1}{L_{ji}} & 0 & 0 & 0 & -\frac{R_{ji}}{L_{ji}} & \omega_o & 0 & 0 & -\frac{1}{L_{ji}} & 0 & 0 & 0 \\
0 & \frac{1}{L_{ji}} & 0 & 0 & -\omega_o & -\frac{R_{ji}}{L_{ji}} & 0 & 0 & 0 & -\frac{1}{L_{ji}} & 0 & 0 \\
0 & 0 & 0 & 0 & 0 & 0 & \frac{1}{C_{tj}} & 0 & 0 & \omega_o & \frac{d_i}{C_{ti}} & 0 \\
0 & 0 & 0 & 0 & 0 & 0 & 0 & \frac{1}{C_{tj}} & -\omega_o & 0 & 0 & \frac{d_i}{C_{ti}} \\
0 & 0 & 0 & 0 & 0 & 0 & 0 & 0 & \frac{d_j}{L_{tj}} & 0 & -\frac{R_{tj}}{L_{tj}} & \omega_o \\
0 & 0 & 0 & 0 & 0 & 0 & 0 & 0 & 0 & -\frac{d_j}{L_{tj}} & -\omega_o & -\frac{R_{tj}}{L_{tj}}
\end{bmatrix},$$

$$\mathbf{B} = \begin{bmatrix}
0 & 0 & 1/L_{ti} & 0 & 0 & 0 & 0 & 0 & 0 & 0 & 0 & 0 \\
0 & 0 & 0 & 1/L_{ti} & 0 & 0 & 0 & 0 & 0 & 0 & 0 & 0 \\
0 & 0 & 0 & 0 & 0 & 0 & 0 & 0 & 0 & 0 & 1/L_{tj} & 0 \\
0 & 0 & 0 & 0 & 0 & 0 & 0 & 0 & 0 & 0 & 0 & 1/L_{ti}
\end{bmatrix}'.$$

and the system input $\mathbf{u} = [V_{ti,d},\ V_{ti,q},\ V_{tj,d},\ V_{tj,q}]'$. The system state matrix $\mathbf{A}$ and input matrix $\mathbf{B}$ are given above.

Now, the above system is expressed as a discrete-time state-space linear model as follows:

$$\mathbf{x}(k+1) = \mathbf{A}_d\mathbf{x}(k) + \mathbf{B}_d\mathbf{u}(k) + \mathbf{n}(k), \tag{8.9}$$

where $\mathbf{A}_d = \mathbf{I} + \mathbf{A}\Delta t$, $\mathbf{I}$ is the identity matrix, Δt is the sampling period, $\mathbf{B}_d = \mathbf{B}\Delta t$ and $\mathbf{n}$ is considered the exogenous disturbance with zero mean and covariance matrix $\mathbf{Q}$. To estimate the system states, the proposed distributed Kalman consensus algorithm is derived in the following section.

8.4 Proposed Distributed Kalman Consensus Algorithm

Let $\mathbf{e}^i$ denote the estimation error between the actual state and estimated state of the i-th estimator as follows:

$$\mathbf{e}^i(k) = \mathbf{x}(k) - \hat{\mathbf{x}}^i(k). \tag{8.10}$$

$$\mathbf{e}^i(k+1) = \mathbf{x}(k+1) - \hat{\mathbf{x}}^i(k+1). \tag{8.11}$$

Substituting (8.3) into (8.11), and using (8.1) as well as (8.2), one can obtain the following error dynamic for the i-th estimator:

$$\begin{aligned}
\mathbf{e}^i(k+1) &= \mathbf{x}(k+1) - \mathbf{A}_d\hat{\mathbf{x}}^i(k) - \mathbf{B}_d\mathbf{u}(k) - \mathbf{K}^i(k)[\mathbf{y}^i(k) - \mathbf{C}^i\hat{\mathbf{x}}^i(k)] - \\
&\qquad \mathbf{L}^i(k)\sum_{r\in N_i}[\hat{\mathbf{x}}^r(k) - \hat{\mathbf{x}}^i(k)] \\
&= \mathbf{A}_d\mathbf{x}(k) + \mathbf{n}_d(k) - \mathbf{A}_d\hat{\mathbf{x}}^i(k) - \mathbf{K}^i(k)[\mathbf{C}^i\mathbf{x}(k) + \mathbf{w}^i(k) - \mathbf{C}^i\hat{\mathbf{x}}^i(k)] - \\
&\qquad \mathbf{L}^i(k)\sum_{r\in N_i}[-\mathbf{x}(k) + \hat{\mathbf{x}}^r(k) + \mathbf{x}(k) - \hat{\mathbf{x}}^i(k)] \\
&= [\mathbf{A}_d - \mathbf{K}^i(k)\mathbf{C}^i]\mathbf{e}^i(k) + \mathbf{L}^i(k)\sum_{r\in N_i}[\mathbf{e}^r(k) - \mathbf{e}^i(k)] + \mathbf{n}_d(k) - \mathbf{K}^i(k)\mathbf{w}^i(k).
\end{aligned} \tag{8.12}$$

Similarly for the j-th estimator, (8.12), can be written as follows:

$$\mathbf{e}^j(k+1) = [\mathbf{A}_d - \mathbf{K}^j(k)\mathbf{C}^j]\mathbf{e}^j(k) + \mathbf{L}^j(k)\sum_{s\in N_j}[\mathbf{e}^s(k) - \mathbf{e}^j(k)] + \mathbf{n}_d(k) - \mathbf{K}^j(k)\mathbf{w}^j(k). \tag{8.13}$$

The state estimation error covariance is defined by:

$$\mathbf{P}^{ij}(k+1) = E[\mathbf{e}^i(k+1)\mathbf{e}'^j(k+1)]. \tag{8.14}$$

By substituting (8.12) and (8.13) into (8.14), one can obtain the following expression:

$$\begin{aligned}
\mathbf{P}^{ij}(k+1) &= E[\{\mathbf{A}_d - \mathbf{K}^i(k)\mathbf{C}^i\}\mathbf{e}^i(k)\mathbf{e}'^j(k)\{\mathbf{A}_d - \\
&\qquad \mathbf{K}^j(k)\mathbf{C}^j\}'] + \sum_{s\in N_j}E[\{\mathbf{A}_d - \mathbf{K}^i(k)\mathbf{C}^i\}\mathbf{e}^i(k)\{\mathbf{e}'^s(k) - \mathbf{e}'^j(k)\}] \\
&\qquad \mathbf{L}'^j(k) + \mathbf{L}^i(k)\sum_{r\in N_i}E[\{\mathbf{e}^r(k) - \mathbf{e}^i(k)\}\mathbf{e}'^j(k)\{\mathbf{A}_d - \\
&\qquad \mathbf{K}^j(k)\mathbf{C}^j\}'] + \mathbf{L}^i(k)\sum_{r\in N_i}\sum_{s\in N_j}E[\{\mathbf{e}^r(k) - \mathbf{e}^i(k)\} \\
&\qquad \{\mathbf{e}^s(k) - \mathbf{e}^j(k)\}']\mathbf{L}'^j(k) + \mathbf{K}^i(k)\mathbf{R}^{ij}\mathbf{K}'^j(k) + \mathbf{Q}.
\end{aligned} \tag{8.15}$$

By setting j=i, one can determine the error covariance matrix of i-th estimator as follows:

$$\begin{aligned}\mathbf{P}^i(k+1) = [\mathbf{A}_d - \mathbf{K}^i(k)\mathbf{C}^i]\mathbf{P}^i(k)[\mathbf{A}_d - \mathbf{K}^i(k)\mathbf{C}^i]' + [\mathbf{A}_d - \\ \mathbf{K}^i(k)\mathbf{C}^i] \sum_{s\in N_i}[\mathbf{P}^{is}(k) - \mathbf{P}^i(k)]\mathbf{L}'^i(k) + \mathbf{L}^i(k) \sum_{r\in N_i} \\ [\mathbf{P}^{ri}(k) - \mathbf{P}^i(k)][\mathbf{A}_d - \mathbf{K}^i(k)\mathbf{C}^i]' + \mathbf{L}^i(k) \sum_{r,s\in N_i} \\ [\mathbf{P}^{rs}(k) - \mathbf{P}^{ri}(k) - \mathbf{P}^{is}(k) + \mathbf{P}^i(k)]\mathbf{L}'^i(k) + \\ \mathbf{K}^i(k)\mathbf{R}^i\mathbf{K}'^i + \mathbf{Q}. \end{aligned} \tag{8.16}$$

The error covariance matrices are: $\mathbf{P}^i(k+1) = \mathbf{P}^{ii}(k+1)$, $\sum_{s\in N_i}[\mathbf{P}^{is}(k) - \mathbf{P}^i(k)] = \sum_{s\in N_i} E[\mathbf{e}^i(k)\{\mathbf{e}'^s(k) - \mathbf{e}'^i(k)\}]$ and $\sum_{r\in N_i}[\mathbf{P}^{ri}(k) - \mathbf{P}^i(k)] = \sum_{r\in N_i} E[\{\mathbf{e}^r(k) - \mathbf{e}^i(k)\}\mathbf{e}'^i(k)]$. In order to find the optimal gain $\mathbf{K}^i(k)$, taking the partial derivative of $tr[\mathbf{P}^i(k+1)]$ in (8.16) with respect to $\mathbf{K}^i(k)$ yields:

$$\begin{aligned}\frac{\partial\{tr[\mathbf{P}^i(k+1)]\}}{\partial\mathbf{K}^i(k)} = -2\mathbf{A}_d\mathbf{P}^i(k)\mathbf{C}'^i + 2\mathbf{K}^i(k)\mathbf{C}^i\mathbf{P}^i(k)\mathbf{C}'^i - 2\mathbf{L}^i(k)\sum_{r\in N_i}[\mathbf{P}^{ri}(k) - \\ \mathbf{P}^i(k)]\mathbf{C}'^i + 2\mathbf{K}^i(k)\mathbf{R}^i(k). \end{aligned} \tag{8.17}$$

Setting $\frac{\partial\{tr[\mathbf{P}^i(k+1)]\}}{\partial\mathbf{K}^i(k)} = 0$ in (8.17), the optimal gain is expressed as follows:

$$\mathbf{K}^i(k) = [\mathbf{A}_d\mathbf{P}^i(k)\mathbf{C}'^i + \mathbf{L}^i(k)\sum_{r\in N_i}\{\mathbf{P}^{ri}(k) - \mathbf{P}^i(k)\}\mathbf{C}'^i][\mathbf{C}^i\mathbf{P}^i(k)\mathbf{C}'^i + \mathbf{R}^i]^{-1}. \tag{8.18}$$

It can be seen that the derived local gain $\mathbf{K}^i(k)$ is a function of consensus gain $\mathbf{L}^i(k)$, which is unknown. To simplify the derivation, a sub-optimal consensus gain is considered, and it is assumed that $\mathbf{L}^i(k) = \mu^i(k)\mathbf{I}$, where $\mu^i(k)$ is a consensus gain coefficient to be designed. Moreover, it can be seen that for computing $\mathbf{K}^i(k)$, it needs to know the neighbouring error covariance matrices $\sum_{r\in N_i}[\mathbf{P}^{ri}(k) - \mathbf{P}^i(k)]$, which are computational expensive in general. In order to reduce the computational burden, one can consider a sub-optimal local gain with $\mathbf{L}^i(k) = \mathbf{0}$, that is without considering the interconnection term in the local gain design [51]. Apparently, the sub-optimal local gain in (8.18) is given by:

$$\mathbf{K}^i(k) = \mathbf{A}_d\bar{\mathbf{P}}^i(k)\mathbf{C}'^i[\mathbf{C}^i\bar{\mathbf{P}}^i(k)\mathbf{C}'^i + \mathbf{R}^i]^{-1}, \tag{8.19}$$

where $\bar{\mathbf{P}}^i(k)$ satisfies the following iterative condition:

$$\bar{\mathbf{P}}^i(k+1) = \mathbf{A}_d\bar{\mathbf{P}}^i(k)\mathbf{A}'_d - \mathbf{A}_d\bar{\mathbf{P}}^i(k)\mathbf{C}'^i[\mathbf{C}^i\bar{\mathbf{P}}^i(k)\mathbf{C}'^i + \mathbf{R}^i]^{-1}\mathbf{C}^i\bar{\mathbf{P}}^i(k)\mathbf{A}'_d + \mathbf{Q}. \tag{8.20}$$

Note that this $\mathbf{K}^i(k)$ in (8.19) and $\bar{\mathbf{P}}^i(k)$ in (8.20) is the local optimal Kalman gain and local minimum error covariance if there is no interconnections with other subsytems. If considering interconnections, $\mathbf{K}^i(k)$ in (8.19) is only a suboptimal Kalman gain, and $\bar{\mathbf{P}}^i(k)$ in (8.20) is different from the corresponding error covariance $\mathbf{P}^i(k)$ by substituting $\mathbf{K}^i(k)$ in (8.19) into (8.16). In the following section, the consensus gain and convergence condition of the proposed algorithm are derived.

8.5 Convergence Analysis of the Proposed Distributed Algorithm

The following steps confirm the convergence of the developed approach.

Step 1. **Stacking all the error dynamics:**

Generally speaking, the Laplacian is a symmetric matrix with zero row sum. Indeed, the node j is called a neighbour of node i if they belong to graph edge E, i.e., $(i, j) \in E$. An edge is the communication link between estimators. If the i-th estimator has a communication link with the j-th estimator, then the element of the Laplacian has a value, otherwise zero [256], [257], [258]. So, the sparse communication graph can be described by the Laplacian matrix $\mathbf{G} \in \mathbb{R}^{n\times n}$ whose entries g^{ij} is given by:

$$g^{ij} = \begin{cases} -\sum_{s\in N_i} g^{is}, & \text{if i = j } (diagonal\ element), \\ -1, & \text{if } (i,j) \in E,\, i \neq \text{j } (adjacence), \\ 0, & \text{otherwise (} (i,j) \notin E, disjoint). \end{cases} \tag{8.21}$$

Here, $[g^{ij}]$ is (i,j)-th element of $\mathbf{G} \in \mathbb{R}^{n\times n}$. Now one can define the following augmented vectors for all estimators:

$$\mathbf{e}(k) = [\mathbf{e}^1(k) \dots \mathbf{e}^n(k)]', \mathbf{v}(k) = [\mathbf{v}^1(k) \dots \mathbf{v}^n(k)]',$$
$$\mathbf{w}(k) = [\mathbf{w}^1(k) \dots \mathbf{w}^n(k)]'.$$

Using (8.12) with $i = 1, 2, \cdots, n$, the overall error dynamic can be written in a compact

form as follows:

$$\begin{aligned}\mathbf{e}(k+1) =&[\mathbf{I}_n \otimes \mathbf{A}_d - bdiag\{\mathbf{K}^i(k)\mathbf{C}^i\} - bdiag\{\mathbf{L}^i(k)\}(\mathbf{G} \otimes \\ &\mathbf{I}_q)]\mathbf{e}(k) + (\mathbf{I}_n \otimes \mathbf{I}_q)\mathbf{n}_d - bdiag\{\mathbf{K}^i(k)\}\mathbf{w}(k) \\ =&\mathbf{\Lambda}(k)\mathbf{e}(k) + \mathbf{V}(k). \end{aligned} \tag{8.22}$$

Here, the symbol $\otimes$ denotes the Kronecker product and the signal as well as noise terms are described by:

$$\mathbf{\Lambda}(k) = \mathbf{I}_n \otimes \mathbf{A}_d - bdiag\{\mathbf{K}^i(k)\mathbf{C}^i\} - bdiag\{\mathbf{L}^i(k)\}(\mathbf{G} \otimes \mathbf{I}_q). \tag{8.23}$$

$$\mathbf{V}_k = (\mathbf{1}_n \otimes \mathbf{I}_q)\mathbf{n}_d - bdiag\{\mathbf{K}^i(k)\}\mathbf{w}(k). \tag{8.24}$$

Here, $\mathbf{1}_n$ denotes the $n \times 1$ vector with all the entries of 1.

Step 2. **Convergence condition**:

Usually, the discrete-time linear system is stable, if the maximum absolute eigenvalue of the system matrix of the overall error system is less than one by designing the appropriate gains. Obviously, it can be seen that if the spectral radius $\rho(\mathbf{\Lambda}(k)) < 1$, the system becomes stable.

Under the assumption 1, the state error covariance $\bar{\mathbf{P}}^i(k)$ in (8.20) converges to $\bar{\mathbf{P}}^i$ [259]. Consequently, the steady state of the sub-optimal gain in (8.19) converges to:

$$\mathbf{K}^i = \mathbf{A}_d\bar{\mathbf{P}}^i\mathbf{C}'^i[\mathbf{C}^i\bar{\mathbf{P}}^i\mathbf{C}'^i + \mathbf{R}^i]^{-1}. \tag{8.25}$$

Using the sub-optimal filter gain $\mathbf{K}^i$ and $\mathbf{L}^i = \mu^i\mathbf{I}$, the error system (8.22) is stable if $\rho(\mathbf{\Lambda}_{\mu^i}) < 1$, i.e.,

$$\rho[\mathbf{I}_n \otimes \mathbf{A}_d - bdiag\{\mathbf{K}^i\mathbf{C}^i\} - \mu^i(\mathbf{G} \otimes \mathbf{I}_q)] < 1. \tag{8.26}$$

Theorem 8.1: For simplicity, it is assumed that $\mu^i = \mu$, now μ can be computed by solving the following optimization problem:

$$\begin{aligned}&\mu = \underset{\mu}{\text{argmax}} \;\; \Psi_\mu(\mathbf{G}) < \mathbf{0}, \\ &\Psi_\mu(\mathbf{G}) = \begin{bmatrix} -\mathbf{I}_{nq} & \mathbf{\Lambda}_\mu \\ \star & -\mathbf{I}_{nq} \end{bmatrix}. \end{aligned} \tag{8.27}$$

Here, $\mathbf{\Lambda}_\mu = \mathbf{I}_n \otimes \mathbf{A}_d - bdiag\{\mathbf{KC}^i\} - \mu(\mathbf{G} \otimes \mathbf{I}_q)$.

Proof: See Appendix F.

It can be seen that the consensus gain is obtained by using the linear matrix inequality approach. In other words, the proposed optimization problem is convex and it can be efficiently solved with the state-of-art LMI solvers [213]. In summary, after computing the local gain by (8.25), the consensus gain is evaluated by (8.27). Then the distributed state estimation and the error-covariance-like matrix is obtained by (8.3) and (8.20), respectively. The performance of the proposed method is analysed in the next section.

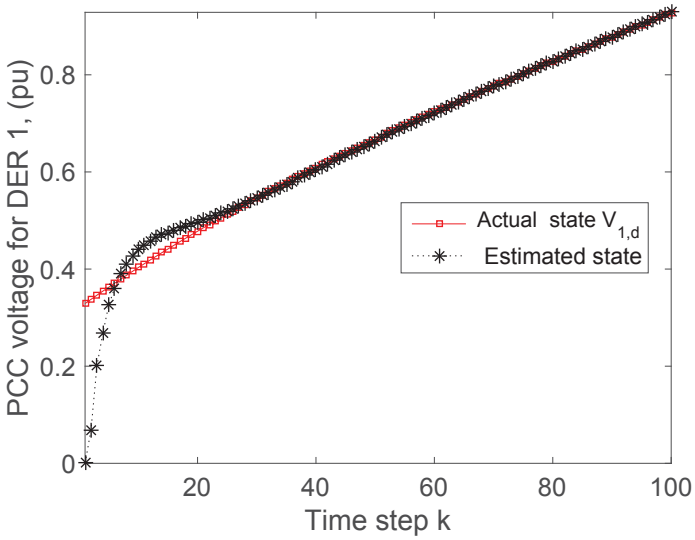

Figure 8.3: d-frame DER 1 PCC voltage $V_{1,d}$ and its estimation.

8.6 Simulation Results Using the Proposed Distributed Consensus Algorithm

The proposed algorithm is applied to the microgrid and IEEE 30-bus power system. The numerical case studies are carried out in Matlab programming environment.

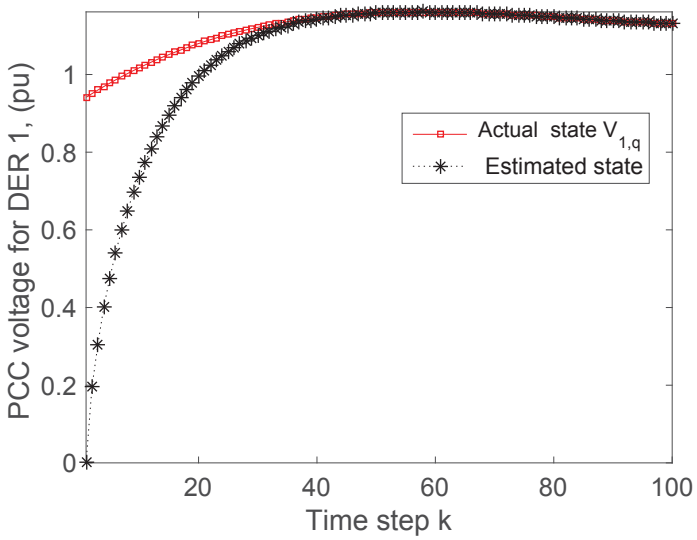

Figure 8.4: q-frame DER 1 PCC voltage $V_{1,q}$ and its estimation.

8.6.1 Estimation Results Using the Microgrid

To verify the performance of the developed algorithm, this study considers a microgrid consisting of two DERs, and there are four observation points as shown in Fig. 8.1. The simulation parameters of microgrid and transmission lines are described in Table 8.1 [16], [17]. The tap voltage ratio of $Y - \Delta$ transformer is specified to $0.6/13.8$.

The dynamic responses of the microgrid are shown in Figs. 8.3-8.14. It can be observed that for every microgrid state, the estimated state response converges to the actual state value as time proceeds. For instance, Fig. 8.4 shows the actual PCC voltage and its estimation result of DER 1. It is evident that the explored algorithm requires about 0.00004 seconds ($k \times \Delta t$) to perfectly estimate the PCC voltage. This is due to the fact that the designed optimal gains can effectively reduce the estimation errors. Similar high estimation accuracy is obtained of all the dynamic states of a microgrid. Finally, Fig. 8.15 shows the mean squared error for all estimators, and it can be seen that the estimators agree with each other as time goes on. This indicates that the proposed distributed estimation algorithm reaches consensus on state estimation, which validates the analytical approach. The maximum spectral radius $\rho(\Lambda_\mu) = 0.892 < 1$, which also verifies the theoretical convergence analysis.

Table 8.1: Simulation parameters of microgrids.

Symbols	Values	Symbols	Values
R_{t1}	$1.2 \times 10^{-3}\Omega$	R_{12}	1.2Ω
R_{t2}	$1.6 \times 10^{-3}\Omega$	R_{21}	$1.2\ \Omega$
C_{t1}	62.86×10^{-6}F	C_{t2}	76×10^{-6}F
L_{t1}	93.7×10^{-6}H	L_{12}	94.8×10^{-6}H
L_{t2}	94.8×10^{-6}H	L_{21}	104.3×10^{-6}H
f_0	60 Hz	d_i	0.6/13.8 $(Y-\Delta)$
Q	0.001*$\mathbf{I}$	$\mathbf{R}^1$	0.01*$\mathbf{I}$
$\mathbf{R}^2$	0.02*$\mathbf{I}$	$\mathbf{R}^3$	0.03*$\mathbf{I}$
$\mathbf{R}^4$	0.04*$\mathbf{I}$	Δt	0.000001

8.6.2 Estimation Results Using the IEEE 30-Bus System

The IEEE 30-bus system is employed to demonstrate the performance of the proposed approach. A single-line diagram of the IEEE 30-bus is depicted in Fig. 8.16 [13]. The system has a total of 12 generators and 20 loads. It has the total generation capacity 335 MW and load capacity 189.2 MW. Basically, the system state vector is comprised of bus voltage magnitudes and phase angles. Generally, for a power system with M buses, the system state vector **x** can be defined as $\mathbf{x} = [\Theta_1\ \Theta_2 \cdots\ \Theta_M,\ V_1\ V_2\ \cdots\ V_M]'$, where Θ_i is the i-th phase angle and V_i is the i-th bus voltage magnitude. The simulation parameters of the IEEE 30-bus system can be found in [220]. The nominal phase angles and bus voltage magnitudes are shown in Table 8.2, where the optimal power flow is evaluated by Matpower tool using the Newton's method.

In order to apply the proposed method in the linear state-space model for estimating the system states, it requires the system state matrix $\mathbf{A}_d$ and input matrix $\mathbf{B}_d$. For virtually computing them, this paper adopts the Holt-Winters method [260], [122], [261] which is summarised by:

$$\mathbf{A}_d = \gamma(1+\beta)\mathbf{I}. \tag{8.28}$$

$$\mathbf{B}_d = diag[(1+\beta)(1-\gamma)\hat{\mathbf{x}}(t-1) - \beta\mathbf{a}(t-1) + (1-\beta)\mathbf{b}(t-1)]. \tag{8.29}$$

Here, the coefficient $\gamma, \beta \in (1, 0)$, the system tuning parameters $\mathbf{a}(t)$ and $\mathbf{b}(t)$ are recursively

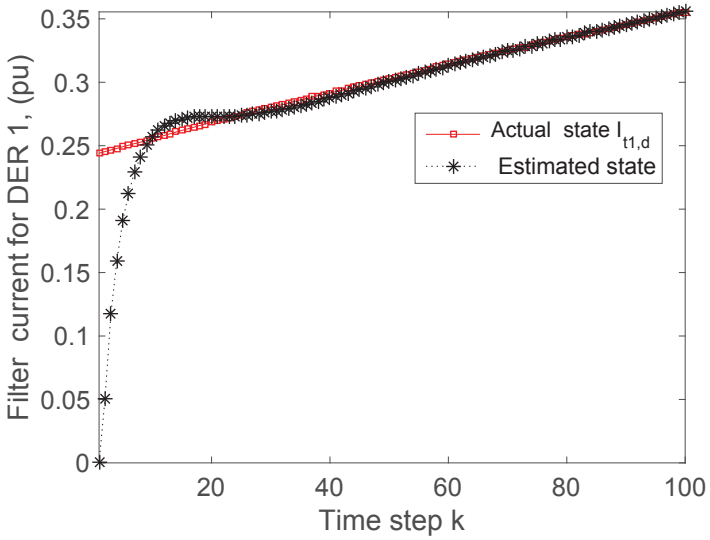

Figure 8.5: d-frame DER 1 filter current $I_{t1,d}$ and its estimation.

computed by:

$$\begin{aligned}\mathbf{a}(t) &= \gamma\mathbf{x}(t) + (1-\gamma)\hat{\mathbf{x}}(t).\\ \mathbf{b}(t) &= \beta[\mathbf{a}(t) - \mathbf{a}(t-1)] + (1-\beta)\mathbf{b}(t-1).\end{aligned} \tag{8.30}$$

Here, $\mathbf{a}(t-1)$ and $\mathbf{b}(t-1)$ are the coefficients of the last step, $\mathbf{x}$ and $\hat{\mathbf{x}}$ are the nominal and predicted states of the system.

For computing $\mathbf{A}_d$ and $\mathbf{B}_d$ in (8.28) and (8.29), this paper uses $\gamma = 0.7$, $\beta = 0.4$, $\mathbf{a}(0) = \mathbf{0}$, $\mathbf{b}(0) = \mathbf{0}$, $\hat{\mathbf{x}}$ is flat started (unit value) and $\mathbf{x}$ is nominal values which are mentioned in Table 8.2. Similar to [122], this study uses the nominal voltage magnitudes and phase angles. For computing the system dynamic parameters $\mathbf{A}_d$ and $\mathbf{B}_d$, the simulation is conducted at time t=1 to 10. Expectedly, it is evident from the dynamic responses in Figs. 8.17-8.18 that the estimation results precisely match the actual system states within a few time steps. This clearly implies that the explored method can accurately monitor the large-scale power systems. Consequently, such an approach can assist the utility operators to monitor the power system and will facilitate future effective controller design.

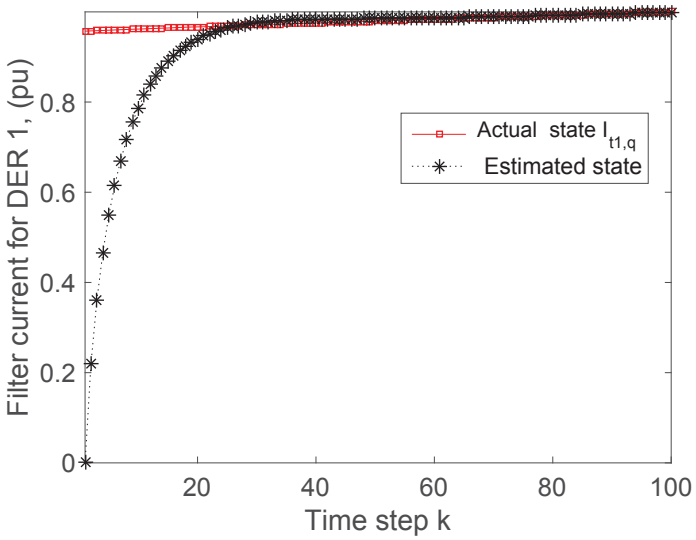

Figure 8.6: q-frame DER 1 filter current $I_{t1,q}$ and its estimation.

8.7 Summary

An algorithm for distributed estimation of the dynamic states of a modern power system has been developed and verified. The convergence analysis of the proposed approach is also justified. After representing the microgrid in a state-space equation, the sensors are deployed in different sub-stations to obtain measurements. To estimate the system states in a distributed way, the designed gains are obtained by minimizing the mean squared error and SDP approaches. Numerical results show that the developed scheme can well estimate the system states. Apparently, it demonstrates that all estimators maintain consensus on estimation. As all the system states have been estimated with high accuracy, they can be used for further designing the effective control strategy to stabilise the grid.

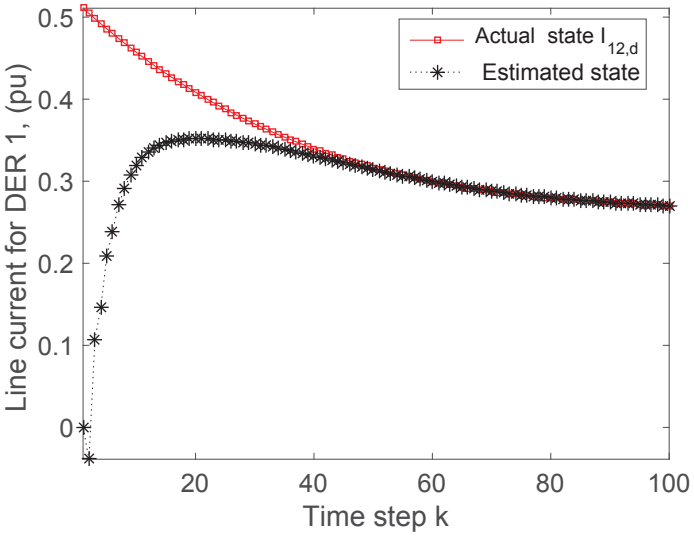

Figure 8.7: d-frame DER 1 line current $I_{12,d}$ and its estimation.

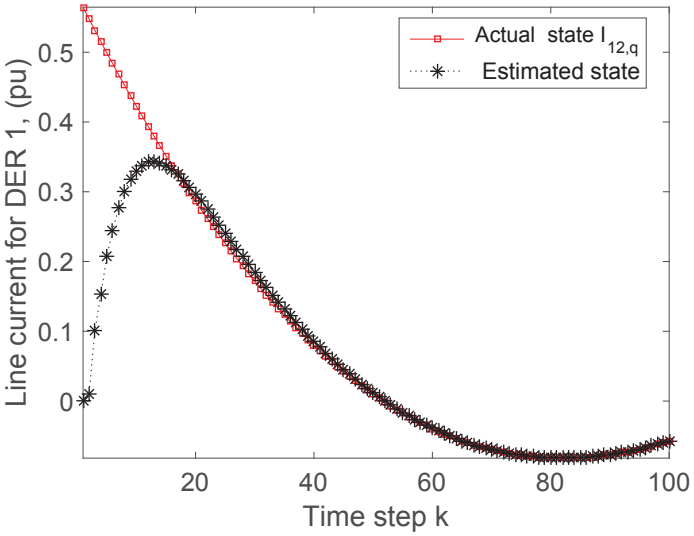

Figure 8.8: q-frame DER 1 line current $I_{12,q}$ and its estimation.

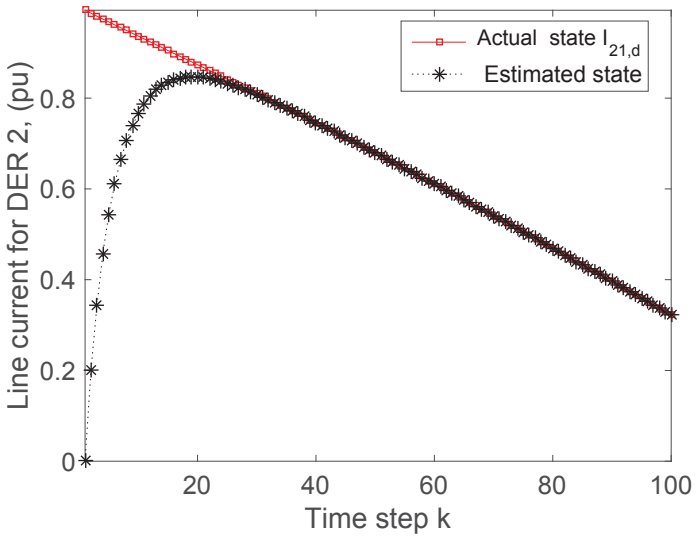

Figure 8.9: d-frame DER 2 line current $I_{21,d}$ and its estimation.

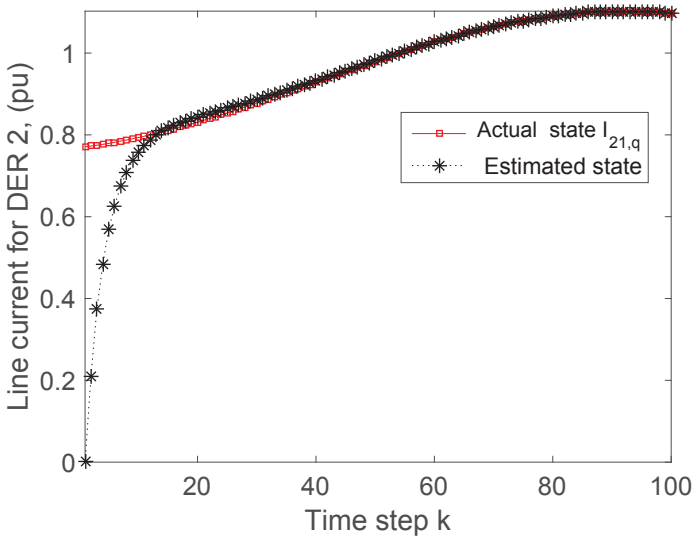

Figure 8.10: q-frame DER 2 line current $I_{21,q}$ and its estimation.

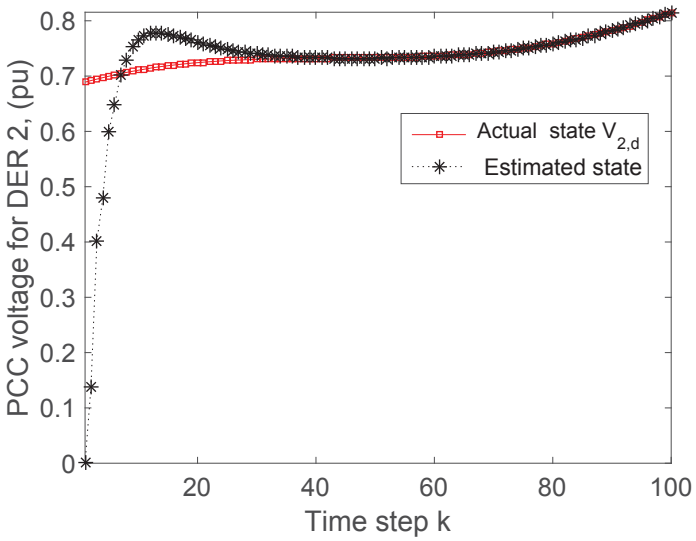

Figure 8.11: d-frame DER 2 PCC voltage $V_{2,d}$ and its estimation.

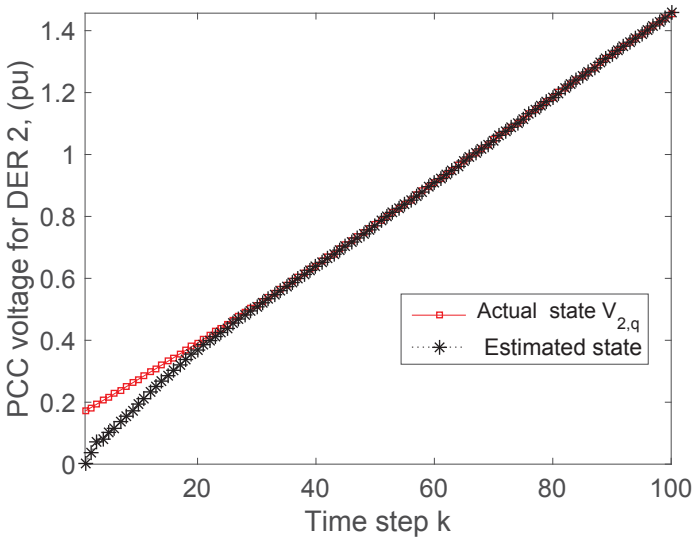

Figure 8.12: q-frame DER 2 PCC voltage $V_{2,q}$ and its estimation.

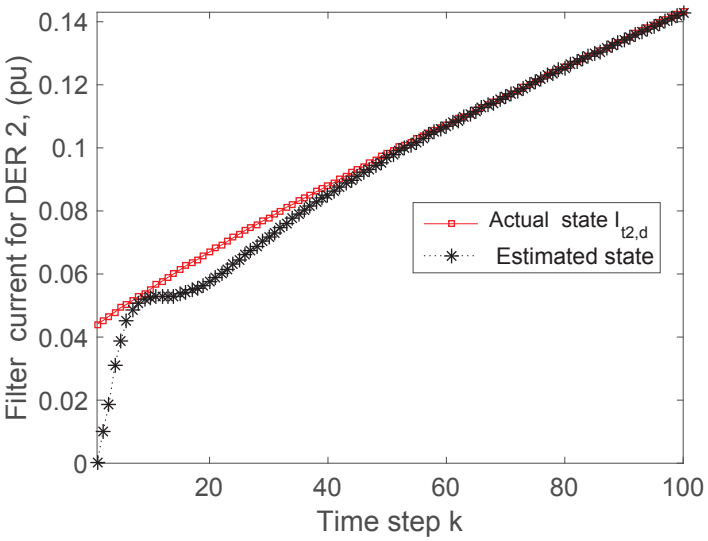

Figure 8.13: d-frame DER 2 filter current $I_{t2,d}$ and its estimation.

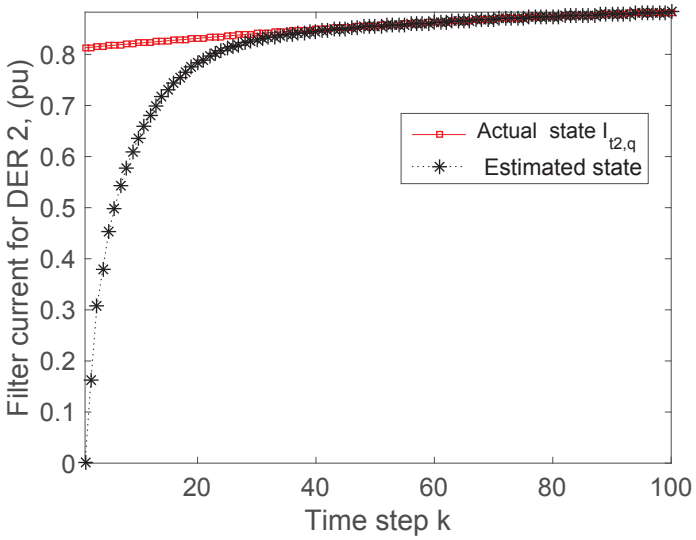

Figure 8.14: q-frame DER 2 filter current $I_{t2,q}$ and its estimation.

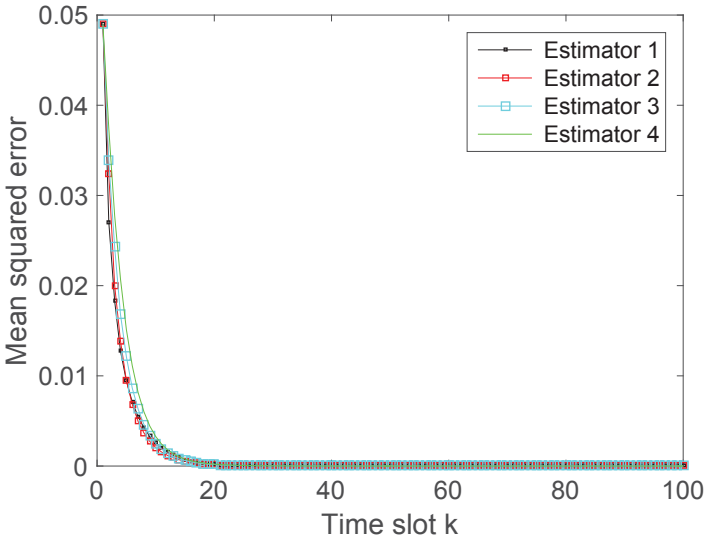

Figure 8.15: Mean squared errors for all estimators to proof the consensus on estimation.

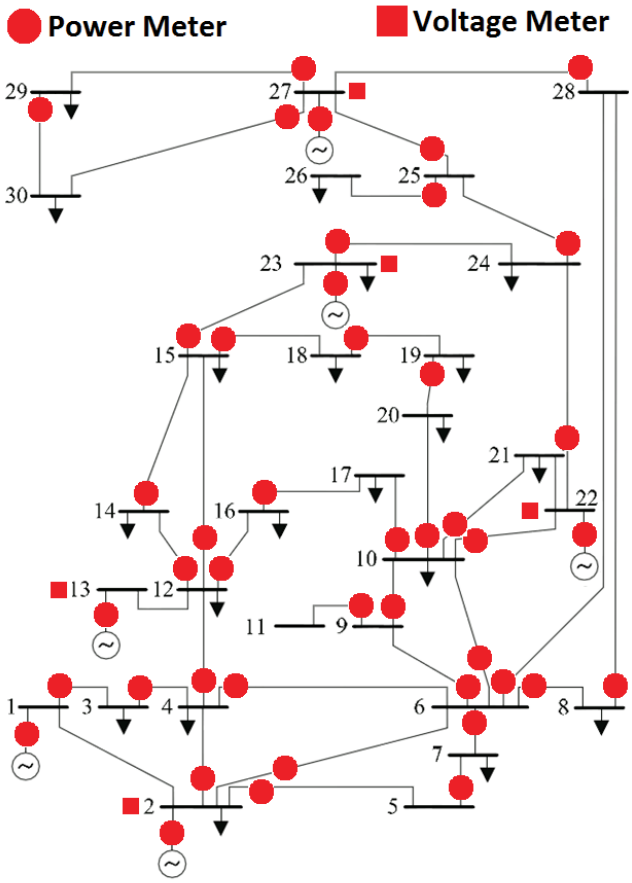

Figure 8.16: Single-line diagram of the IEEE 30-bus system [13].

Table 8.2: The nominal values of the IEEE 30-bus system.

Bus	Θ_N	V_N	Bus	Θ_N	V_N
1	0.000	1	16	-2.644	0.977
2	-0.415	1	17	-3.392	0.977
3	-1.522	0.983	18	-3.478	0.968
4	-1.795	0.983	19	-3.958	0.965
5	-1.864	0.982	20	-3.871	0.969
6	-2.267	0.973	21	-3.488	0.993
7	-2.652	0.967	22	-3.393	1
8	-2.726	0.961	23	-1.589	1
9	-2.997	0.981	24	-2.631	0.989
10	-3.375	0.984	25	-1.690	0.990
11	-2.997	0.981	26	-2.139	0.972
12	-1.537	0.985	27	-0.828	1
13	1.476	1	28	-2.266	0.975
14	-2.308	0.977	29	-2.128	0.980
15	-2.312	0.980	30	-3.042	0.968

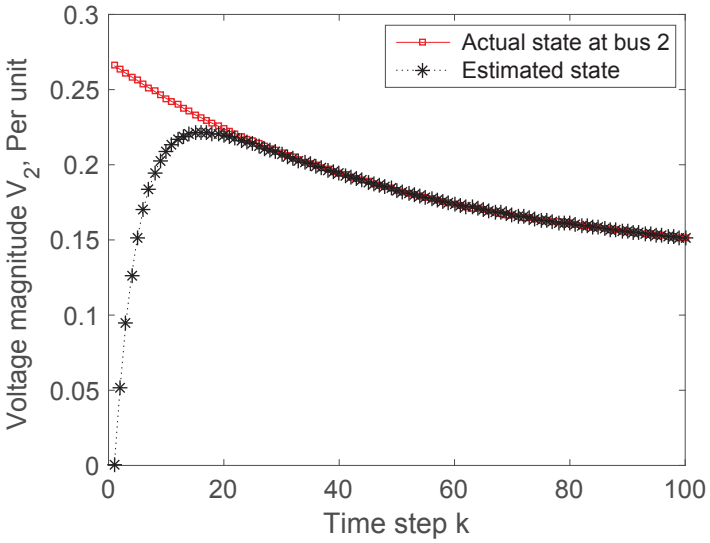

Figure 8.17: Voltage V_2 and its estimation using the IEEE 30-bus.

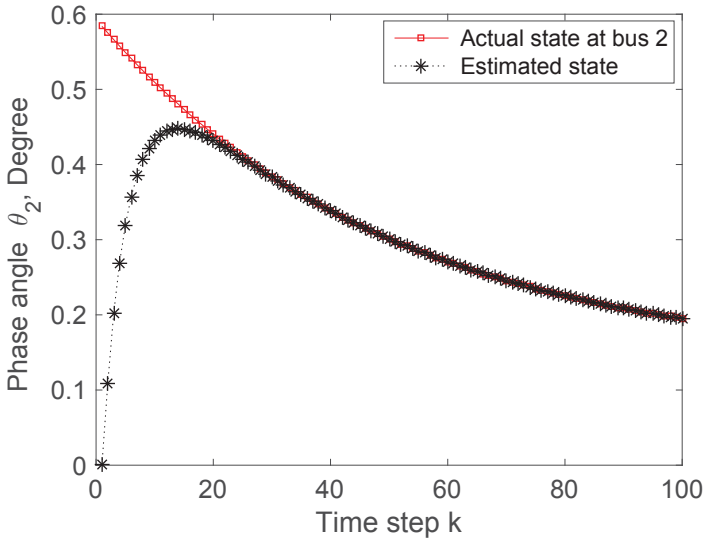

Figure 8.18: Angle θ_2 and its estimation using the IEEE 30-bus.

Chapter 9

Conclusions and Future Work

This research explores the problem of state estimation and stabilization taking disturbances, cyber attacks and packet losses into consideration for the smart grid. The problem has become critical and challenging due to global warming, the increase of green house gas emissions, and the dramatic increase in computational burden of the centralized EMS for the state estimation and stabilization of power networks. To address the impending problem, the KF based smart grid state estimation and stabilization approaches are proposed and verified. It has been shown that the developed methods are practical for microgrids and smart grids. The work also has a wide scope for future research and extensions. This chapter concludes the dissertation with a summary of the presented work and future research directions.

9.1 Conclusions

After giving the motivation of the thesis in Chapter 1, in Chapter 2 a comprehensive literature review on state estimation schemes, communication systems and their applications to the smart grid are presented. Afterwards, the KF based smart grid state estimation and stabilization algorithms are derived. The observation information from the distribution power system is obtained by a set of sensors, then it is transmitted to the energy management system by a communication network. Based on the mean squared error principle and Lyapunov theory, the proposed smart grid state estimation and stabilization algorithms are developed.

Thus, the research gaps have been verified, which has led this research to come up with the following key contributions:

- Environment-friendly renewable microgrid incorporating multiple DERs is modelled to obtain discrete-time state-space linear equations where sensors are deployed to acquire system state information. The proposed smart grid communication system provides an opportunity to address the state regulation challenge by offering two-way communication links for microgrid information collection, estimation and stabilization. The presented least square based centralised KF algorithm is able to properly estimate the system states even at the beginning of the dynamic process. The developed H_2 based optimal feedback controller is able to stabilize the microgrid states in a fairly short time.

- A microgrid incorporating multiple DERs is modelled as a discrete-time state-space equation considering the uncertainty and cyber attack in the measurement. An RSC code is proposed to tolerate the impairments and introduce redundancy in the system states. After estimating the system states, a feedback control strategy for voltage regulation of the microgrid is proposed based on SDP. Test results show that the proposed centralised approach can accurately mitigate the cyber attacks and properly estimate as well as regulate the system states.

- Environment-friendly wind turbine is described as a linear state-space framework, and the system measurements are obtained at EMS under unreliable communication links. After locally estimating the system states, the global estimator combines the local estimation results through a set of designed weighting factors. Convergence of the proposed approach is analyzed based on the Lyapunov approach. The efficacy of the developed approach is verified using the wind turbine and IEEE 6-bus system.

- Based on the mean squared error principle, the optimal local and neighbouring gains are determined to obtain a distributed dynamic state estimation in the context of smart grids. Each estimator exchanges information with the neighbouring estimators for reaching a consensus estimation even though there are unmeasurable states and packet losses. The convergence of the developed approach is theoretically proved. For proper operation and maintaining the stability of the microgrid, a distributed controller is proposed based on the SDP approach. Simulation results demonstrate the accuracy of the developed approaches under the condition of missing measurements.

- The distribution power systems with interconnected synchronous generators and loads are modelled as a discrete-time state-space equation. The sensing information is transmitted to the EMS through a communication network where the proposed optimal estimator runs in a distributed way. The convergence of the developed approach is proved based on the Lyapunov approach. Simulation results demonstrate the efficacy of the developed approach. From the circuit and system point of view, the proposed framework is useful for designing a practical EMS as it has less computational complexity and provides accurate estimation results.
- The distributed algorithm is further modified by considering different observation matrices with both local and consensus steps. To estimate the system states in a distributed way, the designed gains are obtained by minimizing the mean squared error and semidefinite programming approaches. The necessary and sufficient condition for the convergence of the developed algorithm is that the spectral radius of error dynamic is less than one. The efficacy of the developed approach is demonstrated using the environment-friendly renewable microgrid and IEEE 30-bus power system. It shows that the proposed scheme requires maximum 0.00004 seconds for properly estimating the system states.

Overall, the findings, theoretical development and analysis of this research represent a comprehensive source of information for smart grid state estimation and stabilization schemes. Combining the DERs of every place, the community can generate sufficient electricity to keep the police department, the phone systems and the public health centre up and running. Finally, this work involves the engineering communities of communication, control as well as power, and will shed light on green smart EMS and monitoring centre design in the future smart grid implementation.

Based on the research accomplished in this dissertation, some future research directions are highlighted in the next section.

9.2 Future Work

In this research, we have not adopted the state-of-art channel coding and decoding schemes while proposing the smart grid communication systems for the centralized state estimation

and cyber attack protection. Secondly, we apply the dynamic state estimation and control approaches to the discrete-time linear systems. Thirdly, the packet dropouts occur in the communication network from the smart sensors to the estimator and the network from the controller to the actuators. Finally, we assume measurements are lost due to unreliable communication links while it is assumed there are no losses when exchanging information with the neighbouring nodes. Consequently, a number of possible problems for future research have been identified as follows:

- To design the future smart grid communication systems, the low density parity check (LDPC) channel code and belief propagation (BP) decoding can be considered. To illustrate, the future smart grid communication system is described in Fig. 9.1. Basically, the LDPC can add more redundancy in system states, and the BP can effectively recover them. Using the state-of-art channel encoding and decoding schemes, the state estimation performance can be significantly improved [262], [263], [264]. Moreover, the higher order modulation schemes such as quadrature phase shift keying and orthogonal frequency-division multiplexing can be used for long distance data transmission and high speed communication systems [265]. Furthermore, it can be seen that the state estimator has to wait until the decoding has been completed before it can start the estimation process. Due to the information explosion in large grids, this two-step sequential process could result in excessive delays. Therefore, the message updating and passing for each node can be carried out simultaneously without waiting for one another.

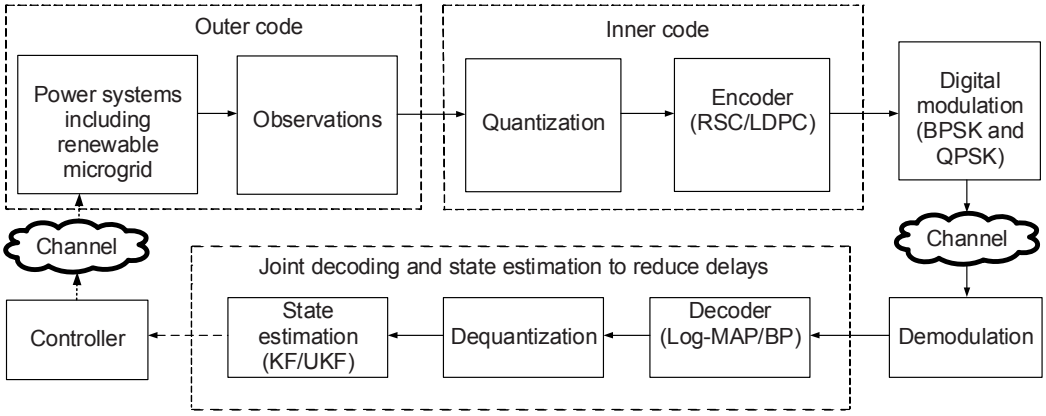

Figure 9.1: Future smart grid communication systems for the smart EMS design.

- The dynamic state estimation technique can be applied to the general case of nonlinear power systems. Usually, the nonlinear systems are tackled by EKF, fractional order EKF and UKF algorithms [106], [107], [108]. The main disadvantage with EKF is that it needs linearized system parameters such as partial derivative of the state transition matrix. Apart from the difficulty of obtaining derivatives for a large-scale power system, if the initial state estimation is wrong, the filter error dynamic may diverge. To deal with these shortcomings, the fractional order EKF is used for estimating the state variables, whereby fractional order partial derivatives can be used [109], [110]. In order to avoid the calculation of Jacobians, the UKF based power system state estimation is explored in [106], [111], [112], [113], and it shows that the UKF preserves high-order estimation accuracy compared with the EKF.

- Generally speaking, the distribution power system is connected to the controller in feedback closed-loop via a real-time shared communication network [266]. Therefore, the state feedback controller can be designed under the condition of packet dropouts in the communication network. In other words, sometimes the control signals are lost in unreliable channels during sending the control signals as shown in Fig. 9.1. Considering such a real-time scenario, the feedback control law can be defined by [267], [266], [268]:

$$\mathbf{u}(k) = \beta(k)\mathbf{F}\mathbf{x}(k). \tag{9.1}$$

  Here, $\mathbf{F}$ is the feedback gain and $\beta(k)$ is the packet loss parameter with

$$\beta(k) = \begin{cases} 1, & \text{no loss,} \\ \gamma(k), \quad 0 < \gamma(k) < 1 & \text{lossy condition,} \end{cases}$$

  where $\gamma(k)$ is the fading parameter at the actuator due to the unreliable communication network. The problem can be solved using the SDP, H_2 and H_∞ approaches [267], [266], [268].

- It can be considered that the estimator exchanges information with the neighboring nodes through a lossy communication network. This is due to the fact that the electricity network and EMS are not located at the same place. Considering there are packet losses in both of the measurements and during exchanging information among

the nodes, the filter structure can be written as follows:

$$\hat{\mathbf{x}}^i(k+1) = \mathbf{A}_d\hat{\mathbf{x}}^i(k) + \mathbf{B}_d\mathbf{u}(k) + \alpha^i(k)\mathbf{K}^i(k)[\mathbf{y}^i(k) - \mathbf{C}\hat{\mathbf{x}}^i(k)] + \sum_{j\neq i}\beta^{ij}(k)\mathbf{L}^{ij}(k)[\hat{\mathbf{x}}^j(k) - \hat{\mathbf{x}}^i(k)]. \tag{9.2}$$

Here, $\beta^{ij}(k)$ is the binary variable indicating whether the information of the *estimator j* is received from the *node i* due to the lossy network, and all other variables are previously well described. The problem can be solved using the mean squared error and H_∞ approaches [269], [156].

Chapter 10

Appendices

Appendix A (Network admittance matrix)

The constant network admittance matrix is given by [15]:

$$\mathbf{Y} = \mathbf{Y}_{rr} - \mathbf{Y}_{re}\mathbf{Y}_{ee}^{-1}\mathbf{Y}'_{re}. \tag{10.1}$$

Here, the simplified term $\mathbf{Y}_{rr} = diag[Y_{17} + jB_{17}, Y_{26} + jB_{26}, Y_{36} + jB_{36}, Y_{46} + jB_{46}, Y_{56} + jB_{56}]$, where the mutual admittance is computed as follows as an example: $Y_{17} = 1/(R_{17} + jX_{17})$, R_{17} is the resistance between node 1 and 7, X_{17} and B_{17} are its reactance and susceptance, respectively. The second simplified term $\mathbf{Y}_{re}$ is given by:

$$\mathbf{Y}_{re} = \begin{bmatrix} 0 & -Y_{17} & 0 \\ -Y_{26} & 0 & 0 \\ -Y_{36} & 0 & 0 \\ 0 & 0 & -Y_{48} \\ -Y_{56} & 0 & 0 \end{bmatrix}. \tag{10.2}$$

The last simplified term $\mathbf{Y}_{ee}$ is given by:

$$\mathbf{Y}_{ee} = \begin{bmatrix} Y_{66} & -Y_{67} & 0 \\ -Y_{67} & Y_{77} & -Y_{78} \\ 0 & -Y_{78} & Y_{88} \end{bmatrix}, \tag{10.3}$$

where Y_{ii} is the self-admittance of bus i.

Appendix B (System matrices)

Let $\delta^\star$ and $E_q^{'\star}$ be the operating points.

$$\mathbf{A}_i = \begin{bmatrix} 0 & 1 & 0 & 0 & 0 \\ -\frac{1}{H_i}\frac{\partial P_{ei}}{\partial \delta i} & -\frac{D_i}{H_i} & -\frac{1}{H_i}\frac{\partial P_{ei}}{\partial E'_{qi}} & 0 & 0 \\ X_i \frac{\partial I_{di}}{\partial \delta_i} & 0 & -\frac{1}{T'_{doi}} + X_i \frac{\partial I_{di}}{\partial E'_{qi}} & \frac{b_{1i}}{T'_{doi}} & \frac{b_{oi}}{T'_{doi}} \\ 0 & 0 & 0 & -c_{1i} & -c_{0i} \\ 0 & 0 & 0 & 1 & 0 \end{bmatrix}_{\substack{\delta=\delta^\star \\ E'_q = E_q^{'\star}}}$$

$$\mathbf{A}_{ij} = \begin{bmatrix} 0 & 0 & 0 & 0 & 0 \\ -\frac{1}{H_i}\frac{\partial P_{ei}}{\partial \delta j} & 0 & -\frac{1}{H_i}\frac{\partial P_{ei}}{\partial E'_{qj}} & 0 & 0 \\ X_i \frac{\partial I_{di}}{\partial \delta_j} & 0 & -\frac{1}{T'_{doi}} + X_i \frac{\partial I_{di}}{\partial E'_{qj}} & \frac{b_{1i}}{T'_{doj}} & \frac{b_{oi}}{T'_{doj}} \\ 0 & 0 & 0 & 0 & 0 \\ 0 & 0 & 0 & 0 & 0 \end{bmatrix}_{\substack{\delta=\delta^\star \\ E'_q = E_q^{'\star}}}$$

$\mathbf{B}_i = [0\ 0\ 0\ 1\ 0]'$ and $X_i = \frac{X_{di} - X'_{di}}{T'_{doi}}$.

Appendix C (Proof of Theorem 7.1)

Let $n^i = n^i(N^i)$ represents the cardinality of N^i. Now substituting (7.4) into (7.20), and using (7.2) one can obtain the following error expression:

$$\begin{aligned}\mathbf{e}^i_{k|k} &= \mathbf{x}_k - \hat{\mathbf{x}}^i_{k|k-1} - \mathbf{K}^i_k \sum_{l\in N^i}(\mathbf{y}^l_k - \mathbf{C}\hat{\mathbf{x}}^i_{k|k-1}) \\ &= (\mathbf{I} - n^i\mathbf{K}^i_k\mathbf{C})(\mathbf{x}_k - \hat{\mathbf{x}}^i_{k|k-1}) - \mathbf{K}^i_k \sum_{l\in N^i}\mathbf{w}^l_k \\ &= (\mathbf{I} - n^i\mathbf{K}^i_k\mathbf{C})\mathbf{e}^i_{k|k-1} - \mathbf{K}^i_k \sum_{l\in N^i}\mathbf{w}^l_k. \end{aligned} \tag{10.4}$$

Now the state estimation error covariance $\mathbf{P}^i_{k|k}$ is defined by:

$$\mathbf{P}^i_{k|k} = E(\mathbf{e}^i_{k|k}\mathbf{e}'^i_{k|k}). \tag{10.5}$$

Substituting (10.4) into (10.5), one can obtain:

$$\mathbf{P}^i_{k|k} = (\mathbf{I} - n^i\mathbf{K}^i_k\mathbf{C})\mathbf{P}^i_{k|k-1}(\mathbf{I} - n^i\mathbf{K}^i_k\mathbf{C})' + \mathbf{K}^i_k \sum_{l\in N^i}\mathbf{R}^l_k\mathbf{K}'^i_k. \tag{10.6}$$

Here, the error covariance $\mathbf{P}^i_{k|k-1} = E(\mathbf{e}^i_{k|k-1}\mathbf{e}'^i_{k|k-1})$. The following partial derivatives are used to obtain the optimal expression of the gain $\mathbf{K}^i_k$. For any two compatible matrices $\mathbf{X}$ and $\mathbf{Y}$, the following partial derivatives holds:

$$\frac{\partial tr(\mathbf{YX})}{\partial \mathbf{X}} = \mathbf{Y}'. \tag{10.7}$$

$$\frac{\partial tr(\mathbf{XYX}')}{\partial \mathbf{X}} = \mathbf{X}(\mathbf{Y} + \mathbf{Y}'). \tag{10.8}$$

In order to find the optimal gain $\mathbf{K}^i_k$, taking the partial derivative of $\mathbf{P}^i_{k|k}$ in (10.6) with respect to $\mathbf{K}^i_k$ and applying (10.7) and (10.8) yields:

$$\frac{\partial[tr\mathbf{P}^i_{k|k}]}{\partial \mathbf{K}^i_k} = -2n^i\mathbf{P}^i_{k|k-1}\mathbf{C}' + 2\mathbf{K}^i_k[(n^i)^2\mathbf{C}\mathbf{P}^i_{k|k-1}\mathbf{C}' + \sum_{l\in N^i}\mathbf{R}^l_k]. \tag{10.9}$$

Now putting $\frac{\partial[tr\mathbf{P}^i_{k|k}]}{\partial \mathbf{K}^i_k} = 0$ in (10.9), the optimal gain $\mathbf{K}^i_k$ is given by:

$$\mathbf{K}^i_k = n^i_k\mathbf{P}^i_{k|k-1}\mathbf{C}'[(n^i)^2\mathbf{C}\mathbf{P}^i_{k|k-1}\mathbf{C}' + \sum_{l\in N^i}\mathbf{R}^l_k]^{-1}. \tag{10.10}$$

The proof is completed.

Appendix D (Proof of Lemma 7.1)

Substituting $\mathbf{K}_k^i$ (10.10) into $\mathbf{P}_{k|k}^i$ (10.6) and after simplifying matrix manipulations, one can obtain:

$$\begin{aligned}\mathbf{P}_{k|k}^i &= \mathbf{P}_{k|k-1}^i - n^i \mathbf{K}_k^i \mathbf{C} \mathbf{P}_{k|k-1}^i \\ &= \mathbf{P}_{k|k-1}^i - n^i \{ n^i \mathbf{P}_{k|k-1}^i \mathbf{C}' [(n^i)^2 \mathbf{C} \mathbf{P}_{k|k-1}^i \mathbf{C}' + \\ &\quad \sum_{l \in N^i} \mathbf{R}_k^l]^{-1} \} \mathbf{C} \mathbf{P}_{k|k-1}^i . \end{aligned} \tag{10.11}$$

Using the matrix inversion Lemma, $\mathbf{A}^{-1} - \mathbf{A}^{-1}\mathbf{B}(\mathbf{C}^{-1} + \mathbf{D}\mathbf{A}^{-1}\mathbf{B})^{-1}\mathbf{D}\mathbf{A}^{-1} = (\mathbf{A} + \mathbf{B}\mathbf{C}\mathbf{D})^{-1}$, the right hand side of (10.11) can be written as follows:

$$\begin{aligned}\mathbf{P}_{k|k}^i &= [(\mathbf{P}_{k|k-1}^i)^{-1} + (n^i)^2 \mathbf{C}' (\sum_{l \in N^i} \mathbf{R}_k^l)^{-1} \mathbf{C}]^{-1} \\ &= [(\mathbf{P}_{k|k-1}^i)^{-1} + \mathbf{S}_k^i]^{-1} . \end{aligned} \tag{10.12}$$

Here, $\mathbf{S}_k^i = (n^i)^2 \mathbf{C}' (\sum_{l \in N^i} \mathbf{R}_k^l)^{-1} \mathbf{C}$.

Appendix E (Proof of Lemma 7.2)

Generally speaking, the stability and convergence study deals with an infinite time horizon. So, throughout this proof without loss of generality, we adopt a notation that is free of the time index k and the updated variable x_{k+1} is denoted by x_+. Inspired by [51], the optimal gain (7.18) can be written in the *information form* as follows:

$$\begin{aligned}\mathbf{K}^i =& n^i\mathbf{P}^i\mathbf{C}'[(n^i)^2\mathbf{C}\mathbf{P}^i\mathbf{C}' + \sum_{l\in N^i}\mathbf{R}^l]^{-1}\\ =&[(\mathbf{P}^i)^{-1} + (n^i)^2\mathbf{C}'(\sum_{l\in N^i}\mathbf{R}^l)^{-1}\mathbf{C}]^{-1}n^i\mathbf{C}'(\sum_{l\in N^i}\mathbf{R}^l)^{-1}\\ =&n^i\mathbf{M}^i\mathbf{C}'(\sum_{l\in N^i}\mathbf{R}^l)^{-1}. \end{aligned} \tag{10.13}$$

Here, from Lemma 7.1 the error covariance matrix $\mathbf{M}^i = \mathbf{P}^i_{k|k}$ in the information form is given by:

$$\mathbf{M}^i = [(\mathbf{P}^i)^{-1} + \mathbf{S}^i]^{-1}. \tag{10.14}$$

The information matrix $\mathbf{S}^i$ is described as follows:

$$\mathbf{S}^i = (n^i)^2\mathbf{C}'(\sum_{l\in N^i}\mathbf{R}^l)^{-1}\mathbf{C}. \tag{10.15}$$

Utilizing (10.13) and (10.15), the simplified term $\mathbf{F}^i$ becomes:

$$\begin{aligned}\mathbf{F}^i &= \mathbf{I} - n^i\mathbf{K}^i\mathbf{C} = \mathbf{I} - (n^i)^2\mathbf{M}^i\mathbf{C}'(\sum_{l\in N^i}\mathbf{R}^l)^{-1}\mathbf{C}\\ &= \mathbf{I} - \mathbf{M}^i\mathbf{S}^i. \end{aligned} \tag{10.16}$$

Motivated by (10.14), we have:

$$\begin{aligned}&[(\mathbf{P}^i)^{-1} + \mathbf{S}^i]^{-1}[(\mathbf{P}^i)^{-1} + \mathbf{S}^i] = \mathbf{I}\\ \Rightarrow&\mathbf{M}^i[(\mathbf{P}^i)^{-1} + \mathbf{S}^i] = \mathbf{I}\\ \Rightarrow&\mathbf{M}^i(\mathbf{P}^i)^{-1} = \mathbf{I} - \mathbf{M}^i\mathbf{S}^i = \mathbf{F}^i. \end{aligned} \tag{10.17}$$

Using (10.4), (10.13), (10.15) and (10.17), the error covariance matrix (7.19) can be rewritten

as follows:

$$
\begin{aligned}
\mathbf{M}_+^i &= \mathbf{F}_+^i \mathbf{P}_+^i \mathbf{F}_+^{'i} + \mathbf{K}_+^i \sum_{l \in N^i} \mathbf{R}_+^l \mathbf{K}_+^{'i} \\
&= \mathbf{F}_+^i (\mathbf{A}_d \mathbf{M}^i \mathbf{A}_d' + \mathbf{Q}) \mathbf{F}_+^{'i} + [n^i \mathbf{M}_+^i \mathbf{C}' (\sum_{l \in N^i} \mathbf{R}_+^l)^{-1}] \\
&\quad (\sum_{l \in N^i} \mathbf{R}_+^l)[n^i \mathbf{M}_+^i \mathbf{C}' (\sum_{l \in N^i} \mathbf{R}_+^l)^{-1}]' \\
&= \mathbf{F}_+^i (\mathbf{A}_d \mathbf{M}^i \mathbf{A}_d' + \mathbf{Q}) \mathbf{F}_+^{'i} + (n^i)^2 \mathbf{M}_+^i \mathbf{C}' (\sum_{l \in N^i} \mathbf{R}_+^l)^{-1} \mathbf{C} \mathbf{M}_+^i \\
&= \mathbf{F}_+^i (\mathbf{A}_d \mathbf{M}^i \mathbf{A}_d' + \mathbf{Q}) \mathbf{F}_+^{'i} + \mathbf{M}_+^i \mathbf{S}_+^i \mathbf{M}_+^i \\
&= \mathbf{F}_+^i (\mathbf{A}_d \mathbf{M}^i \mathbf{A}_d' + \mathbf{Q}) \mathbf{F}_+^{'i} + \mathbf{F}_+^i \mathbf{P}_+^i \mathbf{S}_+^i \mathbf{P}_+^i \mathbf{F}_+^{'i} \\
&= \mathbf{F}_+^i (\mathbf{A}_d \mathbf{M}^i \mathbf{A}_d' + \mathbf{Q} + \mathbf{P}_+^i \mathbf{S}_+^i \mathbf{P}_+^i) \mathbf{F}_+^{'i} \\
\Rightarrow \mathbf{M}_+^i &= \mathbf{F}_+^i \mathbf{G}_+^i \mathbf{F}_+^{'i}. \qquad (10.18)
\end{aligned}
$$

Here, the simplified terms are: $\mathbf{G}_+^i = \mathbf{A}_d \mathbf{M}^i \mathbf{A}_d' + \mathbf{W}_+^i$ and $\mathbf{W}_+^i = \mathbf{Q} + \mathbf{P}_+^i \mathbf{S}_+^i \mathbf{P}_+^i$. The proof is completed.

Appendix F (Proof of Theorem 8.1)

In [51], [259], it is proved that $\mathbf{A}_d - \mathbf{K}^i\mathbf{C}^i$ is stable, i.e., $\rho(\mathbf{A}_d - \mathbf{K}^i\mathbf{C}^i) < 1$ with the fixed sub-optimal local gain (8.25). By continuity, $\rho(\mathbf{\Lambda}_\mu) < 1$ holds for some small value of μ. In this case, the term $\mathbf{\Lambda}_\mu$ (time-independent) satisfies the following condition:

$$\begin{aligned} &\rho(\mathbf{\Lambda}_\mu) < 1 \\ &\mathbf{\Lambda}_\mu \mathbf{\Lambda}_\mu' < \mathbf{I}_{nq}. \end{aligned} \tag{10.19}$$

According to the Schur complement the above inequality can be written as follows:

$$\begin{bmatrix} -\mathbf{I}_{nq} & \mathbf{\Lambda}_\mu \\ \star & -\mathbf{I}_{nq} \end{bmatrix} < \mathbf{0}. \tag{10.20}$$

The proof is completed.

Bibliography

[1] A. Arefi, G. Ledwich, and B. Behi, "An efficient DSE using conditional multivariate complex Gaussian distribution," *IEEE Transactions on Smart Grid*, vol. 6, no. 4, pp. 2147–2156, 2015.

[2] C. H. Lo and N. Ansari, "The progressive smart grid system from both power and communications aspects," *IEEE Communications Surveys and Tutorials*, vol. 14, no. 3, pp. 799–821, 2012.

[3] M. Esmalifalak, G. Shi, Z. Han, and L. Song, "Bad data injection attack and defense in electricity market using game theory study," *IEEE Transactions on Smart Grid*, vol. 4, no. 1, pp. 160–169, 2013.

[4] S. S. S. R. Depuru, L. Wang, and V. Devabhaktuni, "Smart meters for power grid: Challenges, issues, advantages and status," *Renewable and Sustainable Energy Reviews*, vol. 15, no. 6, pp. 2736–2742, 2011.

[5] P. Kundur, *Power System Stability and Control*. New York: McGraw-Hill, 1994.

[6] H. Karimi, H. Nikkhajoei, and R. Iravani, "Control of an electronically-coupled distributed resource unit subsequent to an islanding event," *IEEE Transactions on Power Delivery*, vol. 23, no. 1, pp. 493–501, 2008.

[7] "IEEE PES distribution system analysis subcommittee," *Distribution Test Feeders, available at http://ewh.ieee.org/soc/pes/dsacom/testfeeders/index.html*.

[8] H. Li, L. Lai, and H. V. Poor, "Multicast routing for decentralized control of cyber physical systems with an application in smart grid," *IEEE Journal on Selected Areas in Communications*, vol. 30, no. 6, pp. 1097–1107, 2012.

[9] S. Gong, H. Li, L. Lai, and R. C. Qiu, "Decoding the nature encoded messages for distributed energy generation control in microgrid," in *Proc. of the International Conference on Communications*, 2011, pp. 1–5.

[10] Y. Jing, *A practical guide to error control coding using Matlab*. Boston, London: Artech house, 2010.

[11] D. B. Rawat and C. Bajracharya, "Detection of false data injection attacks in smart grid communication systems," *IEEE Signal Processing Letters*, vol. 22, no. 10, pp. 1652–1656, 2015.

[12] R. M. Imran, D. Akbar Hussain, and Z. Chen, "LQG controller design for pitch regulated variable speed wind turbine," in *Proc. of the International Energy Conference*. IEEE, 2014, pp. 101–105.

[13] A. J. Wood and B. F. Wollenberg, *Power generation, operation, and control*. John Wiley and Sons, 2012.

[14] J. Liu, A. Gusrialdi, S. Hirche, and A. Monti, "Joint controller communication topology design for distributed wide-area damping control of power systems," in *Proc. of the International Federation of Automatic Control World Congress*, 2011, pp. 519–525.

[15] J. Machowski, J. Bialek, and J. Bumby, *Power System Dynamics: Stability and Control*. USA: John Wiley and Sons, 2011.

[16] S. Riverso, F. Sarzo, and G. Ferrari-Trecate, "Plug-and-play voltage and frequency control of islanded microgrids with meshed topology," *IEEE Transactions on Smart Grid*, vol. 6, no. 3, pp. 1176–1184, 2015.

[17] R. Moradi, H. Karimi, and M. Karimi-Ghartemani, "Robust decentralized control for islanded operation of two radially connected DG systems," in *Proc. of the International Symposium on Industrial Electronics*, 2010, pp. 2272–2277.

[18] M. J. Hossain, M. A. Mahmud, F. Milano, S. Bacha, and A. Hably, "Design of robust distributed control for interconnected microgrids," *IEEE Transactions on Smart Grid*, vol. 7, no. 6, pp. 2724–2735, 2016.

[19] E. R. Diaz, J. C. V. Quintero, and J. M. Guerrero, "Intelligent DC homes in future sustainable energy systems: When efficiency and intelligence work together," *IEEE Consumer Electronics Magazine*, vol. 5, no. 1, pp. 74–80, 2016.

[20] A. K. Singh, R. Singh, and B. C. Pal, "Stability analysis of networked control in smart grids," *IEEE Transactions on Smart Grid*, vol. 6, no. 1, pp. 381–390, 2015.

[21] T. Morstyn, B. Hredzak, G. D. Demetriades, and V. G. Agelidis, "Unified distributed control for DC microgrid operating modes," *IEEE Transactions on Power Systems*, vol. 31, no. 1, pp. 802–812, 2016.

[22] A. Abur and A. G. Exposito, *Power system state estimation: Theory and implementation*. CRC press, 2004.

[23] S. Yu, T. Fernando, and H. H.-C. Iu, "Realization of state-estimation-based DFIG wind turbine control design in hybrid power systems using stochastic filtering approaches," *IEEE Transactions on Industrial Informatics*, vol. 12, no. 3, pp. 1084–1092, 2016.

[24] K. Tan, B. Sivaneasan, X. Peng, and P. So, "Control and operation of a DC grid-based wind power generation system in a microgrid," *IEEE Transactions on Energy Conversion*, vol. 31, no. 2, pp. 496–505, 2016.

[25] G. Mendes, J. Von Appen, and C. Ioakimidis, "Integrated energy microgrids for community-scale systems: Case study research in the Azores islands," in *Proc of the International Conference of the European Energy Market*, 2011, pp. 382–387.

[26] X. Yu, Z. Jiang, and Y. Zhang, "Control of parallel inverter-interfaced distributed energy resources," in *Proc of the International Conference on Energy 2030*, 2008, pp. 1–8.

[27] T. Orhan, G. Shafiullah, A. Stojcevski, and A. Oo, "A feasibility study on microgrid for various islands in Australia," in *Proc of the International Conference Power Engineering Conference*, 2014, pp. 1–8.

[28] R. M. Kamel, A. Chaouachi, and K. Nagasaka, "Three control strategies to improve the microgrid transient dynamic response during isolated mode: A comparative study," *IEEE Transactions on Industrial Electronics*, vol. 60, no. 4, pp. 1314–1322, 2013.

[29] A. M. Egwebe, M. Fazeli, P. Igic, and P. Holland, "Implementation and stability study of dynamic droop in islanded microgrids," *IEEE Transactions on Energy Conversion,*, vol. 31, no. 3, pp. 821–832, 2016.

[30] H. Sui and W.-J. Lee, "An AMI based measurement and control system in smart distribution grid," in *Proc of the Industrial and Commercial Power Systems Technical Conference*, 2011, pp. 1–5.

[31] C. Marnay, H. Asano, S. Papathanassiou, and G. Strbac, "Policy making for microgrids," *IEEE Power and Energy Magazine*, vol. 6, no. 3, pp. 66–77, 2008.

[32] E. Alvarez, A. C. Lopez, J. Gómez-Aleixandre, and N. De Abajo, "On-line minimization of running costs, greenhouse gas emissions and the impact of distributed generation using microgrids on the electrical system," in *Proc of the International Conference on Sustainable Alternative Energy*, 2009, pp. 1–10.

[33] Y. Han, P. Shen, X. Zhao, and J. M. Guerrero, "An enhanced power sharing scheme for voltage unbalance and harmonics compensation in an islanded microgrid," *IEEE Transactions on Energy Conversion,*, vol. 31, no. 3, pp. 1037–1050, 2016.

[34] R. Deng, G. Xiao, and R. Lu, "Defending against false data injection attacks on power system state estimation," *IEEE Transactions on Industraial Informatics, to appear in 2017*.

[35] Y. V. Makarov, P. Du, M. C. Kintner-Meyer, C. Jin, and H. F. Illian, "Sizing energy storage to accommodate high penetration of variable energy resources," *IEEE Transactions on Sustainable Energy*, vol. 3, no. 1, pp. 34–40, 2012.

[36] S. Zhang, J. Yang, X. Wu, and R. Zhu, "Dynamic power provisioning for cost minimization in islanding micro-grid with renewable energy," in *Proc of the International Conference Innovative Smart Grid Technologies Conference*, 2014, pp. 1–5.

[37] L. Schenato, "Optimal estimation in networked control systems subject to random delay and packet drop," *IEEE Transactions on Automatic Control*, vol. 53, no. 5, pp. 1311–1317, 2008.

[38] L. Schenato, B. Sinopoli, M. Franceschetti, K. Poolla, and S. S. Sastry, "Foundations of control and estimation over lossy networks," *Proc. of the IEEE*, vol. 95, no. 1, pp. 163–187, 2007.

[39] N. Kayastha, D. Niyato, E. Hossain, and Z. Han, "Smart grid sensor data collection, communication, and networking: A tutorial," *Wireless Communications and Mobile Computing*, vol. 14, no. 11, pp. 1055–1087, 2014.

[40] D. Soldani and A. Manzalini, "Horizon 2020 and beyond: On the 5G operating system for a true digital society," *IEEE Vehicular Technology Magazine*, vol. 10, no. 1, pp. 32–42, 2015.

[41] S. Talwar, D. Choudhury, K. Dimou, E. Aryafar, B. Bangerter, and K. Stewart, "Enabling technologies and architectures for 5G wireless," in *Microwave Symposium*. IEEE, 2014, pp. 1–4.

[42] M. J. Daigle, A. Bregon, and I. Roychoudhury, "Distributed prognostics based on structural model decomposition," *IEEE Transactions on Reliability*, vol. 63, no. 2, pp. 495–510, 2014.

[43] D. E. Olivares, C. A. Cañizares, and M. Kazerani, "A centralized energy management system for isolated microgrids," *IEEE Transactions on Smart Grid*, vol. 5, no. 4, pp. 1864–1875, 2014.

[44] M. Tahir and S. K. Mazumder, "Self-triggered communication enabled control of distributed generation in microgrids," *IEEE Transactions on Industrial Informatics*, vol. 11, no. 2, pp. 441–449, 2015.

[45] H. Li and Z. Han, "Distributed scheduling of wireless communications for voltage control in micro smart grid," in *Proc. of the Global Communications Conference*, 2011, pp. 1188–1193.

[46] E. Song, J. Xu, and Y. Zhu, "Optimal distributed Kalman filtering fusion with singular covariances of filtering errors and measurement noises," *IEEE Transactions on Automatic Control*, vol. 59, no. 5, pp. 1271–1282, 2014.

[47] Y. Wang, P. Yemula, and A. Bose, "Decentralized communication and control systems for power system operation," *IEEE Transactions on Smart Grid*, vol. 6, no. 2, pp. 885–893, 2015.

[48] H. R. Hashemipour, S. Roy, and A. J. Laub, "Decentralized structures for parallel Kalman filtering," *IEEE Transactions on Automatic Control*, vol. 33, no. 1, pp. 88–94, 1988.

[49] S.-C. Huang, C.-N. Lu, and Y.-L. Lo, "Evaluation of AMI and SCADA data synergy for distribution feeder modeling," *IEEE Transactions on Smart Grid*, vol. 6, no. 4, pp. 1639–1647, 2015.

[50] R. Olfati-Saber, "Distributed Kalman filtering for sensor networks," in *Proc. of the Conference on Decision and Control*, 2007, pp. 5492–5498.

[51] ——, "Kalman-consensus filter: Optimality, stability, and performance," in *Proc. of the International Conference on Decision and Control*, 2009, pp. 7036–7042.

[52] F. Cattivelli and A. H. Sayed, "Diffusion distributed Kalman filtering with adaptive weights," in *Proc. of the Conference Record of the Forty Third Asilomar Conference on Signals, Systems and Computers*, 2009, pp. 908–912.

[53] F. S. Cattivelli and A. H. Sayed, "Diffusion strategies for distributed Kalman filtering and smoothing," *IEEE Transactions on Automatic Control*, vol. 55, no. 9, pp. 2069–2084, 2010.

[54] X. Zhang, W. Pei, W. Deng, Y. Du, Z. Qi, and Z. Dong, "Emerging smart grid technology for mitigating global warming," *International Journal of Energy Research*, vol. 39, no. 13, pp. 1742–1756, 2015.

[55] R. Mao and H. Li, "Nobody but you: Sensor selection for voltage regulation in smart grid," *arXiv preprint arXiv:1103.5441*, 2011.

[56] H. Liang and W. Zhuang, "Stochastic modeling and optimization in a microgrid: A survey," *Energies*, vol. 7, no. 4, pp. 2027–2050, 2014.

[57] X. Wang and Q. Liang, "Stabilizing the power supply in microgrid using sensor selection," in *Proc. of the Global Communications Conference*, 2012, pp. 3513–3518.

[58] H. Liang, A. Abdrabou, and W. Zhuang, "Stochastic information management for voltage regulation in smart distribution systems," in *Proc. of the International Conference on Computer Communications*, 2014, pp. 2652–2660.

[59] B. Yan, H. Lev-Ari, and A. Stankovic, "Networked state estimation with delayed and rregularly-spaced time-stamped observations," *IEEE Transactions on Control of Network Systems, to appear in 2017*.

[60] S. A. Salinas and P. Li, "Privacy-preserving energy theft detection in microgrids: A state estimation approach," *IEEE Transactions on Power Systems*, vol. 31, no. 2, pp. 883–894, 2016.

[61] X. Li and H. Gao, "Load mitigation for a floating wind turbine via generalized structural control," *IEEE Transactions on Industrial Electronics*, vol. 63, no. 1, pp. 332–342, 2016.

[62] S. Deshmukh, B. Natarajan, and A. Pahwa, "State estimation over a lossy network in spatially distributed cyber-physical systems," *IEEE Transactions on Signal Processing*, vol. 62, no. 15, pp. 3911–3923, 2014.

[63] B. Sinopoli, L. Schenato, M. Franceschetti, K. Poolla, M. Jordan, and S. Sastry, "Kalman filtering with intermittent observations," *IEEE Transactions on Automatic Control*, vol. 49, no. 9, pp. 1453–1464, 2004.

[64] C. H. Lo and N. Ansari, "Decentralized controls and communications for autonomous distribution networks in smart grid," *IEEE Transactions on Smart Grid*, vol. 4, no. 1, pp. 66–77, 2013.

[65] R. Ma, H. H. Chen, Y. R. Huang, and W. Meng, "Smart grid communication: Its challenges and opportunities," *IEEE Transaction on Smart Grid*, vol. 4, no. 1, pp. 36–46, 2013.

[66] M. Kuzlu, M. Pipattanasomporn, and S. Rahman, "Communication network requirements for major smart grid applications in HAN, NAN and WAN," *Computer Networks*, vol. 67, pp. 74–88, 2014.

[67] F. R. Yu, P. Zhang, W. Xiao, and P. Choudhury, "Communication systems for grid integration of renewable energy resources," *IEEE Network*, vol. 25, no. 5, pp. 22–29, 2011.

[68] L. T. Berger and K. Iniewski, *Smart grid applications, communication and security*. New Jersey, USA: John Wiley and Sons, 2012.

[69] I. R. Casella, C. Capovilla, and E. Ruppert, "A wireless deadbeat power control for wind power generation systems in smart grid applications," in *Proc of the Power Electronics Conference*, 2011, pp. 520–523.

[70] C. W. Taylor, *Power system voltage stability*. New York: McGraw-Hill, 1994.

[71] J. M. J. Bialek and J. Bumby, *Power system dynamics and stability*. UK: John Wiley and Sons, 1997.

[72] R. Moxley and D. Dolezilek, "Case studies: Synchrophasors for wide-area monitoring, protection, and control," in *Proc of the IEEE PES International Conference and Exhibition on Innovative Smart Grid Technologies*, 2011, pp. 1–7.

[73] F. Li, W. Qiao, H. Sun, H. Wan, J. Wang, Y. Xia, Z. Xu, and P. Zhang, "Smart transmission grid: Vision and framework," *IEEE Transactions on Smart Grid*, vol. 1, no. 2, pp. 168–177, 2010.

[74] H. Zhu and G. B. Giannakis, "Sparse overcomplete representations for efficient identification of power line outages," *IEEE Transactions on Power Systems*, vol. 27, no. 4, pp. 2215–2224, 2012.

[75] Shivakumar and A. Jain, "A review of power system dynamic state estimation techniques," in *Proc. of the International Conference on Power System Technology and IEEE Power India*, 2008.

[76] Z. Huang and J. Nieplocha, "Transforming power grid operations via high performance computing," in *Proc of the Power and Energy Society General Meeting-Conversion and Delivery of Electrical Energy in the 21st Century*, 2008, pp. 1–8.

[77] S. Kamireddy, N. N. Schulz, and A. K. Srivastava, "Comparison of state estimation algorithms for extreme contingencies," in *North American Power Symposium*, 2008, pp. 1–5.

[78] V. Aravinthan, B. Karimi, V. Namboodiri, and W. Jewell, "Wireless communication for smart grid applications at distribution level feasibility and requirements," in *Proc. of the Power and Energy Society General Meeting*, 2011, pp. 1–8.

[79] A. G. Exposito, A. Abur, A. D. L. V. Jaen, and C. G. Quiles, "A multilevel state estimation paradigm for smart grids," *Proc. of the IEEE*, vol. 99, no. 6, pp. 952–976, 2011.

[80] F. C. Schweppe and J. Wildes, "Power system static state estimation, part I: Exact model," *IEEE Transactions on Power Apparatus and Systems*, vol. 89, no. 1, pp. 120–125, 1970.

[81] ——, "Power system static state estimation, part II: Approximate model," *IEEE Transactions on Power Apparatus and Systems*, vol. 89, no. 1, pp. 125–130, 1970.

[82] N. Shivakumar and A. Jain, "A review of power system dynamic state estimation techniques," in *Proc. of the Joint International Conference on Power System Technology and IEEE Power India*, 2008, pp. 1–6.

[83] A. S. Debs and R. E. Larson, "A dynamic estimator for tracking the state of a power system," *IEEE Transactions on Power Apparatus and Systems*, vol. 89, no. 7, pp. 1670–1678, 1970.

[84] M. Zhao and A. Abur, "Multi-area state estimation using synchronous phasor measurements," *IEEE Transactions on Power Systems*, vol. 22, no. 2, pp. 611 – 617, 2005.

[85] G. T. Heydt, "The next generation of power distribution systems," *IEEE Transactions on Smart Grid*, vol. 1, no. 3, pp. 225–235, 2010.

[86] C. G. Quiles, A. G. Exposito, and A. D. L. V. Jaen, "State estimation for smart distribution substations," *IEEE Transactions on Smart Grid*, vol. 3, no. 2, pp. 986–995, 2012.

[87] A. G. E. Sito, A. Abur, A. D. L. V. Jaen, and C. G. Quiles, "A multilevel state estimation paradigm for smart grids," *Proc. of the IEEE*, vol. 99, no. 6, pp. 952–976, 2011.

[88] S. Pajic and K. A. Clements, "Power system state estimation via globally convergent methods," *IEEE Transactions on Power Systems*, vol. 20, no. 4, pp. 1683–1689, 2005.

[89] L. Holten, A. Gjelsvik, S. Aam, F. F. Wu, and W. H. E. Liu, "Comparison of different methods for state estimation," *IEEE Transactions on Power Systems*, vol. 3, no. 4, pp. 1798–1806, 1988.

[90] E. Caro, A. J. Conejo, and R. Manguez, "Decentralized state estimation and bad measurement identification: An efficient Lagrangian relaxation approach," *IEEE Transactions on Power Systems*, vol. 33, no. 4, pp. 1331–1336, 1998.

[91] A. Ahmed, M. Moinuddin, and U. M. Al-Saggaf, "State space least mean fourth algorithm for dynamic state estimation in power systems," *Arabian*

Journal for Science and Engineering, pp. 1–17, 2015. [Online]. Available: DOI 10.1007/s13369-015-1698-6

[92] M. B. Malik and M. Salman, "State-space least mean square," *Digital Signal Processing*, vol. 18, no. 3, pp. 334–345, 2008.

[93] J. Ni and F. Li, "A variable step-size matrix normalized subband adaptive filter," *IEEE Transactions on Audio, Speech, and Language Processing*, vol. 18, no. 6, pp. 1290–1299, 2010.

[94] F. Zhang, Y. Wang, and B. Ai, "Variable step-size MLMS algorithm for digital predistortion in wideband OFDM systems," *IEEE Transactions on Consumer Electronics*, vol. 61, no. 1, pp. 10–15, 2015.

[95] H. Cho and S. W. Kim, "Variable step-size normalized LMS algorithm by approximating correlation matrix of estimation error," *Signal Processing*, vol. 90, no. 9, pp. 2792–2799, 2010.

[96] I. Kamwa, B. Baraboi, and R. Wamkeue, "Sensorless ANN-based speed estimation of synchronous generators: Improved performance through physically motivated prefilters," in *Proc. of the Joint Conference on Neural Networks*, 2006, pp. 1710–1718.

[97] D. H. Dini and D. P. Mandic, "Widely linear modeling for frequency estimation in unbalanced three-phase power systems," *IEEE Transactions on Instrumentation and Measurement*, vol. 62, no. 2, pp. 353–363, 2013.

[98] S. Kanna, D. H. Dini, Y. Xia, S. Hui, and D. P. Mandic, "Distributed widely linear Kalman filtering for frequency estimation in power networks," *IEEE Transactions on Signal and Information Processing over Networks*, vol. 1, no. 1, pp. 45–57, 2015.

[99] F. C. Schweppe and R. D. Masiello, "A tracking static state estimator," *IEEE Transactions on Power Apparatus and Systems*, vol. 90, no. 3, pp. 1025–1033, 1971.

[100] X. Bian, X. R. Li, H. Chen, D. Gan, , and J. Qiu, "Joint estimation of state and parameter with synchrophasorspart II: Parameter tracking," *IEEE Transactions on Power Systems*, vol. 26, no. 3, pp. 1209–1220, 2011.

[101] A. M. L. D. Silva, M. B. D. C. Filho, and J. F. D. Queiroz, "State forecasting in electric power systems," in *IEE Generation, Transmission and Distribution*, vol. 130, no. 5, 1983, pp. 237–244.

[102] N. Kashyap, S. Werner, T. Riihonen, and Y. F. Huang, "Reduced-order synchrophasor-assisted state estimation for smart grids," in *Proc. of the International Conference on Smart Grid Communications*, 2012, pp. 1–6.

[103] G. Durgaprasad and S. S. Thakur, "Robust dynamic state estimation of power systems based on M-estimation and realistic modeling of system dynamics," *IEEE Transactions on Power Systems*, vol. 13, no. 4, pp. 1331–1336, 1998.

[104] M. M. Rana and L. Li, "Microgrid state estimation and control for smart grid and the internet of things communication network," *Electronics Letters*, vol. 51, no. 2, pp. 149–151, 2015.

[105] ——, "An overview of distributed microgrid state estimation and control for smart grids," *Sensors*, vol. 15, no. 2, pp. 4302–4325, 2015.

[106] E. Ghahremani and I. Kamwa, "Online state estimation of a synchronous generator using unscented Kalman filter from phasor measurements units," *IEEE Transactions on Energy Conversion*, vol. 26, no. 4, pp. 1099–1108, 2011.

[107] X. Wang, , and E. E. Yaz, "Smart power grid synchronization with fault tolerant nonlinear estimation," *IEEE Transactions on Power Systems, to appear in 2017*.

[108] S. Yu, K. Emami, T. Fernando, H. H. C. Iu, and K. P. Wong, "State estimation of doubly fed induction generator wind turbine in complex power systems," *IEEE Transactions on Power Systems, to appear in 2016*.

[109] S. Metia, S. Oduro, Q. Ha, and H. Due, "Inverse air-pollutant emission and prediction using extended fractional Kalman filtering," *IEEE Journal of Selected Topics in Applied Earth Observations and Remote Sensing, to appear in 2016*.

[110] D. Sierociuk, I. Tejado, and B. M. Vinagre, "Improved fractional Kalman filter and its application to estimation over lossy networks," *Signal Processing*, vol. 91, no. 3, pp. 542–552, 2011.

[111] A. K. Singh and B. C. Pal, "Decentralized dynamic state estimation in power systems using unscented transformation," *IEEE Transactions on Power Systems*, vol. 29, no. 2, pp. 794–804, 2014.

[112] K. Hua, Y. Mishra, and G. Ledwich, "Fast unscented transformation-based transient stability margin estimation incorporating uncertainty of wind generation," *IEEE Transactions on Sustainable Energy*, vol. 6, no. 4, pp. 1254–1262, 2015.

[113] M. Ariff, B. Pal, and A. Singh, "Estimating dynamic model parameters for adaptive protection and control in power system," *IEEE Transactions on Power Systems*, vol. 30, no. 2, pp. 829–839, 2015.

[114] G. Feng, C. Lai, and N. Kar, "Particle filter based magnet flux linkage estimation for PMSM magnet condition monitoring using harmonics in machine speed," *IEEE Transactions on Industrial Informatics, to appear in 2017*.

[115] M. S. Arulampalam, S. Maskell, N. Gordon, and T. Clapp, "A tutorial on particle filters for online nonlinear/non-gaussian Bayesian tracking," *IEEE Transactions on Signal Processing*, vol. 50, no. 2, pp. 174–188, 2002.

[116] J. Zhu, Z. Shi, H. Liang, R. Lu, and X. Shen, "Particle filter based grid synchronization with voltage unbalance and frequency variation in smart grid." in *Proc. of the International Conference on Wireless Communications and Signal Processing*, 2013, pp. 1–6.

[117] S. Nadarajan, B. Bhangu, S. Panda, and A. K. Gupta, "Comparing extended Kalman filter and particle filter for estimating field and damper bar currents in brushless wound field synchronous generator for stator winding fault detection and diagnosis," in *Proc. of the IEEE Applied Power Electronics Conference and Exposition*, 2016, pp. 715–719.

[118] S. Nanchian, A. Majumdar, and B. C. Pal, "Three-phase state estimation using hybrid particle swarm optimization," *IEEE Transactions on Smart Grid, to appear in 2017*.

[119] Y. Cui and R. Kavasseri, "A particle filter for dynamic state estimation in multi-machine systems with detailed models," *IEEE Transactions on Power Systems*, vol. 30, no. 6, pp. 3377–3385, 2015.

[120] Y. Cui, R. Kavasseri, and S. Brahma, "Dynamic state estimation assisted out-of-step detection for generators using angular difference," *IEEE Transactions on Power Delivery, to appear in 2017*.

[121] Y. Hu, A. Kuh, and A. Kavcic, "A belief propagation based power distribution system state estimator," *IEEE Computational Intelligence Magazine*, vol. 6, no. 3, pp. 36–46, 2011.

[122] P. Chavali and A. Nehorai, "Distributed power system state estimation using factor graphs," *IEEE Transactions on Signal Processing*, vol. 63, no. 11, pp. 2864–2876, 2015.

[123] Y. Li, "Fully distributed state estimation of smart grids," in *Proc. of the International Conference on Communications*, 2012, pp. 6580–6585.

[124] Y. Weng, R. Negi, and M. D. Ilic, "Graphical model for state estimation in electric power systems," in *Proc. of the International Conference on Smart Grid Communications*, 2013, pp. 103–108.

[125] B. Ruffer, C. M. Kellett, P. M. Dower, and S. R. Weller, "Belief propagation as a dynamical system: The linear case and open problems," *IET Control Theory and Applications*, vol. 4, no. 7, pp. 1188–1200, 2010.

[126] H.-A. Loeliger, J. Dauwels, J. Hu, S. Korl, L. Ping, and F. R. Kschischang, "The factor graph approach to model-based signal processing," *Proceedings of the IEEE*, vol. 95, no. 6, pp. 1295–1322, 2007.

[127] Y. Hu, A. Kuh, A. Kavcic, and D. Nakafuji, "Real-time state estimation on microgrids," in *Proc. of the International Joint Conference on Neural Networks*, 2011, pp. 1378–1385.

[128] G. Rigatos, P. Siano, and N. Zervos, "A distributed state estimation approach to condition monitoring of nonlinear electric power systems," *Asian Journal of Control*, vol. 15, no. 3, pp. 849–860, 2013.

[129] C.-H. Lo and N. Ansari, "Decentralized controls and communications for autonomous distribution networks in smart grid," *IEEE Transactions on Smart Grid*, vol. 4, no. 1, pp. 66–77, 2013.

[130] L. Xie, D.-H. Choi, S. Kar, and H. V. Poor, "Fully distributed state estimation for wide-area monitoring systems," *IEEE Transactions on Smart Grid*, vol. 3, no. 3, pp. 1154–1169, 2012.

[131] S. Zonouz and W. H. Sanders, "A Kalman based coordination for hierarchical state estimation: Agorithm and analysis," in *Proc. of the 41st Annual Hawaii International Conference on System Sciences*, 2008, pp. 187–187.

[132] T. Van Cutsem, L. Horward, and M. Ribbens-Pavella, "A two-level static state estimator for electric power systems," *IEEE Transactions on Power Apparatus and Systems*, no. 8, pp. 3722–3732, 1981.

[133] T. Yang, H. Sun, and A. Bose, "Transition to a two-level linear state estimatorpart I: Architecture," *IEEE Transactions on Power Systems*, vol. 26, no. 1, pp. 46–53, 2011.

[134] ——, "Transition to a two-level linear state estimatorpart II: Algorithm," *IEEE Transactions on Power Systems*, vol. 26, no. 1, pp. 54–62, 2011.

[135] A. Gómez-Expósito and A. De La Villa Jaén, "Two-level state estimation with local measurement pre-processing," *IEEE Transactions on Power Systems*, vol. 24, no. 2, pp. 676–684, 2009.

[136] A. J. Conejo, F. J. Nogales, and F. J. Prieto, "A decomposition procedure based on approximate Newton directions," *Mathematical Programming*, vol. 93, no. 3, pp. 495–515, 2002.

[137] A. Gómez-Expósito, A. Abur, A. De La Villa Jaén, and C. Gómez-Quiles, "A multilevel state estimation paradigm for smart grids," *Proc. of the IEEE*, vol. 99, no. 6, pp. 952–976, 2011.

[138] G. N. Korres, "A distributed multiarea state estimation," *IEEE Transactions on Power Systems*, vol. 26, no. 1, pp. 73–84, 2011.

[139] A. Minot, Y. M. Lu, and N. Li, "A distributed Gauss-Newton method for power system state estimation," *IEEE Transction on Power Systems*, vol. 31, pp. 3804–3815, 2016.

[140] P. Alriksson and A. Rantzer, "Distributed Kalman filtering using weighted averaging," in *Proc. of the International Symposium on Mathematical Theory of Networks and Systems*, 2006, pp. 2445–2450.

[141] R. Olfati-Saber, "Distributed Kalman filter with embedded consensus filters," in *Proc. of the Conference on Decision and Control and European Control Conference*, 2005, pp. 8179–8184.

[142] R. Olfati-Saber and J. S. Shamma, "Consensus filters for sensor networks and distributed sensor fusion," in *Proc. of the Conference on Decision and Control*, 2005, pp. 6698–6703.

[143] T. Jiang, I. Matei, and J. Baras, "A trust based distributed Kalman filtering approach for mode estimation in power systems," in *Proc. of the First Workshop on Secure Control Systems*, 2010.

[144] K. Dedecius, "Collaborative Kalman filtration Bayesian perspective," in *Proc of the International Conference on Informatics in Control, Automation and Robotics*, vol. 1, 2014, pp. 468–474.

[145] Y. Lu, L. Zhang, and X. Mao, "Distributed information consensus filters for simultaneous input and state estimation," *Circuits, Systems, and Signal Processing*, vol. 32, no. 2, pp. 877–888, 2013.

[146] A. H. Sayed, "Adaptation, learning, and optimization over networks," *Foundations and Trends in Machine Learning*, vol. 7, no. 4-5, pp. 311–801, 2014.

[147] J. Hu, L. Xie, and C. Zhang, "Diffusion Kalman filtering based on covariance intersection," *IEEE Transactions on Signal Processing*, vol. 60, no. 2, pp. 891–902, 2012.

[148] L. Xiao, S. Boyd, and S. Lall, "A scheme for robust distributed sensor fusion based on average consensus," in *Proc. of the Fourth International Symposium on Information Processing in Sensor Networks*, 2005, pp. 63–70.

[149] S. J. Julier and J. K. Uhlmann, "General decentralized data fusion with covariance intersection," *Handbook of multisensor data fusion*, pp. 319–342, 2001.

[150] O. Hlinka, O. Sluciak, F. Hlawatsch, and M. Rupp, "Distributed data fusion using iterative covariance intersection," in *Proc. of the international Conference on Acoustics, Speech and Signal Processing*, 2014, pp. 1861–1865.

[151] F. P. Vista IV, D.-J. Lee, and K. T. Chong, "Design of an EKF-CI based sensor fusion for robust heading estimation of marine vehicle," *International Journal of Precision Engineering and Manufacturing*, vol. 16, no. 2, pp. 403–407, 2015.

[152] C. G. Lopes and A. H. Sayed, "Diffusion least-mean squares over adaptive networks: Formulation and performance analysis," *IEEE Transactions on Signal Processing*, vol. 56, no. 7, pp. 3122–3136, 2008.

[153] S. Xu, R. C. de Lamare, and H. V. Poor, "Dynamic topology adaptation for distributed estimation in smart grids," in *Proc. of the International Workshop on Computational Advances in Multi-Sensor Adaptive Processing*, 2013, pp. 420–423.

[154] K. Fujimoto, Y. Oji, and K. Hamamoto, "On periodic Kalman filters and multi-rate estimation," in *Proc. of the International Conference on Control Applications*, 2016, pp. 934–939.

[155] D. Simon, *Optimal state estimation: Kalman, H infinity, and nonlinear approaches*. New Jersey: John Wiley and Sons, 2006.

[156] V. Ugrinovskii and C. Langbort, "Distributed H_∞ consensus-based estimation of uncertain systems via dissipativity theory," *IET control theory and applications*, vol. 5, no. 12, pp. 1458–1469, 2011.

[157] J. Wu, L. Li, V. Ugrinovskii, and F. Allgower, "Distributed filter design for cooperative H_∞-type estimation," in *Proc. of the International Conference on Control Applications*, 2015, pp. 1373–1378.

[158] V. Ugrinovskii and E. Fridman, "A round-robin protocol for distributed estimation with H_∞ consensus," *arXiv preprint arXiv:1401.1545*, 2014.

[159] M. Zamani and V. Ugrinovskii, "Cooperative robust estimation with local performance guarantees," *arXiv preprint arXiv:1603.05307*, 2016.

[160] A. Mohammadi and A. Asif, "Distributed particle filtering for large scale dynamical systems," in *Proc. of the International Multitopic Conference*. IEEE, 2009, pp. 1–5.

[161] S. Li, Y. Yilmaz, and X. Wang, "Quickest detection of false data injection attack in wide-area smart grids," *IEEE Transactions on Smart Grid*, vol. 6, no. 6, pp. 2725–2735, 2015.

[162] G. Hug and J. A. Giampapa, "Vulnerability assessment of AC state estimation with respect to false data injection cyber-attacks," *IEEE Transactions on Smart Grid*, vol. 3, no. 3, pp. 1362–1370, 2012.

[163] A. Alimardani, F. Therrien, D. Atanackovic, J. Jatskevich, and E. Vaahedi, "Distribution system state estimation based on nonsynchronized smart meters," *IEEE Transactions on Smart Grid*, vol. 6, no. 6, pp. 2919–2928, 2015.

[164] S. Meliopoulos, R. Huang, E. Polymeneas, and G. Cokkinides, "Distributed dynamic state estimation: Fundamental building block for the smart grid," in *Proc. of the Power and Energy Society General Meeting*, 2015, pp. 1–6.

[165] K. C. Sou, H. Sandberg, and K. H. Johansson, "On the exact solution to a smart grid cyber-security analysis problem," *IEEE Transactions on Smart Grid*, vol. 4, no. 2, pp. 856–865, 2013.

[166] G. Chaojun, P. Jirutitijaroen, and M. Motani, "Detecting false data injection attacks in AC state estimation," *IEEE Transactions on Smart Grid*, vol. 6, no. 5, pp. 2476–2483, 2015.

[167] Y. Weng, Q. Li, R. Negi, and M. Ilic, "Distributed algorithm for SDP state estimation," in *Proc. of the International Conference on Innovative Smart Grid Technologies*, 2013, pp. 1–6.

[168] H. Zhang, P. Cheng, L. Shi, and J. Chen, "Optimal denial-of-service attack scheduling with energy constraint," *IEEE Transactions on Automatic Control*, vol. 60, no. 11, pp. 3023–3028, 2015.

[169] L. Shi, P. Cheng, and J. Chen, "Sensor data scheduling for optimal state estimation with communication energy constraint," *Automatica*, vol. 47, no. 8, pp. 1693–1698, 2011.

[170] Y. Li, L. Shi, P. Cheng, J. Chen, and D. E. Quevedo, "Jamming attacks on remote state estimation in cyber-physical systems: A game-theoretic approach," *IEEE Transactions on Automatic Control*, vol. 60, no. 10, pp. 2831–2836, 2015.

[171] H. Zhang, P. Cheng, L. Shi, and J. Chen, "Optimal DoS attack policy against remote state estimation," in *Proc. of the Decision and Control*, 2013, pp. 5444–5449.

[172] D. E. Quevedo and A. Ahlen, "A predictive power control scheme for energy efficient state estimation via wireless sensor networks," in *Proc. of the Decision and Control*, 2008, pp. 1103–1108.

[173] L. Hu, Z. Wang, I. Rahman, and X. Liu, "A constrained optimization approach to dynamic state estimation for power systems including PMU and missing measurements," *IEEE Transactions on Control Systems Technology*, vol. 24, no. 2, pp. 703–710, 2016.

[174] H. Li and Z. Han, "Distributed scheduling of wireless communication for voltage control in micro smart grid," in *Proc. of the International Conference on Smart Grid Communications*, 2011.

[175] H. Cai, G. Hu, F. Lewis, and A. Devoudi, "A distributed feedforward approach to cooperative control of AC microgrids," *IEEE Transactions on Power Systems, to appear in 2016*.

[176] R. Shi, X. Zhang, F. Liu, H. Xu, C. Hu, H. Ni, and Y. Yu, "A differential feedforward control of output current for high performance virtual synchronous generator in microgrid," in *Proc. of the Future Energy Electronics Conference*, 2015, pp. 1–7.

[177] M. M. Rezaei and J. Soltani, "Robust control of an islanded multi-bus microgrid based on input–output feedback linearisation and sliding mode control," *IET Generation, Transmission and Distribution*, vol. 9, no. 15, pp. 2447–2454, 2015.

[178] X.-H. Chang and G.-H. Yang, "New results on output feedback control for linear discrete-time systems," *IEEE Transactions on Automatic Control*, vol. 59, no. 5, pp. 1355–1359, 2014.

[179] A. Rios-Bolivar and F. Narciso, "A robust control by extended static output feedback for discrete-time uncertain linear systems," in *Proc. of the international conference on Automatic control, modelling and simulation*, 2010, pp. 378–383.

[180] M. M. Aghdam, L. Li, J. Zhu, and O. Palizban, "Finite control set model predictive control-a powerful control algorithm for grid-connected power converters," in *Proc. of the Intrnational Conference on Industrial Electronics and Applications*, 2016, pp. 2350–2355.

[181] M. Mahdavi Aghdam, L. Li, and J. Zhu, "A model predictive control of parallel inverters for distributed generations in microgrids," in *Proc. of the International Conference on Power Systems Technology*, 2016.

[182] M. Mahmud, H. Pota, and M. Hossain, "Nonlinear current control scheme for a single-phase grid-connected photovoltaic system," *IEEE Transactions on Sustainable Energy*, vol. 5, no. 1, pp. 218–227, 2014.

[183] ——, "Nonlinear DSTATCOM controller design for distribution network with distributed generation to enhance voltage stability," *International Journal of Electrical Power and Energy Systems*, vol. 53, pp. 974–979, 2013.

[184] ——, "Dynamic stability of three-phase grid-connected photovoltaic system using zero dynamic design approach," *IEEE Journal of Photovoltaics*, vol. 2, no. 4, pp. 564–571, 2012.

[185] ——, "Full-order nonlinear observer-based excitation controller design for interconnected power systems via exact linearization approach," *International Journal of Electrical Power and Energy Systems*, vol. 41, no. 1, pp. 54–62, 2012.

[186] Y. Mo, R. Chabukswar, and B. Sinopoli, "Detecting integrity attacks on SCADA systems," *IEEE Transactions on Control Systems Technology*, vol. 22, no. 4, pp. 1396–1407, 2014.

[187] S. A. Arefifar, Y. A.-R. Mohamed, and T. El-Fouly, "Optimized multiple microgrid-based clustering of active distribution systems considering communication and control requirements," *IEEE Transactions on Industrial Electronics*, vol. 62, no. 2, pp. 711–723, 2015.

[188] S. Saat, S. K. Nguang, J. Wu, and G. Zeng, "Disturbance attenuation for a class of uncertain polynomial discrete-time systems: An integrator approach," in *Proc. of the International Conference on Control Automation Robotics and Vision*, 2012, pp. 787–792.

[189] N. Azman, S. Saat, and S. K. Nguang, "Nonlinear observer design with integrator for a class of polynomial discrete-time systems," in *Proc. of the International Conference on Computer, Communications, and Control Technology*, 2015, pp. 422–426.

[190] A. Sargolzaei, K. K. Yen, and M. N. Abdelghani, "Preventing time-delay switch attack on load frequency control in distributed power systems," *IEEE Transactions on Smart Grid*, vol. 7, no. 2, pp. 1176–1185, 2016.

[191] Y. Song, H. Lou, and S. Liu, "Distributed model predictive control with actuator saturation for Markovian jump linear system," *IEEE/CAA Journal of Automatica Sinica*, vol. 2, no. 4, pp. 374–381, 2015.

[192] P. Massioni and M. Verhaegen, "Distributed control for identical dynamically coupled systems: A decomposition approach," *IEEE Transactions on Automatic Control*, vol. 54, no. 1, pp. 124–135, 2009.

[193] S. P. Ribas, L. A. Maccari, H. Pinheiro, R. Oliveira, and V. Montagner, "Design and implementation of a discrete-time H-infinity controller for uninterruptible power supply systems," *IET Power Electronics*, vol. 7, no. 9, pp. 2233–2241, 2014.

[194] A. P. S. Meliopoulos, G. J. Cokkinides, R. Huang, E. Farantatos, S. Choi, Y. Lee, and X. Yu, "Smart grid technologies for autonomous operation and control," *IEEE Transactions on Smart Grid*, vol. 2, no. 1, pp. 1–10, 2011.

[195] I. Esnaola, S. M. Perlaza, H. V. Poor, and O. Kosut, "Maximum distortion attacks in electricity grids," *IEEE Transactions on Smart Grid, to appear in 2016*.

[196] L. Yu, T. Jiang, Y. Cao, and Q. Qi, "Carbon-aware energy cost minimization for distributed internet data centers in smart microgrids," *IEEE Internet of Things Journal*, vol. 1, no. 3, pp. 255–264, 2014.

[197] K.-L. Nguyen, D.-J. Won, S.-J. Ahn, and I.-Y. Chung, "Power sharing method for a grid connected microgrid with multiple distributed generators," *Journal of Electrical Engineering & Technology*, vol. 7, no. 4, pp. 459–467, 2012.

[198] J.-D. Park and J. Candelaria, "Fault detection and isolation in low-voltage DC-bus microgrid system," *IEEE Transactions on Power Delivery*, vol. 28, no. 2, pp. 779–787, 2013.

[199] D. Chen and L. Xu, "Autonomous DC voltage control of a DC microgrid with multiple slack terminals," *IEEE Transactions on Power Systems*, vol. 27, no. 4, pp. 1897–1905, 2012.

[200] A. Maknouninejad, Z. Qu, F. L. Lewis, and A. Davoudi, "Optimal, nonlinear, and distributed designs of droop controls for DC microgrids," *IEEE Transactions on Smart Grid*, vol. 5, no. 5, pp. 2508–2516, 2014.

[201] Y. Gu, W. Li, and X. He, "Passivity-based control of DC microgrid for self-disciplined stabilization," *IEEE Transactions on Power Systems*, vol. 30, no. 5, pp. 2623–2632, 2015.

[202] A. T. Elsayed, A. A. Mohamed, and O. A. Mohammed, "DC microgrids and distribution systems: An overview," *Electric Power Systems Research*, vol. 119, pp. 407–417, 2015.

[203] C. Dou, D. Yue, J. M. Guerrero, X. Xie, and S. Hu, "Multiagent system-based distributed coordinated control for radial DC microgrid considering transmission time delays," *IEEE Transactions on Smart Grid, to appear in 2016*.

[204] M. Tucci, S. Riverso, J. C. Vasquez, J. M. Guerrero, and G. Ferrari-Trecate, "A decentralized scalable approach to voltage control of DC islanded microgrids," *arXiv preprint arXiv:1503.06292*, 2015.

[205] D. Buchstaller, E. C. Kerrigan, and G. A. Constantinides, "Sampling and controlling faster than the computational delay," *IET Control Theory and Applications*, vol. 6, no. 8, pp. 1071–1079, 2012.

[206] H. Yang, Y. Xia, P. Shi, and M. Fu, "A novel delta operator Kalman filter design and convergence analysis," *IEEE Transactions on Circuits and Systems I: Regular Papers*, vol. 58, no. 10, pp. 2458–2468, 2011.

[207] T. Sui, K. You, M. Fu, and D. Marelli, "Stability of MMSE state estimators over lossy networks using linear coding," *Automatica*, vol. 51, pp. 167–174, 2015.

[208] V. Radisavljevic-Gajic, "Linear observers design and implementation," in *Proc. of the Zone 1 Conference of th American Society for Engineering Education*, 2014, pp. 1–6.

[209] C. Johnson, "Optimal initial conditions for full-order observers," *International Journal of Control*, vol. 48, no. 3, pp. 857–864, 1988.

[210] M. Gopal, *Digital Control and State Variable methods Conventional and Neural-Fuzzy Control System*. New Delhi, India: McGraw-Hill, 2003.

[211] K. Zhou, J. C. Doyle, and K. Glover, *Robust and optimal control*. Prentice Hall, New Jersey, USA, 1996, vol. 40.

[212] M. Fardad and M. R. Jovanovic, "On the design of optimal structured and sparse feedback gains via sequential convex programming," in *Proc. of the American Control Conference*, 2014, pp. 2426–2431.

[213] J. Löfberg, "YALMIP: A toolbox for modeling and optimization in Matlab," in *Proc. of the International Symposium on Computer Aided Control Systems Design*, 2004, pp. 284–289.

[214] L. Kojovic, "Impact of DG on voltage regulation," in *IEEE Power Engineering Society Summer Meeting*, 2002.

[215] H. Li, F. Li, Y. Xu, D. T. Rizy, and J. D. Kueck, "Adaptive voltage control with distributed energy resources: Algorithm, theoretical analysis, simulation, and field test verification," *IEEE Transactions on Power Systems*, vol. 25, no. 3, pp. 1638–1647, 2010.

[216] S. Ntalampiras, "Detection of integrity attacks in cyber-physical critical infrastructures using ensemble modeling," *IEEE Transactions on Industrial Informatics*, vol. 11, no. 1, pp. 104–111, 2015.

[217] Y. Chakhchoukh and H. Ishii, "Coordinated cyber-attacks on the measurement function in hybrid state estimation," *IEEE Transactions on Power Systems*, vol. 30, no. 5, pp. 2487–2487, 2015.

[218] C. Vladeanu and S. El Assad, *Nonlinear Digital Encoders for Data Communications*. USA: John Wiley and Sons, 2014.

[219] B. Vucetic and J. Yuan, *Turbo coding: Principles and applications*. Netherlands: Kluwer Academic Publishers, 2001.

[220] R. D. Zimmerman, C. E. Murillo-Sánchez, and R. J. Thomas, "Matpower: Steady-state operations, planning, and analysis tools for power systems research and education," *IEEE Transactions on Power Systems*, vol. 26, no. 1, pp. 12–19, 2011.

[221] L. Hu, Z. Wang, and X. Liu, "Dynamic state estimation of power systems with quantization effects: A recursive filter approach," *IEEE Transactions on Neural Networks and Learning Systems*, vol. 27, no. 8, pp. 1604–1614, 2015.

[222] J. Zhang and L. Sankar, "Implementation of unobservable state-preserving topology attacks," in *Proc. of the North American Power Symposium*, 2015, pp. 1–6.

[223] M. Malinowski, A. Milczarek, R. Kot, Z. Goryca, and J. T. Szuster, "Optimized energy-conversion systems for small wind turbines: Renewable energy sources in

modern distributed power generation systems," *IEEE Power Electronics Magazine*, vol. 2, no. 3, pp. 16–30, 2015.

[224] C. Jauch and S. Hippel, "Hydraulic-pneumatic flywheel system in a wind turbine rotor for inertia control," *IET Renewable Power Generation*, vol. 10, no. 1, pp. 33–41, 2016.

[225] A. D. Wright, *Modern control design for flexible wind turbines*. National Renewable Energy Laboratory Golden, CO, USA, 2004.

[226] Y. Liu and D.-L. Yu, "Robust fault detection for wind turbine systems," in *Proc. of the International Conference on Automation and Computing*, 2014, pp. 38–42.

[227] H. A. Mohammadpour, Y.-J. Shin, and E. Santi, "SSR analysis of a DFIG-based wind farm interfaced with a gate-controlled series capacitor," in *Proc. of the Applied Power Electronics Conference and Exposition*, 2014, pp. 3110–3117.

[228] Z. Wu, W. Gao, D. Yang, and Y. Shi, "Comprehensive modeling and analysis of permanent magnet synchronous generator-wind turbine system with enhanced low voltage ride through capability," in *Proc. of the Energy Conversion Congress and Exposition*, 2012, pp. 2091–2098.

[229] X. Yu, J. W. Modestino, and X. Tian, "The accuracy of Markov chain models in predicting packet-loss statistics for a single multiplexer," *IEEE Transactions on Information Theory*, vol. 54, no. 1, pp. 489–501, 2008.

[230] P. Almstrom, M. Rabi, and M. Johansson, "Networked state estimation over a Gilbert-Elliot type channel," in *Proc. of the Joint 48th IEEE Conference on Decision and Control and 28th Chinese Control Conference*, 2009, pp. 2711–2716.

[231] W. Niehsen, "Information fusion based on fast covariance intersection filtering," in *Proc of the Fifth International Conference on Information Fusion*, vol. 2, 2002, pp. 901–904.

[232] Q. Guo, S. Chen, H. Leung, and S. Liu, "Covariance intersection based image fusion technique with application to pansharpening in remote sensing," *Information Sciences*, vol. 180, no. 18, pp. 3434–3443, 2010.

[233] E. Aranda-Escolastico, M. Guinaldo, and S. Dormido, "Stability of output event-based control systems through quadratic trigger functions," in *Proc. of the International Conference on Emerging Technologies and Factory Automation*, 2015, pp. 1–7.

[234] R. Vadigepalli and F. J. Doyle, "A distributed state estimation and control algorithm for plantwide processes," *IEEE Transactions on Control Systems Technology*, vol. 11, no. 1, pp. 119–127, 2003.

[235] J. Chen, X. Cao, P. Cheng, Y. Xiao, and Y. Sun, "Distributed collaborative control for industrial automation with wireless sensor and actuator networks," *IEEE Transactions on Industrial Electronics*, vol. 57, no. 12, pp. 4219–4230, 2010.

[236] H. Karimipour and V. Dinavahi, "Parallel domain decomposition based distributed state estimation for large-scale power systems," in *Proc. of the Industrial and Commercial Power Systems Technical Conference*, 2015, pp. 1–5.

[237] B. Chen, W.-A. Zhang, and L. Yu, "Distributed fusion estimation with missing measurements, random transmission delays and packet dropouts," *IEEE Transactions on Automatic Control*, vol. 59, no. 7, pp. 1961–1967, 2014.

[238] M. Moayedi, Y. K. Foo, and Y. C. Soh, "Adaptive Kalman filtering in networked systems with random sensor delays, multiple packet dropouts and missing measurements," *IEEE Transactions on Signal Processing*, vol. 58, no. 3, pp. 1577–1588, 2010.

[239] Z.-g. Yin, C. Zhao, Y.-R. Zhong, and J. Liu, "Research on robust performance of speed-sensorless vector control for the induction motor using an interfacing multiple-model extended Kalman filter," *IEEE Transactions on Power Electronics*, vol. 29, no. 6, pp. 3011–3019, 2014.

[240] C.-L. Su and C.-N. Lu, "Interconnected network state estimation using randomly delayed measurements," *IEEE Transactions on Power Systems*, vol. 16, no. 4, pp. 870–878, 2001.

[241] R. Ambrosino, B. Sinopoli, K. Poolla, and S. Sastry, "Optimal sensor density for remote estimation over wireless sensor networks," in *Proc. of the International Annual Allerton Conference*, 2008, pp. 599–606.

[242] D. Han, Y. Mo, and L. Xie, "Resilience and performance analysis for state estimation against integrity attacks," *IFAC-PapersOnLine*, vol. 49, no. 22, pp. 55–60, 2016.

[243] J. Zhao, M. Netto, and L. Mili, "A robust iterated extended Kalman filter for power system dynamic state estimation," *IEEE Transactions on Power Systems, to apper in 2017*.

[244] W. Zhang, W. Liu, C. Zang, and L. Liu, "Multi-agent system based integrated solution for topology identification and state estimation," *IEEE Transactions on Industrial Informatics, to appear in 2017*.

[245] P. Gaj, A. Malinowski, T. Sauter, and A. Valenzano, "Guest editorial: Distributed data processing in industrial applications," *IEEE Transactions on Industrial Informatics*, vol. 11, no. 3, pp. 737–740, 2015.

[246] D. Han, Y. Mo, and L. Xie, "Robust state estimation against sparse integrity attacks," *arXiv preprint arXiv:1601.04180*, 2016.

[247] M. J. Hossain, H. R. Pota, M. A. Mahmud, and R. A. Ramos, "Investigation of the impacts of large scale wind power penetration on the angle and voltage stability of power systems," *IEEE Systems Journal*, vol. 6, no. 1, pp. 76–84, 2012.

[248] W. Hu, P. Wang, and H. Gooi, "Towards optimal energy management of microgrids via robust two-stage optimization," *IEEE Transactions on Smart Grid, to appear in 2017*.

[249] X. Yin, K. Arulmaran, and J. Liu, "Subsystem decomposition for distributed state estimation of nonlinear systems," in *Proc. of the American Control Conference*, 2016, pp. 5569–5574.

[250] S. Kar, G. Hug, J. Mohammadi, and J. M. Moura, "Distributed state estimation and energy management in smart grids: A consensus innovations approach," *IEEE Journal of Selected Topics in Signal Processing*, vol. 8, no. 6, pp. 1022–1038, 2014.

[251] T. Bouchoucha, M. F. Ahmed, T. Y. Al-Naffouri, and M.-S. Alouini, "Distributed estimation based on observations prediction in wireless sensor networks," *IEEE Signal Processing Letters*, vol. 22, no. 10, pp. 1530–1533, 2015.

[252] L. Mo, X. Cao, J. Chen, and Y. Sun, "Collaborative estimation and actuation for wireless sensor and actuator networks," *IFAC Proceedings*, vol. 47, no. 3, pp. 5544–5549, 2014.

[253] W. Pei, Y. Du, W. Deng, K. Sheng, H. Xiao, and H. Qu, "Optimal bidding strategy and intramarket mechanism of microgrid aggregator in real-time balancing market," *IEEE Transactions on Industrial Informatics*, vol. 12, no. 2, pp. 587–596, 2016.

[254] W.-J. Ma, J. Wang, X. Lu, and V. Gupta, "Optimal operation mode selection for a dc microgrid," *IEEE Transactions on Smart Grid, to appear in 2017*.

[255] A. H. Etemadi, E. J. Davison, and R. Iravani, "A decentralized robust control strategy for multi-DER microgridspart i: Fundamental concepts," *IEEE Transactions on Power Delivery*, vol. 27, no. 4, pp. 1843–1853, 2012.

[256] Y. Zhang and Y.-P. Tian, "Maximum allowable loss probability for consensus of multi-agent systems over random weighted lossy networks," *IEEE Transactions on Automatic Control*, vol. 57, no. 8, pp. 2127–2132, 2012.

[257] H. Chen, H. Bing, M. Xi, and L. Gang, "Distributed H_∞ consensus estimation for moving target using constant gain," in *Proc. of the Chinese Control Conference*, 2015, pp. 7159–7164.

[258] W.-M. Zhou and J.-W. Xiao, "Dynamic average consensus and consensusability of general linear multiagent systems with random packet dropout," in *Abstract and Applied Analysis*, vol. 2013, 2013.

[259] B. D. Anderson and J. B. Moore, *Optimal filtering*. Courier Corporation, 2012.

[260] A. L. Da Silva, M. Do Coutto Filho, and J. De Queiroz, "State forecasting in electric power systems," in *IEE Proceedings in Generation, Transmission and Distribution*, vol. 130, no. 5, 1983, pp. 237–244.

[261] N. Kashyap, S. Werner, T. Riihonen, and Y.-F. Huang, "Reduced-order synchrophasor-assisted state estimation for smart grids," in *Proc. of the International Conference on Smart Grid Communications*, 2012, pp. 605–610.

[262] Y. Fang, G. Bi, Y. L. Guan, and F. C. Lau, "A survey on protograph LDPC codes and their applications," *IEEE Communications Surveys and Tutorials*, vol. 17, no. 4, pp. 1989–2016, 2015.

[263] X. Liu, Y. Zhang, and R. Cui, "Variable-node-based dynamic scheduling strategy for belief-propagation decoding of LDPC codes," *IEEE Communications Letters*, vol. 19, no. 2, pp. 147–150, 2015.

[264] C.-H. Huang, Y. Li, and L. Dolecek, "Belief propagation algorithms on noisy hardware," *IEEE Transactions on Communications*, vol. 63, no. 1, pp. 11–24, 2015.

[265] J. G. Proakis, *Digital communications*, 3rd ed. McGraw-Hill, 1995.

[266] S. Hu and W.-Y. Yan, "Stability of networked control systems subject to input and output packet loss," in *Proc. of the Joint 48th IEEE Conference on Decision and Control and 28th Chinese Control Conference*, 2009.

[267] L. Su and G. Chesi, "On the robust stability of uncertain discrete-time networked control systems over fading channels," in *Proc. of the American Control Conference*, 2015, pp. 6010–6015.

[268] N. Xiao, L. Xie, and L. Qiu, "Feedback stabilization of discrete-time networked systems over fading channels," *IEEE Transactions on Automatic Control*, vol. 57, no. 9, pp. 2176–2189, 2012.

[269] S. S. Alam, B. Natarajan, and A. Pahwa, "Agent based optimally weighted Kalman consensus filter over a lossy network," in *Proc. of the International Global Communications Conference*, 2015, pp. 1–6.